State-of-the-art review of inherent variability and uncertainty in geotechnical properties and models

Ching, Jianye ; Schweckendiek, T.

Publication date
2021

Document Version
Final published version

Citation (APA)
Ching, J., & Schweckendiek, T. (Eds.) (2021). *State-of-the-art review of inherent variability and uncertainty in geotechnical properties and models*. ISSMGE Technical Committee 304. http://140.112.12.21/issmge/2021/SOA_Review_on_geotechnical_property_variablity_and_model_uncertainty.pdf

Important note
To cite this publication, please use the final published version (if applicable).
Please check the document version above.

STATE-OF-THE-ART REVIEW

OF

INHERENT VARIABILITY AND UNCERTAINTY

IN

GEOTECHNICAL PROPERTIES AND MODELS

March 2, 2021

PREPARED BY

Technical Committee of Engineering Practice of Risk Assessment & Management (TC304)

EDITED BY

Jianye Ching (Chair of TC304, ISSMGE)
Timo Schweckendiek (member of TC304, ISSMGE)

Citation: ISSMGE-TC304 (2021). State-of-the-art review of inherent variability and uncertainty in geotechnical properties and models. International Society of Soil Mechanics and Geotechnical Engineering (ISSMGE) - Technical Committee TC304 'Engineering Practice of Risk Assessment and Management', March 2nd., 2021. Download: http://140.112.12.21/issmge/2021/SOA_Review_on_geotechnical_property_variablity_and_model_uncertainty.pdf

Preface

CEN committee TC250 is currently working on an update of the Eurocodes. Sub-committee SC10, in charge of updating EN 1990 (Basis of structural and geotechnical design), has installed a working group to produce a background document with the working title 'Reliability Backgrounds of the Eurocodes', with the intention to document and explain the reliability framework underlying all Eurocodes and the implementation of reliability aspects in them. As part of that effort, quantitative information on the inherent variability and uncertainty in loads, material properties and models is compiled. ISSMGE-TC304 identified this as an opportunity to provide an overview of the relevant information available in the geotechnical literature such as the statistics of soil/rock properties. The EPRI TR-105000 report (Phoon et al. 1995) provided an overview of the statistics of inherent soil properties and measurement errors, but these statistics have not yet been updated systematically since 1995. Also, rock properties were not covered by the TR-105000 report. Other than soil/rock properties and measurement errors, there are also other important statistics, such as the statistics of transformation uncertainties and model factors.

The current technical report is entitled "State-of-the-Art Review of Inherent Variability and Uncertainty in Geotechnical Properties and Models". It contains the following seven chapters as shown in the following table.

Table P1. Titles of the seven chapters in the report

Chap	Title	Contributors
1	Site-specific statistics for geotechnical properties	Zheng Guan, Yu-Chi Chang, Yu Wang (lead), Adeyemi Aladejare, Dongming Zhang, and Jianye Ching
2	Site-specific correlations between soil/rock properties	Yelu Zhou, Dongming Zhang (lead), and Jianye Ching
3	Summary of random field parameters of geotechnical properties	Armin W. Stuedlein (lead), Brigid Cami, Diego Di Curzio, Sina Javankhoshdel, Shin-ichi Nishimura, Wojciech Pula, Giovanna Vessia, Yu Wang, and Jianye Ching
4	Statistics for geotechnical design model factors	Chong Tang (lead) and Richard Bathurst
5	Statistics for transformation uncertainties	Jianye Ching (lead) and Ali Noorzad
6	Determining characteristic values of geotechnical parameters and resistance: an overview	Zi-Jun Cao (lead), Jianye Ching, Guo-Hui Gao, Mikhail Kholmyansky, Ali Noorzad, Timo Schweckendiek, Johan Spross, Mohammad Tabarroki, Xiaohui Tan, Yu Wang, Tengyuan Zhao, and Yan-Guo Zhou
7	Numerical evidences for worst-case scale of fluctuation	Giovanna Vessia (lead), Yan-Guo Zhou, Andy Leung, Wojciech Pula, Diego Di Curzio, Mohammad Tabarroki, and Jianye Ching

The current technical report has the following features:

1. It serves as an update for the TR-105000 report on the statistics of inherent soil properties. Chapter 1 compiles the site-specific statistics for univariate soil properties. Chapter 3 compiles the random field parameters (e.g., the scales of fluctuation) for spatial variability of soils. Many of the statistics are new.
2. It contains statistics that are not covered by the TR-105000 report. Chapter 1 compiles the

site-specific statistics for some rock and rock mass properties. Chapter 2 compiles the site-specific correlations between soil/rock properties. Chapter 5 compiles the statistics for transformation uncertainties.

3. Chapter 4 compiles the statistics of geotechnical design model factors. Chapter 6 reviews methods that determine the characteristic value defined by the Eurocode 7. Chapter 7 reviews some numerical evidences for the worst-case scale of fluctuation.

Many of the new updates in #1 and #2 above are based on the databases in 304dB, an open-access database sharing initiative developed by ISSMGE TC304:
http://140.112.12.21/issmge/tc304.htm?=6

While updating of the Eurocodes triggered the work on the present state-of-the-art review, we trust that the information contained will be a valuable resource for other codes of practice as well as for researchers and practitioners in the field of geotechnical reliability.

We would like to acknowledge the tremendous efforts contributed by the seven groups of experts. This report would not be possible without their efforts.

Editors
Jianye Ching (Chair of TC304, ISSMGE)
Timo Schweckendiek (member of TC304, ISSMGE)

References

Phoon, K.K., Kulhawy, F.H., and Grigoriu, M.D. (1995). Reliability-Based Design of Foundations for Transmission Line Structure, Report TR-105000, Palo Alto, Electric Power Research Institute.

Contents

1. Site-specific statistics for geotechnical properties

Zheng Guan, Yu-Chi Chang, Yu Wang, Adeyemi Aladejare, Dongming Zhang, and Jianye Ching

1.1 Introduction

The proper characterization of the variability of geotechnical properties for a specific site plays a critical role in reliability-based design (RBD) of geotechnical structures (e.g., Phoon and Kulhawy 1999; Baecher and Christian 2003; Fenton and Griffiths 2008; Cao et al. 2016). However, in geotechnical site investigation, site-specific measurement data are usually sparse and limited, particularly for small or medium-sized projects (e.g., Wang and Cao 2013). This leads to the difficulty in obtaining meaningful site-specific statistics (e.g., mean, μ, and coefficient of variation, COV) of geotechnical properties from site-specific measurement data. To deal with these challenges, sparse site-specific data might be integrated with prior knowledge such as typical ranges of μ and COV (e.g., Phoon and Kulhawy 1999; Wang and Cao 2013). This underlines a need to summarize the typical values of site-specific μ and COV from previous studies and reports.

The EPRI TR-105000 report (Phoon et al. 1995), denoted by TR-105000 later, complied statistics of some soil properties from the literature. Since then, soil property statistics have not been systematically updated. Nonetheless, some soil/rock databases have been collected recently, as shown in Table 1.1. The purpose of the current report is to extract site-specific statistics from these databases to serve as an update for TR-105000.

Table 1.1. Soil/rock databases

Database	Reference	Parameters of interest	# data points	# sites/ studies
CLAY/10/7490	Ching and Phoon (2014)	LL, PI, LI, σ'_v/P_a, σ'_p/P_a, s_u/σ'_v, S_t, q_{t1}, q_{tu}, B_q	7490	251 studies
SAND/7/2794	Ching et al. (2017)	D_{50}, C_u, D_r, σ'_v/P_a, ϕ', q_{c1n}, $(N_1)_{60}$	2794	176 studies
ROCK/13	Aladejare and Wang (2017)	ρ, G_s, I_{d2}, n, w, γ, R_L, S_h, σ_{bt}, I_{s50}, σ_{ci}, E_i, ν		
ROCK/9/4069	Ching et al. (2018)	γ, n, R_L, S_h, σ_{bt}, I_{s50}, V_p, σ_{ci}, E_i	4069	184 studies
ROCKMass/9/5876	Ching et al. (2020)	RQD, RMR, Q, GSI, E_m, E_{em}, E_{dm}, E_i, σ_{ci}	5784	225 studies
CLAY/8/12225	Ching (2020)	LL, PI, w, e, σ'_v/P_a, C_c, C_{ur}, c_v	12225	427 studies
CLAY/12/3997	Ching (2020)	LL, PI, LI, σ'_v/P_a, σ'_p/P_a, s_u/σ'_v, K_0, E_u/σ'_v, B_q, q_{t1}, $N_{60}/(\sigma'_v/P_a)$	3997	237 studies
SAND/13/4113	Ching (2020)	e, D_r, σ'_v/P_a, σ'_p/P_a, K_0, E_{dn}, q_{c1n}, B_q, $(N_1)_{60}$, K_{DMTn}, E_{DMTn}, E_{PMTn}, M_{dn}	4113	172 studies
SH-CLAY/11/4051	Zhang et al. (2020)	LL, PI, LI, e, K_0, σ'_v/P_a, $s_{u(UCST)}/\sigma'_v$, $s_{u(VST)}/\sigma'_v$, $S_{t(UCST)}$, $S_{t(VST)}$, p_s/σ'_v	4051	50 sites in Shanghai

ρ = density; ν = Poisson ratio; γ = unit weight; ϕ' = effective friction angle; σ'_p = preconsolidation stress; σ'_v = vertical effective stress; σ_{bt} = Brazilian tensile strength; σ_{ci} = uniaxial compressive strength of intact rock; $(N_1)_{60} = N_{60}/(\sigma'_v/P_a)^{0.5}$; B_q = CPT pore pressure ratio = $(u_2-u_0)/(q_t-\sigma_v)$; C_c = compression index; C_{ur} = unload/reload index; C_u = coefficient of uniformity; c_v = coefficient of consolidation; D_{50} = median grain size; D_r = relative density; e = void ratio; E_{DMT} = soil modulus determined by DMT; E_{DMTn} = normalized $E_{DMT} = (E_{DMT}/P_a)/(\sigma'_v/P_a)^{0.5}$; E_{PMT} = soil modulus determined by PMT; E_d = drained modulus of sand; E_{PMTn} = normalized $E_{PMT} = (E_{PMT}/P_a)/(\sigma'_v/P_a)^{0.5}$; $E_{dn} = (E_d/P_a)/(\sigma'_v/P_a)^{0.5}$; E_{dm} = dynamic modulus of rock mass; E_{em} = elasticity modulus of rock mass; E_i = Young's modulus of intact rock; E_m = deformation modulus of rock mass; E_u = undrained modulus of clay; G_s = specific gravity; GSI = geological strength index; I_{d2} = slake durability index; I_{s50} = point load strength index for diameter 50 mm; K_0 = at-rest lateral earth pressure coefficient; K_{DMT} = dilatometer horizontal stress index; LI = liquidity index; LL = liquid limit; n = porosity; M_d = effective constrained modulus determined by oedometer; M_{dn} = normalized $M_d = (M_d/P_a)/(\sigma'_v/P_a)^{0.5}$; N_{60} = corrected SPT-N; P_a = atmospheric pressure = 101.3 kPa; PI = plasticity index; p_s = specific penetration resistance from the CPT (unique to China); Q = Q-system; q_c = cone tip resistance; q_t = corrected cone tip resistance; $q_{c1n} = (q_c/P_a)/(\sigma'_v/P_a)^{0.5}$; $q_{t1} = (q_t-\sigma_v)/\sigma'_v$ = normalized cone tip resistance; $q_{tu} = (q_t-u_2)/\sigma'_v$ = effective cone tip resistance; R_L = L-type Schmidt hammer hardness; RMR = rock mass rating; RQD = rock quality designation; S_h = Shore scleroscope hardness; SPT-N = standard penetration test blow count; S_t = sensitivity; s_u = undrained shear strength for clay; s_u^{re} = remoulded s_u; u_0 = hydrostatic pore pressure; u_2 = CPTU pore pressure; UCST = unconfined compression soil test; V_p = P-wave velocity; VST = vane shear test; w = water content.

To extract reliable statistics, only sites in the databases with more than 10 data points are used. There are also sites in the databases with more than 30 data points. The site-specific statistics for these sites are considered to be very reliable. In Table 1.1, there is a municipal database of Shanghai (SH-CLAY/11/4051).

1.2 Data Tables

The data tables for site-specific statistics of clay, sand, and rock properties are shown in the Appendix. These site-specific statistics are extracted from the databases in Table 1.1. The site-specific statistics in TR-105000 are not included in these data tables.

1.3 Summary Figures

Based on the data tables in the Appendix, summary figures for clay, sand, and rock are developed. These figures show the distributions of site-specific statistics. Site-specific statistics for more than 30 data points are marked as red, whereas those for 10-30 data points are marked as yellow. The city-specific statistics for this municipal database are shown as blue crosses '**x**'. For comparison, the results for TR-105000 are also shown in the figures as grey triangles.

1.3.1 Figures for clay properties

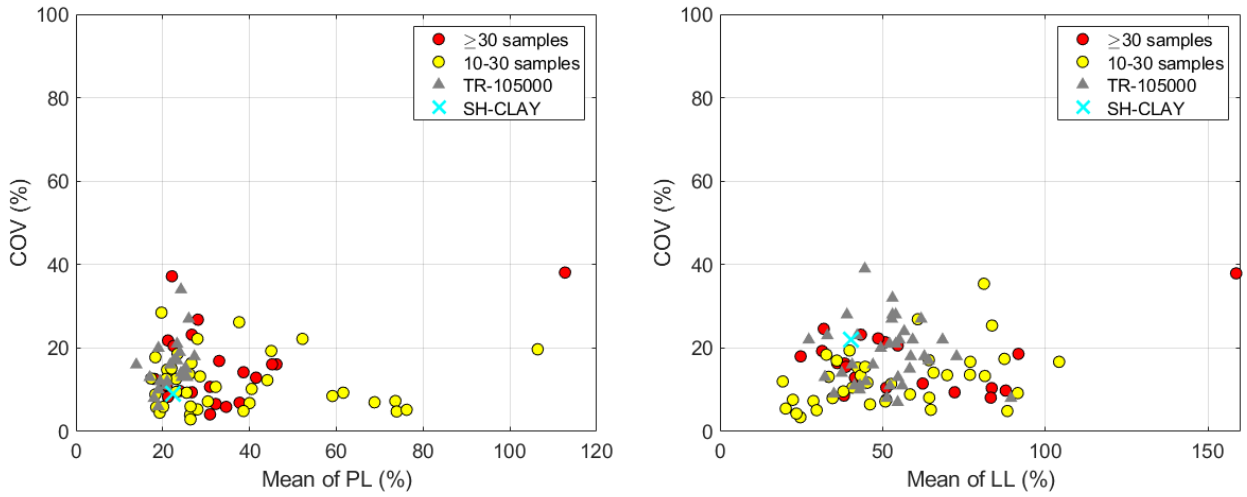

Figure 1.1. Statistics for Atterberg limits (PL and LL) of clays

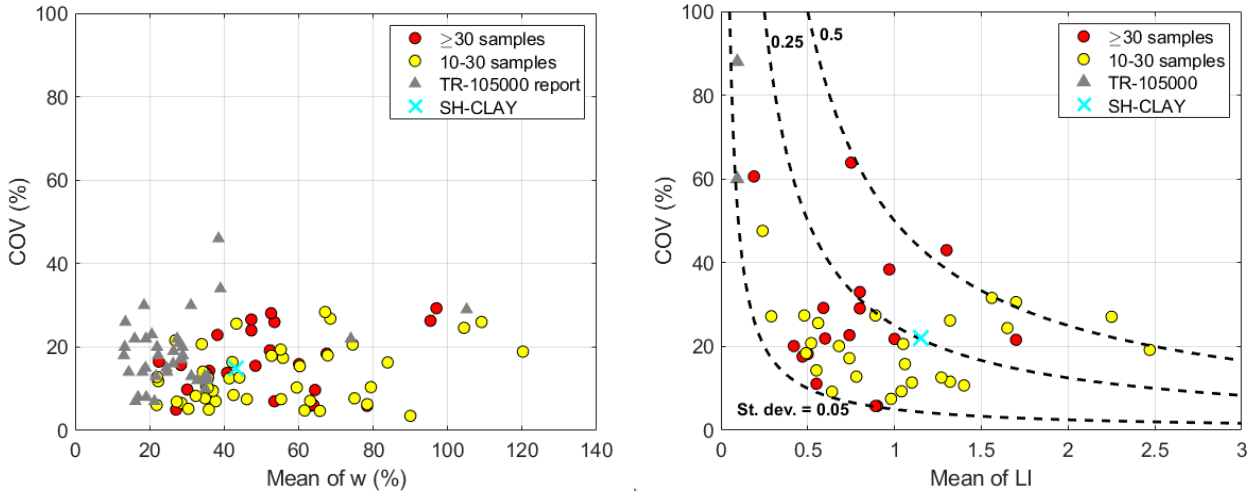

Figure 1.2. Statistics for water content (w) and liquidity index (LI) of clays

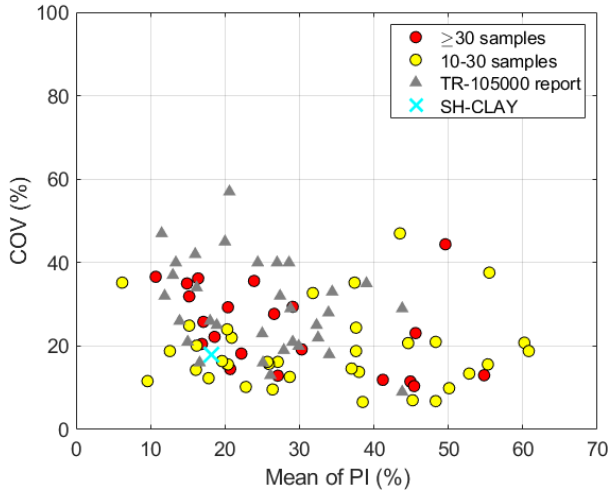

Figure 1.3. Site-specific statistics for plasticity index (PI) of clays

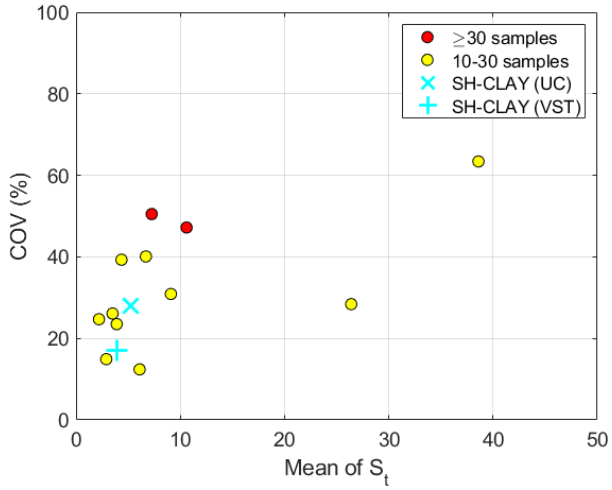

Figure 1.4. Statistics for sensitivity (S_t) of clays

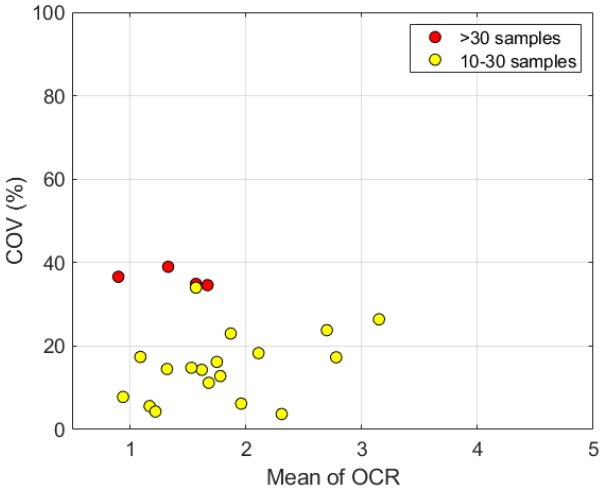

Figure 1.5. Statistics for overconsolidation ratio (OCR) of clays

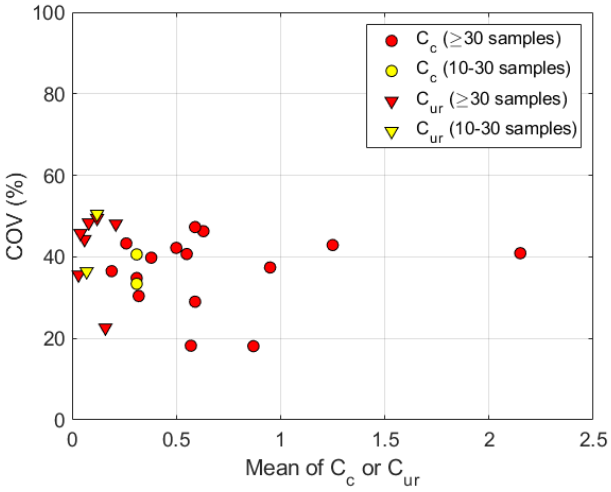

Figure 1.6. Statistics for compression (C_c) and unload-reload (C_{ur}) indices of clays

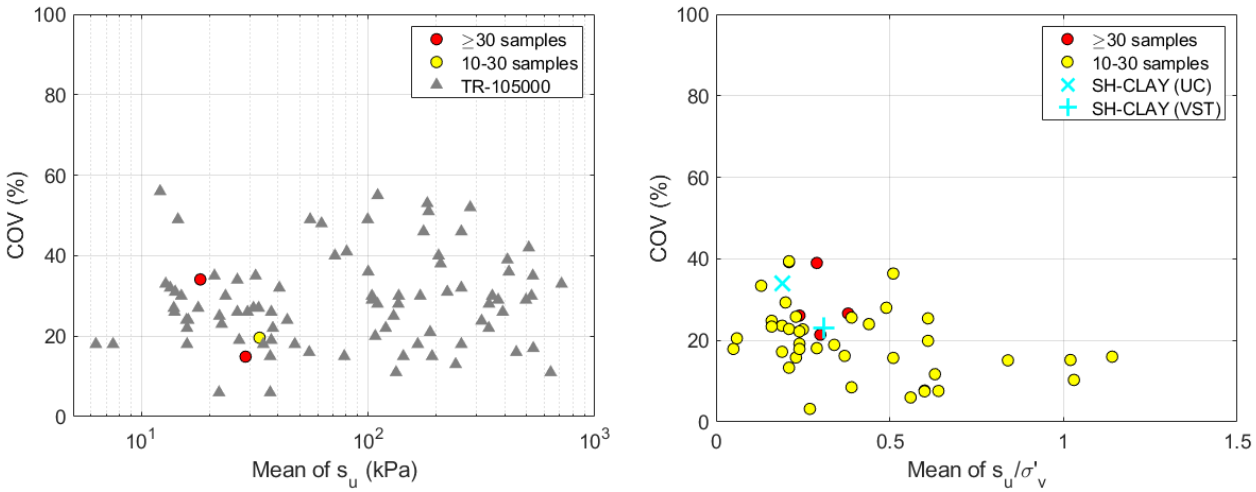

Figure 1.7. Statistics for undrained strength (s_u) and normalized strength (s_u/σ'_v) of clays

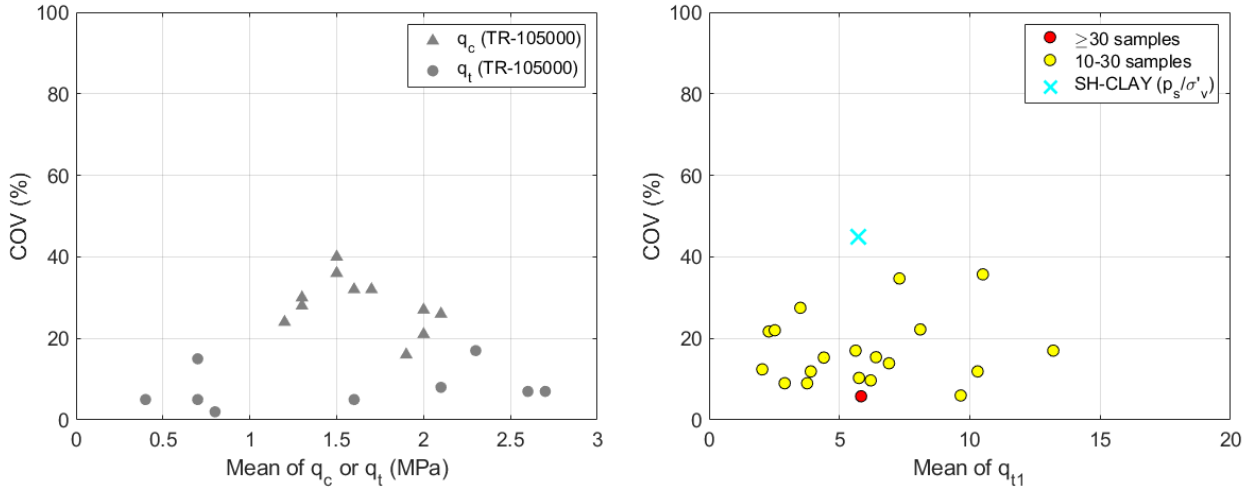

Figure 1.8. Statistics for CPT tip resistance (q_c or q_t) and normalized tip resistance (q_{t1}) of clays

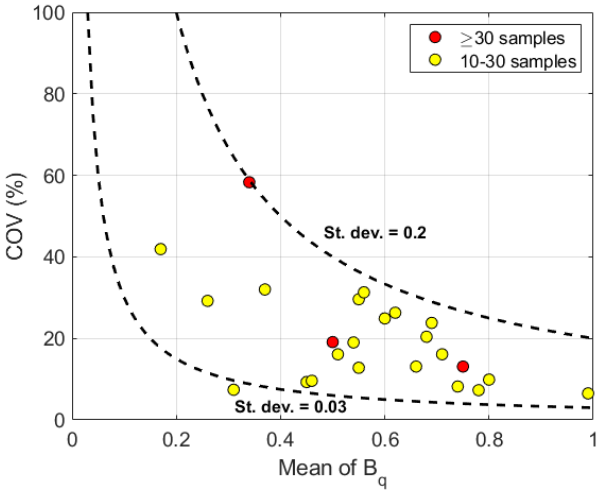

Figure 1.9. Statistics for CPT pore pressure coefficient (B_q) of clays

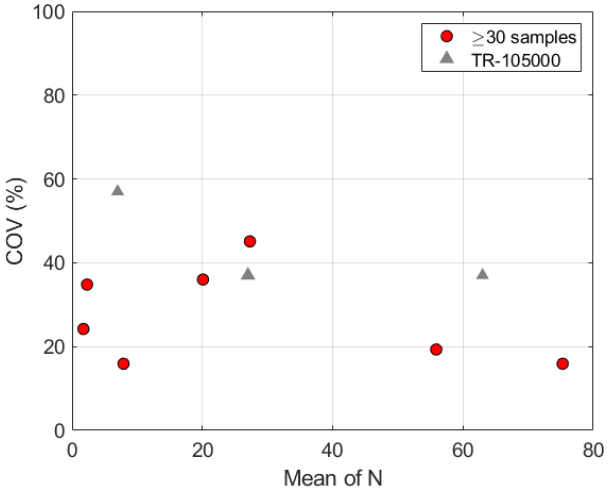

Figure 1.10. Statistics for SPT blow count (N) of clays

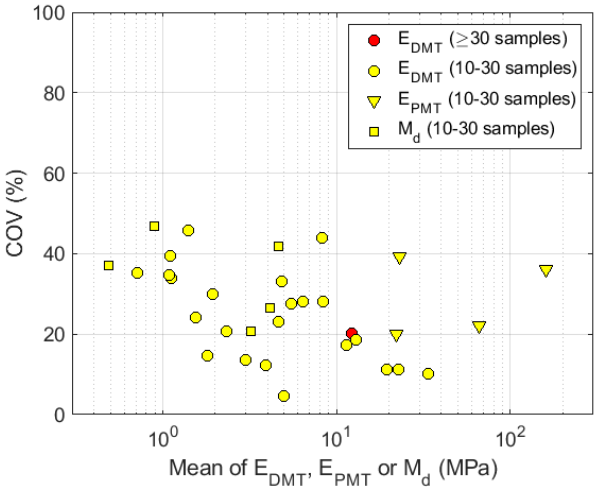

Figure 1.11. Statistics for E_{DMT}, E_{PMT}, and M_d of clays

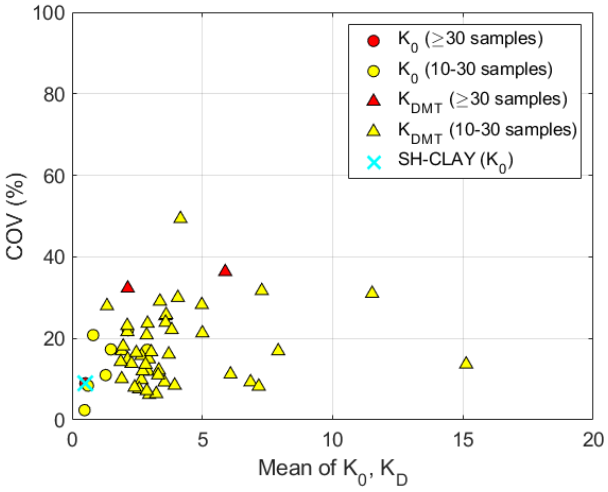

Figure 1.12. Statistics for K_0 and K_{DMT} of clays

1.3.2 Figures for sand properties

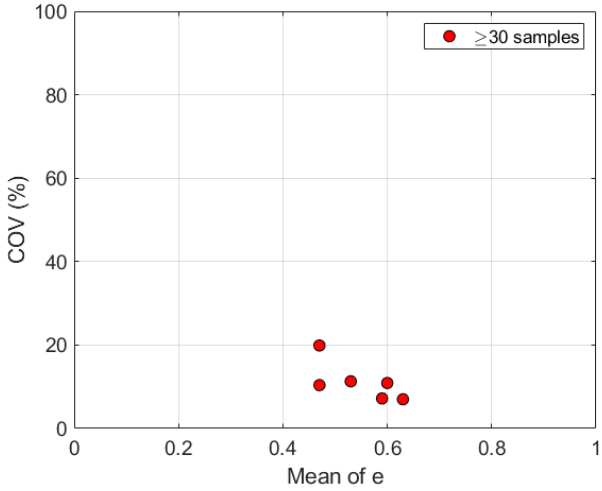

Figure 1.13. Statistics for void ratio (e) of sands

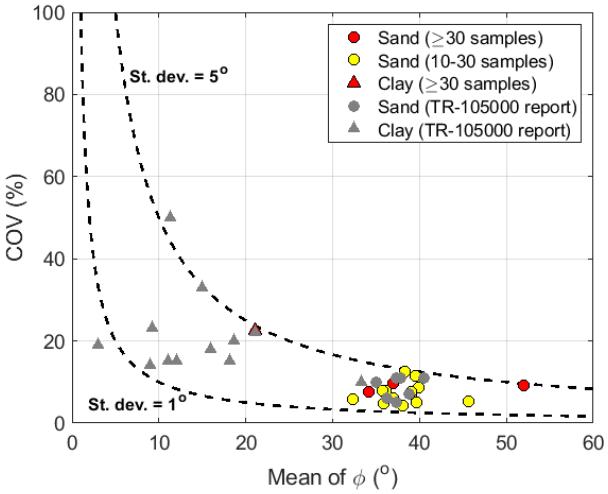

Figure 1.14. Site-specific statistics for friction angle (ϕ) of sands and clays

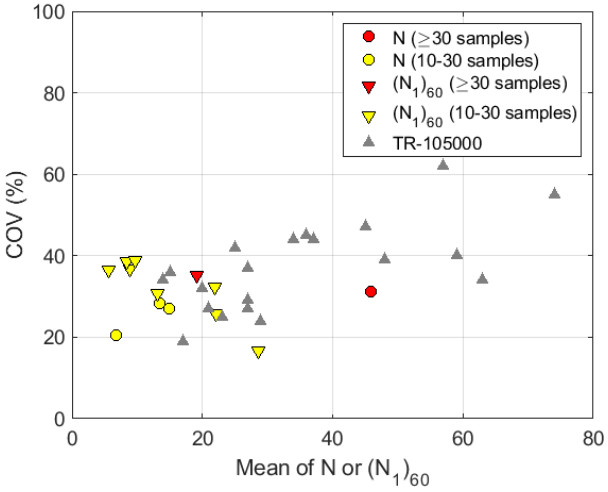

Figure 1.15. Statistics for SPT blow count (N) of sands

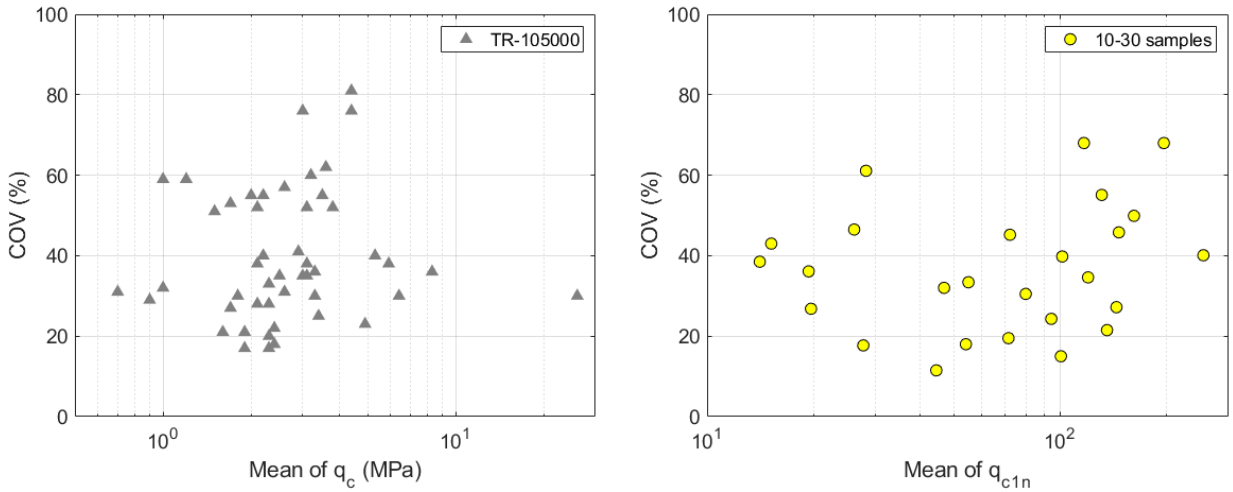

Figure 1.16. Statistics for tip resistance (q_c) and normalized tip resistance (q_{c1n}) of sands

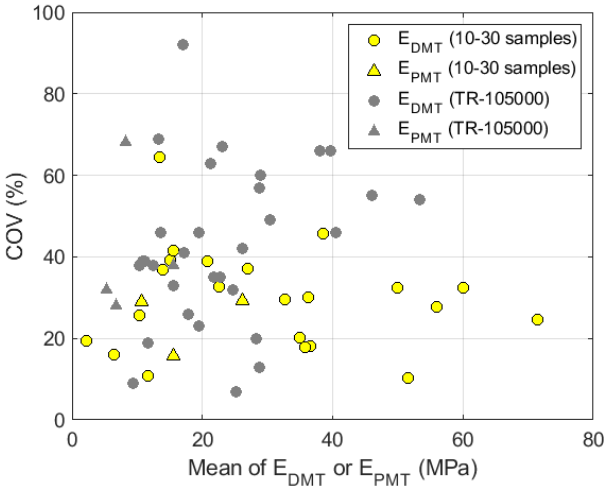

Figure 1.17. Statistics for E_{DMT} and E_{PMT} of sands

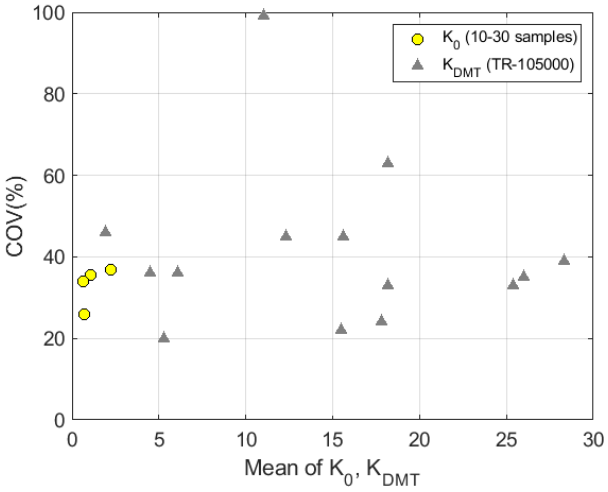

Figure 1.18. Statistics for K_0 and K_{DMT} of sands

1.3.3 Figures for intact rock properties

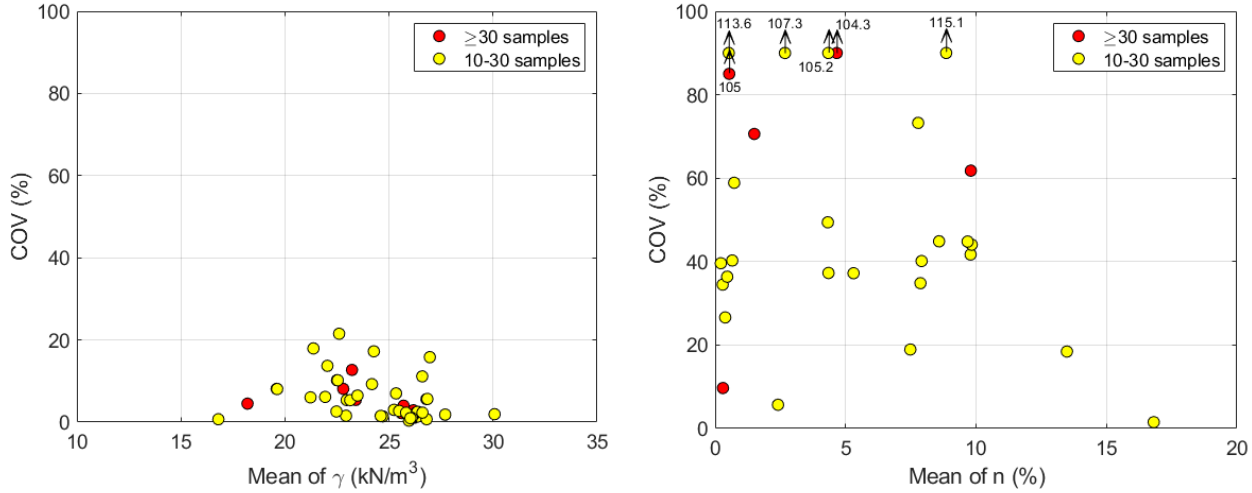

Figure 1.19. Statistics for unit weight (γ) and porosity (n) of intact rocks

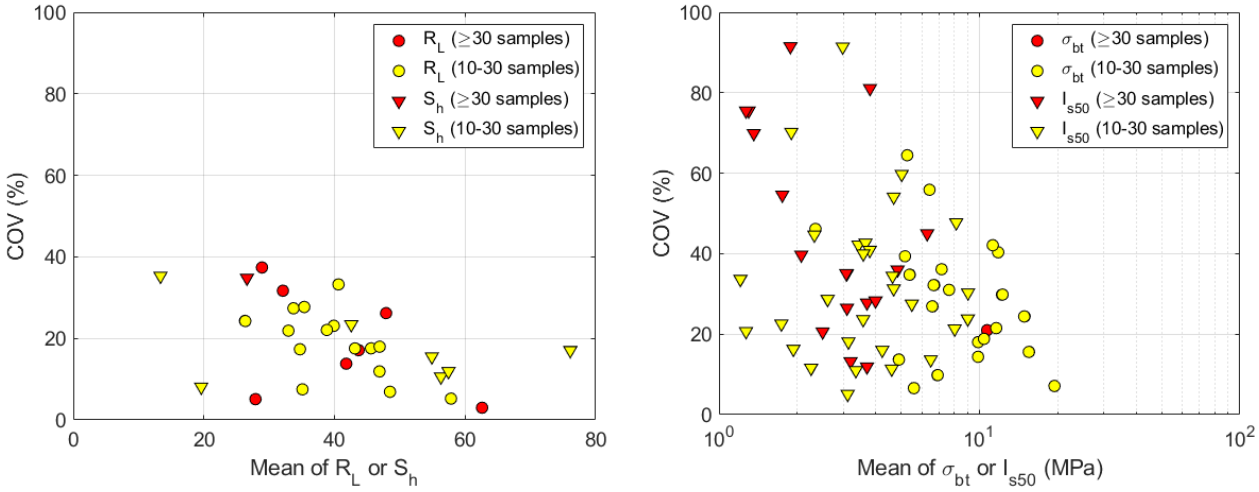

Figure 1.20. Statistics for hardnesses (R_L and S_h) and strengths (σ_{bt} and I_{s50}) of intact rocks

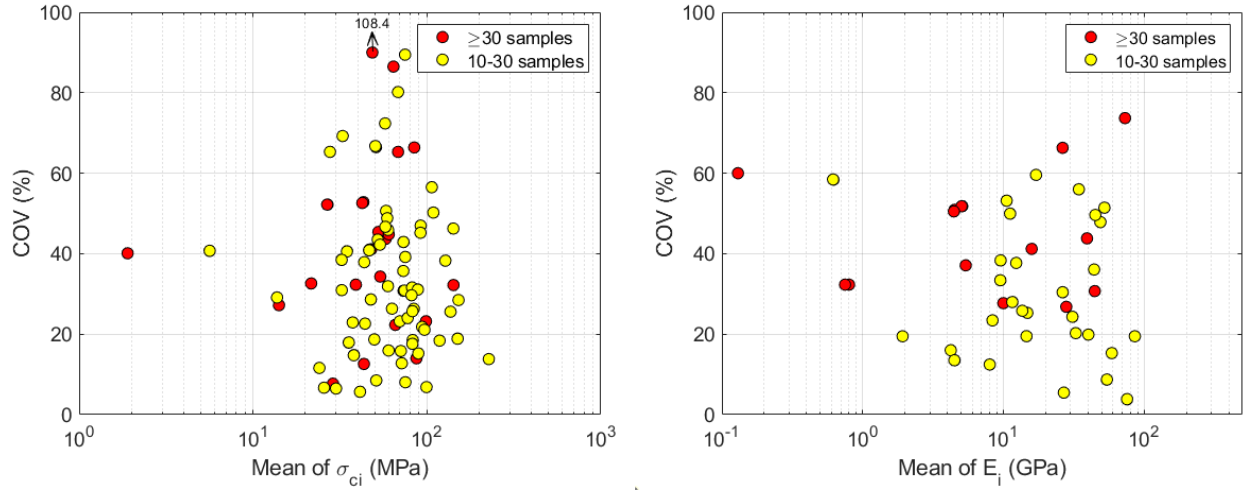

Figure 1.21. Statistics for uniaxial compressive strength (σ_{ci}) and Young's modulus (E_i) of intact rocks

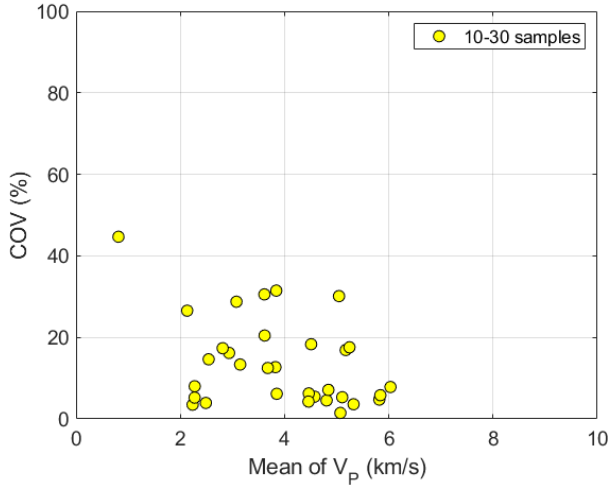

Figure 1.22. Statistics for P-wave velocity (V_p) of intact rocks

1.3.4 Figures for rock mass properties

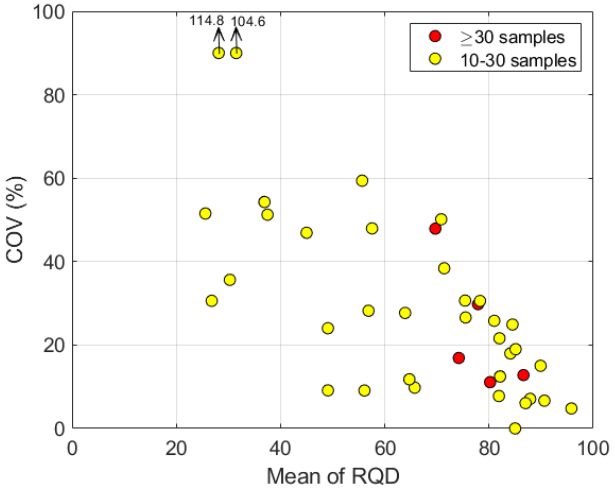

Figure 1.23. Statistics for RQD of rock masses

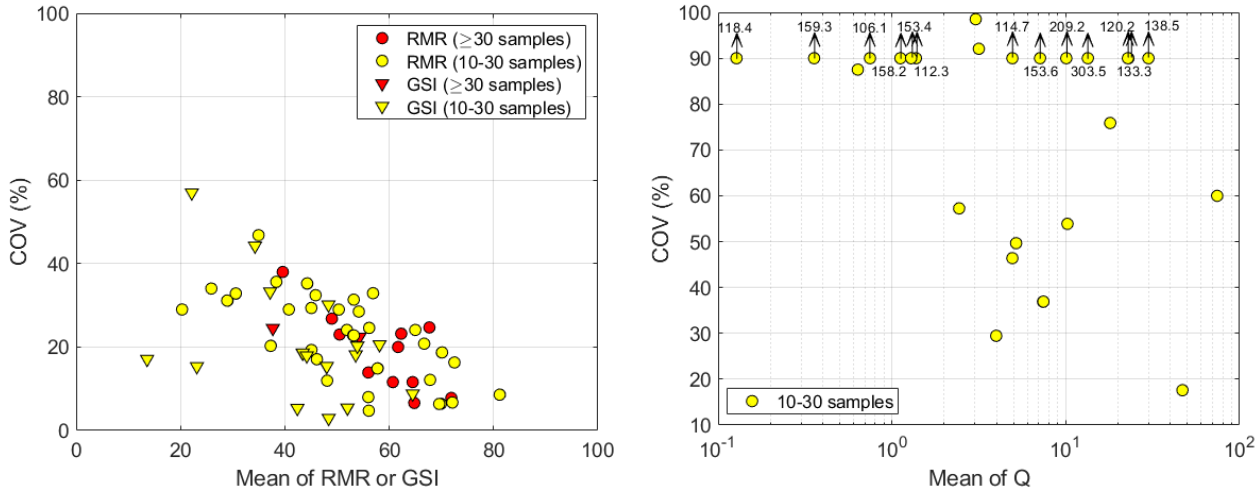

Figure 1.24. Statistics for RMR, GSI, and Q of rock masses

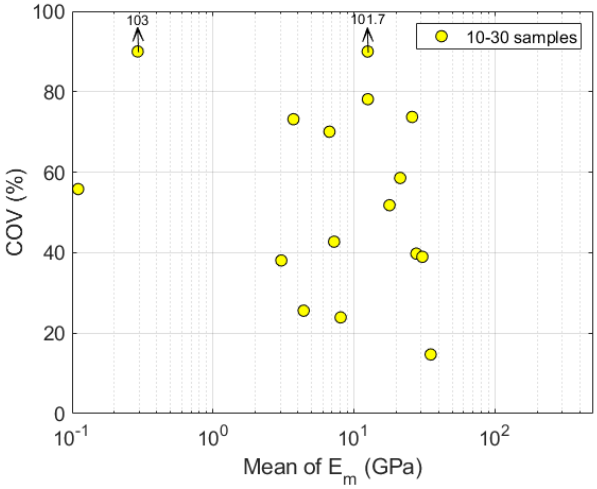

Figure 1.25. Statistics for deformation modulus (E_m) of rock masses

1.4 Summary Tables

Based on the site-specific statistics in the Appendix and those in TR-105000, summary tables (Tables 1.2, 1.3, and 1.4) for clay, sand, and rock are developed. These summary tables summarize the mean and range of the site-specific statistics. For example, the first item in Table 1.2 indicates that the site-specific COV for LL of clay ranges from 3.4-39% with mean = 15.6%. Note that these tables are developed based on the combined results of Appendix and TR-105000.

Table 1.2. Summary of site-specific statistics for clay

Property	# groups	# cases/group		Site-specific mean			Site-specific COV		
		Range	Mean	Range	Mean	95% CI	Range	Mean	95% CI
LL (%)	103	10-2229	69	19.3-158.6	55.6	24.7-95.1	3.4-39	15.6	4.8-35.1
PL (%)	87	10-299	41	13.9-112.7	29.1	17.2-76.2	2.9-38.1	13.5	3.9-35.0
PI (%)	94	10-4044	93	6.2-60.8	29.0	10.5-56.2	6.5-57	23.5	6.8-47
w (%)	111	10-439	76	13.1-120.2	43.5	13.7-104.9	3.5-46	15.3	4.9-30
LI	49	10-2067	68	0.09-2.47	0.93	0.09-2.31	5.8-88	24.5	5.8-70.5
OCR	24	10-56	17	0.90-3.15	1.69	0.90-3.11	1.2-39	17.8	1.5-38.8
C_c	18	17-136	53	0.19-2.15	0.63	0.19-2.15	18.1-47.3	35.6	18.1-47.3
C_{ur}	9	17-115	44	0.03-0.21	0.10	0.03-0.21	22.6-50.5	42.4	22.6-50.5
ϕ (°)	13	5-51	19	3-33.3	15.3	3-33.3	10-50	21.3	10-50
s_u (kPa)	91	9-393	59	6.3-712.8	148.0	7.2-558.4	6-56	28.2	9.9-53.5
s_u/σ'_v	45	10-352	27	0.05-1.14	0.39	0.06-1.07	3.2-39.4	20.8	5.0-39.3
S_t	17	10-384	51	2.2-38.6	8.8	2.2-38.6	12.4-63.4	30.8	12.4-63.4
q_c	11	47-53	50	1.2-2.1	1.65	1.2-2.1	16-40	28.4	16-40
q_t	9	-	-	0.4-2.7	1.54	0.4-2.7	2-17	7.9	2-17
q_{t1}	21	12-42	17	2.04-13.2	5.99	2.04-13.13	5.8-39.8	17.5	5.8-39.7
B_q	26	11-47	20	0.17-0.99	0.57	0.18-0.96	6.5-58.3	20.3	6.6-55.8
SPT-N	11	12-61	27	1.75-75.3	33.0	1.75-75.3	15.9-57	30.7	15.9-57
E_{DMT} (MPa)	25	10-32	17	0.71-33.7	7.2	0.76-32.36	4.6-45.8	24.0	5.3-56.6
E_{PMT} (MPa)	4	10-22	15	22.1-160.6	68.0	22.1-160.6	19.8-39.1	29.3	19.8-39.1
M_d (MPa)	5	10-13	11	0.49-4.60	2.66	0.49-4.60	20.8-46.8	34.6	20.8-46.8
K_0	8	10-264	45	0.48-2.88	1.28	0.48-2.88	2.4-22	13.5	2.4-22.0
K_{DMT}	47	10-50	18	1.34-15.12	3.91	1.70-12.69	6.2-49.4	18.2	6.3-40.6

Table 1.3. Summary of site-specific statistics for sand

Property	# groups	# cases/group		Site-specific mean			Site-specific COV		
		Range	Mean	Range	Mean	95% CI	Range	Mean	95% CI
e	6	11-17	14	0.47-0.63	0.55	0.47-0.63	7-19.9	11.1	7-19.9
ϕ (°)	23	10-136	32	32.3-52	38.4	32.4-51.5	4.2-12.5	7.9	4.3-12.4
q_c	49	10-2039	125	0.7-26	3.3	0.85-13.17	17-81	39.7	17.0-77.4
q_{c1n}	25	10-28	15	14.1-254.6	90.4	14.2-247.4	11.5-68	36.9	11.9-68
SPT-N	26	10-300	62	6.8-74	32.9	6.8-73.3	18.4-62	34.3	18.5-61.0
$(N_1)_{60}$	9	11-35	21	5.7-28.6	15.3	5.7-28.6	16.5-38.8	32.2	16.5-38.8
E_{DMT} (MPa)	53	10-25	14	2.21-71.4	26.2	5.63-62.0	7-92	37.0	8.7-73.0
E_{PMT} (MPa)	7	10-53	26	5.24-26.1	12.6	5.24-26.1	15.7-68	34.3	15.7-68
K_0	4	13-15	15	0.64-2.20	1.16	0.64-2.20	25.8-36.9	33.1	25.8-36.9
K_{DMT}	15	10-25	15	1.9-28.3	15.1	1.9-28.3	20-99	44.3	20-99

Table 1.4. Summary of site-specific statistics for rock and rock mass

Property	# groups	# cases/group		Site-specific mean			Site-specific COV		
		Range	Mean	Range	Mean	95% CI	Range	Mean	95% CI
n (%)	31	10-262	38	0.2-36.2	6.9	0.2-33.1	1.5-115.1	50.1	2.7-114.7
γ (kN/m^3)	56	10-778	44	5.4-30.1	24.6	18.0-28.1	0.4-21.5	5.2	0.6-18.5
V_P (km/s)	32	10-27	15	0.81-6.03	3.90	1.20-5.97	1.47-44.7	14.1	2.1-40.7
R_L	23	10-355	53	26.3-62.6	39.9	26.3-62.2	3.0-37.4	19.1	3.2-37.1
S_h	9	11-31	22	13.4-76.1	47.0	13.4-76.1	8.1-35.3	19.1	8.1-35.3
I_{s50} (MPa)	58	10-1305	63	0.17-9.04	3.69	1.21-9.02	5.1-91.5	34.4	5.1-91.4
σ_{bt} (MPa)	31	10-43	18	2.35-19.4	9.23	3.2-19.4	6.6-64.5	25.8	6.6-61.7
σ_{ci} (MPa)	116	10-470	29	1.9-226.9	66.6	8.7-151.2	5.7-108.4	33.8	6.6-84.1
E_i (GPa)	53	10-99	26	0.13-85.9	24.37	0.53-77.49	3.8-73.7	33.4	3.8-67.6
RQD	43	10-80	21	25.6-95.8	65.6	26.3-92.8	4.8-114.8	29.9	5.5-108.9
RMR	55	10-330	31	20.3-81.2	53.7	25.2-81.2	4.7-46.8	21.3	6.2-39.1
GSI	22	10-111	23	13.6-64.5	44.4	14.0-64.2	3.0-57.0	19.9	3.1-56.4
Q	26	10-28	18	0.13-74.28	11.7	0.16-70.17	17.6-303.5	104.7	19.4-289.4
E_m (GPa)	16	10-28	19	0.11-35.1	13.6	0.11-35.1	14.7-103.0	55.6	14.7-103.0

1.5 References

Abdou, M., & Mahmoud, A. N. (2013). Correlation of Sandstone Rock Properties Obtained From Field and Laboratory Tests. International Journal of Civil and Structural Engineering, 4(1), 1-11.

Adebayo, B., & Umeh, E. C. (2007). Influence of Some Rock Properties on Blasting Performance-A Case Study. Journal of Engineering and Applied Science, 2(1), 41-44.

Agarwal, K. B. (1967). The Influence of Size and Orientation of Sample on the Undrained Strength of London Clay. (Ph.D.). University of London, London, UK.

Aggistalis, G., Alivizatos, A., Stamoulis, D., & Stournaras, G. (1980). Correlating uniaxial compressive strength with schmidt hardness, point load index, young's modulus, and mineralogy of gabbros and basalts (Northern Greece). Bulletin of the International Association of Engineering Geology, 22(1), 3-11.

Aladejare, A.E. and Wang, Y. (2017). Evaluation of rock property variability. Georisk: Assessment and Management of Risk for Engineered Systems and Geohazards, 11(1), 22-41.

Aladejare, A. E. (2020). Characterization of the petrographic and physicomechanical properties of rocks from Otanmäki, Finland. Geotechnical and Geological Engineering (In Preses).

Aggistalis, G., Alivizatos, A., Stamoulis, D., & Stournaras, G. (1996). Correlating uniaxial compressive strength with Schmidt hardness, point load index, Young's modulus, and mineralogy of gabbros and basalts (Northern Greece). Bulletin of Engineering Geology and the Environment, 22, 3–11.

Ajalloeian, R., & Mohammadi, M. (2013). Estimation of limestone rock mass deformation modulus using empirical equations. Bulletin of Engineering Geology and the Environment, 73(2), 541-550.

Akbar, A., Arshad, M., & Clarke, B. G. (2008, April 1-4). Site Characterization Using CPT, DMT, SPT and Laboratory Tests Results. Paper presented at the 3rd International Conference on Site Characterization (ISC'3), Taipei, Taiwan.

Alexander, L. G. (1960). Field and Laboratory Tests in Rock Mechanics. Paper presented at the 3rd Australian-New Zealand Conference on Soil Mechanics and Foundation Engineering, Sydney, Australia.

Al-Quadhi, A.-A. A., & Janardhana, M. R. (2016). Geotechnical Characterization of the Volcaniclastic Rocks in and around Taiz City, Yemen. Global Journal of Advanced Engineering Technologies and Sciences, 3(4), 14-31.

Amundsen, T., Lunne, T., Christophersen, H. P., Bayne, J. M., & Barnwell, C. L. (1985). Advanced Deep-water Soil Investigation at the Troll East Field. Paper presented at the Offshore Site Investigation, London, UK.

Anderson, J. B., Ogunro, V. O., Detwiler, J. M., & Starnes, J. R. (2006). DMT Testing for the Estimation of Lateral Earth Pressure in Piedmont Residual Soils. Paper presented at the 2nd International Conference on the Flat Dilatometer, Washington D.C.

Anderson, T. C. (1982). Discussion: Cam-Clay Prediction of Undrained Strength. Journal of the Geotechnical Engineering Division, 108(1), 93-120.

Arman, H., Ramazanoglu, S., & Akinci, A. (2007). Mechanical and physical properties of the Kandira stone, Kandira, Turkey. Bulletin of Engineering Geology and the Environment, 66(3), 331-333.

Arroyo, M., Di Mariano, A., Monaco, P., Devincenzi, M., & Perez, N. (2008, April 1-4). SDMT-based Deep Excavation Design. Paper presented at the 3rd International Conference on Site Characterization (ISC'3), Taipei, Taiwan.

Arslan, M., Khan, S. M., & Yaqub, M. (2015). Prediction of durability and strength from Schmidt rebound hammer number for limestone rocks from Salt Range, Pakistan. Journal of Himalayan Earth Sciences, 48(1), 9-13.

Aydin, A., & Basu, A. (2005). The Schmidt hammer in rock material characterization. Engineering Geology, 81(1), 1-14.

Azimian, A., & Ajalloeian, R. (2014). Empirical correlation of physical and mechanical properties of marly rocks with P wave velocity. Arabian Journal of Geosciences, 8(4), 2069-2079.

Azzouz, A. S., & Lutz, D. G. (1986). Shaft Behavior of a Model Pile in Plastic Empire Clays. Journal of Geotechnical Engineering, 112(4), 389-406.

Azzouz, A. S., Baligh, M. M., & Ladd, C. C. (1982). Cone Penetration and Engineering Properties of The Soft Orinoco Clay. Paper presented at the 3rd International Conference on the Behaviour of Off-shore Structures, Cambridge, Massachusetts, United States.

Baecher, G. B. & Christian, J. T. (2003). Reliability and statistics in geotechnical engineering. John Wiley & Sons, Hoboken, New Jersey.

Bagde, M. N., Raina, A. K., Chakraborty, A. K., & Jethwa, J. L. (2002). Rock mass characterization by fractal dimension. Engineering Geology, 63(1-2), 141-155.

Balci, C., Copur, H., & Tuncdemir, H. (2004). Estimation of optimum specific energy based on rock properties for assessment of roadheader performance. South African Institute of Mining and Metallurgy, 104(11), 633-642.

Baligh, M. M., Ladd, C. C., & Vivatrat, V. (1980). Cone Penetration in Soil Profiling. Journal of the Geotechnical Engineering Division, 106(4), 447-461.

Baroni, M., & Almeida, M. de S. S. (2017). Compressibility and Stress History of Very Soft Organic Clays. Proceedings of the Institution of Civil Engineers - Geotechnical Engineering, 170(2), 148–160.

Bartlett, S. F., & Lee, H. S. (2004). Estimation of Compression Properties of Clayey Soils, Salt Lake Valley,

Utah (UT-04.28).

Bastola, S., & Chugh, Y. P. (2015). Shear Strength and Stiffness of Bedding Planes and Discontinuities in the Immediate Roof Rocks Overlying the NO 6 Coal Seam in Illinois. Paper presented at the International Symposium on Rock and Mechanics, Montreal, Canada.

Basu, A., & Kamran, M. (2010). Point load test on schistose rocks and its applicability in predicting uniaxial compressive strength. International Journal of Rock Mechanics and Mining Sciences, 47(5), 823-828.

Basu, A., Celestino, T. B., & Bortolucci, A. A. (2008). Evaluation of rock mechanical behaviors under uniaxial compression with reference to assessed weathering grades. Rock Mechanics and Rock Engineering, 42(1), 73-93.

Battaglio, M., Bruzzi, D., Jamiolkowski, M., & Lancellotta, R. (1986). Interpretation of CPT's and CPTU's. Paper presented at the 4th International Geotechnical Seminar, Singapore.

Bearman, R. A. (1999). The use of the point load test for the rapid estimation of Mode I fracture toughness. International Journal of Rock Mechanics and Mining Sciences, 36(2), 257-263.

Been, K., Lingnau, B. E., Crooks, J. H. A., & Leach, B. (1987). Cone penetration test calibration for Erksak (Beaufort Sea) sand. Canadian Geotechnical Journal, 24(4), 601-610.

Begonha, A., & Sequeira Braga, M. A. (2002). Weathering of the Oporto granite: geotechnical and physical properties. Catena, 49(1-2), 57-76.

Bell, F. G. (1978). The physical and mechanical properties of the fell sandstones, Northumberland, England. Engineering Geology, 12, 1-29.

Bell, F. G., & Lindsay, P. (1999). The petrographic and geomechanical properties of some sandstones from the Newspaper Member of the Natal Group near Durban, South Africa. Engineering Geology, 53(1), 57-81.

Bell, F. G., Entwisle, D. C., & Culshaw, M. G. (1997). A geotechnical survey of some British Coal Measures mudstones, with particular emphasis on durability. Engineering Geology, 46(2), 115-129.

Bieniawski, Z. T. (1978). Determining rock mass deformability: experience from case histories. International Journal of Rock Mechanics and Mining Sciences & Geomechanics Abstracts, 15(5), 237-247.

Bihs, A., Marchetti, D., & Long, M. (2010). Interpretation of CPTU and SDMT in Organic, Irish Soils.

Bihs, A., Nordal, S., Boylan, N., & Long, M. (2013, September 17-21). Interpretation of Consolidation Parameters from CPTU Results in Sensitive Clays. Paper presented at the 4th International Conference on Site Characterization ISC-4, Porto de Galinhas-Pernamuco, Brazil.

Birid, K. (2014). Comparative Study of Rock Mass Deformation Modulus Using Different Approaches. Paper presented at the 8th Asian Rock Mechanics Symposium, 14-16, Octobor 2014, Sapporo, Japan.

Bjerrum, L. (1954). Geotechnical Properties of Norwegian Marine Clays. Géotechnique, 4(2), 49-69.

Bjerrum, L. (1967). Engineering Geology of Norwegian Normally-Consolidated Marine Clays as Related to Settlements of Buildings. Géotechnique, 17(2), 83-118.

Bjerrum, L., & Lo, K. Y. (1963). Effect of Again of the Shear-Strength Properties of a Normally Consolidated Clay. Géotechnique, 13(2), 147-157.

Borsetto, M., Giuseppetti, G., Martinetti, S., Ribacchi, R., & Silvestri, T. (1983). Design and construction of the Timpagrande Powerhouse. Rock Mechanics and Rock Engineering, 16, 85-115.

Bosco, G., & Monaco, P. (2016, September 5-9). Strain Moduli of Alluvial Soils from CPT, DMT, Vs, and

Lab Tests. Paper presented at the 5th International Conference on Geotechnical and Geophysical Site Characterization ISC-5, Gold Coast, Queensland, Australia.

Bozbey, I., & Togrol, E. (2010). Correlation of standard penetration test and pressuremeter data: a case study from Istanbul, Turkey. Bulletin of Engineering Geology and the Environment, 69(4), 505-515.

Brahana, D. C., & Wang, J. (1998). Performance of In Situ Testing Methods in Predicting Deep Foundation Capacity. Paper presented at the 1st International Conference on Site Characterization (ISC'98), Atlanta, Georgia, USA.

Briaud, J. L. (1997). The National Geptechnical Experiment Sites at Texas A&M University: Clay and Sand, A Summary (NGES-TAMU-007).

Briaud, J. L., Nicks, J., Rhee, K., & Stieben, G. (2007). San Jacinto Monument Case History. Journal of Geotechnical and Geoenvironmental Engineering, 133(11), 1337-1351.

Cabrera, M., Combarros, M., & Macedo, A. (2013). Reliability of Pressuremeter Tests. Paper presented at the 4th International Conference on Site Characterization ISC-4, Porto de Galinhas-Pernamuco, Brazil.

Cadling, L., & Odenstad, S. (1950). The Vane Borer. Paper presented at the Royal Swedish Institution, Stockholm.

Cameron-Clarke, I. S., & Budavari, S. (1981). Correlation of rock mass classification parameters obtained from borecore and In-situ observations. Engineering Geology, 17(1-2), 19-53.

Cao, L. F., Chang, M. F., Teh, C. I., & Na, Y. M. (2001). Back-calculation of consolidation parameters from field measurements at a reclamation site. Canadian Geotechnical Journal, 38(4), 755-769.

Cao, L. F., Chang, M. F., Teh, C. I., Choa, V., & Na, Y. M. (2008). Characterization of reclaimed sand fill by seismic cone test. 3rd International Conference on Site Characterization (ISC'3), Taipei, Taiwan.

Cao, L. F., Peaker, S. M., & Ahmad, S. (2016, September 5-9). Use of Flat Dilatometer in Ontario. Paper presented at the 5th International Conference on Geotechnical and Geophysical Site Characterization ISC-5, Gold Coast, Queensland, Australia.

Cao, Z., Wang, Y., and Li, D. (2016). Site-specific characterization of soil properties using multiple measurements from different test procedures at different locations – A Bayesian sequential updating approach. Engineering Geology, 211, 150-161.

Carrassco, A. L., Soto, A. R., & Torres, M. (2006). Geotechnical Correlations in Madrid Soil from SPT and Pressuremeter Tests. Paper presented at the 2nd International Conference on the Flat Dilatometer, Washington D.C.

Cavallaro, A., Grasso, S., & Ferraro, A. (2016, September 5-9). Study on Seismic Response Analysis in "Vincenzo Bellini" Garden area by Seismic Dilatometer Marchetti Tests. Paper presented at the 5th International Conference on Geotechnical and Geophysical Site Characterization ISC-5, Gold Coast, Queensland, Australia.

Cavallaro, A., Grasso, S., & Maugeri, M. (2006). Clay Soil Characterization by The New Seismic Dilatometer Marchetti Test (SDMT). Paper presented at the 2nd International Conference on the Flat Dilatometer, Washington D.C.

Ceryan, N., Okkan, U., & Kesimal, A. (2012). Prediction of unconfined compressive strength of carbonate rocks using artificial neural networks. Environmental Earth Sciences, 68(3), 807-819.

Ceryan, S., Zorlu, K., Gokceoglu, C., & Temel, A. (2008). The use of cation packing index for characterizing

the weathering degree of granitic rocks. Engineering Geology, 98(1-2), 60-74.

Chang, M. F. (1991). Interpretation of overconsolidation ratio from in situ tests in Recent clay deposits in Singapore and Malaysia. Canadian Geotechnical Journal, 28(2), 210-225.

Chapman, G. A., & Donald, I. B. (1981, June 15-19). Interprtation of Static Penetration Test in Sand. Paper presented at the 10th International Conference on Soil Mechanics and Foundation Engineering, Stockholm.

Chatziangelou, M., Christaras, B., Dimopoulos, G., Soulios, G., & Kilias, A. (2002). Support of unstable wedges along the Platamon railway tunnel under construction, in northern Greece. Engineering Geology, 65(4), 233-243.

Chen, C. S., & Hsu, S. C. (2001). Measurement of Indirect Tensile Strength of Anisotropic Rocks by the Ring Test. Rock Mechanics and Rock Engineering, 34(4), 293-321.

Chen, B. S., & Mayne, P. W. (1994). Profiling the Overconsolidation Ratio of Clays by Piezocone Tests (GIT-CEEGEO-91-1).

Cheshomi, A., & Ghodrati, M. (2014). Estimating Menard pressuremeter modulus and limit pressure from SPT in silty sand and silty clay soils. A case study in Mashhad, Iran. Geomechanics and Geoengineering, 10(3), 194-202.

Chin, C. T., Cheng, T. Y, and Liu, C. J. (1989). Relationship between undrained shear strength and overconsolidation retio of Taipei silt. Journal of the Chinese Institue of Civil and Hydraulic Engineering, 1(3), 245-250.

Chin, C. T., Duann, S. W., & Kao, T. C. (1988). SPT-CPT Correlations for Granular Soils. Paper presented at the 1st International Symposium on Penetration Testing, Orlando, USA.

Chin, C., Crooks, J., & Moh, Z. (1994). Geotechnical properties of the cohesive Sungshan deposits, Taipei. Geotechnical Engineering, 25(2).

Ching, J. and Phoon, K.K. (2014). Transformations and correlations among some parameters of clays – the global database. Canadian Geotechnical Journal, 51(6), 663-685.

Ching, J., Lin, G.H., Chen, J.R., and Phoon, K.K. (2017). Transformation models for effective friction angle and relative density calibrated based on a multivariate database of coarse-grained soils. Canadian Geotechnical Journal, 54(4), 481-501.

Ching, J., Li, K.H., Phoon, K.K., and Weng, M.C. (2018). Generic transformation models for some intact rock properties. Canadian Geotechnical Journal, 55(12), 1702-1741.

Ching, J. (2020). Unpublished databases.

Chitty, D. E., Blouin, S. E., Sun, X., & Kim, K. J. (1994). Laboratory Investigation and Analysis of the Strength and Deformation of Joints and Fluid Flow in Salem Limestone (DNA-TR-93-63).

Chun, B.-S., Lee, Y.-J., Seo, D.-D., & Lim, B.-S. (2006). Correlation deformation modulus by PMT with RMR and rock mass condition. Tunnelling and Underground Space Technology, 21(3-4), 231-232.

Chun, B.-S., Ryu, W. R., Sagong, M., & Do, J.-N. (2009). Indirect estimation of the rock deformation modulus based on polynomial and multiple regression analyses of the RMR system. International Journal of Rock Mechanics and Mining Sciences, 46(3), 649-658.

Chung, S. G., Ryu, C. K., Jo, K. Y., & Huh, D. Y. (2005). Geological and Geotechnical Characteristics of Marine Clays at the Busan New Port. Marine Georesources & Geotechnology, 23(3), 235-251.

Clough, G. W., & Denby, G. M. (1980). Self-Boring Pressuremeter Study of San Francisco Bay Mud. Journal of the Geotechnical Engineering Division, 106(1), 45-63.

Cooling, L. F., & Skempton, A. W. (1942). A Laboratory Study of London Clay. Journal of the Institution of Civil Engineers, 17(3), 251-276.

Coon, R. F. (1968). Correlation of Engineering Behavior with the Classification of in-situ Rock. (Ph.D). University of Illinois, Urbana, Illinois.

Coutinho, R. Q., Bello, M. I. M., & Pereira, A. C. (2006). Geotechnical Investigation of the Recife Soft Clays by Dilatometer Tests. Paper presented at the 2nd International Conference on the Flat Dilatometer, Washington D.C.

Coutinho, R. Q., Bello, M. I. M., & Soares, F. L. (2008). Geotechnical Investigation of the Recife Soft Clays by Piezocone Tests. Paper presented at the 3rd International Conference on Site Characterization, Taipei, Taiwan.

Cozzolino, E. V. M. (1961). Statistical Forecasting of Compression Index. Proceeding of the 5th International Conference on Soil Mechanics and Foundation Engineering, Paris, 1, 51-53.

Cruz, I. R. (2009). An Evaluation of Seimic Flat Dilatometer and Lateral Stress Seismic Piezocone. (MASc). University of British Columbia (Vancouver), Vancouver.

陳厚銘, & 謝百鍾. (1996). 以現地試驗調查基隆河新生地粘土之工程性質. [Geotechnical Properties of the Clay Deposits from In-Situ Test on Keelung River Reclaimed Land]. 地工技術(54), 55-66.

da Fonesca, A. V., & Coutinho, R. Q. (2008, April 1-4). Characterization of Residual Soils. Paper presented at the 3rd International Conference on Site Characterization (ISC'3), Taipei, Taiwan.

Danielsen, B. E., & Dahlin, T. (2009). Comparison of geoelectrical imaging and tunnel documentation at the Hallandsås Tunnel, Sweden. Engineering Geology, 107(3-4), 118-129.

DeGroot, D. J., & Lutenegger, A. J. (2002). Geology and Engineering Properties of Connecticut Valley Varved Clay. Paper presented at the International Workshop on Characterisation and Engineering Properties of Natural Soils, Singapore.

Dehghan, S., Sattari, G., Chehreh Chelgani, S., & Aliabadi, M. A. (2010). Prediction of uniaxial compressive strength and modulus of elasticity for Travertine samples using regression and artificial neural networks. Mining Science and Technology (China), 20(1), 41-46.

del Potro, R., & Hürlimann, M. (2008). Geotechnical classification and characterisation of materials for stability analyses of large volcanic slopes. Engineering Geology, 98(1-2), 1-17.

Di Mariano, A., Amoroso, S., Arroyo, M., Monaco, P., & Gens, A. (2019). SDMT-Based Numerical Analyses of Deep Excavation in Soft Soil. Journal of Geotechnical and Geoenvironmental Engineering, 145(1).

Diamantis, K., Bellas, S., Migiros, G., & Gartzos, E. (2011). Correlating Wave Velocities with Physical, Mechanical Properties and Petrographic Characteristics of Peridotites from the Central Greece. Geotechnical and Geological Engineering, 29(6), 1049-1062.

Diamantis, K., Gartzos, E., & Migiros, G. (2009). Study on uniaxial compressive strength, point load strength index, dynamic and physical properties of serpentinites from Central Greece: Test results and empirical relations. Engineering Geology, 108(3-4), 199-207.

Dinçer, İ., Acar, A., & Ural, S. (2008). Estimation of strength and deformation properties of Quaternary

caliche deposits. Bulletin of Engineering Geology and the Environment, 67(3), 353-366.

Dinçer, I., Acar, A., Çobanoğlu, I., & Uras, Y. (2004). Correlation between Schmidt hardness, uniaxial compressive strength and Young's modulus for andesites, basalts and tuffs. Bulletin of Engineering Geology and the Environment, 63(2), 141-148.

Eden, W. J., & Crawford, C. B. (1957). Geotechnical Properties of Leda Clay in the Ottawa Area. Paper presented at the 4th International Conference on Soil Mechanics and Foundation Engineering, London.

Eden, W. J., & Hamilton, J. J. (1957). The Use of A Field Vane Apparatus in Sensitive Clay. In Symposium on Vane Shear Testing of Soils (pp. 41-53): A.S.T.M.

El-Naqa, A. (1996). Assessment of geomechanical characterization of a rock mass using a seismic geophysical technique. Geotechnical and Geological Engineering, 14(4), 291-305.

El-Naqa, A., & Al Kuisi, M. (2002). Engineering geological characterisation of the rock masses at Tannur Dam site, South Jordan. Environmental Geology, 42(7), 817-826.

Endait, M., & Juneja, A. (2014). New correlations between uniaxial compressive strength and point load strength of basalt. International Journal of Geotechnical Engineering, 9(4), 348-353.

Exadaktylos, G., Stavropoulou, M., Xiroudakis, G., de Broissia, M., & Schwarz, H. (2008). A spatial estimation model for continuous rock mass characterization from the specific energy of a TBM. Rock Mechanics and Rock Engineering, 41(6), 797-834.

Fenton, G. A., & Griffiths, D. V. (2008). Risk assessment in geotechnical engineering. John Wiley & Sons, New York, USA.

Finno, R. J. (1989). Subsurface Conditions and Pile Installation Data. 1989 Foundation Engineering Congress Test Section. Geotechnical Special Publication(23), 1-74.

Finno, R. J., & Chung, C. K. (1992). Stress-Strain-Strength Responses of Compressible Chicago Glacial Clays. Journal of Geotechnical Engineering, 118(10), 1607-1625.

Foa, S. B., Passos, P. G. O., Assis, A. P., & Farias, M. M. (2004). Site Characterisation for Tunnel-Building Interaction Problem in Brazil. Paper presented at the 2nd International Conference on Site Characterization, Porto, Portugal.

Frough, O., & Torabi, S. R. (2013). An application of rock engineering systems for estimating TBM downtimes. Engineering Geology, 157, 112-123.

Frough, O., Torabi, S. R., & Yagiz, S. (2014). Application of RMR for Estimating Rock-Mass–Related TBM Utilization and Performance Parameters: A Case Study. Rock Mechanics and Rock Engineering, 48(3), 1305-1312.

Geotechnical Engineering Office (GEO), 1989. Cut slopes 11 NW-A/C55 and C56 Ching Cheung Road, Unpublished. Civil Engineering and Development Department of the Government of the Hong Kong Special Administrative Region.

Ghionna, V. N., & Jamiolkowski, M. (1991). A Critical Appraisal of Calibration Chamber Testing of Sands. Paper presented at the 1st International Symposium on Calibration Chamber Testing, Potsdam, New York.

Ghosh, D. K., & Srivastava, M. (1991). Point-load strength: An index for classification of rock material. Bulletin of the International Association of Engineering Geology, 44(1), 27-33.

Giacheti, H. L., Peixoto, A. S. P., Mio, G. D., & Carcalho, D. d. (2006). Flat Dilatometer Testing in Brazilian

Tropical Soils. Paper presented at the 2nd International Conference on the Flat Dilatometer, Washington D.C.

Giao, P. H., & Hien, D. H. (2007). Geotechnical characterization of soft clay along a highway in the Red River. Lowland Technology International, 9(1), 18-27.

Gorski, B., Conlon, B., & Ljunggren, B. (2007). Forsmark Site Investigation: Determination of the Direct and Indirect Tensile Strength on Cores from Borehole KFM01D (P-07-76).

Greeuw, G., Smits, F. P., & Van Driel, P. (1988). Cone Penetration Test in Dry Oostershelde Sand and The Relation with A Cavity Expansion Model. Paper presented at the 1st International Symposium on Penetration Testing, ISOPT-1, Orlando.

Gregersen, O., & Løken, T. (1979). The quick-clay slide at Baastad, Norway, 1974. Engineering Geology, 14(2-3), 183-196.

Gupta, V., & Sharma, R. (2012). Relationship between textural, petrophysical and mechanical properties of quartzites: A case study from northwestern Himalaya. Engineering Geology, 135-136, 1-9.

Hanzawa, H. (1979). Undrained Strength Characteristics of an Alluvial Marine Clay in the Tokyo Bay. Soils and Foundations, 19(4), 69-84.

Hasancebi, N. (2016). Effect of Porosity on Uniaxial Compressive Strength of Sasaltic Rock from Diyarbakir, Turkey. In R. Ulusay, O. Aydan, H. Gerçek, M. Ali Hindistan, & E. Tuncay (Eds.), Rock Mechanics and Rock Engineering: From the Past to the Future (1 ed., pp. 337-340): CRC Press.

Hashemi, M., Moghaddas, S., & Ajalloeian, R. (2009). Application of Rock Mass Characterization for Determining the Mechanical Properties of Rock Mass: a Comparative Study. Rock Mechanics and Rock Engineering, 43(3), 305-320.

Hassanpour, J., Rostami, J., Khamehchiyan, M., Bruland, A., & Tavakoli, H. R. (2009). TBM Performance Analysis in Pyroclastic Rocks: A Case History of Karaj Water Conveyance Tunnel. Rock Mechanics and Rock Engineering, 43(4), 427-445.

Heidari, M., Momeni, A. A., Rafiei, B., Khodabakhsh, S., & Torabi-Kaveh, M. (2012). Relationship Between Petrographic Characteristics and the Engineering Properties of Jurassic Sandstones, Hamedan, Iran. Rock Mechanics and Rock Engineering, 46(5), 1091-1101.

Hight, D. W., McMillan, F., Powell, J. J. M., Jardine, R. J., & Allenou, C. P. (2003). Some Characteristics of London Clay. In T. S. Tan, K. K. Phoon, D. W. Hight, & S. Leroueil (Eds.), Characterisation and Engineering Properties of Natural Soils (Vol. 2, pp. 851-907). Netherlands: Balkema, A A.

Houlsby, G. T., & Hitchman, R. (1988). Calibration chamber tests of a cone penetrometer in sand. Géotechnique, 38(1), 39-44.

Huang, A. B. (1991). Calibration Chamber Testing: Proceedings of the First International Symposium on Calibration Chamber Testing/ISOCCT1, Potsdam, New York, 28-29 June 1991: Elsevier.

Huang, A. B., Hsu, H. H., & Chang, J. W. (1999). The Behaviour of A Compressible Silty Fine Sand. Canadian Geotechnical Journal, 36(1), 88-101.

Huang, A. B., Hsueh, C. K., O'Neill, M. W., Chern, S., & Chen, C. (2001). Effects of Construction on Laterally Loaded Pile Groups. Journal of Geotechnical and Geoenvironmental Engineering, 127(5), 385-397.

Huntsman, S. R., Mitchell, J. K., & Klejbuk Jr., L. W. (1986). Lateral Stress Measurement During Cone

Penetration. Paper presented at the In Situ'86, Virginia Tech, Blackburg, Virginia.

Isik, N. S., Doyuran, V., & Ulusay, R. (2008). Assessment of deformation modulus of weak rock masses from pressuremeter tests and seismic surveys. Bulletin of Engineering Geology and the Environment, 67(3), 293-304.

Iwasaki, K., Tsuchiya, H., Sakai, Y., & Yammamoto, Y. (1991, September 3-6). Applicability of the Marchetti Dilatometer Test to Soft Ground in Japan. Paper presented at the International Conference on Geotechnical Engineering for Coastal Development: Theory and Practice on Soft Ground (GEO-COAST'91), Yokohama, Japan.

Jacob, K., & G, H. (2016). Study on the Relationaship of Compression Index from Water Content, Atteberg Limits and Field Density for Kuttanad Clay. International Journal of Innovative Research in Technology, 3(4), 33-38.

Jafari, A., Mollaee, M., & Shamsi, H. (2007). Investigation into ground convergence effect on TBM oerformance in squeezing ground. Paper presented at the 11th Congress of the International Society for Rock Mechanics, 9-13 July, 2007, Lisbon, Portugal.

Jhanwar, J. C., Jethwa, J. L., & Reddy, A. H. (2000). Influence of air-deck blasting on fragmentation in jointed rocks in an open-pit manganese mine. Engineering Geology, 57(1-2), 13-29.

Jizba, D. L. (1991). Mechanics and Acoustical Properties of Sandstones and Shales. (Ph.D.). Stanford University,

Jordá-Bordehore, L. (2017). Stability Assessment of Natural Caves Using Empirical Approaches and Rock Mass Classifications. Rock Mechanics and Rock Engineering, 50(8), 2143-2154.

Jordá-Bordehore, L., Toulkeridis, T., Romero-Crespo, P. L., Jordá-Bordehore, R., & García- Garizabal, I. (2016). Stability assessment of volcanic lava tubes in the Galápagos using engineering rock mass classifications and an empirical approach. International Journal of Rock Mechanics and Mining Sciences, 89, 55-67.

Judeel, G. d. T. (2003). Study of the effects of shaft pillar extraction on a vertical shaft located in highly stratified and poor quality rock masses. Paper presented at the 10th International Congress on Rock Mechanics, Jonhannesburg, South Africa.

Kahraman, S. (2001). Evaluation of simple methods for assessing the uniaxial compressive strength of rock. International Journal of Rock Mechanics and Mining Sciences, 38(7), 981-994.

Kahraman, S., & Alber, M. (2006). Estimating unconfined compressive strength and elastic modulus of a fault breccia mixture of weak blocks and strong matrix. International Journal of Rock Mechanics and Mining Sciences, 43(8), 1277-1287.

Kahraman, S., Fener, M., & Gunaydin, O. (2004). Predicting the sawability of carbonate rocks using multiple curvilinear regression analysis. International Journal of Rock Mechanics and Mining Sciences, 41(7), 1123-1131.

Kahraman, S., Gunaydin, O., & Fener, M. (2005). The effect of porosity on the relation between uniaxial compressive strength and point load index. International Journal of Rock Mechanics and Mining Sciences, 42(4), 584-589.

Kaiser, P. K., MacKay, C., & Gale, A. D. (1986). Evaluation of rock classifications at B. C. Rail tumbler ridge tunnels. Rock Mechanics and Rock Engineering, 19(4), 205-234.

Kamei, T., & Tanaka, M. (2003). The Interpretation of The Flat Dilatometer Tests in Ariake Clay, Southwest Japan. Memoirs of the Graduate School of Science and Engineering Shimane University. Series A, 37, 1-6.

Kasim, M., & Shakoor, A. (1996). An investigation of the relationship between uniaxial compressive strength and degradation for selected rock types. Engineering Geology, 44(1-4), 213-227.

Kavur, B., Štambuk Cvitanović, N., & Hrženjak, P. (2015). Comparison between plate jacking and large flat jack test results of rock mass deformation modulus. International Journal of Rock Mechanics and Mining Sciences, 73, 102-114.

Keffeler, E. R. (2014). Measurement and Prediction of In-Situ Weak Rock Mass Modulus: Case Studies from Nevada, Puerto Rico, and Iran. (Ph.D. doctoral dissertation). University of Nevada, Reno, Reno, Nevada, USA. (UMI 3638210)

Kelly, R. B., Pineda, J. A., Bates, L., Suwal, L. P., & Fitzallen, A. (2017). Site characterisation for the Ballina field testing facility. Géotechnique, 67(4), 279-300.

Khabbazi, A., Ghafoori, M., Lashkaripour, G. R., & Cheshomi, A. (2013). Estimation of the rock mass deformation modulus using a rock classification system. Geomechanics and Geoengineering, 8(1), 46-52.

Khaksar, Griffiths, & McCann. (1999). Compressional- and shear-wave velocities as a function of confining stress in dry sandstones. Geophysical Prospecting, 47(4), 487-508.

Khanlari, G., & Abdilor, Y. (2011). Estimation of Strength Parameters of Limestone Using Artificial Neural Networks and

Khanlari, G., meybodi, R. G., & Mokhtari, E. (2012). Engineering geological study of the second part of water supply Karaj to Tehran tunnel with emphasis on squeezing problems. Engineering Geology, 145-146, 9-17.

Kinner, E. B. (1970). Load-Deformation Behavior of Saturated Clays During Undrained Shear. (Doctor of Science). Massachusetts Institute of Technology.

Kinner, E. B. (1970). Load-Deformation Behavior of Saturated Clays During Undrained Shear. (Doctor of Science). Massachusetts Institute of Technology.

Kiran Jacob, Hari G (2016). Study on the relationship of shear strength from water content, Atterberg limits and field density for Kuttand clay. International Journal of Innovative Research in Technology, 3(4), 33-38.

Kitagawa, T., Kumeta, T., Ichizyo, T., Soga, S., Sato, M., & Yasukawa, M. (1991). Application of Convergence Confinement Analysis to the study of preceding displacement of a squeezing rock tunnel. Rock Mechanics and Rock Engineering, 24(1), 31-51.

Klanphumeesri, S. (2010). Direct Tension Testing of Rock Specimens. (M.Eng.). Suranaree University of Technology.

Kocbay, A., & Kilic, R. (2006). Engineering geological assessment of the Obruk dam site (Corum, Turkey). Engineering Geology, 87, 141–148.

Koçkar, M. K., & Akgün, H. (2003a). Engineering geological investigations along the Ilıksu Tunnels, Alanya, southern Turkey. Engineering Geology, 68(3-4), 141-158.

Koçkar, M. K., & Akgün, H. (2003b). Methodology for tunnel and portal support design in mixed limestone, schist and phyllite conditions: a case study in Turkey. International Journal of Rock Mechanics and

Mining Sciences, 40(2), 173-196.

Koncagül, E. C., & Santi, P. M. (1999). Predicting the unconfined compressive strength of the Breathitt shale using slake durability, Shore hardness and rock structural properties. International Journal of Rock Mechanics and Mining Sciences, 36(2), 139-153.

Konrad, J. M., & Law, K. T. (1987a). Undrained shear strength from piezocone tests. Canadian Geotechnical Journal, 24(3), 392-405.

Konrad, J. M., & Law, K. T. (1987b). Preconsolidation pressure from piezocone tests in marine clays. Géotechnique, 37(2), 177-190.

Koutsoftas, D. C., & Ladd, C. C. (1985). Design Strengths for an Offshore Clay. Journal of Geotechnical Engineering, 111(3), 337-355.

Koutsoftas, D. C., Foott, R., & Handfelt, L. D. (1987). Geotechnical Investigations Offshore Hong Kong. Journal of Geotechnical Engineering, 113(2), 87-105.

Kramadibrata, S., Saptono, S., Wattimena, R. K., Simangunsong, G. M., & Sulistianto, B. (2011, October 18-21). Developing a Slope Stability Curve of Open Pit Coal Mine by Using Dimensional Analysis Method. Paper presented at the 12th International Congress on Rock Mechanics, ISRM, Beijing, China.

Ku, T., & Mayne, P. W. (2015). In Situ Lateral Stress Coefficient (K0) from Shear Wave Velocity Measurements in Soils. Journal of Geotechnical and Geoenvironmental Engineering, 141(12).

Kulhawy, F. H., & Mayne, P. W. (1990). Manual on Estimating Soil Properties for Foundation Design. EPRI Report EL-6800, Electric Power Research Inst., Palo Alto, CA, United States.

Phoon, K.K., Kulhawy, F.H., and Grigoriu, M.D. (1995). Reliability-based Design of Foundations for Transmission Line Structures. EPRI Report TR-105000, Electric Power Research Inst., Palo Alto, CA, United States.

Kumar, S., Kumar, K., & Dogra, N. N. (2017). Rock mass classification and assessment of stability of critical slopes on national highway-22 in Himachal Pradesh. Journal of the Geological Society of India, 89(4), 407-412.

Kumari, W. G. P., Ranjith, P. G., Perera, M. S. A., & Chen, B. K. (2016). Investigation on temperature dependent mechanical behaviour. In R. Ulusay, O. Aydan, H. Gerçek, M. Ali Hindistan, & E. Tuncay (Eds.), Rock Mechanics and Rock Engineering: From the Past to the Future (1 ed., pp. 253-258).

Kuo, C. C. (1994). 平板膨脹儀(DMT)試驗評估土層大地應力之研究. (MSc). National Taiwan University, Taipei, Taiwan.

Kurtulus, C., Bozkurt, A., & Endes, H. (2011). Physical and Mechanical Properties of Serpentinized Ultrabasic Rocks in NW Turkey. Pure and Applied Geophysics, 169(7), 1205-1215.

Kurtulus, C., CakIr, S., & Yoğurtcuoğlu, A. C. (2016). Ultrasound Study of Limestone Rock Physical and Mechanical Properties. Soil Mechanics and Foundation Engineering, 52(6), 348-354.

Lacasse, S., & Lunne, T. (1982). Penetration Tests in Two Norwegian Clays. Paper presented at the 2nd European Symposium on Penetration Testing, Amsterdam.

Ladd, C. C. (1972). Test embankment on sensitive clay. Paper presented at the Specialty Conference on Performance of Earth and Earth-Supported Structures, Purdue University, Lafayette, Indiana, USA.

Lama, R. D., & Vutukuri, V. S. (1978). Handbook on Mechanical Properties of Rocks (Vol. 3).

Larsson, R., & Eskilson, S. (1989). Dilatometerförsök i lera: Statens Geotekniska Institut.

Larsson, R., & Mulabdic, M. (1991). Shear Moduli in Scandinavian Clays.

Lee, K. L., & Seed, H. B. (1967). Drained Strength Characteristics of Sands. Journal of the Soil Mechanics and Foundations Division, 93(6), 117-141.

Leong, E. C., & Rahardjo, H. (2002). Characterization and Engineering Properties of Singapore Residual Soils. Paper presented at the International Workshop on Characterisation and Engineering Properties of Natural Soils, Singapore.

Liu, C. C. (1999). A Generalized Effective Stress Constitutive Model for Taipei Clay. (Ph.D.). National Taiwan University of Sceince and Technology, Taipei, Taiwan.

Liu, S. Y., Shao, G. H., Du, Y. J., & Cai, G. J. (2011). Depositional and geotechnical properties of marine clays in Lianyungang, China. Engineering Geology, 121(1-2), 66-74.

Long, M. M., Gudjonsson, G. & Callanan, F.(2007). Sampling, In Situ Testing and Long Term Settlement of Soft Soils at the Loughmore Link Embankments. Proceedings of the Soft Ground Engineering Conference, Athlone, Ireland.

Lunne, T., Christophersen, H. P., & Tjelta, T. I. (1985). Engineering use of piezocone data in North Sea clays. Paper presented at the 11th International Conference on Soil Mechanics and Foundation Engineering, San Francisco.

Lunne, T., Powell, J. J. M., Hauge, E. A., Mokkelbost, K. H., & Uglow, I. M. (1990). Correlation of Dilatometer Readings with Lateral Stress in Clays. In N. R. C. (NRC) & T. R. B. (TRB) (Eds.), Dynamic Testing of Aggregates and Soils and Lateral Stress Measurements 1990 (Vol. 1278, pp. 183-193). Washington, D.C.: Transportation Research Board.

Lutenegger, A. J. (1986). Dynamic Compaction in Friable Loess. Journal of Geotechnical Engineering, 112(6), 663-667.

Majdi, A., & Beiki, M. (2010). Evolving neural network using a genetic algorithm for predicting the deformation modulus of rock masses. International Journal of Rock Mechanics and Mining Sciences, 47(2), 246-253.

Marchetti, S. (1980). In Situ Tests by Flat Dilatometer. Journal of the Geotechnical Engineering Division, 106(3), 299-321.

Marchetti, S. (1985). On the Field Determination of K0 in Sand. Paper presented at the 6th International Conference on Soil Mechanics and Foundation Engineering, San Francisco, USA.

Marchetti, S. (1991). Discussion of “Settlement of Shallow Foundations on Granular Soils” by G. A. Leonards and J. D. Frost (July, 1988, Vol. 114, No. 7). Journal of Geotechnical Engineering, 117(1), 174-179.

Marchetti, S., Monaco, P., Totani, G., & Calabrese, M. (2001). The Flat Dilatometer Test (DMT) in Soil Investigation - A Report by the ISSMGE Committee TC16.

Marques, A. d. A., Paes, B. S. T., Marques, E. A. G., & Pereira, L. C. (2014). Correlations between Uniaxial Compressive Strength and Point Load Strength for Some Brazilian High-Grade Metamorphic Rocks. Revista Brasileira de Geologia de Engenharia e Ambiental (RBGEA), 4(1), 47-58.

Maugeri, M., & Monaco, P. (2006). Liquefaction Potential Evaluation by SDMT. Paper presented at the 2nd International Conference on the Flat Dilatometer, Washington D.C.

Mayer, J. M., & Stead, D. (2016). A Comparison of Traditional, Step-Path, and Geostatistical Techniques in

the Stability Analysis of a Large Open Pit. Rock Mechanics and Rock Engineering, 50(4), 927-949.

Mayne, P. W. (1991). Determination of OCR in Clays by Piezocone Tests Using Cavity Expansion and Critical State Concepts. Soils and Foundations, 31(2), 65-76.

Mayne, P. W. (2008). piezocone profiling of clays for maritime site investigation. Paper presented at the 11th Baltic Sea Geotechnical Conference, Gdansk, Poland.

Mayne, P. W., & Frost, D. D. (1988). Dilatometer Experience in Washington, D.C., and Vicinity. Tranportation Research Record(1169), 16-23.

Mio, G. D., & Giacheti, H. L. (2004). Integration of Testing Data in A Site Investigation Program: Examples from Tropical Soils Sites. Paper presented at the 2nd International Conference on Site Characterization, Porto, Portugal.

Mishra, D. A., & Basu, A. (2013). Estimation of uniaxial compressive strength of rock materials by index tests using regression analysis and fuzzy inference system. Engineering Geology, 160, 54-68.

Mlynarek, Z., Gogolik, S., Gryczmanski, M., & Uliniarz, R. (2012). Settlement Analysis of A Cylindrical Tank Based on CPTU and SDMT Results. Paper presented at the 4th International Conference on Geotechnical and Geophysical Site Characterization, Porto de Galinhas, Brazil.

Modoni, G., & Bzówka, J. (2012). Analysis of Foundations Reinforced with Jet Grouting. Journal of Geotechnical and Geoenvironmental Engineering, 138(12), 1442-1454.

Mohamad, E. T., Jahed Armaghani, D., Momeni, E., & Alavi Nezhad Khalil Abad, S. V. (2014). Prediction of the unconfined compressive strength of soft rocks: a PSO-based ANN approach. Bulletin of Engineering Geology and the Environment, 74(3), 745-757.

Moon, V., Russell, G., & Stewart, M. (2001). The value of rock mass classification systems for weak rock masses: a case example from Huntly, New Zealand. Engineering Geology, 61(1), 53-67.

Moradi, M. R., & Farsangi, M. A. E. (2013). Application of the Risk Matrix Method for Geotechnical Risk Analysis and Prediction of the Advance Rate in Rock TBM Tunneling. Rock Mechanics and Rock Engineering, 47(5), 1951-1960.

Moradian, Z. A., & Behnia, M. (2009). Predicting the Uniaxial Compressive Strength and Static Young's Modulus of Intact Sedimentary Rocks Using the Ultrasonic Test. International Journal of Geomechanics, 9(1), 14-19.

Munshi, M. K. (2003). Geotechnical Characterization of Soft Soil along Mollahat-Noapara Road Section at Bagerhat. (Master Thesis). Bangladesh University of Engineering and Technology, Bangladesh.

Mustafa, S., Khan, M. A., Khan, M. R., Hameed, F., Mughal, M. S., Asghar, A., & Niaz, A. (2015). Geotechnical study of marble, schist, and granite as dimension stone: a case study from parts of Lesser Himalaya, Neelum Valley Area, Azad Kashmir, Pakistan. Bulletin of Engineering Geology and the Environment, 74(4), 1475-1487.

Nazir, R., Momeni, E., Armaghani, D. J., & Amin, M. F. M. (2013a). Prediction of Unconfined Compressive Strength of Limestone Rock Samples Using L-Type Schmidt Hammer. Electronic Journal of Geotechnical Engineering, 18/I, 1767-1775.

Nazir, R., Momeni, E., Armaghani, D. J., & Amin, M. F. M. (2013b). Correlation Between Unconfined Compressive Strength and Indirect Tensile Strength of Limestone Rock Samples. Electronic Journal of Geotechnical Engineering, 18/I, 1737-1746.

Nefeslioglu, H. A. (2013). Evaluation of geo-mechanical properties of very weak and weak rock materials by using non-destructive techniques: Ultrasonic pulse velocity measurements and reflectance spectroscopy. Engineering Geology, 160, 8-20.

Nejati, H. R., Ghazvinian, A., Moosavi, S. A., & Sarfarazi, V. (2013). On the use of the RMR system for estimation of rock mass deformation modulus. Bulletin of Engineering Geology and the Environment, 73(2), 531-540.

Ng, I.T., Yuen, K.-V., & Lau, C.-H. (2015). Predictive model for uniaxial compressive strength for Grade III granitic rocks from Macao. Engineering Geology, 199, 28-37.

Nicksiar, M., & Martin, C. D. (2012). Evaluation of Methods for Determining Crack Initiation in Compression Tests on Low-Porosity Rocks. Rock Mechanics and Rock Engineering, 45(4), 607-617.

Ohtsubo, M., Higashi, T., Kanayama, M., & Takayama, M. (2007). Depositional geochemistry and geotechnical properties of marine clays in the Ariake Bay area, Japan. Paper presented at the 1st International Workshop on Characterisation and Engineering Properties of Natural Soils.

Ohtsubo, M., Takayama, M., & Egashira, K. (1982). Marine Quick Clays from Ariake Bay Area, Japan. Soils and Foundations, 22(4), 71-80.

Olsen, H. W. (1982). Geptechnical Profiles for Thirty-One Sites on the Mid-Atlantic Upper Contenental Slope: U.S.G.S.

Özkan, İ., Erdem, B., & Ceylanoğlu, A. (2015). Characterization of jointed rock masses for geotechnical classifications utilized in mine shaft stability analyses. International Journal of Rock Mechanics and Mining Sciences, 73, 28-41.

Palchik, V., & Hatzor, Y. H. (2004). The Influence of Porosity on Tensile and Compressive Strength of Porous Chalks. Rock Mechanics and Rock Engineering, 37(4), 331-341.

Palchik, V. (1999). Influence of Porosity and Elastic Modulus on Uniaxial Compressive Strength in Soft Brittle Porous Sandstones. Rock Mechanics and Rock Engineering, 32(4), 303-309.

Panthi, K. K., & Shrestha, P. K. (2018). Estimating Tunnel Strain in the Weak and Schistose Rock Mass Influenced by Stress Anisotropy: An Evaluation Based on Three Tunnel Cases from Nepal. Rock Mechanics and Rock Engineering, 51(6), 1823-1838.

Pappalardo, G. (2014). Correlation Between P-Wave Velocity and Physical–Mechanical Properties of Intensely Jointed Dolostones, Peloritani Mounts, NE Sicily. Rock Mechanics and Rock Engineering, 48(4), 1711-1721.

Parkin, A., Holden, J., Aamot, K., Last, N., & Lunne, T. (1980). Laboratory Investigation of CPT's in Sand (52108-9).

Parry, R. H. G. (1968). Field and Laboratory Behaviour of a Lightly Overconsolidated Clay. Géotechnique, 18(2), 151-171.

Pavlovic, M. (1970, September 21-26). Determining of Quasihomogeneous Zones of Elasticity and Deformability of Rock Mass in Tunnel, on the Basis of in situ Investigation. Paper presented at the Second Congress of the International Society for Rock Mechnaics, Belgrade, Yugoslavia.

Penna, A. S. D. (2006). Some Recent Experience Obtained with DMT in Brazilian Soils. Paper presented at the 2nd International Conference on the Flat Dilatometer, Washington D.C.

Phoon, K. K., & Kulhawy, F. H. (1999). Characterization of geotechnical variability. Can. Geotech., 36(4):

612-624.

Phoon, K.K., Kulhawy, F.H., and Grigoriu, M.D. (1995). Reliability-Based Design of Foundations for Transmission Line Structure, Report TR-105000, Palo Alto, Electric Power Research Institute.

Pinto da Cunha, A. (1991). Scale effects in the determination of mechanical properties of joints and rock masses. Paper presented at the 7th International Congress on Rock Mechanics, Aachen, Deutschland.

Pittino, G., Gegenhuber, N., Reiter, F., & Frohlich, R. (2016). Ultrasonic wave measurement during uniaxial compression tests. In R. Ulusay, O. Aydan, H. Gerçek, M. Ali Hindistan, & E. Tuncay (Eds.), Rock Mechanics and Rock Engineering: From the Past to the Future (1 ed., pp. 365-369).

Powell, J. J. M. & Uglow, I. M. (1988). The interpretation of Marchetti dilameter tests in UK clays. Proceedings of ICE Penetration Testing in the UK, Birmingham, pp. 269-273.

Quiros, G. W., & Young, A. G. (1988). Comparison of Field Vane, CPT, and Laboratory Strength Data at Santa Barbara Channel Site. In A. F. Richards (Ed.), Vane Shear Strength Testing in Soils: Field and Laboratory Studies (pp. 306-317). West Conshohocken: A.S.T.M.Regression Analysis. Australian Journal of Basic and Applied Sciences, 5(11), 1049-1053.

Radhakrishnan, R., & Leung, C. F. (1989). Load Transfer Behavior of Rock-Socketed Piles. Journal of Geotechnical Engineering, 115(6), 755-768.

Rajabzadeh, M. A., Moosavinasab, Z., & Rakhshandehroo, G. (2011). Effects of Rock Classes and Porosity on the Relation between Uniaxial Compressive Strength and Some Rock Properties for Carbonate Rocks. Rock Mechanics and Rock Engineering, 45(1), 113-122.

Ramana, Y. V., & Venkatanarayana, B. (1973). Laboratory studies on kolar rocks. International Journal of Rock Mechanics and Mining Sciences & Geomechanics Abstracts, 10(5), 465-489.

Ranasooriya, J. (2009). The Reliability of Rock Mass Classification System as Underground Excavation Support Design Tools. (Ph.D). Curtin University, Perth, Australia.

Robertson, P. K., Campenella, R. G., & Gillespie, D. (1988). Excess Pore Pressure and the Flat Dilatometer Test. Paper presented at the 1st International Symposium on Penetration Testing, Orlando, USA.

Rocha, B. P., dos Santos, R. A., Bezerra, R. C., Rodrigues, R. A., & Giacheti, H. L. (2016). Characterization of Unsaturated Tropical Soil Site by In Situ Tests. Paper presented at the 5th International Conference on Geotechnical and Geophysical Site Characterization, Gold Coast, Queensland, Australia.

Rochelle, P. L., Zebdi, M., Leroueil, S., Tavenas, F., & Virely, D. (1988). Piezocone tests in sensitive clays of eastern Canada. Paper presented at the First International Symposium on Penetration Testing, Orlando, United States.

Roque, R., Janbu, N., & Senneset, K. (1988). Basic Interpretation Procedures of Flat Dilatometer Tests. Paper presented at the 1st International Symposium on Penetration Testing, Orlando, USA.

Rouainia, M., Elia, G., Panayides, S., & Scott, P. (2017). Nonlinear Finite-Element Prediction of the Performance of a Deep Excavation in Boston Blue Clay. Journal of Geotechnical and Geoenvironmental Engineering, 143(5).

Roy, M., Tremblay, M., Tavenas, F., & Rochelle, P. L. (1982). Development of a quasi-static piezocone apparatus. Canadian Geotechnical Journal, 19(2), 180-188.

Rutledge, P. C. (1939). Compression Characteristics of Clays and Application to Settlement Analysis. (doctoral dissertation). Harvard University.

Sabatakakis, N., Koukis, G., Tsiambaos, G., Papanakli, S. (2008). Index properties and strength variation controlled by microstructure for sedimentary rocks. Engineering Geology, 97, 80–90.

Sabatini, P. J., Bachus, R. C., Mayne, P. W., Schneider, J. A., & Zettler, T. E. (2002). Geotechnical Engineering Circular NO.5: Evaluation of Soil and Rock Properties (FHWA-IF-02-034).

Salgado, R., Bandini, P., & Karim, A. (2000). Shear Strength and Stiffness of Silty Sand. Journal of Geotechnical and Geoenvironmental Engineering, 126(5), 451-462.

Sandven, R. (2003). Geotechnical Properties of a Natural Silt Deposit Obtained from Field and Laboratory Tests. In T. S. Tan (Ed.), Characterisation and Engineering Properties of Natural Soils (Vol. 2, pp. 1237-1276): CRC Press.

Sandven, R., Orbech, T., & Lunne, T. (2004). Sample Distribution in Highly Sensitive Clays. Paper presented at the 2nd International Conference on Geotechnical and Geophysical Site Characterization, Porto, Portugal.

Santagata, M., Germaine, J. T., & Ladd, C. C. (2005). Factors Affecting the Initial Stiffness of Cohesive Soils. Journal of Geotechnical and Geoenvironmental Engineering, 131(4), 430-441.

Sapigni, M., Berti, M., Bethaz, E., Busillo, A., & Cardone, G. (2002). TBM performance estimation using rock mass classifications. International Journal of Rock Mechanics and Mining Sciences, 39(6), 771-788.

Sarkar, K., Tiwary, A., & Singh, T. N. (2010). Estimation of strength parameters of rock using artificial neural networks. Bulletin of Engineering Geology and the Environment, 69(4), 599-606.

Sarkar, K., Vishal, V., & Singh, T. N. (2011). An Empirical Correlation of Index Geomechanical Parameters with the Compressional Wave Velocity. Geotechnical and Geological Engineering, 30(2), 469-479.

Sarpun, Y. H., Hersat, S., B, Ozkan, V., Tuncel, S., & Yildiz, A. (2010, June 7-11). The Elastic Properties Determination of Volcanic Rocks by Using Ultrasonic Method. Paper presented at the 10th European Conference on Non-Destructive Testing 2010, Moscow, Russia.

Senneset, K., Sandven, R., Lunne, T., By, T., & Amundsen, T. (1988). Piezocone Tests in Dilty Soils. Paper presented at the First International Symposium on Penetration Testing, Orlando, United States.

Shalabi, F. I., Cording, E. J., & Al-Hattamleh, O. H. (2007). Estimation of rock engineering properties using hardness tests. Engineering Geology, 90(3-4), 138-147.

Sharma, P. K., & Singh, T. N. (2007). A correlation between P-wave velocity, impact strength index, slake durability index and uniaxial compressive strength. Bulletin of Engineering Geology and the Environment, 67(1), 17-22.

Shrestha, G. L. (2005). Stress Induced Problems in Himalayan Tunnels with Special Reference to Squeezing. (Eng.D.). Norwegian University of Science and Technology, Trondheim.

Silvestri, V. (2003). Assessment of self-boring pressuremeter tests in sensitive clay. Canadian Geotechnical Journal, 40(2), 365-387.

Simons, N. E. (1960, June). Comprehensive investigations on the shear strength of an undisturbed Drammen clay. Paper presented at the Research Conference on Shear Strength of Cohesive Soils, Boulder, Colorado, United State.

Singh, R. (2011). Deformability of rock mass and a comparison between plate jacking and Goodman jack tests. International Journal of Rock Mechanics and Mining Sciences, 48(7), 1208-1214.

Singh, R., Vishal, V., Singh, T. N., & Ranjith, P. G. (2012). A comparative study of generalized regression neural network approach and adaptive neuro-fuzzy inference systems for prediction of unconfined compressive strength of rocks. Neural Computing and Applications, 23(2), 499-506.

Skempton, A. W. (1961). Horizontal Stresses in An Overconsolidated Eocence Clay. Paper presented at the 5th International Conference on Soil Mechanics and Foundation Engineering (5th ICSFE), Paris.

Swolfs, H. S., & Kibler, J. D. (1982). A Note on the Goodman Jack. Rock Mechanics, 15, 57-66.

Taheri, A., & Tani, K. (2009). Assessment of the Stability of Rock Slopes by the Slope Stability Rating Classification System. Rock Mechanics and Rock Engineering, 43(3), 321-333

Tahir, M., Mohammad, N., & Dia, F. (2011). Strength Parameters and Their Inter-Relationship for Limestones of Cherat and Kohat Areas of Khyber Pakhtunkhwa. Journal of Himalayan Earth Sciences, 44(2), 45-51.

Takemura, J., Watabe, Y., & Tanaka, M. (2006, November 16). Characterization of Alluvial Deposits in Mekong Delta. Paper presented at the 2nd International Workshop on Characterisation and Engineering Properties of Natural Soils, Singapore.

Tamrakar, N. K., Yokota, S., & Shrestha, S. D. (2007). Relationships among mechanical, physical and petrographic properties of Siwalik sandstones, Central Nepal Sub-Himalayas. Engineering Geology, 90(3-4), 105-123.

Tan, Y.C., Gue. S.S., Ng, H.B. & Lee, PT. (2003). Design Parameters of Klang Clay, Malaysia. 12th Asian Regional Conference on Soil Mechanics and Geotechnical Engineering, Singapore, 4th - 8th August, 2003, 4-7.

Tanaka, H., Locat, J., Shibuya, S., Soon, T. T., & Shiwakoti, D. R. (2001). Characterization of Singapore, Bangkok, and Ariake clays. Canadian Geotechnical Journal, 38(2), 378-400.

Tanaka, H., Shiwakoti, D. R., Mishima, O., Watabe, Y., & Tanaka, M. (2001). Comparison of Mechanical Behavior of Two Overconsolidated Clays: Yamashita and Louiseville Clays. Soils and Foundations, 41(4), 73-87.

Tavenas, F. A., Blanchette, G., Leroueil, S., Roy, M., & Rochelle, P. L. (1975, June 1-4). Difficulties in the In Situ Determination of Ko in Soft Sensitive Clays. Paper presented at the Geotechnical Specialty Conference on In Situ Measurement of Soil Properties, Raleigh, North Carolina, United States.

Tong, L. Y., Liu, S. Y., Qiang, W., Du, G. Y., & Cai, G. J. (2013). In Situ Evaluation of K_0 Using Piezocone Tests for Bridge Foundations. Paper presented at the 4th International Conference on Site Characterization ISC-4, Porto de Galinhas-Pernamuco, Brazil.

Török, Á., & Vásárhelyi, B. (2010). The influence of fabric and water content on selected rock mechanical parameters of travertine, examples from Hungary. Engineering Geology, 115(3-4), 237-245.

Totani, G., Calabrese, M., & Monaco, P. (1998). In Situ Determination of c_h by Flat Dilatometer (DMT). Paper presented at the 1st International Conference on Site Characterization (ISC'98), Atlanta, Georgia, USA.

Totani, G., Totani, F., Monaco, P., & Simeoni, L. (2016, September 5-9). Site Investigation, Monitoring and Stability Analysis of a Built-up Slope Involved by Gas Pipeline Explosion. Paper presented at the 5th International Conference on Geotechnical and Geophysical Site Characterization ISC-5, Gold Coast, Queensland, Australia.

Tschuschke, W., Kmiecik, G., & Mikos, A. (2013). G_0 Profiling in Mine Tailings Based on SCPTU and SDMT. Paper presented at the 4th International Conference on Site Characterization ISC-4, Porto de Galinhas-Pernamuco, Brazil.

Tuğrul, A. (1998). The application of rock mass classification systems to underground excavation in weak limestone, Atatürk dam, Turkey. Engineering Geology, 50(3-4), 337-345.

Tumac, D., Bilgin, N., Feridunoglu, C., & Ergin, H. (2006). Estimation of Rock Cuttability from Shore Hardness and Compressive Strength Properties. Rock Mechanics and Rock Engineering, 40(5), 477-490.

Ulusay, R., Türeli, K., & Ider, M. H. (1994). Prediction of engineering properties of a selected litharenite sandstone from its petrographic characteristics using correlation and multivariate statistical techniques. Engineering Geology, 38(1-2), 135-157.

Vasconcelos, G., Lourenco, P. B., Alves, C., & Pamplona, J. (2007). Prediction of the mechanical properties of granites by ultrasonic pulse velocity and Schmidt hammer hardness. Paper presented at the 10th North American Masonry Conference, St. Louis, Missouri, USA.

Verwaal, W., & Mulder, A. (1993). Estimating rock strength with the equotip hardness tester. International Journal of Rock Mechanics and Mining Sciences & Geomechanics Abstracts, 30(6), 659-662.

Villet, W. C. B., & Mitchell, J. K. (1981). Cone Resistance, Relative Density, and Friction Angle. Paper presented at the ASCE Symposium on Cone Penetration Testing and Experience, New York.

Wang, C. C., Huang, A. B., Ho, Y. T., & Lee, J. T. (2013). Geotechnical Site Characterization for Reservoir Sediment. Paper presented at the 4th International Conference on Site Characterization ISC-4, Porto de Galinhas-Pernamuco, Brazil.

Wang, C., & Zhu, H. (2016). Combination of Kriging methods and multi-fractal analysis for estimating spatial distribution of geotechnical parameters. Bulletin of Engineering Geology and the Environment, 75(1), 413-423.

Wang, Y. & Cao, Z. J. (2013). Probabilistic characterization of Young's modulus of soil using equivalent samples. Engineering Geology, 159, 106-118.

Watabe, Y., Tanaka, M., & Takemura, J. (2004). Evaluation of In-situ K0 for Ariake, Bangkok and Hai-Phong Clays. Paper presented at the 2nd International Conference on Geotechnical and Geophysical Site Characterization, Porto, Portugal.

Watabe, Y., Tanaka, M., Tanaka, H., & Tsuchida, T. (2003). K0-Consolidation in a Triaxial Cell and Evaluation of In-Situ K0 for Marine Clays with Various Characteristics. Soils and Foundations, 43(1), 1-20.

Wei, L., Pant, R., & Tumay, M. T. (2010). Evaluation of undrained shear strength of soft New Orleans clay using piezocone. Paper presented at the 2nd International Symposium on Cone Penetration Testing, Huntington Beach, CA, USA.

White, D. J., Pham, H. T. V., & Hoevelkamp, K. K. (2007). Support Mechanisms of Rammed Aggregate Piers. I: Experimental Results. Journal of Geotechnical and Geoenvironmental Engineering, 133(12), 1503-1511.

Windle, D., & Wroth, C. P. (1977). In Situ Measurement of the Properties of Stiff Clays. Paper presented at the 9th International Conference on Soil Mechanics and Foundation Engineering, Tokyo, Japan.

Yagiz, S., Akyol, E., & Sen, G. (2008). Relationship between the standard penetration test and the

pressuremeter test on sandy silty clays: a case study from Denizli. Bulletin of Engineering Geology and the Environment, 67(3), 405-410.

Yanjun, S., Yongyue, S., Guangxiang, Y., & Yuanchun, S. (2007, July 9-13). Discontinuity Distribution in Granite and Its Effects on Rock Mass Classification. Paper presented at the 11th Congress of the International Society for Rock Mechanics, Lisbon, Protugal.

Yılmaz, I., & Yuksek, A. G. (2008). An example of artificial neural network (ANN) application for indirect estimation of rock parameters. Rock Mechanics and Rock Engineering, 41(5), 781–795.

Yin, J. H. (1999). Properties and behaviour of Hong Kong marine deposits with different clay contents. Canadian Geotechnical Journal, 36(6), 1085-1095.

Zhang, D., Zhou, Y., Phoon, K. K., and Huang, H. (2020). Multivariate probability distribution of shanghai clay properties. Engineering Geology, 273, 105675.

Zhao, J., & Li, H. B. (2000). Experimental determination of dynamic tensile properties of a granite. International Journal of Rock Mechanics and Mining Sciences, 37(5), 861-866.

Zhu, G., Yin, J.-H., & Graham, J. (2001). Consolidation modelling of soils under the test embankment at Chek Lap Kok International Airport in Hong Kong using a simplified finite element method. Canadian Geotechnical Journal, 38(2), 349-363.

Zolfaghari, A., Sohrabi Bidar, A., Maleki Javan, M. R., Haftani, M., & Mehinrad, A. (2015). Evaluation of rock mass improvement due to cement grouting by Q-system at Bakhtiary dam site. International Journal of Rock Mechanics and Mining Sciences, 74, 38-44.

Zorlu, K., Gokceoglu, C., Ocakoglu, F., Nefeslioglu, H. A., and Acikalin, S. 2008. Prediction of uniaxial compressive strength of sandstones using petrography-based models. Engineering Geology, 96, 141–158.

1.6 Appendix: data tables for site-specific statistics of clay, sand, and rock properties

Table 1.A1. Site-specific clay property statistics (databases: CLAY/10/7490, CLAY/8/12225, CLAY/12/3997 & SH-CLAY/11/4051)

Source	Site Description	Property		No. of tests (≥30)	Range of data	Property mean	Property COV (%)
Wang and Zhu 2016	2010 Expo Park in Shanghai (Silty clay)	c (kPa)	Cohesion	42	4.0-29.0	13.7	38.0
		ϕ (°)	Friction angle	42	8.4-32.5	21.1	22.7
		E (MPa)	Young's modulus	42	2.3-13.9	5.2	51.9
Chin et al. 1994	Taipei City Hall Station in Taiwan (Clay)	w (%)	Natural moisture content	56	26.6-48.1	36	14.3
		LL (%)	Liquid limit	56	21.9-46.8	36	16.4
		PI (%)	Plasticity index	56	5.9-29.1	14.9	35.0
		γ_t (kN/m^3)	Total unit weight	56	17.9-20.9	19.0	3.3
Zhang et al. (2020)	Shanghai Clay Database SH-CLAY/11/4051	LL (%)	Liquid limit	2229	26.3-58.7	40.3	22
		PL (%)	Plastic limit	2350	13.8-43.50	22.25	9
		PI (%)	Plasticity index	4044	10.3-30.9	18.2	18
		w (%)	Water content	4011	23.30-63.60	43.29	15
		LI	Liquidity index	2067	0.49-2.19	1.15	22
		e	Void ratio	3875	0.67-1.86	1.24	14
		K_0	At-rest lateral pressure coefficient	264	0.43-0.65	0.51	9
		s_u/σ'_v	Normalized UC	148	0.10-0.59	0.19	34
		S_t	UC	181	1.5-7.6	5.2	28
		s_u/σ'_v	Normalized VST	352	0.22-0.71	0.31	23
		S_t	VST	384	2.7-7.8	3.95	17
		p_s/σ'_v	Specific penetration resistance ratio	1148	2.55-46.05	5.71	45
Gregersen and	Baastad (Norway)	w (%)	Natural moisture content	32	25.0-35.7	30.1	9.8

Løken (1979)		LL (%)	Liquid limit	30	19.1-43.2	31.9	24.6
		PL (%)	Plastic limit	30	11.2-28.7	21.2	21.8
		PI (%)	Plasticity index	30	5.0-17.5	10.7	36.6
		S_t	Sensitivity	21	1.5-6.0	3.7	35.7
Hanzawa (1979)	Natsushima (Japan)	w (%)	Natural moisture content	47	27.7-74.0	60.1	15.9
		LL (%)	Liquid limit	47	60.5-96.6	83.5	10.4
		PL (%)	Plastic limit	47	25.2-60.8	38.6	14.2
		PI (%)	Plasticity index	47	35.3-54.7	44.9	11.5
		LI	Liquid index	47	0.8-1.0	0.9	5.8
		s_u/σ'_v	Normalized VST	17	0.50-0.67	0.60	7.7
Ladd (1972)	Portsmouth, New Hampshire (USA)	w (%)	Natural moisture content	31	28.9-57.8	48.4	15.5
		LL (%)	Liquid limit	31	24.5-51.2	38.3	16.3
		PL (%)	Plastic limit	31	16.7-24.8	21.2	9.3
		PI (%)	Plasticity index	31	7.8-26.8	17.1	25.8
		LI	Liquid index	28	1.33-2.53	1.76	15.2
		s_u/σ'_v	Normalized VST	19	0.18-0.31	0.24	19.2
		S_t	Sensitivity	18	7.3-12.9	9.5	18.6
Bjerrum and Lo (1963)	Skabo, Oslo (Norway)	w (%)	Natural moisture content	55	32.4-50.5	40.8	13.8
		LL (%)	Liquid limit	54	40.8-60.0	51.1	10.5
		PL (%)	Plastic limit	54	20.8-29.2	23.9	9.7
		PI (%)	Plasticity index	54	19.2-31.7	27.1	12.9
		LI	Liquid index	54	0.3-0.8	0.6	21.9
		s_u (kPa)	VST	42	21.4-37.8	28.8	14.9
		s_u (kPa)	UC	20	21.7-45.9	30.4	19.4
		S_t	Sensitivity	48	2.6-8.9	5.2	23.5
陳厚銘 and 謝百鍾	Taipei (Taiwan)	w (%)	Natural moisture content	23	25.5-40.8	36.2	10.6
		LL (%)	Liquid limit	23	30.1-48.4	39.4	12.3

(1996)		PL (%)	Plastic limit	23	19.5-24.6	22.6	6.6
		PI (%)	Plasticity index	23	8.8-23.7	16.8	22.5
		B_q	Pore pressure parameter	23	0.10-0.77	0.61	27.7
		OCR	Over consolidation ratio	17	1.13-1.53	1.30	10.2
Jacob and G (2016)	Kuttanad (India)	w (%)	Natural moisture content	60	50-95	67.5	18.4
		LL (%)	Liquid limit	60	68-131	91.7	18.6
		PL (%)	Plastic limit	60	29-69	46.2	16.1
		PI (%)	Plasticity index	60	27-62	45.6	23.1
		LI	Liquid index	60	0.3-0.7	0.5	17.6
		C_c	Compression index	60	0.38-0.79	0.57	18.2
Kinner (1970)	Boston (USA)	w (%)	Natural moisture content	40	20.5-36.8	28.4	15.7
		LL (%)	Liquid limit	39	30.0-45.5	38.7	15.5
		PL (%)	Plastic limit	39	17.5-23.9	20.1	12.0
		PI (%)	Plasticity index	39	12.5-22.5	18.6	22.2
		LI	Liquid index	36	0.24-0.61	0.42	20.1
Lunne et al. (1985)	Sleipner Area (Norway)	w (%)	Natural moisture content	35	14.9-27.7	22.5	16.5
		LL (%)	Liquid limit	30	32.7-56.4	41.5	12.9
		PL (%)	Plastic limit	30	16.0-23.9	19.4	8.3
		PI (%)	Plasticity index	30	15.9-32.6	22.2	18.2
		LI	Liquid index	30	-0.11-0.35	0.19	60.6
		B_q	CPTu pore pressure parameter	32	-0.03-0.63	0.34	58.3
		q_{t1}	Normalized cone tip resistance	26	2.64-9.92	4.68	39.8
Mayne (1991)	Jamestown, Virginia (USA)	w (%)	Natural moisture content	33	27.7-43.4	35.2	10.7
Bjerrum (1954)	Toyon, Oslo (Norway)	LL (%)	Liquid limit	32	23.1-41.4	31.4	19.3
		PL (%)	Plastic limit	32	16.4-26.6	20.9	11.1
		LI	Liquid index	32	0.6-3.1	0.8	33.0

	Manglerud (Norway)	w (%)	Natural moisture content	37	26.5-41.3	35.5	10.6
		LL (%)	Liquid limit	37	19.4-39.0	24.8	18.0
		PL (%)	Plastic limit	37	14.9-24.8	18.1	12.6
		s_u/σ'_v	Normalized VST	20	0.05-0.22	0.13	33.4
		s_u/σ'_v	Normalized UC	13	0.03-0.17	0.05	17.9
	Drammen (Norway)	w (%)	Natural moisture content	38	28.5-44.7	35.2	13.7
		LL (%)	Liquid limit	38	31.8-45.8	38.1	8.6
		PL (%)	Plastic limit	38	18.2-24.8	21.2	8.3
		PI (%)	Plasticity index	38	9.4-23.4	16.9	20.5
		LI	Liquid index	35	0.5-1.38	0.80	29.1
		B_q	CPTu pore pressure parameter	40	0.45-0.90	0.71	16.1
Olsen (1982)	Mid-Atlantic (USA)	LL (%)	Liquid limit	48	22.0-61.0	43.3	23.2
		PL (%)	Plastic limit	48	15.0-30.0	22.5	20.5
		PI (%)	Plasticity index	48	6.0-34.0	20.4	29.3
		LI	Liquid index	48	0-3.7	1.3	43.0
		C_c	Compression index	40	0.1-0.7	0.38	39.8
		C_{ur}	Swell index	40	0.01-0.11	0.06	44.3
Cao et al. (2001)	Singapore	w (%)	Natural moisture content	33	54.7-80.4	64.6	9.7
		LL (%)	Liquid limit	33	64.1-104.2	87.8	9.8
		PL (%)	Plastic limit	33	24.5-41.6	33.0	16.9
		PI (%)	Plasticity index	33	39.6-70.2	54.8	13.0
		LI	Liquid index	33	0.24-0.98	0.59	29.2
		OCR	Over consolidation ratio	30	1.12-2.37	1.67	34.6
		C_c	Compression index	46	0.56-1.27	0.87	18.1
		C_{ur}	Swell index	46	0.05-0.25	0.16	22.6
Chung et al.	Busan	w (%)	Natural moisture content	55	23.2-77.3	53.5	26.0

(2005)	(South Korea)	LL (%)	Liquid limit	55	30.9-74.3	54.6	20.6
		PL (%)	Plastic limit	55	14.6-55.7	28.1	26.8
		PI (%)	Plasticity index	55	10.7-40.0	26.6	27.7
		LI	Liquid index	55	0.19-2.04	0.97	38.4
		s_u/σ'_v	Normalized VST	26	0.28-0.70	0.39	25.6
		OCR	Over consolidation ratio	56	0.13-1.60	0.90	36.6
		s_u/σ'_v	Normalized UC	46	0.04-0.56	0.29	39.0
		C_c	Compression index	56	0.15-1.05	0.55	40.7
Munshi (2003)	Bangladesh	w (%)	Natural moisture content	33	32.0-78.0	47.3	26.6
		LL (%)	Liquid limit	33	34.0-78.0	50.7	21.4
		PL (%)	Plastic limit	33	13.0-50.0	26.7	23.2
		PI (%)	Plasticity index	33	7.0-51.0	23.9	35.6
		LI	Liquid index	29	-0.332-1.89	0.75	63.9
		C_c	Compression index	33	0.19-0.65	0.32	30.4
Quiros and Young (1988)	Santa Barbara Channel, California (USA)	w (%)	Natural moisture content	32	32.3-86.5	47.3	24.0
		LL (%)	Liquid limit	31	48.5-84.1	62.3	11.5
		PL (%)	Plastic limit	32	28.5-37.4	32.2	6.6
		PI (%)	Plasticity index	31	16.0-48.1	30.3	19.2
		s_u/σ'_v	Normalized VST	15	0.3-0.7	0.49	28.0
		s_u/σ'_v	Normalized UU	10	0.32-0.69	0.44	24.0
Lacasse and Lunne (1982)	Norway	LL (%)	Liquid limit	35	50.2-74.4	63.5	11.6
		PL (%)	Plastic limit	35	29.0-38.3	34.6	5.9
		LI	Liquid index	35	0.7-1.8	1.0	21.8
		s_u/σ'_v	Normalized VST	30	0.2-0.5	0.3	21.4
		w (%)	Natural moisture content	45	57.3-70.0	63.4	6.0
		LI	Liquid index	40	0.42-1.14	0.74	22.7
		B_q	CPTu pore pressure	47	0.3-0.7	0.5	19.1

			parameter				
		q_{t1}	Normalized cone tip resistance	42	4.92-6.67	5.83	5.8
Cooling and Skempton (1942)	London (UK)	PL (%)	Plastic limit	100	21.7-31.9	26.7	9.4
Carrassco et al. (2004)	Madrid (Spain)	SPT-N	Standard penetration test blow count	40	42.3-95.9	75.3	15.9
Totani et al. (1998)	large clay waste disposal at Santa Barbara open-pit mine (center Italy)	E_{DMT} (MPa)	Modulus from DMT	32	8.69-18.15	12.22	20.2
Liu (1999)	Taipei (Taiwan)	PI (%)	Plasticity index	48	5.76-25.46	15.23	31.9
		s_u/σ'_v	Normalized CIUC	43	0.15-0.37	0.24	26.1
Chin et al. (1989)	Taipei (Taiwan)	w (%)	Natural water content	32	23.7-52.6	38.2	22.9
		PI (%)	Plasticity index	32	7.6-26.2	16.4	36.2
DeGroot and Lutenegger (2002)	Amherst, Massachusetts (USA)	w (%)	Natural water content	49	56.6-74.0	64.0	6.1
		LL (%)	Liquid limit	49	39.6-55.5	51.1	7.6
		PL (%)	Plastic limit	46	27.8-32.3	30.9	4.1
		PI (%)	Plasticity index	49	11.8-25.0	20.7	14.5
		LI	Liquidity index	49	1.2-2.9	1.7	21.6
		B_q	CPTu pore pressure parameter	32	0.63-0.96	0.75	13.1
		S_t	Sensitivity	47	4.8-23.2	10.6	47.2
		s_u/σ'_v	Normalized VST	50	0.23-0.68	0.38	26.6
Hanzawa (1979)	Natsushima (Japan)	w (%)	Natural water content	42	70.8-90.0	78.4	5.9
		LL (%)	Liquid limit	46	60.5-96.6	83.2	8.1
		PL (%)	Plastic limit	42	32.4-42.5	37.7	6.9
		PI (%)	Plasticity index	41	37.8-54.7	45.4	10.4
		LI	Liquidity index	46	0.76-0.99	0.89	5.8
		s_u/σ'_v	Normalized VST	18	0.50-0.67	0.60	7.5

Agarwal (1967)	Wraysbury (UK)	w (%)	Natural water content	33	25.0-29.4	27.1	5.0
		s_u/σ'_v	Normalized CIUC	21	0.16-0.29	0.23	15.8
			Normalized UU	12	0.39-1.24	0.71	32.8
Cozzolino (1961)	Santos (Spain)	LL (%)	Liquid limit	35	47.1-136.4	95.4	26.3
		C_c	Compression index	52	0.34-1.75	0.95	37.4
Bartlett and Lee (2004)	Salt Lake City, Utah (USA)	LL (%)	Liquid limit	26	27-70	48.6	22.3
		PL (%)	Plastic limit	26	9-45	22.1	37.2
		OCR	Over consolidation ratio	27	0.66-2.68	1.33	39.0
		C_c	Compression index	35	0.13-1.03	0.50	42.2
Finno and Chung (1992)	Chicago (USA)	w (%)	Natural water content	47	18.4	52.6	28.1
		OCR	Over consolidated ratio	16	0.81-2.41	1.57	34.9
Briaud et al. (2007)	Houston (USA)	C_c	Compression index	32	0.06-0.48	0.26	43.3
		C_{ur}	Swell index	30	0.03-0.15	0.08	48.4
Liu et al. (2011)	Lianyungang (China)	w (%)	Natural water content	136	30.3-753	52.3	19.2
		C_c	Compression index	136	0.20-1.03	0.59	29.0
Giao and Hien (2007)	Red River Delta (Vietnam)	C_c	Compression index	115	0.07-0.33	0.19	36.5
		C_{ur}	Swell index	115	0.006-0.106	0.04	45.8
Baroni et al. (2017)	Jacarepaguá Lowlands (Brazil)	LL (%)	Liquid limit	15	66.9-257.3	158.6	37.9
		PL (%)	Plastic limit	12	48.2-182.6	112.7	38.1
		PI (%)	Plasticity index	12	18.8-96.3	49.6	44.4
		S_t	Sensitivity	21	1.22-13.41	7.26	50.5
		C_c	Compression index	44	0.35-4.22	2.15	40.9
		C_{ur}	Swell index	28	0.06-0.47	0.21	48.1
Tan et al. (2003)	Klang (Malaysia)	w (%)	Natural water content	65	90.5-136.3	97.0	29.3
		C_c	Compression index	63	0.23-2.39	1.25	42.9
Long et al. (2007)	Belfast (Northern Ireland)	C_c	Compression index	40	0.08-1.26	0.63	46.3
		C_{ur}	Swell index	38	0.01-0.26	0.12	49.5

Kiran Jacob (2016)	Kuttanad (India)	w (%)	Natural water content	60	50-95	67.5	18.4
		LL (%)	Liquid limit	60	68-131	91.7	18.6
		PL (%)	Plastic limit	60	29-69	46.2	16.1
		PI (%)	Plasticity index	60	27-62	45.6	23.1
		LI	Liquidity index	60	0.25-0.74	0.47	17.6
		C_c	Compression index	60	0.38-0.79	0.57	18.2
Yin (1999)	Tseung Kwan O (Hong Kong)	PI (%)	Plasticity index	35	8.57-49.0	29.1	29.4
		C_c	Compression index	35	0.09-1.24	0.59	47.3
Zhu and Graham (2001)	Chek Lap Kok International Airport (Hong Kong)	C_c	Compression index	62	0.097-0.498	0.305	34.8
		C_{ur}	Swell index	62	0.009-0.060	0.031	35.6
Koutsoftas and Ladd (1985)	New Jersey Offshore (USA)	w (%)	Natural moisture content	14	49.0-61.5	53.5	7.0
		LL (%)	Liquid limit	14	61.7-88.4	72.1	9.4
		PL (%)	Plastic limit	14	26.4-36.1	30.9	10.7
		PI (%)	Plasticity index	14	32.7-52.3	41.2	11.9
		LI	Liquid index	14	0.47-0.63	0.55	11.1
		s_u/σ'_v	Normalized UC	14	0.82-1.42	1.02	15.2
		s_u/σ'_v	Normalized VST	12	0.89-1.20	1.03	10.3
Tavenas et al. (1975)	Saint-Alban, Quebec (Canada)	w (%)	Natural moisture content	10	43.6-68.9	55.8	17.4
		LL (%)	Liquid limit	10	28.4-44.3	35.9	17.0
		PL (%)	Plastic limit	10	16.9-24.3	23.1	12.6
		PI (%)	Plasticity index	10	10.5-20.0	15.2	24.9
		LI	Liquid index	10	1.95-3.42	2.47	19.2
		s_u/σ'_v	Normalized UU	11	0.53-0.75	0.63	11.7
		s_u/σ'_v	Normalized VST	15	0.52-1.01	0.61	19.9
Clough and	Hamilton Air Force	w (%)	Natural moisture content	16	82.0-93.9	90.0	3.5

Denby (1980)	Base (USA)	LL (%)	Liquid limit	16	81.2-96.0	88.3	4.9
		PL (%)	Plastic limit	16	36.5-46.9	40.0	6.8
		PI (%)	Plasticity index	16	42.6-52.1	48.3	6.8
		LI	Liquid index	16	0.89-1.22	1.04	9.3
		s_u/σ'_v	Normalized VST	16	0.23-0.44	0.34	18.9
Azzouz and Lutz (1986)	Empire, Louisiana (USA)	w (%)	Natural moisture content	19	28.1-49.9	42.2	16.4
		LL (%)	Liquid limit	19	49.8-98.5	81.4	13.3
		PL (%)	Plastic limit	19	16.9-31.4	26.1	13.8
		PI (%)	Plasticity index	19	32.9-68.6	55.3	15.6
		LI	Liquid index	19	0.09-0.41	0.29	27.2
		s_u/σ'_v	Normalized VST	13	0.11-0.25	0.19	23.6
		B_q	Pore pressure parameter	13	0.22-0.62	0.54	19.0
		s_u/σ'_v	Normalized UU	10	0.10-0.41	0.21	39.2
		s_u/σ'_v	Normalized UC	13	0.06-0.28	0.20	29.3
		q_{t1}	Normalized cone tip resistance	13	5.15-6.44	5.75	10.3
Simons (1960)	Drammen (Norway)	w (%)	Natural moisture content	12	30.7-40.4	34.9	7.7
		LL (%)	Liquid limit	10	19.3-38.6	34.6	8.0
		PL (%)	Plastic limit	10	16.7-20.1	18.5	5.8
		PI (%)	Plasticity index	10	11.4-19.4	16.1	14.3
		LI	Liquid index	10	0.71-1.33	1.06	15.8
		s_u/σ'_v	Normalized VST	12	0.08-0.22	0.16	24.8
Finno (1989)	Evanston (USA)	w (%)	Natural moisture content	13	31.0-41.0	37.7	7.0
		LL (%)	Liquid limit	13	15.0-23.0	19.3	12.0
		PL (%)	Plastic limit	13	10.0-23.0	18.3	17.8
		PI (%)	Plasticity index	14	17.0-28.0	22.8	10.2
		LI	Liquid index	13	0.06-0.35	0.24	47.6

		s_u/σ'_v	Normalized VST	11	0.17-0.37	0.25	22.7
		B_q	Pore pressure parameter	14	0.28-0.89	0.69	23.8
		S_t	Sensitivity	12	1.6-3.4	2.2	24.7
		s_u/σ'_v	Normalized UC	10	0.12-0.36	0.21	39.4
		q_{t1}	Normalized cone tip resistance	14	2.6-5.3	3.5	27.5
Konrad and Law (1987a)	Gloucester, Ontario (Canada)	w (%)	Natural moisture content	13	42.1-89.8	68.5	26.8
		LL (%)	Liquid limit	13	41.5-59.6	52.6	11.4
		PL (%)	Plastic limit	13	22.4-28.8	25.5	9.3
		PI (%)	Plasticity index	13	18.8-32.1	27.1	16.2
		LI	Liquid index	13	0.68-2.41	1.56	31.6
		B_q	Pore pressure parameter	13	0.67-0.84	0.74	8.2
		OCR	Over consolidation ratio	13	1.43-2.16	1.68	11.2
		s_u/σ'_v	Normalized VST	11	0.42-0.64	0.51	15.7
		q_{t1}	Normalized cone tip resistance	13	5.2-7.3	6.2	9.7
Koutsoftas et al. (1987)	Hong Kong	w (%)	Natural moisture content	13	25.8-64.1	43.3	25.6
		LL (%)	Liquid limit	13	39.0-87.7	60.8	26.9
		PL (%)	Plastic limit	13	17.1-32.5	23.4	18.6
		PI (%)	Plasticity index	13	21.0-65.1	37.4	35.2
		LI	Liquid index	11	0.34-0.75	0.56	25.6
		s_u/σ'_v	Normalized VST	13	0.45-0.88	0.61	25.4
		B_q	Pore pressure parameter	13	0.26-0.83	0.62	26.3
		OCR	Over consolidation ratio	12	1.9-3.8	2.7	23.8
		q_{t1}	Normalized cone tip resistance	13	5.8-16.9	10.5	35.7
Rochelle et al. (1988)	Louiseville, Quebec (Canada)	w (%)	Natural moisture content	12	61.9-85.3	75.0	7.7
		LL (%)	Liquid limit	12	61.5-71.1	64.8	5.2
		PL (%)	Plastic limit	12	25.2-28.4	26.3	4.0

		PI (%)	Plasticity index	12	35.8-43.6	38.5	6.6
		LI	Liquid index	12	1.01-1.56	1.27	12.6
		B_q	Pore pressure parameter	11	0.18-0.71	0.60	24.9
		q_{t1}	Normalized cone tip resistance	12	10.2-16.6	13.2	17.0
Chang (1991)	Norfolk Road (Singapore)	LI	Liquid index	13	0.54-0.92	0.74	17.2
		s_u/σ'_v	Normalized UU	13	0.11-0.22	0.16	23.4
		s_u/σ'_v	Normalized VST	12	0.20-0.36	0.24	17.9
		q_{t1}	Normalized cone tip resistance	12	1.59-3.26	2.29	21.7
Azzouz et al. (1982)	Delta Amacuro Offshore (Venezuela)	B_q	Pore pressure parameter	14	0.36-0.60	0.51	16.1
		s_u/σ'_v	Normalized VST	14	0.14-0.33	0.21	22.8
		q_{t1}	Normalized cone tip resistance	14	3.4-5.1	3.9	11.9
Azzouz et al. (1982)	Tucupita Offshore (Venezuela)	w (%)	Natural moisture content	12	60.9-73.2	65.7	4.7
		LL (%)	Liquid limit	12	73.6-104.5	91.5	9.2
		PL (%)	Plastic limit	12	34.5-40.4	38.6	4.9
		PI (%)	Plasticity index	12	39.1-64.5	52.8	13.4
		LI	Liquid index	12	0.41-0.78	0.52	20.8
		B_q	Pore pressure parameter	13	0.39-0.52	0.45	9.3
		s_u/σ'_v	Normalized VST	10	0.18-0.38	0.24	22.2
		q_{t1}	Normalized cone tip resistance	13	3.5-6.2	4.4	15.3
Roy et al. (1982)	Saint-Alban, Quebec (Canada)	w (%)	Natural moisture content	17	43.1-102.7	67.1	28.4
		LL (%)	Liquid limit	15	27.5-52.0	39.8	19.4
		PL (%)	Plastic limit	15	14.8-25.2	21.0	14.8
		PI (%)	Plasticity index	10	11.8-20.7	16.2	20.1
		LI	Liquid index	15	0.96-3.32	2.25	27.1
		B_q	Pore pressure parameter	17	0.27-0.34	0.31	7.4

		OCR	Over consolidation ratio	14	2.18-2.43	2.31	3.7
		s_u/σ'_v	Normalized VST	14	0.53-0.63	0.56	6.0
		q_{t1}	Normalized cone tip resistance	14	8.72-10.64	9.65	6.0
Baligh et al. (1980)	East Atchafalaya Basin (USA)	w (%)	Natural moisture content	17	39.4-79.5	55.2	19.4
		LL (%)	Liquid limit	17	61.4-437.8	83.6	25.4
		PL (%)	Plastic limit	17	19.6-40.0	28.0	22.2
		PI (%)	Plasticity index	17	37.5-116.6	55.5	37.6
		LI	Liquid index	16	0.23-0.66	0.48	27.4
		B_q	Pore pressure parameter	17	0.17-0.39	0.26	29.2
		OCR	Over consolidation ratio	17	1.11-1.94	1.32	14.5
		s_u/σ'_v	Normalized VST	18	0.31-0.44	0.39	8.5
		q_{t1}	Normalized cone tip resistance	17	3.05-4.10	3.76	9.0
Amundsen et al. (1985)	Troll East, North Sea (Norway)	B_q	Pore pressure parameter	20	0.62-0.94	0.80	9.9
		s_u/σ'_v	Normalized VST	18	0.23-0.46	0.29	18.1
		q_{t1}	Normalized cone tip resistance	18	4.67-8.46	5.62	17.0
Battaglio et al. (1986)	Upplands-Vasby (Sweden)	LI	Liquid index	15	0.88-1.20	0.98	7.5
		B_q	Pore pressure parameter	15	0.83-1.07	0.99	6.5
		OCR	Over consolidation ratio	15	1.12-1.40	1.17	5.6
Wei et al. (2010)	New Orleans (USA)	w (%)	Natural moisture content	11	42.0-76.4	52.7	17.9
		LL (%)	Liquid limit	11	57.5-105.1	76.9	16.7
		PL (%)	Plastic limit	11	24.0-37.1	28.6	13.2
		PI (%)	Plasticity index	11	30.6-68.0	48.3	21.0
		LI	Liquid index	11	0.30-0.61	0.49	18.4
		B_q	Pore pressure parameter	12	0.24-0.76	0.55	29.6
		s_u/σ'_v	Normalized UU	12	0.13-0.24	0.19	17.2
		q_{t1}	Normalized cone tip	12	1.92-4.00	2.52	22.0

			resistance				
Chang (1991)	Kallang Basin (Singapore)	w (%)	Natural moisture content	12	37.1-73.3	60.3	15.4
		B_q	Pore pressure parameter	13	0.55-0.80	0.66	13.1
		q_{t1}	Normalized cone tip resistance	13	1.54-2.40	2.04	12.4
Baligh et al. (1980)	Boston (USA)	w (%)	Natural moisture content	13	30.0-47.0	41.4	12.5
		LL (%)	Liquid limit	13	32.1-51.1	43.9	12.1
		PL (%)	Plastic limit	13	19.5-26.0	23.1	9.5
		PI (%)	Plasticity index	13	12.6-28.7	20.9	22.0
		LI	Liquid index	13	0.59-1.48	0.89	27.4
		B_q	Pore pressure parameter	12	0.13-0.73	0.56	31.3
Konrad and Law (1987b)	Saint-Marcel (Canada)	B_q	Pore pressure parameter	17	0.38-0.52	0.46	9.6
Lunne et al. (1985a)	Gullfaks A, North Sea (Norway)	w (%)	Natural moisture content	26	14.5-26.2	22.3	11.8
		LL (%)	Liquid limit	26	37.1-49.7	46.1	6.5
		PL (%)	Plastic limit	26	16.3-21.3	19.7	5.8
		PI (%)	Plasticity index	26	17.8-29.9	26.4	9.6
		B_q	Pore pressure parameter	26	0.08-0.51	0.37	32.0
		q_{t1}	Normalized cone tip resistance	13	8.2-12.2	10.3	11.9
Mayne (1991)	Jamestown, Virginia (USA)	w (%)	Natural moisture content	33	27.7-43.4	35.2	10.7
		B_q	Pore pressure parameter	19	0.34-0.67	0.55	12.8
		OCR	Over consolidation ratio	19	1.72-3.50	2.78	17.3
		q_{t1}	Normalized cone tip resistance	19	4.8-8.3	6.9	13.9
Senneset et al. (1988)	Stjørdal (Norway)	B_q	Pore pressure parameter	18	0.07-0.29	0.17	41.9
		q_{t1}	Normalized cone tip resistance	18	4.5-13.5	7.3	34.7
Mayne (2008)	Anchorage, Alaska (USA)	B_q	Pore pressure parameter	22	0.43-0.91	0.68	20.4
		q_{t1}	Normalized cone tip	22	5.3-11.0	8.1	22.2

			resistance				
Mayne (2008)	Brisbane (Australia)	B_q	Pore pressure parameter	18	0.68-0.86	0.78	7.3
		q_{t1}	Normalized cone tip resistance	18	2.4-3.3	2.9	9.0
Cadling and Odenstad (1950)	Gothenburg (Sweden)	S_t	Sensitivity	17	4.5-15.4	9.1	30.9
Ohtsubo et al. (1982)	Shiroishi, Saga (Japan)	w (%)	Natural moisture content	18	62.9-152.5	104.4	24.6
		LL (%)	Liquid limit	18	51.7-146.3	81.1	35.4
		PL (%)	Plastic limit	18	22.3-56.0	37.6	26.2
		PI (%)	Plasticity index	18	22.3-96.5	43.5	47.0
		LI	Liquid index	18	0.89-2.62	1.70	30.6
		S_t	Sensitivity	14	13.4-101.2	38.6	63.4
Eden and Hamilton (1957)	Hawkesbury, Ontario (Canada)	w (%)	Natural moisture content	13	61-90	79.4	10.4
		LL (%)	Liquid limit	13	53-72	64.3	8.1
		PL (%)	Plastic limit	13	25-28	26.4	2.9
		PI (%)	Plasticity index	13	26-46	38.0	13.8
		LI	Liquid index	13	1.20-1.68	1.40	10.7
		S_t	Sensitivity	12	2.57-7.84	4.36	39.3
		s_u/σ'_v	Normalized VST	12	0.62-1.04	0.84	15.1
Eden and Crawford (1957)	National Research Council, Ottawa (Canada)	w (%)	Natural moisture content	10	70.4-84.0	78.4	6.3
		LL (%)	Liquid limit	10	46.2-75.8	65.6	14.1
		PL (%)	Plastic limit	10	25.4-30.2	28.0	5.3
		PI (%)	Plasticity index	10	17.2-46.5	37.6	24.4
		S_t	Sensitivity	10	3.0-11.7	6.7	40.1
		s_u/σ'_v	Normalized VST	10	0.91-1.51	1.14	16.0
Andresen and Bjerrum 1957	Olso (Norway)	w (%)	Natural moisture content	17	26.4-43.6	35.7	12.6
		LL (%)	Liquid limit	17	30.5-53.0	42.3	15.3

		PL (%)	Plastic limit	17	18.1-30.7	22.0	15.1
		PI (%)	Plasticity index	17	11.6-31.9	20.3	24.0
		LI	Liquid index	17	0.48-0.95	0.68	20.1
		S_t	Sensitivity	17	2.0-4.8	3.5	26.1
		s_u	VST	15	21.9-45.3	33.2	19.6
Anderson (1982)	Rio de Janeiro (Brazil)	PL (%)	Plastic limit	15	33.78-76.5	52.2	22.2
		LI	Liquid index	15	1.09-1.63	1.32	11.6
		S_t	Sensitivity	13	2.2-5.0	3.9	23.5
Parry (1968)	Launceston, Tasmania (Australia)	s_u/σ'_v	Normalized VST	17	0.25-0.77	0.64	7.6
Lunne et al. (1985b)	Gullfaks Location C, North Sea (Norway)	w (%)	Natural moisture content	20	15.5-54.1	44.1	12.7
		LL (%)	Liquid limit	19	27.3-57.0	45.3	11.7
		PL (%)	Plastic limit	19	15.4-20.9	19.3	4.5
		PI (%)	Plasticity index	15	23.8-36.3	28.7	12.6
		LI	Liquid index	16	0.61-1.40	1.05	20.6
		B_q	Pore pressure parameter	40	0.45-0.90	0.71	16.1
		OCR	Over consolidation ratio	25	1.49-2.90	2.11	18.3
		q_{t1}	Normalized cone tip resistance	15	5.3-9.0	6.4	15.4
Rutledge (1939)	Boston (USA)	w (%)	Natural moisture content	24	22.4-46.5	34.0	20.7
		C_c	Compression index	24	0.16-0.47	0.31	33.4
		C_{ur}	Swell index	24	0.03-0.11	0.07	36.4
Briaud et al. (2007)	Houston (USA)	OCR	Over consolidation ratio	16	0.81-2.41	1.57	34.0
		C_c	Compression index	17	0.09-0.48	0.31	40.6
		C_{ur}	Swell index	17	0.03-0.26	0.12	50.5
Ohtsubo et al. (2007)	Shiroishi, Saga (Japan)	w (%)	Natural moisture content	18	57.1-155.9	109.1	26.0
		LI	Liquid index	18	0.89-2.41	1.32	26.2
		s_u/σ'_v	Normalized VST	18	0.26-1.15	0.51	36.4

		S_t	Sensitivity	18	15-41	26.4	28.4
Bjerrum (1967)	Norway	s_u/σ'_v	Normalized VST	18	0.16-0.25	0.21	13.3
Mayne and Frost (1988)	The confluence of the Anacostia and Potomac rivers, Washington, D.C. (USA)	w (%)	Natural moisture content	20	44.4-90.0	67.8	18.0
		LL (%)	Liquid limit	20	60.0-93.0	76.8	13.6
		PL (%)	Plastic limit	20	24.1-68.6	45.0	19.3
		PI (%)	Plasticity index	20	17.6-54.0	31.8	32.7
		OCR	Over consolidation ratio	22	1.37-3.00	1.87	23.0
		SPT-N	Standard penetration test blow count	17	1.05-2.76	1.75	24.2
		E_{DMT} (MPa)	Modulus from DMT	21	3.11-8.78	4.85	33.0
		K_{DMT}	Lateral earth pressure coefficient from DMT	20	2.40-3.89	2.92	11.9
Marchetti (1980)	Montalto (Italy)	E_{DMT} (MPa)	Modulus from DMT	18	8.96-18.15	12.91	18.7
		K_{DMT}	Lateral earth pressure coefficient from DMT	18	3.13-4.35	3.55	9.2
	Porto Tolle (Italy)	K_{DMT}	Lateral earth pressure coefficient from DMT	20	1.46-2.16	1.91	10.1
	Conca del Fuuno (Italy)	K_{DMT}	Lateral earth pressure coefficient from DMT	25	2.65-3.30	2.96	6.2
Cheshomi and Ghodrati (2014)	Mashhad (Iran)	SPT-N	Standard penetration test blow count	15	8.97-50.33	27.33	45.1
		E_{PMT} (MPa)	Modulus from PMT	15	10.3-43.8	23.0	39.1
Briaud (1997)	TAMU Riverside Campus, Texas (USA)	w (%)	Natural moisture content	10	19.2-39.2	26.9	21.6
		LL (%)	Liquid limit	10	42.5-76.7	64.2	17.1
		PL (%)	Plastic limit	10	13.6-32.3	19.7	28.5
		PI (%)	Plasticity index	10	28.9-60.9	44.6	20.7
Skempton (1961)	Bradwell (UK)	K_0	coefficient of earth pressure at rest	12	1.46-2.8	2.14	22.0
Watabe et al. (2003);Larsson and Mulabdic	Drammen (Norway)	w (%)	Natural moisture content	16	32.1-43.7	37.0	9.5
		LL (%)	Liquid limit	16	18.2-22.1	20.2	5.5
		PL (%)	Plastic limit	16	34.8-48.1	40.5	10.2

(1991)		PI (%)	Plasticity index	16	15.5-26.0	20.3	15.6
		K_{DMT}	Lateral earth pressure coefficient from DMT	16	2.96-4.52	3.85	16.2
Watabe et al. (2003)	Pusan, Yangsan	w (%)	Natural moisture content	18	16.5-68.7	59.5	10.3
		LL (%)	Liquid limit	18	22.9-25.8	24.7	3.4
		PL (%)	Plastic limit	18	52.4-71.7	61.6	9.3
		PI (%)	Plasticity index	18	29.6-16.1	37.0	14.6
		OCR	Over consolidation ratio	10	1.15-1.31	1.22	4.3
		K_{DMT}	Lateral earth pressure coefficient from DMT	24	2.08-3.16	2.67	9.9
Watabe et al. (2003);Tanaka et al. (2001a)	Yokohama port, Yamashita (Japan)	OCR	Over consolidation ratio	16	1.81-2.21	1.96	6.2
		w (%)	Natural moisture content	24	51.0-99.9	83.9	16.3
		LL (%)	Liquid limit	24	28.5-54.2	44.6	15.5
		PL (%)	Plastic limit	24	54.9-125.0	106.4	19.7
		PI (%)	Plasticity index	24	29.6-46.1	37.0	14.6
		K_{DMT}	Lateral earth pressure coefficient from DMT	26	2.10-3.11	2.57	7.6
Tanaka et al. (2001a);Silvestri (2003)	Louiseville, Quebec (Canada)	w (%)	Natural moisture content	13	64.0-87.2	73.8	9.1
		LL (%)	Liquid limit	13	61.2-72.1	66.6	4.7
		PL (%)	Plastic limit	13	23.3-26.0	24.7	3.6
		PI (%)	Plasticity index	13	36.8-46.1	41..9	6.5
		LI	Liquid index	13	0.98-1.48	1.17	12.4
		K_{DMT}	Lateral earth pressure coefficient from DMT	13	5.07-11.95	7.28	31.7
Kamei and Tanaka (2003)	Ariake Sea (Japan)	OCR	Over consolidation ratio	17	1.39-2.18	1.62	14.3
		w (%)	Natural moisture content	16	91.6-152.4	120.2	18.9
		LL (%)	Liquid limit	16	68.0-128.3	104.2	16.7
		PL (%)	Plastic limit	16	31.5-52.2	44.1	12.3
		PI (%)	Plasticity index	16	36.5-80.6	60.2	20.8

		LI	Liquid index	16	1.07-1.65	1.27	12.6
		s_u/σ'_v	Normalized VST	15	0.27-0.49	0.37	16.2
		K_{DMT}	Lateral earth pressure coefficient from DMT	17	1.73-3.36	2.12	21.6
Watabe et al. (2004)	Ekachai, Bangkok (Thailand)	w (%)	Natural moisture content	10	47.7-98.0	74.5	20.6
		LL (%)	Liquid limit	10	61.6-109.3	87.4	17.4
		PL (%)	Plastic limit	10	22.6-35.8	26.6	16.4
		PI (%)	Plasticity index	10	39.0-75.4	60.8	18.8
		LI	Liquid index	10	0.61-0.90	0.78	12.8
		OCR	Over consolidation ratio	10	1.17-1.87	1.53	14.8
		E_{DMT} (MPa)	Modulus from DMT	13	1.02-2.46	1.12	33.9
		K_{DMT}	Lateral earth pressure coefficient from DMT	13	2.28-4.48	2.86	20.8
Tanaka et al. (2001b);Watabe et al. (2003)	Merlion park (Singapore)	w (%)	Natural moisture content	13	46.6-60.2	55.3	7.5
		PL (%)	Plastic limit	13	21.0-25.1	23.5	4.3
		LL (%)	Liquid limit	13	62.8-82.2	73.6	7.3
		PI (%)	Plasticity index	13	40.0-57.0	50.1	9.9
		LI	Liquid index	13	0.57-0.74	0.64	9.2
		s_u/σ'_v	Normalized VST	10	0.14-0.35	0.23	25.8
		K_{DMT}	Lateral earth pressure coefficient from DMT	15	2.38-3.94	2.95	14.9
Lunne et al. (1990)	Onsoy (Norway)	w (%)	Natural moisture content	10	58.3-66.5	61.6	4.8
		PL (%)	Plastic limit	10	29.1-36.5	33.4	7.6
		LL (%)	Liquid limit	10	53.7-69.0	59.1	8.5
		PI (%)	Plasticity index	10	19.2-32.5	25.9	15.7
		LI	Liquid index	10	0.91-1.30	1.10	11.4
		K_0	coefficient of earth pressure at rest	13	0.53-0.68	0.61	8.4
		s_u/σ'_v	Normalized VST	16	0.26-0.28	0.27	3.2

		K_{DMT}	Lateral earth pressure coefficient from DMT	20	2.97-3.67	3.23	6.4
Lunne et al. (1990)	Madingley England (UK)	w (%)	Natural moisture content	17	23.8-31.3	28.5	6.6
		PL (%)	Plastic limit	17	25.9-33.2	28.7	7.3
		LL (%)	Liquid limit	17	67.4-81.2	73.9	4.8
		PI (%)	Plasticity index	17	40.2-52.7	45.2	7.0
		K_0	coefficient of earth pressure at rest	10	1.07-1.73	1.49	17.3
		K_{DMT}	Lateral earth pressure coefficient from DMT	13	6.15-10.8	7.91	16.9
Hight et al. (2003)	Canons Park, London (UK)	w (%)	Natural moisture content	16	27.9-33.1	30.4	5.2
		PL (%)	Plastic limit	16	49.5-66.3	58.4	8.9
		LL (%)	Liquid limit	16	71.3-83.3	76.2	5.2
		PI (%)	Plasticity index	16	13.4-21.8	17.8	12.3
		E_{DMT} (MPa)	Modulus from DMT	10	18.29-27.82	22.8	11.1
		K_{DMT}	Lateral earth pressure coefficient from DMT	16	3.30-19.53	11.51	31.0
Hight et al. (2003)	Waterloo, London (UK)	w (%)	Natural moisture content	11	23.7-29.2	27.3	6.9
		PL (%)	Plastic limit	11	35.8-51.4	43.2	13.4
		LL (%)	Liquid limit	11	58.0-72.1	68.8	7.0
		PI (%)	Plasticity index	11	20.5-34.0	25.7	16.2
		K_0	coefficient of earth pressure at rest	13	1.09-1.54	1.29	11.0
Takemura et al. (2006)	Can Tho site, Mekong Delta (Vietnam)	E_{DMT} (MPa)	Modulus from DMT	11	3.04-4.55	3.71	12.2
		K_{DMT}	Lateral earth pressure coefficient from DMT	11	2.52-3.11	2.87	7.1
Coutinho et al. (2006);Coutinho et al. (2008)	RRS1, Recife (Brazil)	E_{DMT} (MPa)	Modulus from DMT	16	2.41-3.82	3.01	13.7
		SPT-N		23	1-4	2.3	34.8
		M_d (MPa)	Constrained tangent modulus	13	2.38-4.45	3.21	20.8
		K_{DMT}	Lateral earth pressure coefficient from DMT	23	2.59-5.28	3.61	25.8

	RRS2, Recife (Brazil)	OCR	Over consolidation ratio	11	0.84-1.04	0.94	7.8
		M_d (MPa)	Constrained tangent modulus	11	0.31-0.86	0.49	37.2
		K_{DMT}	Lateral earth pressure coefficient from DMT	17	2.28-3.66	2.71	12.0
DeGroot and Lutenegger (2002)	CVVC, New England (USA)	w (%)	Natural moisture content	17	56.1-72.2	63.1	7.1
		LL (%)	Liquid limit	17	39.8-55.5	50.8	7.2
		PL (%)	Plastic limit	17	24.3-33.5	30.4	7.2
		PI (%)	Plasticity index	17	12.1-23.9	20.4	15.6
		LI	Liquid index	17	1.23-2.91	1.65	24.4
		E_{DMT} (MPa)	Modulus from DMT	13	4.7-3.4	5.0	4.6
		S_t	Sensitivity	19	4.6-7.6	6.11	12.4
		s_u/σ'_v	Normalized VST	17	4.6-7.5	0.06	20.5
		K_{DMT}	Lateral earth pressure coefficient from DMT	17	2.45-5.25	3.59	23.9
Leong and Rahardjo (2002)	Jurong Formation - residual soil (Singapore)	SPT-N	Standard penetration test blow count	14	6.8-29.2	20.1	36.0
Bihs et al. (2013)	Kvennild (Norway)	w (%)	Natural moisture content	12	30.5-40.0	35.6	10.2
		PI (%)	Plasticity index	12	3.2-9.0	6.2	35.2
		OCR	Over consolidation ratio	11	1.45-2.62	1.09	17.4
		M_d (MPa)	Constrained tangent modulus	10	2.32-5.51	4.11	26.4
Cabrera et al. (2013)	tunnel next Barcelona (Spain)	w (%)	Natural moisture content	13	19.9-23.5	21.9	6.1
		PL (%)	Plastic limit	13	17.9-21.2	20.1	5.9
		LL (%)	Liquid limit	13	26.3-31.8	29.7	5.1
		PI (%)	Plasticity index	13	7.1-11.4	9.6	11.6
		E_{PMT} (MPa)	Modulus from PMT	13	15.0-26.9	22.1	19.8
Tong et al. (2013)	Nanjing Fourth Bridge site A, China	w (%)	Natural moisture content	18	299.1-46.6	34.3	14.1
		PL (%)	Plastic limit	18	16.5-25.2	20.8	12.6

		LL (%)	Liquid limit	18	27.4-39.4	33.4	13.1
		PI (%)	Plasticity index	18	9.2-16.4	12.6	18.8
		SPT-N	Standard penetration test blow count	12	6.3-1.0	7.9	15.9
Wang et al. (2013)	Tsengwen reservoir (Taiwan)	E_{DMT} (MPa)	Modulus from DMT	10	1.47-2.43	1.80	14.6
Bosco and Monaco (2016)	N1, north side of Tevere river (Italy)	K_{DMT}	Lateral earth pressure coefficient from DMT	24	1.35-3.90	1.96	18.1
	N2, north side of Tevere river (Italy)	E_{DMT} (MPa)	Modulus from DMT	18	3.90-11.48	8.40	28.0
		K_{DMT}	Lateral earth pressure coefficient from DMT	18	1.57-2.51	2.13	14.9
	N3, north side of Tevere river (Italy)	E_{DMT} (MPa)	Modulus from DMT	24	2.38-14.74	8.23	43.9
		K_{DMT}	Lateral earth pressure coefficient from DMT	24	1.54-2.96	2.28	13.8
	South side of Tevere river (Italy)	K_{DMT}	Lateral earth pressure coefficient from DMT	16	1.14-3.01	2.12	23.1
Cao et al. (2016)	Bradford West Gwillimbury, Ontario (Canada)	E_{DMT} (MPa)	Modulus from DMT	23	1.34-8.59	5.49	27.6
		K_{DMT}	Lateral earth pressure coefficient from DMT	21	3.09-6.64	5.00	21.3
Bihs et al. (2010)	Limerick (Ireland)	M_d (MPa)	Constrained tangent modulus	10	0.48-1.52	0.89	46.8
		K_{DMT}	Lateral earth pressure coefficient from DMT	10	2.51-5.14	3.37	29.1
Cruz (2009)	200th Street Overpass test, Vancouver (Canada)	E_{DMT} (MPa)	Modulus from DMT	11	0.99-2.10	1.54	24.2
		K_{DMT}	Lateral earth pressure coefficient from DMT	10	2.38-3.45	2.82	13.6
	Colebrook Overpass, Surrey, Vancouver (Canada)	w (%)	Natural moisture content	10	38.4-49.9	42.5	8.5
		PL (%)	Plastic limit	10	22.9-28.3	26.4	6.0
		LL (%)	Liquid limit	10	34.4-48.4	40.7	10.5
		E_{DMT} (MPa)	Modulus from DMT	12	0.24-1.09	0.71	35.3
		K_{DMT}	Lateral earth pressure coefficient from DMT	13	2.12-2.80	2.40	8.0
Iwasaki et al.	Komatsugawa, Tokyo	OCR	Over consolidation ratio	10	1.42-2.22	1.75	16.2

(1991)	Bay (Japan)	K_{DMT}	Lateral earth pressure coefficient from DMT	12	3.91-4.01	3.30	11.0
Windle and Wroth (1977)	Hendon, London (UK)	K_0	coefficient of earth pressure at rest	10	2.20-3.60	2.88	17.2
		E_{PMT} (MPa)	Modulus from PMT	10	38.0-90.6	66.2	22.0
Larsson and Eskilson (1989)	Lilla Mellosa, Stockholm (Sweden)	OCR	Over consolidation ratio	11	1.15-1.19	1.17	1.2
		E_{DMT} (MPa)	Modulus from DMT	13	0.60-2.01	1.10	39.4
		K_{DMT}	Lateral earth pressure coefficient from DMT	12	2.96-5.19	3.71	16.1
	Ska-Edeby, Stockholm (Sweden)	K_{DMT}	Lateral earth pressure coefficient from DMT	11	3.11-5.57	3.82	22.1
	Norrkoping (Sweden)	E_{DMT} (MPa)	Modulus from DMT	13	0.50-1.79	1.08	34.8
		K_{DMT}	Lateral earth pressure coefficient from DMT	13	2.08-3.65	3.04	16.7
Robertson et al. (1988)	Langley site, BC (Canada)	E_{DMT} (MPa)	Modulus from DMT	14	1.16-3.98	1.93	29.9
		K_{DMT}	Lateral earth pressure coefficient from DMT	16	5.21-7.57	6.08	11.2
Roque et al. (1988)	Glava, Stjordal (Norway)	E_{DMT} (MPa)	Modulus from DMT	15	1.52-3.00	2.32	20.7
		K_{DMT}	Lateral earth pressure coefficient from DMT	18	3.58-8.79	4.98	28.3
Carrassco et al. (2004)	Madrid (Spain)	SPT-N	Standard penetration test blow count	19	39.3-78.4	55.9	19.3
Carrassco et al. (2004)	Madrid (Spain)	SPT-N	Standard penetration test blow count	40	42.3-95.9	75.3	15.9
		E_{PMT} (MPa)	Modulus from PMT	22	68.3-271.0	160.6	36.1
Sandven et al. (2004)	Trondheim (Norway)	OCR	Over consolidation ratio	14	2.25-5.07	3.15	26.4
		M_d (MPa)	Constrained tangent modulus	13	2-8	4.6	41.9
Cavallaro et al. (2006)	Catania STM M6 (Italy)	E_{DMT} (MPa)	Modulus from DMT	19	2.58-7.05	4.63	23.2
		K_{DMT}	Lateral earth pressure coefficient from DMT	19	2.03-3.41	2.47	16.5
Cavallaro et al. (2016)	Bellini Garden, Catania (Italy)	E_{DMT} (MPa)	Modulus from DMT	19	16.67-24.37	19.32	11.1
		K_{DMT}	Lateral earth pressure coefficient from DMT	18	5.62-8.00	6.85	9.3

Totani et al. (2016)	Colle Cretone, Pineto (Italy)	E_{DMT} (MPa)	Modulus from DMT	19	27.71-28.58	33.72	10.1
		K_{DMT}	Lateral earth pressure coefficient from DMT	19	6.36-8.54	7.16	8.2
Totani et al. (1998)	Garigliano river, (Italy)	w (%)	Natural moisture content	17	39.5-52.0	46.1	7.5
		PL (%)	Plastic limit	19	26.0-39.1	32.2	10.7
		LL (%)	Liquid limit	19	53.0-84.5	69.8	13.5
		PI (%)	Plasticity index	19	22.2-49.9	37.6	18.8
		E_{DMT} (MPa)	Modulus from DMT	21	9.21-15.19	11.40	17.2
		K_{DMT}	Lateral earth pressure coefficient from DMT	21	3.35-5.58	4.67	17.5
	Santa Barbara (Italy)	K_{DMT}	Lateral earth pressure coefficient from DMT	48	1.49-3.11	2.03	20.2
Chen and Mayne (1994)	Port Huron, Michigan (USA)	w (%)	Natural moisture content	15	17.6-27.2	22.0	12.8
		PL (%)	Plastic limit	15	15.1-21.3	17.3	12.7
		LL (%)	Liquid limit	15	26.0-41.2	32.7	18.4
		E_{DMT} (MPa)	Modulus from DMT	26	4.24-10.72	6.38	28.2
		K_{DMT}	Lateral earth pressure coefficient from DMT	16	3.50-4.50	3.94	8.5
Rouainia et al. (2017)	Western Avenue in Allston, Boston (USA)	w (%)	Natural moisture content	14	29.3-38.3	32.4	8.3
		PL (%)	Plastic limit	14	16.5-21.6	18.3	8.9
		LL (%)	Liquid limit	14	32.1-44.8	37.9	9.6
		PI (%)	Plasticity index	14	14.4-24.7	19.6	16.4
		K_0	coefficient of earth pressure at rest	18	0.52-1.12	0.81	20.8
Kelly et al. (2017)	Ballina, New South Wales (Australia)	OCR	Over consolidation ratio	10	1.31-2.14	1.78	12.8
		S_t	Sensitivity	13	2.3-3.8	2.9	14.9
		K_{DMT}	Lateral earth pressure coefficient from DMT	24	1.68-9.95	4.16	49.4
White et al. (2007)	IA Highway 191 (Neola, Iowa) (USA)	E_{DMT} (MPa)	Modulus from DMT	12	0.51-2.59	1.40	45.8
		K_{DMT}	Lateral earth pressure coefficient from DMT	12	0.82-2.08	1.34	28.0

Santagata et al. (2005)		K_0	coefficient of earth pressure at rest	17	0.46-0.50	0.48	2.4
		w (%)	Natural moisture content	17	33.4-39.0	35.9	5.0
		LI	Liquid index	17	0.43-0.68	0.55	14.3
Kuo (1994)	National Taiwan University (Taiwan)	K_{DMT}	Lateral earth pressure coefficient from DMT	12	2.35-5.41	3.58	25.5
Powell and Uglow (1988)	Grangemouth	K_{DMT}	Lateral earth pressure coefficient from DMT	15	2.83-4.29	3.33	12.2
Penna (2006)	Alemoa-Santos, Sao Paulo (Brazil)	K_{DMT}	Lateral earth pressure coefficient from DMT	23	0.85-2.11	1.87	14.3
Sabatini et al. (2002)	Connecticut River Valley, Massachusetts (USA)	K_{DMT}	Lateral earth pressure coefficient from DMT	17	2.59-6.80	4.06	30.0
Huang et al. (2001)	sugarcane field beside high-speed rail (Taiwan)	K_{DMT}	Lateral earth pressure coefficient from DMT	10	2.03-3.99	2.90	23.7
Marchetti et al. (2001)	Venezia Lido (Italy)	K_{DMT}	Lateral earth pressure coefficient from DMT	23	1.42-2.80	1.91	16.9
	Stagno Livorno (Italy)	K_{DMT}	Lateral earth pressure coefficient from DMT	23	2.06-3.89	2.66	15.8
	S. Barbara (Italy)	K_{DMT}	Lateral earth pressure coefficient from DMT	11	12.16-19.84	15.12	13.7

Table 1.A2. Site-specific sand property statistics (databases: SAND/7/2794 & SAND/13/4113)

Source	Site Description	Property		No. of tests (≥10)	Range of data	Property mean	Property COV (%)
Lee and Seed (1967)	Sacramento River Sand	ϕ (°)	Friction angle	39	30.9-40.9	34.2	7.7
Kulhawy and Mayne (1990)	Ticino	ϕ (°)	Friction angle	64	32.6-47.5	52.0	9.3
Chin et al. (1988)	Hsinta Power Plant, Kaohsiung, Taiwan	q_{c1n}	Normalized cone tip resistance	35	17.6-106.8	62.4	31.2
		$(N_1)_{60}$	Normalized SPT-N	35	6.2-33.3	19.1	35.0
Huang et al. (1999)	Mia-Liao, Taiwan	q_{c1n}	Normalized cone tip resistance	40	40.4-245.2	142.4	34.1

Huang (1991)	Washed mortar sand	q_{c1n}	Normalized cone tip resistance	42	15.3-406.7	160.8	71.7
Bozbey and Togrol (2010)	Istanbul (Turkey)	SPT-N	Corrected SPT-N	53	15.1-70.5	45.9	31.3
		E_{PMT} (MPa)	Modulus from PMT	53	11.7-39.6	26.1	29.2
GEO (1989)	Ching Cheung Road landslide in Hong Kong (Completely decomposed granite)	w (%)	Natural moisture content	31	14.7-45.8	24.1	27
		ρ_b (kg/m^3)	Bulk density	31	1.7-2.1	2.0	4.9
		ρ_d (kg/m^3)	Dry density	31	1.1-1.9	1.6	9.5
		c (kPa)	Cohesion	30	1.7-39.6	17.5	51.4
		ϕ (°)	Friction angle	30	29.2-45.6	37.0	9.6
Been et al. (1987)	Erksak (Man-made)	γ_d(kN/m^2)	Dry unit weight	14	15.7-17.0	16.4	2.6
		e	Initial void ratio	14	0.53-0.66	0.59	7.2
		D_r (%)	Initial relative density	14	69.2-98.9	86.3	11.1
		q_{c1n}	Corrected normalized qc	14	30.2-265.6	146.7	45.8
		Φ (°)	Friction angle	14	31.4-40.2	36.1	7.8
Parkin et al. (1980)	Hokksund	q_{c1n}	Corrected normalized qc	28	68.5-430.9	254.6	40.1
		Φ (°)	Friction angle	28	38.5-49.8	45.7	5.3
Houlsby and Hitchman (1988)	Leighton Buzzard	q_{c1n}	Corrected normalized qc	19	26.2-484.3	196.7	68.0
		Φ (°)	Friction angle	19	33.2-46.4	39.5	11.5
Villet and Mitchell (1981)	Lone Star 60#	q_{c1n}	Corrected normalized qc	16	46.2-171.9	101.4	39.8
		Φ (°)	Friction angle	16	35.5-45.4	39.9	8.7
	Monterey 0	q_{c1n}	Corrected normalized qc	15	73.0-199.4	144.4	27.2
		Φ (°)	Friction angle	16	36.1-40.7	38.1	4.2
Greeuw et al. (1988)	Oostershelde	q_{c1n}	Corrected normalized qc	10	63.6-261.4	131.2	55.1
		Φ (°)	Friction angle	10	35.5-43.2	39.0	7.2
Unknown	Toyoura	q_{c1n}	Corrected normalized	11	27.6-297.0	116.8	68.0

		qc					
		Φ (°)	Friction angle	11	34.6-44.1	39.1	7.6
Salgado et al. (2000)	A Ottawa	e	Initial void ratio	17	0.54-0.70	0.63	7.0
		ϕ (°)	Friction angle	17	20.1-36.5	32.3	5.9
	B Ottawa	e	Initial void ratio	13	0.48-0.66	0.60	10.9
		ϕ (°)	Friction angle	13	32.5-40.8	35.7	7.9
	C Ottawa	e	Initial void ratio	12	0.42-0.58	0.53	11.3
		ϕ (°)	Friction angle	12	33.7-41.3	37.0	6.2
	D Ottawa	e	Initial void ratio	17	0.32-0.61	0.47	19.9
		ϕ (°)	Friction angle	17	32.4-45.5	38.3	12.5
	E Ottawa	e	Initial void ratio	11	0.38-0.54	0.47	10.4
		ϕ (°)	Friction angle	11	34.3-38.8	35.9	4.8
Huang (1991)	Messina	D_{50} (mm)	Median grain size	25	2.18-3.67	2.80	14.3
		$(N_1)_{60}$	Normalized SPT-N	25	21.2-39.5	28.6	16.5
Ghionna and Jamiolkowski (1991)	Holocene Coastal Plain	D_{50} (mm)	Median grain size	22	1.45-4.96	3.00	32.0
		$(N_1)_{60}$	Normalized SPT-N	25	14.4-31.9	22.1	25.6
Chapman and Donald (1981)	Frankston	ϕ (°)	Friction angle	11	35.2-41.4	39.6	5.0
Huntsman et al. (1986)	Caisson-retained Island, Canadian Beaufort Sea (Canada)	K_0	coefficient of earth pressure at rest	15	0.75-1.99	1.09	35.6
Unknown	Mantova (Italy)	K_0	coefficient of earth pressure at rest	15	0.32-1.23	0.64	34.0
		q_{c1n}	Normalized cone tip resistance	15	66.9-148.9	94.4	24.3
Marchetti (1980)	Torre Oglio (Italy)	$(N_1)_{60}$	Normalized SPT-N	17	5.9-19.1	13.1	30.6
		q_{c1n}	Normalized cone tip resistance	22	13.1-145.7	72.1	45.2
Marchetti et al. (2001)	Chieti (Italy)	E_{DMT} (MPa)	Modulus from DMT	13	10.7-35.3	20.8	38.9

Yagiz et al. (2008)	Denizli (Turkey)	E_{PMT} (MPa)	Modulus from PMT	10	8.2-15.4	10.6	29.0
Kuo (1994)	Wugu Industrial Area (Taiwan)	q_{c1n}	Normalized cone tip resistance	11	27.8-74.9	46.9	32.0
Marchetti (1985)	Po River Valley (Italy)	E_{DMT} (MPa)	Modulus from DMT	25	30.0-105.0	60.0	32.5
		q_{c1n}	Normalized cone tip resistance	25	66.0-220.9	120.0	34.6
Sandven (2003)	Halen (Norway)	E_{DMT} (MPa)	Modulus from DMT	10	5.14-8.32	6.36	16.0
Tong et al. (2012)	Nanjing Fourth Bridge site A (China)	$(N_1)_{60}$	Normalized SPT-N	29	4.3-11.7	5.7	36.3
		SPT-N	Standard penetration test blow count	24	4.3-11.0	7.3	18.4
Mlynarek et al. (2012)	Cylindrical tank (Poland)	E_{DMT} (MPa)	Modulus from DMT	11	30.2-84.5	56.0	27.7
		q_{c1n}	Normalized cone tip resistance	12	62.8-297.5	161.9	49.9
Tschuschke et al. (2013)	Zelazny Most dump (Poland)	q_{c1n}	Normalized cone tip resistance	28	19.9-101.3	55.0	33.4
Bosco and Monaco (2016)	N1, north side of Tevere river (Italy)	q_{c1n}	Normalized cone tip resistance	18	6.1-57.2	28.2	61.1
	N3, north side of Tevere river (Italy)	q_{c1n}	Normalized cone tip resistance	11	8.0-30.2	15.2	43.0
	south side of Tevere river (Italy)	q_{c1n}	Normalized cone tip resistance	14	6.3-25.1	14.1	38.5
Cruz (2009)	Fraser River Delta in Richmond, Vancouver (Canada)	$(N_1)_{60}$	Normalized SPT-N	16	13.6-34.9	21.9	32.2
		q_{c1n}	Normalized cone tip resistance	12	56.7-140.3	79.9	30.5
	Massey Tunnel, Richmond, Vancouver (Canada)	q_{c1n}	Normalized cone tip resistance	15	41.1-77.0	54.1	18.0
	Patterson Park, Delta, Vancouver (Canada)	q_{c1n}	Normalized cone tip resistance	10	83.3-122.6	100.5	15.0
Giacheti et al. (2006);Mio and Giacheti (2004)	Bauru, Sao Paulo (Brazil)	q_{c1n}	Normalized cone tip resistance	15	37.0-53.5	44.6	11.5
	Sao Carlos, Sao	$(N_1)_{60}$	Normalized SPT-N	18	3.4-13.5	8.9	36.7

	Paulo (Brazil)	q_{c1n}	Normalized cone tip resistance	12	11.5-37.6	19.4	36.1
Foa et al. (2004)	Salvador, Bahia state (Brazil)	$(N_1)_{60}$	Normalized SPT-N	11	4.0-15.0	8.4	38.4
Carrassco et al. (2006)	Madrid (Spain)	SPT-N	Standard penetration test blow count	22	40.5-99.0	69.4	23.8
Penna (2006)	Cajamar, Sao Paulo (Brazil)	E_{DMT} (MPa)	Modulus from DMT	19	20.2-62.1	32.6	29.6
	Embu, Sao Paulo (Brazil)	$(N_1)_{60}$	Normalized SPT-N	17	1.8-14.3	9.7	38.8
		E_{DMT} (MPa)	Modulus from DMT	14	8.9-33.4	22.6	32.8
Anderson et al. (2006)	Statesville, Iredell County, North Carolina (USA)	N_{60}	Corrected SPT-N	12	5.2-10.0	6.8	20.6
		E_{DMT} (MPa)	Modulus from DMT	12	8.75-13.17	11.72	10.9
Maugeri and Monaco (2006)	San Giuseppe La Rena, Catania (Italy)	E_{DMT} (MPa)	Modulus from DMT	18	37.9-98.8	71.4	24.6
Rocha et al. (2016)	UNESP research site, Bauru, Sao Paulo (Brazil)	E_{DMT} (MPa)	Modulus from DMT	20	27.1-48.8	36.5	18.1
		E_{PMT} (MPa)	Modulus from PMT	14	19.5-32.8	15.6	15.7
da Fonesca and Coutinho (2008)	Subway Station, Sao Paulo (Brazil)	K_0	coefficient of earth pressure at rest	13	1.0-3.8	2.2	36.9
Akbar et al. (2008)	River Ravi, Lahore (Pakistan)	N_{60}	Corrected SPT-N	10	9.6-21.5	14.9	27.1
Cao et al. (2008)	Changi East reclamation site (Singapore)	E_{DMT} (MPa)	Modulus from DMT	12	23.3-53.5	36.2	30.0
Cao et al. (2008)	Changi East reclamation site (Singapore)	E_{DMT} (MPa)	Modulus from DMT	10	27.6-46.4	35.7	17.9
Arroyo et al. (2008)	Rampa1 (fine sand)	E_{DMT} (MPa)	Modulus from DMT	11	39.1-59.5	51.5	10.4
		q_{c1n}	Normalized cone tip resistance	11	53.5-103.1	71.4	19.5
	Rampa1 (silt)	E_{DMT} (MPa)	Modulus from DMT	11	9.3-57.2	38.6	45.7
		q_{c1n}	Normalized cone tip resistance	11	10.9-53.4	26.1	46.5
Totani et al.	Parma in Po River	E_{DMT} (MPa)	Modulus from DMT	13	8.0-25.8	14.0	36.8

(1998)	plain (Italy) (clay) Parma in Po River plain (Italy) (silt)	E_{DMT} (MPa)	Modulus from DMT	12	5.2-30.3	15.0	39.3
Brahana and Wang (1998)	Atlanta Olympic Stadium (USA)	N_{60}	Corrected SPT-N	12	7-18	13.4	28.2
		E_{DMT} (MPa)	Modulus from DMT	11	5.68-13.47	10.28	25.6
Sabatini et al. (2002)	Piedmont Province, in west-central Alabama (USA)	q_{c1n}	Normalized cone tip resistance	11	18.9-36.1	27.7	17.7
		E_{DMT} (MPa)	Modulus from DMT	10	1.47-2.83	2.21	19.4
Di Mariano et al. (2019)	Verge de Montserrat Station, Llobregat River delta, Bercelona (Spain)	E_{DMT} (MPa)	Modulus from DMT	12	10.9-42.0	26.9	37.2
Lutenegger (1986)	Russe (Bulgaria)	E_{DMT} (MPa)	Modulus from DMT	12	5.63-26.63	13.40	46.4
Huang et al. (2001)	sugarcane field beside high-speed rail (Taiwan)	E_{DMT} (MPa)	Modulus from DMT	12	7.13-27.34	15.61	41.6
Marchetti (1991)	Po river (Italy)	E_{DMT} (MPa)	Modulus from DMT	15	25.26-52.00	34.93	20.3
Modoni and Bzówka (2012)	Bojszowy Nowe (Poland)	E_{DMT} (MPa)	Modulus from DMT	15	26.7-78.2	49.9	32.5
		q_{c1n}	Normalized cone tip resistance	14	81.7-185.3	135.8	21.5
Ku and Mayne (2015)	San Matteo (Italy)	K_0	coefficient of earth pressure at rest	15	0.43-1.15	0.71	25.8

Table 1.A3. Site-specific intact rock property statistics (databases: ROCK/13 & ROCK/9/4069)

Source	Site Description	Property		No. of tests (≥30)	Range of data	Property mean	Property COV (%)
Diamantis et al. (2009)	Western Othrys mt., Greece, (Serpentinite)	σ_{ci} (MPa)	Uniaxial compressive strength	32	19.2-125.7	60.3	44.8
		I_{s50} (MPa)	Point load index	32	1.0-4.9	3.1	35.1

		n (%)	Porosity	32	0.4-4.6	1.5	70.6
		γ (kN/m^3)	Unit weight	32	24.4-26.7	25.6	2.2
Aggistalis et al. (1996)	Metsovo road tunnel, Epirus, Northern Greece (Gabbro)	σ_{ci} (MPa)	Uniaxial compressive strength	63	6.3-107.5	43.1	52.8
		I_{s50} (MPa)	Point load index	63	0.3-4.5	1.36	69.85
		E_i (GPa)	Young's modulus	63	1.0-9.8	4.5	50.9
		R_L	Schmidt hammer rebound number	63	19.5-57.2	32.2	25.0
	Metsovo road tunnel, Epirus, Northern Greece (Basalt)	σ_{ci} (MPa)	Uniaxial compressive strength	30	17.1-91.2	46.7	41.0
		I_{s50} (MPa)	Point load index	30	0.7-3.4	3.1	26.5
		E_i (GPa)	Young's modulus	30	1.2-12.1	5.1	51.8
		R_L	Schmidt hammer rebound number	30	21.8 – 55.0	42.4	16.1
Tamrakar et al. (2007)	Siwalik Hills, central Nepal (Sandstone)	σ_{ci} (MPa)	Uniaxial compressive strength	44	1.3-51.6	26.8	52.2
		I_{s50} (MPa)	Point load index	44	0.1-4.0	1.3	75.5
		E_i (GPa)	Young's modulus	44	0.1-1.1	0.8	32.3
		R_L	Schmidt hammer rebound number	44	12-53	31.6	32.5
Zorlu et al. (2008)	Karakaya, Greece (Sandstone)	σ_{ci} (MPa)	Uniaxial compressive strength	61	17.5-107.8	57.9	43.7
Arman et al. (2007)	Kandira, Turkey (Limestone)	σ_{ci} (MPa)	Uniaxial compressive strength	43	35-52	43.4	12.6
		I_{s50} (MPa)	Point load index	43	3.0-4.0	3.7	11.9
		σ_{bt} (MPa)	Brazilian tensile strength	43	4.0 -16.0	10.7	21.0
		R_L	Schmidt hammer rebound number	43	33-40	36.0	5.7
Yilmaz and Yuksek (2008)	Sivas, Turkey (Gypsum)	σ_{ci} (MPa)	Uniaxial compressive strength	39	8.1-35.6	21.6	32.6
		I_{s50} (MPa)	Point load index	39	1.2-3.2	2.5	20.6
		E_i (GPa)	Young's modulus	39	15.7-42.8	28.0	26.8
		R_L	Schmidt hammer	39	27-48	37.1	14.9

			rebound number				
Aydin and Basu (2005)	Hong Kong (Granite)	σ_{ci} (MPa)	Uniaxial compressive strength	40	6.3-196.5	64.2	86.5
		ρ (g/cm^3)	Density	40	2.1-2.7	2.5	5.6
		E_i (GPa)	Young's modulus	40	4.5-53.2	22.6	17.0
		n (%)	Porosity	40	1.3-21.0	9.8	61.8
		R_L	Schmidt hammer hardness	40	20-65.8	47.9	26.2
Kocbay and Kilic (2006)	North Anatolian Fault Zone, Turkey (Basalt)	σ_{ci} (MPa)	Uniaxial compressive strength	114	9.8-130.2	52.6	45.4
		I_{s50} (MPa)	Point load index	149	1.2- 15.1	6.3	45.0
		γ (kN/m^3)	Unit weight	172	22.3-28.3	25.7	4.0
		E_i (GPa)	Young's modulus	99	8.9-89.1	39.3	43.8
		n (%)	Porosity	172	2.1-14.9	7.2	35.7
		v	Poisson ratio	172	0.2-0.4	0.3	9.7
		G_s	Specific gravity	172	2.8-3.0	2.9	1.7
Bastola and Chugh (2015)	Illinois (USA)	γ (kN/m^3)	Unit weight	44	17.5-25.9	22.8	8.1
Nefeslioglu (2013)	Firuzköy, Istanbul (Turkey)	γ (kN/m^3)	Unit weight	66	16.3-20.1	18.2	4.5
		σ_{ci} (MPa)	Uniaxial compression strength	66	0.7-4.1	1.9	40.1
		E_i (GPa)	Young's Modulus	65	0.03-0.44	0.13	60.0
Azimian and Ajalloeian (2014)	Shiraz, Fars Province (Iran)	γ (kN/m^3)	Unit weight	40	20.5-25.7	23.4	5.4
		σ_{ci} (MPa)	Uniaxial compression strength	40	15.3-88.9	47.8	41.1
		E_i (GPa)	Young's Modulus	40	5.6-30.7	15.9	41.2
Khanlari and Abdilor (2011)	Hamadan Province (Iran)	γ (kN/m^3)	Unit weight	40	25.4-27.1	26.3	1.5
		I_{s50} (MPa)	Point load index	40	1.2-5.5	3.7	27.8
		σ_{ci} (MPa)	Uniaxial compression strength	40	56.2-104.0	87.1	14.0
Diamantis et al. (2011)	Greece	R_L	Schmidt hammer hardness	35	59-65	62.6	3.0

		σ_{ci} (MPa)	Uniaxial compression strength	35	65.2-241.6	142.1	32.2
		E_i (GPa)	Young's Modulus	35	26.4-69.3	44.6	30.7
Dehghan et al. (2010)	Haji Mine, Bamyan Province (Afghanistan)	R_L	Schmidt hammer hardness	30	25.6-30.5	27.9	5.1
		I_{s50} (MPa)	Point load index	30	2.3-4.0	3.2	13.2
		σ_{ci} (MPa)	Uniaxial compression strength	30	22.7-71.5	39.0	32.3
		E_i (GPa)	Young's Modulus	30	3.0-11.5	5.4	37.1
Tamrakar et al. (2007)	Siwalik Hills (Nepal)	R_L	Schmidt hammer hardness	44	12-53	32.1	31.7
		I_{s50} (MPa)	Point load index	44	0.05-4.00	1.27	75.5
		σ_{ci} (MPa)	Uniaxial compression strength	44	1.3-51.6	26.7	52.2
		E_i (GPa)	Young's Modulus	44	0.06-1.09	0.75	32.3
Ng et al. (2015)	Cotai,Taipa,Coloane,Macau Peninsula (Macao)	R_L	Schmidt hammer hardness	145	16.8-56.5	43.7	17.1
		I_{s50} (MPa)	Point load index	145	1.08-8.56	4.85	36.0
		σ_{ci} (MPa)	Uniaxial compression strength	145	20.3-112.9	53.9	34.3
Aggistalis et al. (1980)	Epirus (Greece)	I_{s50} (MPa)	Point load index	30	0.67-3.43	2.07	39.7
		σ_{ci} (MPa)	Uniaxial compression strength	30	17.1-91.2	46.7	41.0
		E_i (GPa)	Young's Modulus	30	1.20-12.07	5.05	51.8
Endait and Juneja (2014)	Mumbai (India)	I_{s50} (MPa)	Point load index	41	0.1-9.1	3.8	81.1
		σ_{ci} (MPa)	Uniaxial compression strength	41	2.2-181.7	84.5	66.4
Diamantis et al. (2009)	Mount Othrys (Greece)	I_{s50} (MPa)	Point load index	32	1.04-4.93	3.08	35.1
		σ_{ci} (MPa)	Uniaxial compression strength	32	19.2-125.7	60.3	44.8
Aggistalis et al. (1980)	Epirus (Greece)	I_{s50} (MPa))	Point load index	62	0.34-4.54	1.75	54.6
		σ_{ci} (MPa)	Uniaxial compression strength	62	6.3-107.5	42.5	52.6

		E_i (GPa)	Young's Modulus	62	0.96-9.84	4.45	50.5
Abdou and Mahmoud (2013)	Al-Jouf university (KSA)	σ_{ci} (MPa)	Uniaxial compression strength	30	26.0-36.2	28.8	7.7
Koncagül and Santi (1999)	Breathitt (USA)	S_h	Shore Scleroscope hardness	31	14.9-47.6	26.6	34.8
		σ_{ci} (MPa)	Uniaxial compression strength	31	30.7-99.5	65.8	22.3
Ceryan et al. (2012)	Trabzon (Turkey)	σ_{ci} (MPa)	Uniaxial compression strength	55	7.3-24.1	14.1	27.2
Begonha and Sequeira Braga (2002)	Oporto (Portugal)	σ_{ci} (MPa)	Uniaxial compression strength	48	60-157	98.7	23.2
		E_i (GPa)	Young's Modulus	48	5.03-16.94	9.99	27.7
Shalabi et al. (2007)	Chicago (USA)	γ (kN/m^3)	Unit weight	21	19.5-23.9	21.9	6.1
		R_L	Schmidt hammer hardness	21	24-45	33.0	21.9
		σ_{ci} (MPa)	Uniaxial compressive strength	21	21.4-96.6	53.6	42.2
Palchik (1999)	Donetsk (Ukraine)	n (%)	Porosity	15	27.5-47.2	36.2	15.7
		σ_{ci} (MPa)	Uniaxial compressive strength	15	7.1-19.8	12.7	29.1
		E_i (GPa)	Young's Modulus	15	1.4-2.5	1.92	19.5
Bell and Lindsay (1999)	Durban (South Africa)	n (%)	Porosity	27	5.6-10.1	7.5	18.9
		S_h	Shore scleroscope hardness	27	49-98	76.1	17.1
		σ_{bt} (MPa)	Brazilian tensile strength	27	6-20	14.9	24.4
		I_{s50} (MPa)	Point load index	27	3-13	9.0	30.3
		σ_{ci} (MPa)	Uniaxial compressive strength	27	77-214	136.6	25.6
		E_i (GPa)	Young's Modulus	27	10.9-99.9	52.3	51.4
Bell (1978)	England (UK)	n (%)	Porosity	25	10.2-20.5	13.5	18.4
		S_h	Shore scleroscope hardness	28	24-60	42.6	23.4
		σ_{bt} (MPa)	Brazilian tensile strength	27	2.1-9.5	6.6	26.9

		I_{s50} (MPa)	Point load index	28	0.2-9.5	4.68	54.1
		σ_{ci} (MPa)	Uniaxial compressive strength	29	33.2-112.4	78.4	30.8
		E_i (GPa)	Young's Modulus	18	19.7-46.2	32.7	20.3
Bell et al. (1997)	England (UK)	γ (kN/m^3)	Unit weight	10	23.8-25.1	24.6	1.5
		σ_{ci} (MPa)	Uniaxial compressive strength	10	25.7-45.4	35.5	17.9
Ghosh and Srivastava (1991)	Chamba (India)	I_{s50} (MPa)	Point load index	11	2.04-5.88	3.65	42.7
		σ_{ci} (MPa)	Uniaxial compressive strength	11	25-119	58.2	50.6
Heidari et al. (2012)	Hamedan (Iran)	n (%)	Porosity	20	3.4-17.5	8.6	44.9
		I_{s50} (MPa)	Point load index	20	3.17-5.56	4.23	16.0
		σ_{ci} (MPa)	Uniaxial compressive strength	20	44.9-92.5	69.8	23.2
		E_i (GPa)	Young's Modulus	18	6.1-12.4	8.4	23.4
Jizba (1991)	Texas (USA)	γ (kN/m^3)	Unit weight	10	25.9-26.2	25.9	0.4
		n (%)	Porosity	10	4-14	7.9	40.1
		V_P (km/s)	P-wave velocity	10	4.50-5.13	4.81	4.5
	Texas (USA)	γ (kN/m^3)	Unit weight	17	26-26.8	26.2	1.1
		n (%)	Porosity	17	0.87-9.5	4.3	49.4
		V_P (km/s)	P-wave velocity	17	4.51-5.54	5.11	5.3
	Texas (USA)	γ (kN/m^3)	Unit weight	13	23.9-26.5	25.2	3.0
		n (%)	Porosity	13	4-13.5	7.9	34.8
		V_P (km/s)	P-wave velocity	13	4.06-4.90	4.57	5.5
	Texas (USA)	γ (kN/m^3)	Unit weight	15	25.9-26.7	26.2	1.2
		n (%)	Porosity	15	4.9-20.0	9.8	41.7
		V_P (km/s)	P-wave velocity	15	4.05-5.00	4.46	6.3
	Texas (USA)	γ (kN/m^3)	Unit weight	12	25.9-27.6	26.3	1.8
		n (%)	Porosity	12	1.2-6.6	4.3	37.3

		V_P (km/s)	P-wave velocity	10	5.21-5.86	5.32	3.6
Arslan et al. (2015)	Salt Range (Pakistan)	γ (kN/m^3)	Unit weight	18	22.9-27.1	25.3	7.0
		R_L	Schmidt hammer hardness	18	19-44	33.7	27.4
		σ_{ci} (MPa)	Uniaxial compressive strength	18	42-108	74.3	30.8
Palchik and Hatzor (2004)	Adulam (Israel)	σ_{bt} (MPa)	Brazilian tensile strength	20	2.5-8.7	5.4	34.8
		I_{s50} (MPa)	Point load index	18	1.69-4.28	2.61	28.7
		σ_{ci} (MPa)	Uniaxial compressive strength	12	20.9-63.3	47.6	28.6
		E_i (GPa)	Young's Modulus	12	9.3-20.5	14.8	25.3
Moradian and Behnia (2009)	Ghareh Tikan (Iran)	γ (kN/m^3)	Unit weight	27	25.7-27.2	26.	1.4
		V_P (km/s)	P-wave velocity	27	1.84-6.54	5.05	30.1
		σ_{ci} (MPa)	Uniaxial compressive strength	27	40.7-143.1	82.2	31.6
		E_i (GPa)	Young's Modulus	27	13.7-90.5	48.9	47.8
Sharma and Singh (2007)	Jharia (India)	σ_{ci} (MPa)	Uniaxial compressive strength	10	22-28	25.6	6.7
Pappalardo (2014)	Taormina (Italy)	γ (kN/m^3)	Unit weight	25	25.2-27.5	26.3	2.3
		n (%)	Porosity	25	2.4-10.4	5.3	37.2
		V_P (km/s)	P-wave velocity	25	3.3-6.32	5.17	16.9
		σ_{ci} (MPa)	Uniaxial compressive strength	25	15.2-112	75.0	39.2
		E_i (GPa)	Young's Modulus	25	2.4-18.8	11.2	50.0
Mishra and Basu (2013)	Malanjkhand (India)	γ (kN/m^3)	Unit weight	20	26.5-27.2	26.8	0.7
		n (%)	Porosity	20	0.06-0.4	0.22	39.6
		V_P (km/s)	P-wave velocity	20	5.36-6.25	5.82	4.7
		σ_{bt} (MPa)	Brazilian tensile strength	20	10.5-19.8	15.5	15.6
		I_{s50} (MPa)	Point load index	19	5.66-14.13	9.02	23.8
		σ_{ci} (MPa)	Uniaxial compressive strength	20	91.5-201.7	150.1	18.9

	Jharkhand (India)	γ (kN/m^3)	Unit weight	20	26.9-28.6	27.7	1.8
		n (%)	Porosity	20	0.2-0.54	0.39	26.6
		V_P (km/s)	P-wave velocity	20	5.12-6.25	5.84	5.8
		σ_{bt} (MPa)	Brazilian tensile strength	20	6.14-19.5	12.3	29.8
		I_{s50} (MPa)	Point load index	20	1.15-7.42	3.79	40.9
		σ_{ci} (MPa)	Uniaxial compressive strength	20	21.4-95.1	46.5	40.8
	Andhra Pradesh (India)	γ (kN/m^3)	Unit weight	20	21.3-25.5	23.0	5.4
		n (%)	Porosity	19	2.9-15.5	9.8	44.1
		V_P (km/s)	P-wave velocity	20	2.73-4.99	3.62	20.5
		σ_{bt} (MPa)	Brazilian tensile strength	20	2.0-14.3	6.4	55.9
		I_{s50} (MPa)	Point load index	18	1.25-11.49	5.03	59.8
		σ_{ci} (MPa)	Uniaxial compressive strength	20	12.8-172.0	57.4	72.4
Gorski et al. (2007)	Forsmark (Sweden)	V_P (km/s)	P-wave velocity	20	4.93-5.21	5.07	1.5
		σ_{bt} (MPa)	Brazilian tensile strength	20	17.2-22.1	19.4	7.1
Dinçer et al. (2008)	Adana (Turkey)	γ (kN/m^3)	Unit weight	18	17.2-22.9	19.6	8.1
		n (%)	Porosity	18	16.2-32.5	25.0	17.2
		R_L	Schmidt hammer hardness	18	16.9-40.3	26.3	24.3
		S_h	Shore scleroscope hardness	18	8.4-24.6	13.4	35.3
		V_P (km/s)	P-wave velocity	18	0.44-1.58	0.81	44.7
		I_{s50} (MPa)	Point load index	18	0.78-2.08	1.21	33.7
		σ_{ci} (MPa)	Uniaxial compressive strength	18	2.7-10.4	5.6	40.7
		E_i (GPa)	Young's Modulus	18	0.18-1.40	0.62	58.4
Khaksar et al. (1999)	Cooper Basin (Australia)	γ (kN/m^3)	Unit weight	22	20.9-25.1	23.2	5.3
		n (%)	Porosity	22	2.6-16.6	9.7	44.8
Kahraman and	Attendorn (Germany)	σ_{ci} (MPa)	Uniaxial compressive	24	9.8-86.6	32.8	69.2

Alber (2006)			strength				
		E_i (GPa)	Young's Modulus	24	3-16.8	9.6	38.3
Dinçer et al. (2004)	Bodrum Peninsula (Turkey)	γ (kN/m^3)	Unit weight	10	17.5-26.5	21.4	17.9
		R_L	Schmidt hammer hardness	10	24.8-53.4	35.4	27.7
		σ_{ci} (MPa)	Uniaxial compressive strength	10	32.9-108	59.8	45.9
		E_i (GPa)	Young's Modulus	10	5.1-21.2	10.6	53.2
Rajabzadeh et al. (2011)	Dehbid (Iran)	n (%)	Porosity	14	0.30-0.86	0.46	36.4
	Neyqiz (Iran)	n (%)	Porosity	24	0.17-2.89	0.52	113.6
		σ_{bt} (MPa)	Brazilian tensile strength	10	4.4-10.6	6.7	32.2
		σ_{ci} (MPa)	Uniaxial compressive strength	10	43.1-101.8	63.0	26.3
		E_i (GPa)	Young's Modulus	10	5.9-15.9	11.6	30.0
Koçkar and Akgün (2003a)	Antalya (Turkey)	σ_{ci} (MPa)	Uniaxial compressive strength	12	28-117	73.3	42.9
Nicksiar and Martin (2012)	Oskarshamn (Sweden)	σ_{ci} (MPa)	Uniaxial compressive strength	10	171-294	226.9	13.8
		E_i (GPa)	Young's Modulus	10	72-80	75.7	3.8
Basu et al. (2008)	Sao Paulo (Brazil)	R_L	Schmidt hammer hardness	20	20.6-55.4	45.6	17.6
		S_h	Shore scleroscope hardness	20	28.3-65.3	54.9	15.5
		V_P (km/s)	P-wave velocity	20	1.93-5.51	4.51	18.3
		σ_{ci} (MPa)	Uniaxial compressive strength	20	73-214	151.9	28.5
		E_i (GPa)	Young's Modulus	20	41.1-70.2	58.9	15.3
Basu and Kamran (2010)	Jharkhand (India)	I_{s50} (MPa)	Point load index	15	1.08-5.93	3.58	40.0
		σ_{ci} (MPa)	Uniaxial compressive strength	15	40.1-107.9	77.4	24.0
Gupta and Sharma (2012)	Himalaya (India)	γ (kN/m^3)	Unit weight	18	17.5-26.5	21.4	17.9
		n (%)	Porosity	18	0.3-1.5	0.66	40.3

		V_P (km/s)	P-wave velocity	18	1.48-5.53	3.84	31.5
		σ_{ci} (MPa)	Uniaxial compressive strength	18	46-141	88.6	31.1
Kurtulus et al. (2011)	Ezine (Turkey)	V_P (km/s)	P-wave velocity	20	4.11-5.29	4.84	7.1
		I_{s50} (MPa)	Point load index	20	2.41-7.85	5.50	27.5
		σ_{ci} (MPa)	Uniaxial compressive strength	20	32.7-114.3	81.5	29.7
		E_i (GPa)	Young's Modulus	20	3.4-5.4	4.5	13.5
Sarpun et al. (2010)	Afyonkarahisar (Turkey)	γ (kN/m^3)	Unit weight	14	23.3-29.1	26.8	5.6
		V_P (km/s)	P-wave velocity	14	3.26-4.71	3.83	12.7
		σ_{ci} (MPa)	Uniaxial compressive strength	14	13.2-57.1	34.7	40.6
		E_i (GPa)	Young's Modulus	14	18.4-47.1	30.9	24.3
Sarkar et al. (2011)	Siwalik (India)	γ (kN/m^3)	Unit weight	10	20.0-23.3	21.2	6.0
		V_P (km/s)	P-wave velocity	10	2.10-2.54	2.28	8.0
		σ_{ci} (MPa)	Uniaxial compressive strength	10	20.1-48.6	32.4	30.9
	Gondwana (India)	γ (kN/m^3)	Unit weight	10	22.5-23.6	22.9	1.5
		V_P (km/s)	P-wave velocity	10	2.35-2.64	2.49	3.9
		σ_{ci} (MPa)	Uniaxial compressive strength	10	39.0-45.5	41.2	5.7
	Deccan Trap (India)	γ (kN/m^3)	Unit weight	10	21.9-23.6	22.5	2.6
		V_P (km/s)	P-wave velocity	10	2.15-3.02	2.54	14.6
		σ_{ci} (MPa)	Uniaxial compressive strength	10	50.3-73.2	60.2	15.9
Sarkar et al. (2010)	Himachal Pradesh (India)	γ (kN/m^3)	Unit weight	10	24.5-26.5	25.5	2.7
		V_P (km/s)	P-wave velocity	10	2.55-3.85	3.15	13.4
		I_{s50} (MPa)	Point load index	10	2.81-3.91	3.35	11.0
		σ_{ci} (MPa)	Uniaxial compressive strength	10	68.4-84.5	75.2	8.0
Tahir et al. (2011)	Kohat (Pakistan)	σ_{bt} (MPa)	Brazilian tensile strength	15	3.99-6.82	4.91	13.7

		I_{s50} (MPa)	Point load index	15	1.50-2.89	1.93	16.3
		σ_{ci} (MPa)	Uniaxial compressive strength	15	26.6-49.0	38.0	14.7
	Cherat (Pakistan)	σ_{bt} (MPa)	Brazilian tensile strength	15	5.54-7.89	6.97	9.8
		I_{s50} (MPa)	Point load index	15	1.95-2.70	2.26	11.6
		σ_{ci} (MPa)	Uniaxial compressive strength	15	29.4-61.8	49.8	18.7
Ceryan et al. (2008)	Kurtun (Turkey)	n (%)	Porosity	20	1.3-18.5	7.9	73.2
		V_P (km/s)	P-wave velocity	20	2.06-5.32	3.61	30.6
		σ_{ci} (MPa)	Uniaxial compressive strength	20	2.8-200.3	74.9	89.5
		E_i (GPa)	Young's Modulus	15	4-37.5	17.1	59.6
Kurtulus et al. (2016)	Akveren (Turkey)	n (%)	Porosity	10	2.2-2.6	2.4	5.7
		V_P (km/s)	P-wave velocity	10	4.20-4.70	4.46	4.3
		σ_{bt} (MPa)	Brazilian tensile strength	10	5.0-6.2	5.6	6.6
		I_{s50} (MPa)	Point load index	10	2.88-3.32	3.12	5.1
		σ_{ci} (MPa)	Uniaxial compressive strength	10	28-33	30	6.5
		E_i (GPa)	Young's Modulus	10	49-65	54.4	8.7
Adebayo and Umeh (2007)	Nigeria	σ_{ci} (MPa)	Uniaxial compressive strength	10	59.8-99.8	82.8	18.5
	Shagamu (Nigeria)	σ_{ci} (MPa)	Uniaxial compressive strength	10	60.3-97.4	82.5	17.6
	Lagos (Nigeria)	σ_{ci} (MPa)	Uniaxial compressive strength	10	67.3-119.2	96.8	21.1
Chitty et al. (1994)	Salem (USA)	n (%)	Porosity	18	16.2-17.2	16.8	1.5
		σ_{ci} (MPa)	Uniaxial compressive strength	14	46-59.3	51.1	8.5
		E_i (GPa)	Young's Modulus	14	25.2-29.6	26.9	5.5
Pittino et al. (2016)	Tauern Window (Austria)	V_P (km/s)	P-wave velocity	13	2.34-3.53	2.94	16.2
Kumari et al. (2016)	Strathbogie (Australia)	σ_{ci} (MPa)	Uniaxial compressive strength	11	76.3-143.3	118.2	18.4

		E_i (GPa)	Young's Modulus	11	6.3-9.1	8.0	12.4
Chen and Hsu (2001)	Hualien (Taiwan)	σ_{bt} (MPa)	Brazilian tensile strength	12	3.45-10.97	7.65	31.0
Ulusay et al. (1994)	Kozlu-Zonguldak (Turkey)	I_{s50} (MPa)	Point load index	15	2.2-4.0	3.14	18.1
		E_i (GPa)	Young's Modulus	15	17-112	59.1	48.8
Mustafa et al. (2015)	Azad Kashmir (Pakistan)	I_{s50} (MPa)	Point load index	13	0.52-4.54	2.32	44.7
Shalabi et al. (2007)	Puerto Rico (USA)	γ (kN/m^3)	Unit weight	11	24.5-26.6	25.8	2.3
		S_h	Shore scleroscope hardness	11	49-71	57.5	11.9
		σ_{ci} (MPa)	Uniaxial compressive strength	11	11.2-55.1	32.3	38.5
		E_i (GPa)	Young's Modulus	11	16.2-41.1	26.4	30.4
	Detroit (USA)	γ (kN/m^3)	Unit weight	14	20.4-25.9	23.5	6.5
		R_L	Schmidt hammer hardness	14	23-45	34.7	17.3
		σ_{ci} (MPa)	Uniaxial compressive strength	14	19.9-109.9	57.7	46.7
Dinçer et al. (2004)	Bodrum Peninsula (Turkey)	γ (kN/m^3)	Unit weight	14	18.3-25.2	22.5	10.2
		R_L	Schmidt hammer hardness	14	27.9-52.4	43.1	17.5
		σ_{ci} (MPa)	Uniaxial compressive strength	14	38.5-112.7	82.5	25.7
		E_i (GPa)	Young's Modulus	14	7.8-28.3	13.6	25.8
Koçkar and Akgün (2003a)	Antalya (Turkey)	σ_{ci} (MPa)	Uniaxial compressive strength	15	3-104	50.9	66.5
Marques et al. (2014)	Brazil	I_{s50} (MPa)	Point load index	10	5.0-7.9	6.5	13.7
		I_{s50} (MPa)	Point load index	10	5.1-10.7	8.0	21.3
		I_{s50} (MPa)	Point load index	10	1.8-5.1	3.6	23.7
		I_{s50} (MPa)	Point load index	11	3.2-9.0	4.6	34.5
Sarkar et al. (2010)	Himachal Pradesh (India)	γ (kN/m^3)	Unit weight	10	25.9-27.6	26.6	2.3
		V_P (km/s)	P-wave velocity	10	3.05-4.26	3.68	12.5

		I_{s50} (MPa)	Point load index	10	1.2-2.3	1.7	22.6
		σ_{ci} (MPa)	Uniaxial compressive strength	10	24.2-49.3	37.4	22.9
		γ (kN/m^3)	Unit weight	10	25.8-26.5	26.1	1.0
		V_P (km/s)	P-wave velocity	10	3.52-4.23	3.85	6.2
		I_{s50} (MPa)	Point load index	10	3.8-5.3	4.6	11.4
		σ_{ci} (MPa)	Uniaxial compressive strength	10	93.2-112.3	99.4	6.8
		γ (kN/m^3)	Unit weight	10	25.7-26.4	26.0	1.0
		V_P (km/s)	P-wave velocity	10	2.14-2.49	2.27	5.2
		I_{s50} (MPa)	Point load index	10	1.0-1.8	1.3	20.7
		σ_{ci} (MPa)	Uniaxial compressive strength	10	30.3-28.5	24.1	11.6
Mohamad et al. (2014)	Nusajaya, Desa Tebrau and Mersing, Johor (Malaysia)	γ (kN/m^3)	Unit weight	24	20.2-34.7	27.0	15.8
		V_P (km/s)	P-wave velocity	24	1.25-3.91	2.13	26.5
		σ_{bt} (MPa)	Brazilian tensile strength	24	0.8-4.2	2.35	46.2
		I_{s50} (MPa)	Point load index	24	0.3-4.1	1.9	70.2
		σ_{ci} (MPa)	Uniaxial compressive strength	24	5.5-61.1	27.7	65.3
Vasconcelos et al. (2007)	Portugal	R_L	Schmidt hammer hardness	19	52.7-61.3	57.8	5.2
		V_P (km/s)	P-wave velocity	19	1.90-4.78	3.08	28.8
		σ_{ci} (MPa)	Uniaxial compressive strength	19	26-159.8	92.0	47.0
		E_i (GPa)	Young's Modulus	19	11.0-63.8	34.4	56.0
Ramana and Venkatanarayana (1973)	Mysore State (India)	γ (kN/m^3)	Unit weight	10	29.4-31.0	30.1	1.9
		V_P (km/s)	P-wave velocity	10	5.22-6.65	6.03	7.8
		E_i (GPa)	Young's Modulus	10	59.1-109.3	85.9	19.5
Nazir et al. (2013a)	Malaysia	R_L	Schmidt hammer hardness	20	28.9-39	35.1	7.5
		σ_{ci} (MPa)	Uniaxial compressive strength	20	52.2-85.6	71.6	12.8

Kahraman (2001)	Turkey	γ (kN/m^3)	Unit weight	12	16.3-29.2	24.3	17.2
		R_L	Schmidt hammer hardness	26	8.1-65.8	40.6	33.2
		I_{s50} (MPa)	Point load index	28	0.23-12.01	2.99	91.4
		σ_{ci} (MPa)	Uniaxial compressive strength	28	4.4-152.7	50.5	66.8
Nazir et al. (2013b)	Malaysia	σ_{bt} (MPa)	Brazilian tensile strength	20	3.02-14.2	7.16	36.1
		σ_{ci} (MPa)	Uniaxial compressive strength	20	21.2-100.7	59.6	31.9
Bearman (1999)	UK	R_L	Schmidt hammer hardness	12	23-50	38.3	22.1
		σ_{bt} (MPa)	Brazilian tensile strength	12	3.84-18.42	11.80	40.3
		σ_{ci} (MPa)	Uniaxial compressive strength	12	47.8-274.8	141.9	46.3
		E_i (GPa)	Young's Modulus	12	15.9-64.2	44.1	36.1
Zhao and Li (2000)	Singapore	σ_{bt} (MPa)	Brazilian tensile strength	23	7.7-17.1	11.6	21.5
		E_i (GPa)	Young's Modulus	22	25.7-56.	40.2	19.9
Kahraman et al. (2004)	Turkey	n (%)	Porosity	13	0.18-13.3	4.3	105.2
		R_L	Schmidt hammer hardness	13	32.1-56.	16.9	18.0
		V_P (km/s)	P-wave velocity	13	3.7-6.2	5.24	17.6
		σ_{bt} (MPa)	Brazilian tensile strength	13	2.2-10.2	5.18	39.6
		σ_{ci} (MPa)	Uniaxial compressive strength	13	45.4-175.0	91.8	45.2
		I_{s50} (MPa)	Point load index	13	1.6-7.1	4.7	31.3
Balci et al. (2004)	Turkey	γ (kN/m^3)	Unit weight	10	16.7-27.1	22.6	21.5
		σ_{bt} (MPa)	Brazilian tensile strength	10	1.2-11.6	5.3	64.5
		σ_{ci} (MPa)	Uniaxial compressive strength	10	10.8-173.6	68.2	80.2
Singh et al. (2012)	India	γ (kN/m^3)	Unit weight	15	20.8-31.3	26.6	11.1
		V_P (km/s)	P-wave velocity	15	2.15-3.67	2.81	17.3
		σ_{ci} (MPa)	Uniaxial compressive	15	29-61.8	44.0	22.6

			strength				
Kasim and Shakoor (1996)	US	σ_{ci} (MPa)	Uniaxial compressive strength	22	34-209.6	127.6	38.3
Klanphumeesri (2010)	Thailand	σ_{bt} (MPa)	Brazilian tensile strength	15	7.8-11.8	9.9	14.4
Kahraman et al. (2005)	Turkey	n (%)	Porosity	22	0.06-10.7	2.68	107.3
		R_L	Schmidt hammer hardness	15	44.3-56.5	48.5	6.9
		σ_{bt} (MPa)	Brazilian tensile strength	11	5.7-18.1	11.2	42.1
		I_{s50} (MPa)	Point load index	22	2.9-13.3	8.1	47.7
		σ_{ci} (MPa)	Uniaxial compressive strength	22	26.1-210.6	108.9	50.2
Verwaal and Mulder (1993)	Netherlands	γ (kN/m^3)	Unit weight	25	19.0-26.6	24.2	9.24
		n (%)	Porosity	21	0.4-37.9	8.86	115.1
		σ_{ci} (MPa)	Uniaxial compressive strength	25	22-203	106.7	56.5
		E_i (GPa)	Young's Modulus	25	9-80	45.0	49.6
Török and Vásárhelyi (2010)	Sutto (Hungary)	γ (kN/m^3)	Unit weight	27	23.9-25.4	24.7	1.4
		σ_{ci} (MPa)	Uniaxial compression strength	27	66.8-124.3	93.8	21.8
		σ_{ci} (MPa)	Uniaxial compression strength	32	19.2-125.7	60.3	44.8
Pittino et al. (2016)	Diyarbakir (Turkey)	σ_{ci} (MPa)	Uniaxial compression strength	28	24.0-90.5	43.6	37.9
Bell and Lindsay (1999)	Durban (South Africa)	σ_{ci} (MPa)	Uniaxial compression strength	27	77.0-214.0	136.6	25.6
		S_h	Shore scleroscope hardness	27	49-98	76.1	17.1
		σ_{bt} (MPa)	Brazilian tensile strength	20	6-20	14.9	24.4
Bell (1978)	England (UK)	σ_{bt} (MPa)	Brazilian tensile strength	27	2.1-9.5	6.6	26.9
Bell et al. (1997)	England (UK)	σ_{ci} (MPa)	Uniaxial compression strength	10	25.7-45.4	35.5	17.9
		γ (kN/m^3)	Unit weight	10	23.8-25.1	24.6	1.5

Ghosh and Srivastava (1991)	Chamba (India)	σ_{ci} (MPa)	Uniaxial compression strength	10	25.0-83.3	52.1	43.5
		I_{s50} (MPa)	Point load index	10	2.04-5.47	3.43	42.2
Heidari et al. (2012)	Hamedan (Iran)	σ_{ci} (MPa)	Uniaxial compression strength	20	44.9-82.5	69.8	23.2
		E_i (GPa)	Young's Modulus	20	3.17-5.56	4.23	16.0
Palchik and Hatzor (2004)	Adulam (Israel)	σ_{ci} (MPa)	Uniaxial compression strength	12	20.9-63.3	47.6	28.6
		I_{s50} (MPa)	Point load index	18	1.69-4.28	2.61	28.7
		E_i (GPa)	Young's Modulus	12	9.3-20.5	14.8	25.3
		σ_{bt} (MPa)	Brazilian tensile strength	20	2.5-8.7	5.4	34.8
Moradian and Behnia (2009)	Ghareh Tikan (Israel)	σ_{ci} (MPa)	Uniaxial compression strength	27	40.7-143.1	82.2	31.6
		γ (kN/m^3)	Unit weight	27	25.7-27.2	26.4	1.4
Pappalardo (2014)	Castelmola (Italy)	σ_{ci} (MPa)	Uniaxial compression strength	21	47.3-112.0	84.0	26.3
		γ (kN/m^3)	Unit weight	25	25.2-27.5	26.3	2.3
Mishra and Basu (2013)	Malanjkhand (India)	γ (kN/m^3)	Unit weight	20	16.49-27.17	16.81	0.7
		σ_{ci} (MPa)	Uniaxial compression strength	20	91.5-201.7	150.1	18.9
		I_{s50} (MPa)	Point load index	19	5.66-14.13	9.02	23.8
		σ_{bt} (MPa)	Brazilian tensile strength	20	10.5-19.8	15.5	15.6
	Jharkhand (India)	γ (kN/m^3)	Unit weight	20	26.88-28.55	27.70	1.8
		σ_{bt} (MPa)	Brazilian tensile strength	20	6.14-17.47	12.16	29.8
		I_{s50} (MPa)	Point load index	20	1.15-7.42	3.79	40.9
		σ_{ci} (MPa)	Uniaxial compression strength	20	21.36-95.14	46.53	40.8
Gorski et al. (2007)	Forsmark (Sweden)	σ_{bt} (MPa)	Brazilian tensile strength	20	17.2-22.1	19.4	7.1
Dinçer et al. (2008)	Adana (Turkey)	γ (kN/m^3)	Unit weight	18	17.32-22.94	19.63	8.1
		σ_{ci} (MPa)	Uniaxial compression strength	18	2.65-10.41	5.63	40.7

		I_{s50} (MPa)	Point load index	18	0.78-2.08	1.21	33.7
		E_i (GPa)	Young's Modulus	18	0.18-1.4	0.62	58.4
		R_L	Schmidt hammer hardness	18	16.9-40.3	26.3	24.3
		S_h	Shore scleroscope hardness	18	8.4-24.6	13.4	35.3
		γ (kN/m^3)	Unit weight	18	17.3-22.9	19.6	8.1
Kahraman and Alber (2006)	Attrndorn (Germany)	E_i (GPa)	Young's Modulus	22	4.6-15.8	9.52	33.4
Rajabzadeh et al. (2011)	Neyriz (Iran)	E_i (GPa)	Young's Modulus	10	5.9-15.9	11.6	28.0
		σ_{bt} (MPa)	Brazilian tensile strength	10	4.4-10.6	6.7	32.2
Koçkar and Akgün (2003a)	Antalya (Turkey)	σ_{ci} (MPa)	Uniaxial compression strength	12	28-117	73.3	42.9
Nicksiar and Martin (2012)	Oskarshamn (Sweden)	σ_{ci} (MPa)	Uniaxial compression strength	10	171-294	226.9	13.8
		E_i (GPa)	Young's Modulus	10	72-80	75.7	3.8
Basu et al. (2008)	Sao Paulo (Brazil)	R_L	Schmidt hammer hardness	19	36.24-55.38	46.91	11.9
		S_h	Shore scleroscope hardness	19	44.95-65.32	56.31	10.6
Basu and Kamran (2010)	Jharkhand (India)	σ_{ci} (MPa)	Uniaxial compression strength	15	40.1-107.9	77.4	24.0
		I_{s50} (MPa)	Point load index	15	1.08-5.93	3.58	40.0
Gupta and Sharma (2012)	Himalaya (India)	σ_{ci} (MPa)	Uniaxial compression strength	18	46.0-141.0	88.6	31.1
		γ (kN/m^3)	Unit weight	18	25.5-27.7	26.4	2.5
Kurtulus et al. (2011)	Ezine (Turkey)	σ_{ci} (MPa)	Uniaxial compression strength	20	32.7-114.3	81.5	29.7
		I_{s50} (MPa)	Point load index	20	2.41-7.85	5.50	27.5
		E_i (GPa)	Young's Modulus	20	3.4-5.4	4.5	13.5
Sarpun et al. (2010)	Afyonkarahisar (Turkey)	σ_{ci} (MPa)	Uniaxial compression strength	14	13.2-57.1	34.7	40.6
		E_i (GPa)	Young's Modulus	14	18.4-47.1	31.0	24.3

		γ (kN/m^3)	Unit weight	14	23.2-29.1	26.8	5.6
Sarkar et al. (2010)	Himachal Pradesh (India)	I_{s50} (MPa)	Point load index	10	2.81-3.91	3.35	11.0
Tahir et al. (2011)	Kohat (Pakistan)	σ_{ci} (MPa)	Uniaxial compression strength	15	26.6-49.0	38.0	14.8
		I_{s50} (MPa)	Point load index	15	1.5-2.9	1.93	16.3
		σ_{bt} (MPa)	Brazilian tensile strength	15	4.0-6.8	4.9	13.7
	Cherat (Pakistan)	σ_{ci} (MPa)	Uniaxial compression strength	15	29.4-61.8	49.8	18.7
		I_{s50} (MPa)	Point load index	15	2.0-2.7	2.26	11.6
		σ_{bt} (MPa)	Brazilian tensile strength	15	5.5-7.9	6.9	9.8
Kurtulus et al. (2016)	Akveren (Turkey)	σ_{ci} (MPa)	Uniaxial compression strength	10	28-33	30.0	6.5
		I_{s50} (MPa)	Point load index	10	2.9-3.3	3.12	5.1
		E_i (GPa)	Young's Modulus	10	49-65	54.4	8.7
		σ_{bt} (MPa)	Brazilian tensile strength	10	5.0-6.2	5.6	6.6
Adebayo and Umeh (2007)	Nigeria	σ_{ci} (MPa)	Uniaxial compression strength	10	59.8-99.8	82.8	18.5
	Shagamu (Nigeria)	σ_{ci} (MPa)	Uniaxial compression strength	10	60.3-97.4	82.5	17.6
	Lagos (Nigeria)	σ_{ci} (MPa)	Uniaxial compression strength	10	67.3-119.2	96.8	21.1
Chitty et al. (1994)	Salem (USA)	σ_{ci} (MPa)	Uniaxial compression strength	14	46.0-59.3	51.1	8.5
Ulusay et al. (1994)	Kozlu-Zonguldak (Turkey)	σ_{ci} (MPa)	Uniaxial compression strength	15	55.0-96.0	70.7	15.8
		I_{s50} (MPa)	Point load index	15	2.2-4.0	3.14	18.1
Shalabi et al. (2007)	Puerto Rico (USA)	σ_{ci} (MPa)	Uniaxial compression strength	11	11.2-55.1	32.3	38.5
		E_i (GPa)	Young's Modulus	11	16.2-41.1	26.4	30.4
		γ (kN/m^3)	Unit weight	11	24.5-26.6	25.8	2.3
Dinçer et al. (2004)	Bodrum Peninsula (Turkey)	σ_{ci} (MPa)	Uniaxial compression strength	12	70-112.7	89.2	15.2

		E_i (GPa)	Young's Modulus	12	9.3-18.3	14.6	19.5
		γ (kN/m^3)	Unit weight	14	18.3-25.1	22.5	10.2
Dincer et al. (2004)	Turkey	R_L	Schmidt hammer hardness	24	24.80-53.40	39.9	23.1
		σ_{ci} (MPa)	Uniaxial compression strength	24	32.93-112.7	73.05	35.7
		E_i (GPa)	Youngs' modulus	24	5.05-21.18	12.34	37.7
		γ (kN/m^3)	Unit weight	24	17.45-26-50	22.04	13.7
Sabatakakis et al. (2008)	Greece (Sandstone)	n (%)	Porosity	204	0.2-29.3	4.66	104.3
		γ (kN/m^3)	Unit weight	468	14-26.3	23.22	12.7
		R_L	Schmidt hammer hardness	280	11-52	28.9	37.4
		I_{s50} (MPa))	Point load index	828	0.2-7.6	1.88	91.5
		σ_{ci} (MPa)	Uniaxial compression strength	226	2.5-252	48.53	108.4
		E_i (GPa)	Youngs' modulus	36	3.42-71.75	26.36	66.31
	Greece (Limestone)	n (%)	Porosity	262	0.04-4.25	0.54	105
		γ (kN/m^3)	Unit weight	778	22-28.2	26.17	2.9
		N	Schmidt hammer hardness	355	16-57	41.8	13.8
		I_{s50} (MPa)	Point load index	1305	2-7	3.99	28.3
		σ_{ci} (MPa)	Uniaxial compression strength	470	25-294.05	68.23	65.3
		E_i (GPa)	Youngs' modulus	85	4.7-196.26	73.17	73.7
Aladejare (2020)	Otanmäki, Finland (Gabbro)	w_c (%)	Water content	15	0.01-0.04	0.02	50.00
		n (%)	Porosity	15	0.13-0.48	0.29	34.48
		σ_{bt} (MPa)	Brazilian tensile strength	15	6.8-12.6	9.88	18.02
	Otanmäki, Finland (Granite)	w_c (%)	Water content	10	0.02-0.12	0.05	80.00
		n (%)	Porosity	10	0.29-1.64	0.73	58.90
		σ_{bt} (MPa)	Brazilian tensile strength	10	7.1-12.7	10.41	18.83

Table 1.A4. Site-specific rock mass property statistics (database: ROCKMass/9/5876)

Source	Site Description	Property		No. of tests (≥30)	Range of data	Property mean	Property COV (%)
Bieniawki (1978)	Orange–Fish Tunnel (South Africa)	RQD	Rock quality designation	44	56.4-99.1	86.6	12.8
	Dworshak Dam (USA)	RQD	Rock quality designation	21	59.6-93.2	82.1	12.5
	Orange-Fish Tunnel (South Africa)	E_m (GPa)	Modulus of deformation	7	0.22-1	0.69	41.4
Sapigni et al. (2002)	Maen Tunnel (Italy)	RMR	Rock mass rating	330	13-96	67.7	24.7
Ö zkan et al. (2015)	The Divriği open-pit mine (Turkey)	RQD	Rock quality designation	42	10-100	69.7	47.9
		RMR	Rock mass rating	39	51-80	64.5	11.6
	The Divriği open-pit mine (Turkey)	RMR	Rock mass rating	35	50-72	60.7	11.6
Nejati et al. (2013)	Gotvand Dam (Iran)	RMR	Rock mass rating	49	30-76	50.5	23.0
Hassanpour et al. (2009)	Karaj Water Conveyance Tunnel (Iran)	RMR	Rock mass rating	37	36-74	56.0	13.9
Kaiser et al. (1986)	Tumbler Ridge Tunnels (Canada)	RMR	Rock mass rating	49	20-71	49.0	26.8
Chatziangelou et al. (2002)	Platamon Railway Tunnel (Greece)	RMR	Rock mass rating	43	14.5-70	39.6	38.0
		GSI	Geological strength index	43	22.5-52.5	37.7	24.5
Moon et al. (2001)	Waikato Coal Region (New Zealand)	RQD	Rock quality designation	80	58-94	80.2	11.1
		RMR	Rock mass rating	65	51.2-72	64.8	6.6
	Jinzhou (China)	RMR	Rock mass rating	32	56-78	71.9	7.8
	Iran	RMR	Rock mass rating	74	39-85	61.7	20.0
Chun et al. (2009)	Korea	RQD	Rock quality designation	61	15-100	77.9	29.8
		RMR	Rock mass rating	61	21-92	62.3	23.2
Coon (1968)	Dworshak (USA)	RQD	Rock quality designation	40	35-92	74.18	16.9
Majdi and Beiki (2010)	Iran	GSI	Geological strength index	111	26-89	54.3	22.4

Yanjun et al. (2007)	Daya Bay (China)	RMR	Rock mass rating	23	67-92	81.2	8.6
		Q	Rock mass quality	11	33.6-57.6	46.9	17.6
	Jinzhou (China)	RMR	Rock mass rating	32	56-78	71.9	7.8
Kramadibrata et al. (2011)	Tutupan open pit coal mine (Indonesia)	RMR	Rock mass rating	22	23-71	44.3	35.2
Khabbazi et al. (2013)	Iran	RQD	Rock quality designation	10	30-85	63.9	27.7
		RMR	Rock mass rating	10	39-56	488.1	11.9
	Iran	RMR	Rock mass rating	74	39-85	61.7	20.0
El-Naqa (1996)	Wadi Mujib (Jordan)	RMR	Rock mass rating	16	48-63	56	8.0
		Q	Rock mass quality	16	2.8-18.3	10.2	53.9
Cameron-Clarke and Budavari (1981)	The Bushkoppies Tunnel (South Africa)	RMR	Rock mass rating	24	38-87	70.1	18.7
		Q	Rock mass quality	24	0.02-200	13.4	303.5
	The Du Toitskloof Pilot Tunnel (South Africa)	RMR	Rock mass rating	22	30-81	54.2	28.5
		Q	Rock mass quality	22	0.09-89.7	10.1	209.2
	The Delvers Street Tunnel (South Africa)	RMR	Rock mass rating	10	28-74	45.9	32.4
		Q	Rock mass quality	10	0.01-4.75	1.37	112.3
Tuğrul (1998)	Atatürk Dam (Turkey)	RMR	Rock mass rating	21	13-42	29.0	31.1
		Q	Rock mass quality	21	0.05-1.9	0.64	87.5
Kumar et al. (2017)	Himachal Pradesh (India)	RMR	Rock mass rating	29	34-63	46.1	17.1
		GSI	Geological strength index	29	17-33	23.1	15.4
Hashemi et al. (2009)	Borujen (Iran)	RMR	Rock mass rating	23	14-58	30.6	32.8
		GSI	Geological strength index	23	22-60	43.4	18.6
		Q	Rock mass quality	23	0.005-2.5	0.36	159.3
Bieniawski (1978)	Orange–Fish Tunnel (South Africa)	RQD	Rock quality designation	44	56.4-99.1	86.6	12.8
	Dworshak Dam (USA)	RQD	Rock quality designation	21	59.6-93.2	82.1	12.5
	Orange-Fish Tunnel (South Africa)	E_m (GPa)	Modulus of deformation	7	0.22-1	0.69	41.4
El-Naqa and Al	Tannur Dam (Jordan)	RQD	Rock quality designation	11	44-57	49.1	9.1

Kuisi (2002)		RMR	Rock mass rating	11	52-60	56.1	4.8
		GSI	Geological strength index	11	48-57	52	5.4
		Q	Rock mass quality	11	2.43-5.92	3.98	29.5
	Taiz (Yemen)	RQD	Rock quality designation	17	50.3-100	89.9	15.0
		RMR	Rock mass rating	17	52.1-80.3	67.8	12.1
		GSI	Geological strength index	17	33.6-72	58.2	20.6
Ajalloeian and Mohammadi (2013)	Khersan II Dam (Iran)	RMR	Rock mass rating	28	41-70	57.8	14.9
		GSI	Geological strength index	28	37-64	48.0	15.4
		E_m (GPa)	Modulus of deformation	28	3.4-40.5	21.3	58.6
Al-Quadhi and Janardhana (2016)	Taiz (Yemen)	RQD	Rock quality designation	12	85.2-100	95.8	4.8
		RMR	Rock mass rating	12	62.8-80.3	72.1	6.7
		GSI	Geological strength index	12	52.9-72	64.5	8.8
Jordá-Bordehore et al. (2016)	Mirador (Ecuador)	RQD	Rock quality designation	15	41-100	84.1	18.0
Jordá-Bordehore et al. (2016);Jordá-Bordehore (2017)	Sucre, Isabela (Ecuador)	Q	Rock mass quality	12	4.3-12.2	7.4	36.9
	Chato (Ecuador)	RQD	Rock quality designation	10	10-86	75.4	30.7
		Q	Rock mass quality	10	0.3-15	4.93	114.7
Jordá-Bordehore (2017)	Primicias (Ecuador)	RQD	Rock quality designation	15	35-100	78.3	30.6
		Q	Rock mass quality	15	0.22-100	22.9	133.3
	Cueva de Los Verdes (Spain)	RQD	Rock quality designation	27	76-100	87.9	7.1
		Q	Rock mass quality	27	2.8-150	29.9	138.5
Kumar (2002)	Himalaya	RMR	Rock mass rating	31	31-80	55.7	19.0
		RQD	Rock quality designation	15	55-75	65.7	9.8
		GSI	Geological strength index	12	32-67	53.6	18.2
Zolfaghari et al. (2015)	Bakhtiary dam site (Iran)	RQD	Rock quality designation	21	46.9-78.1	64.7	11.8
		Q	Rock mass quality	21	0.92-5.02	2.44	57.3
		E_m (GPa)	Modulus of deformation	21	2.9-5.5	4.4	25.6

Kavur et al. (2015)	Karun3 (Iran)	RMR	Rock mass rating	19	32-77	53.2	22.8
		E_m (GPa)	Modulus of deformation	19	1.2-54	12.5	101.7
Shrestha (2005)	Khimti tunnel (Nepal)	RQD	Rock quality designation	26	10-50	25.6	51.5
		Q	Rock mass quality	26	0.005-0.60	0.13	118.4
Hassanpour et al. (2009)	Karaj Water Conveyance Tunnel (Iran)	RMR	Rock mass rating	37	36-74	56.0	13.9
Kitagawa et al. (1991)	Nou Tunnel (Japan)	RQD	Rock quality designation	26	11.2-80.3	36.9	54.3
Exadaktylos et al. (2008)	West Rail Line (Hong Kong)	RMR	Rock mass rating	12	62.5-78.5	69.6	6.4
		Q	Rock mass quality	12	2.5-79.2	22.8	120.2
Bagde et al. (2002)	Dongargaon fluorite mine (India)	RMR	Rock mass rating	14	23-52	37.3	20.3
del Potro and Hürlimann (2008)	Tenerife (Spain)	GSI	Geological strength index	26	39-80	53.9	20.3
Khanlari et al. (2012)	Karaj–Tehran tunnel (Iran)	RMR	Rock mass rating	24	21-75	20.3	29.0
Pavlovic (1970)	Unknown	E_m (GPa)	Modulus of deformation	27	3.5-45.1	30.6	39.0
Yanjun et al. (2007)	Daya Bay (China)	RMR	Rock mass rating	23	67-92	81.2	8.6
		Q	Rock mass quality	23	33.6-180.5	74.3	60.0
	Jinzhou (China)	RMR	Rock mass rating	32	56-78	71.9	7.8
Kramadibrata et al. (2011)	Tutupan open pit coal mine (Indonesia)	RMR	Rock mass rating	22	23-71	44.3	35.2
Chun et al. (2006)	Chungcheong-do and Kyungsang-do (Korea)	RQD	Rock quality designation	26	34.9-100	85.1	19.0
		RMR	Rock mass rating	26	46-86	71.5	16.3
		E_m (GPa)	Modulus of deformation	26	3.02-35.7	17.9	51.8
	Chungcheong-do and Kyungsang-do (Korea)	RQD	Rock quality designation	18	13.1-99.8	71.4	38.4
		RMR	Rock mass rating	18	43-94	66.7	20.8
	Chungcheong-do and Kyungsang-do (Korea)	RQD	Rock quality designation	23	35.9-99.9	75.5	26.6
		RMR	Rock mass rating	22	32-84	65	24.1
Koçkar and	Ilıksu tunnels (Turkey)	RMR	Rock mass rating	27	31-59	45.1	29.4

Akgün (2003b)		Q	Rock mass quality	27	0.13-7.31	3.03	98.5
Keffeler (2014)	Nevada (USA)	RMR	Rock mass rating	17	18-54	40.8	29.0
		GSI	Geological strength index	14	10-50	34.3	44.3
		Q	Rock mass quality	17	0.008-6.6	1.12	158.2
		E_m (GPa)	Modulus of deformation	14	0.001-1.03	0.29	103.0
Ranasooriya (2009)	The Huai Saphan Hin Power (HSHP) Tunnel (Thailand)	RQD	Rock quality designation	10	32-99	81	25.8
		Q	Rock mass quality	10	0.04-6.6	3.16	92.1
	The Ramboda Pass Highway Tunnel (Sri Lanka)	RMR	Rock mass rating	19	30-73	56.2	24.6
	The Namroud Water Resources Project Diversion Tunnel (Iran)	RMR	Rock mass rating	11	17-40	26.9	34.0
Birid (2014)	Mumbai (India)	RMR	Rock mass rating	22	9-67	35.0	46.8
Alexander (1960)	Turmut (Australia)	E_m (GPa)	Modulus of deformation	18	4.98-12.0	8.1	23.9
Singh (2011)	Baspa Hydroelectric project (India)	RQD	Rock quality designation	24	73.2-87.5	81.9	7.8
		Q	Rock mass quality	24	1.7-7.6	5.2	49.7
		E_m (GPa)	Modulus of deformation	24	3.6-13.9	7.2	42.7
Isik et al. (2008)	Ankara (Turkey)	RQD	Rock quality designation	10	9.8-100	55.7	59.4
		GSI	Geological strength index	12	8-53	22.2	57.0
		E_m (GPa)	Modulus of deformation	23	0.02-0.27	0.11	55.8
Tumac et al. (2006)	Küçüksu tunnel (Turkey)	RQD	Rock quality designation	15	75-90	87	6.1
Borsetto et al. (1983)	Timpagrande Powerhouse (Italy)	RQD	Rock quality designation	189	0-100	54.6	54.4
		E_m (GPa)	Modulus of deformation	21	0.3-26.2	6.7	70.1
Frough et al. (2014)	Karaj-Tehran water conveyance tunnel (Iran)	RMR	Rock mass rating	10	21-75	53.2	31.4
Moradi and Farsangi (2013)	Zagros long water conveyance tunnel (Iran)	RQD	Rock quality designation	15	12.5-79	45	46.9
Panthi and Shrestha (2018)	Kaligandaki headrace tunnel (Nepal)	Q	Rock mass quality	14	0.02-2	0.75	106.1
Mayer and Stead (2016)	Ok Tedi mine site (Papua New Guinea)	GSI	Geological strength index	10	29-53	44.2	17.9

Swolfs and Kibler (1982)	South Table Mountain (USA)	RQD	Rock quality designation	10	16.4-98.6	70.8	50.1
		E_m (GPa)	Modulus of deformation	10	12.9-43.2	27.8	39.8
Danielsen and Dahlin (2009)	Hallandsås Tunnel (Sweden)	RQD	Rock quality designation	12	12.5-62.5	37.5	51.3
		Q	Rock mass quality	12	0.01-5.5	1.29	153.4
Frough and Torabi (2013)	Karaj–Tehran tunnel (Iran)	RQD	Rock quality designation	16	15-95	57.6	47.9
		RMR	Rock mass rating	24	21-75	50.3	29.0
		Q	Rock mass quality	24	0.003-50	7.11	153.6
Jhanwar et al. (2000)	Dongri-Buzurg mine (India)	RQD	Rock quality designation	11	40-65	49.1	24.0
		RMR	Rock mass rating	11	24-65	38.4	35.6
Lama and Vutukuri (1978)	Japanese Hydro Projects (Japan)	E_m (GPa)	Modulus of deformation	21	1.0-10.1	3.73	73.2
Jafari et al. (2007)	Nosoud water tunnel (Iran)	GSI	Geological strength index	11	21-56	37.2	33.3
Pinto da Cunha (1991)	Karun dam site (Iran)	E_m (GPa)	Modulus of deformation	11	6-57	26.9	73.7
Judeel (2003)	Klerksdorp gold field (South Africa)	GSI	Geological strength index	11	27-65	48.4	30.1
Radhakrishnan and Leung (1989)	Singapore	RQD	Rock quality designation	16	15-53.8	30.3	35.6
Taheri and Tani (2009)	Australia	GSI	Geological strength index	10	46-50	48.4	3.0
		GSI	Geological strength index	10	40-45	42.4	5.4

2. Site-specific correlations between geotechnical properties

Yelu Zhou, Dongming Zhang, and Jianye Ching

2.1 Introduction

It is well known that soil parameters are generally "correlated" to each other. The existence of a large number of transformation models demonstrate the usefulness of bivariate relationships between soil parameters. The concept of a correlation expands the deterministic notion of a relationship, such as a mean trend, to a probabilistic notion that describes the strength of the relationship on top of the mean trend. In this report, the site-specific bivariate correlation coefficients are computed based on the multivariate soil databases shown in Table 2.1. Note that for the soil databases (clay and sand), most parameters do not have a unit (dimensionless), but for the rock and rock mass databases, most parameters have units. Most databases are generic (global), except that SH-CLAY/11/4051 is a municipal clay database of Shanghai. Three types of correlation coefficients are considered: (a) the Pearson product-moment correlation coefficient (ρ); (b) the Spearman rank correlation coefficient (r); and (c) the Kendall's tau rank correlation coefficient (τ).

Table 2.1. Soil/rock databases

Database	Reference	Parameters of interest	# data points	# sites/ studies
CLAY/10/7490	Ching and Phoon (2014)	LL, PI, LI, σ'_v/P_a, σ'_p/P_a, s_u/σ'_v, S_t, q_{t1}, q_{tu}, B_q	7490	251 studies
SAND/7/2794	Ching et al. (2017)	D_{50}, C_u, D_r, σ'_v/P_a, ϕ', Q_{tn}, $(N_1)_{60}$	2794	176 studies
ROCK/9/4069	Ching et al. (2018)	γ, n, R_L, S_h, σ_{bt}, I_{s50}, V_p, σ_{ci}, E_i	4069	184 studies
ROCKMass/9/5876	Ching et al. (2020)	RQD, RMR, Q, GSI, E_m, E_{em}, E_{dm}, E_i, σ_{ci}	5784	225 studies
CLAY/8/12225	Ching (2020)	LL, PI, w, e, σ'_v/P_a, C_c, C_s, c_v	12225	427 studies
CLAY/12/3997	Ching (2020)	LL, PI, LI, σ'_v/P_a, σ'_p/P_a, s_u/σ'_v, K_0, E_u/σ'_v, B_q, q_{t1}, $N_{60}/(\sigma'_v/P_a)$	3997	237 studies
SAND/13/4113	Ching (2020)	e, D_r, σ'_v/P_a, σ'_p/P_a, K_0, E_{dn}, Q_{tn}, B_q, $(N_1)_{60}$, K_{DMT}, E_{DMTn}, E_{PMTn}, M_n	4113	172 studies
SH-CLAY/11/4051	Zhang et al. (2020)	LL, PI, LI, e, K_0, σ'_v/P_a, $s_{u(UCST)}/\sigma'_v$, $s_{u(VST)}/\sigma'_v$, $S_{t(UCST)}$, $S_{t(VST)}$, p_s/σ'_v	4051	50 sites in Shanghai

γ = unit weight; ϕ' = effective friction angle; σ'_p = preconsolidation stress; σ'_v = vertical effective stress; σ_{bt} = Brazilian tensile strength; σ_{ci} = uniaxial compressive strength of intact rock; $(N_1)_{60} = N_{60}/(\sigma'_v/P_a)^{0.5}$; B_q = CPT pore pressure ratio = $(u_2-u_0)/(q_t-\sigma_v)$; C_c = compression index; C_s = swelling index; C_u = coefficient of uniformity; c_v = coefficient of consolidation; D_{50} = median grain size; D_r = relative density; e = void ratio; E_{DMT} = soil modulus determined by DMT; E_{DMTn} = normalized $E_{DMT} = (E_{DMT}/P_a)/(\sigma'_v/P_a)^{0.5}$; E_{PMT} = soil modulus determined by PMT; E_d = drained modulus of sand; E_{PMTn} = normalized $E_{PMT} = (E_{PMT}/P_a)/(\sigma'_v/P_a)^{0.5}$; $E_{dn} = (E_d/P_a)/(\sigma'_v/P_a)^{0.5}$; E_{dm} = dynamic modulus of rock mass; E_{em} = elasticity modulus of rock mass; E_i = Young's modulus of intact rock; E_m = deformation modulus of rock mass; E_u = undrained modulus of clay; GSI = geological strength index; I_{s50} = point load strength index for diameter 50 mm; K_0 = at-rest lateral earth pressure coefficient; K_{DMT} = dilatometer horizontal stress index; LI = liquidity index; LL = liquid limit; n = porosity; M = effective constrained modulus determined by oedometer; M_n = normalized $M = (M/P_a)/(\sigma'_v/P_a)^{0.5}$; N_{60} = corrected SPT-N; P_a = atmospheric pressure = 101.3 kPa; PI = plasticity index; p_s = specific penetration resistance from the CPT (unique to China); Q = Q-system; q_c = cone tip resistance; q_t = corrected cone tip resistance; $Q_{tn} = (q_t/P_a)/(\sigma'_v/P_a)^{0.5}$; $q_{t1} = (q_t-\sigma_v)/\sigma'_v$ = normalized cone tip resistance; $q_{tu} = (q_t-u_2)/\sigma'_v$ = effective cone tip resistance; R_L = L-type Schmidt hammer hardness; RMR = rock mass rating; RQD = rock quality designation; S_h = Shore scleroscope hardness; SPT-N = standard penetration test blow count; S_t = sensitivity; s_u = undrained shear strength for clay; s_u^{re} = remoulded s_u; u_0 = hydrostatic pore pressure; u_2 = CPTU pore pressure; UCST = unconfined compression soil test; V_p = P-wave velocity; VST = vane shear test; w = water content.

2.2 Summary Tables

Tables 2.2-2.6 summarize some site-specific correlation coefficients between different parameter pairs for the databases in Table 2.1. All correlation coefficients in this report are site-specific in the

sense that they are computed for each site, not for the entire soil/rock database.

2.3 Key observations

1. Figure 2.1 compares the site-specific ρ coefficients for the global vs. Shanghai municipal databases. It shows that the site-specific ρ's for the Shanghai database mostly span in a narrower range than those for the global database.
2. Evans (1996) classified ρ into 5 categories based on its magnitude. The correlation is very strong when $|\rho| \geq 0.8$, strong when $0.6 \leq |\rho| < 0.8$, moderate when $0.4 \leq |\rho| < 0.6$, weak when $0.2 \leq |\rho| < 0.4$, and very weak when $|\rho| < 0.2$. The results in Tables 2.1-2.5 are shaded by different colors according to the ρ median value (ρ_{median}): red means very strong, orange means strong, yellow means moderate, green means weak, and blue means very weak.
3. Figure 2.2 compares the histograms of site-specific ρ_{median} for normalized vs. non-normalized parameter pairs in ROCK/9/4069 (e.g., I_{s50}-E_i vs. I_{s50}/σ_{ci}-E_i/σ_{ci}). It shows that |site-specific ρ_{median}| decreases after normalization.
4. Figure 2.3 compares the histograms of site-specific ρ_{median} for global vs. Shanghai municipal sites. It shows that the site-specific ρ's at a municipal scale seem stronger than those at a global scale.
5. Figure 2.4 compares the histograms of site-specific ρ_{median} between non-dimensional parameters for clay vs. rock. There is no clear difference between soil and rock in the general trends.

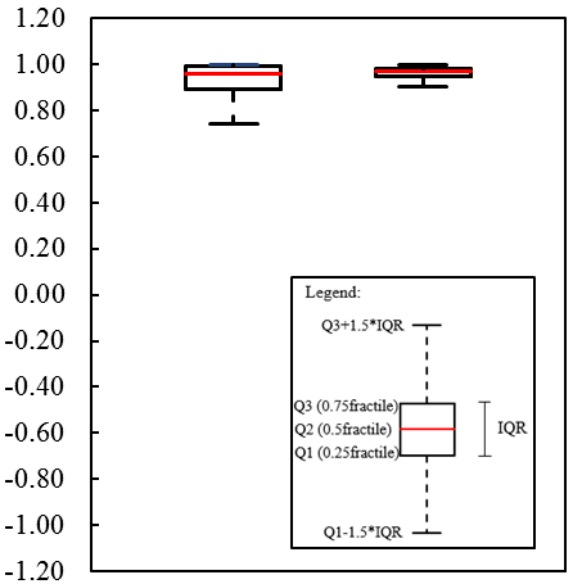

LL-PI

a)

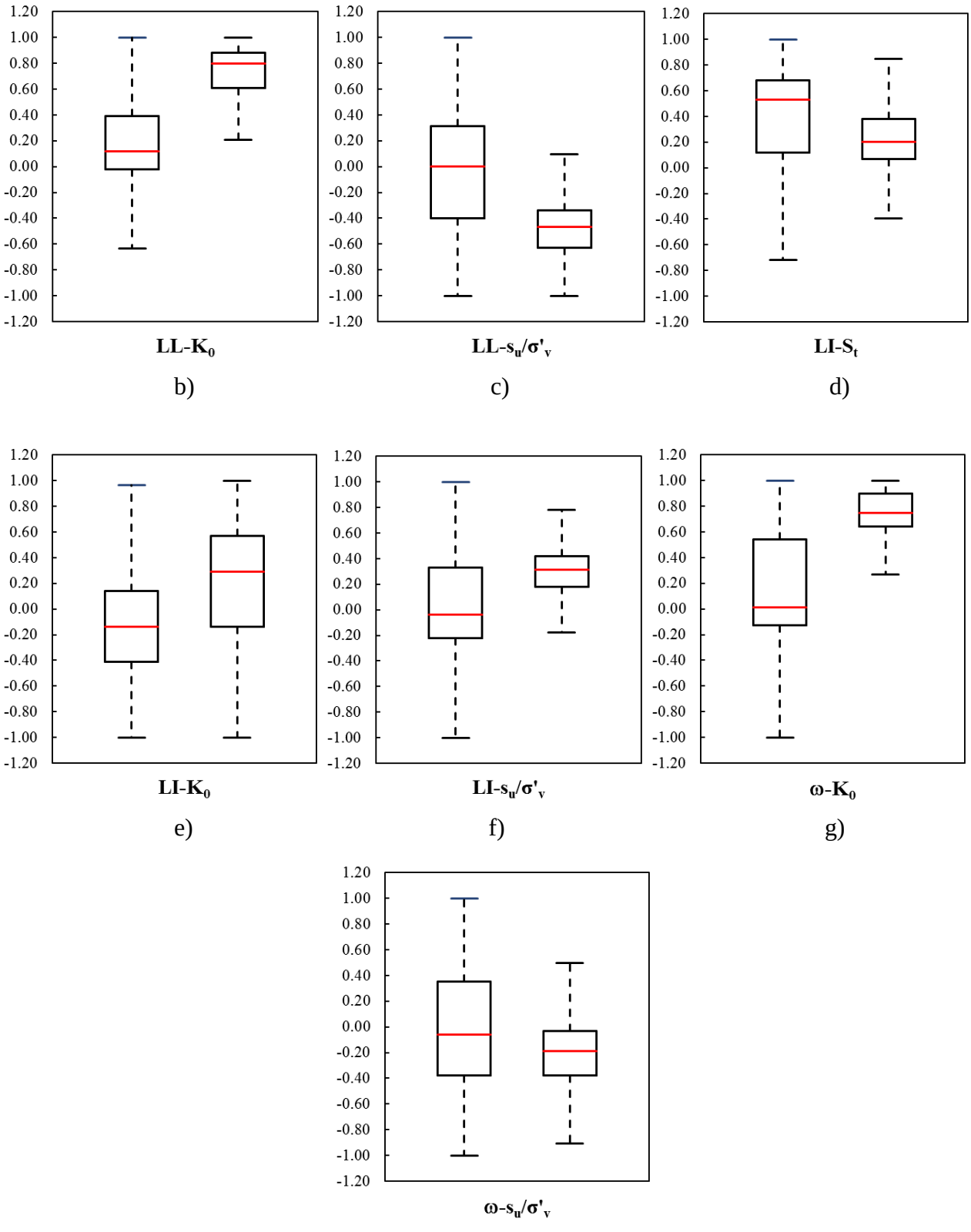

Figure 2.1. Boxplots of site-specific ρ for: a) LL-PI; b) LL-K_0; c) LL-s_u/σ'_v; d) LI-S_t; e) LI-K_0; f) LI-s_u/σ'_v; g) ω-K_0; h) ω-s_u/σ'_v. The lower and upper edges of the box mean first and third quartiles (25% at 75% percentiles), whereas the lower and upper bars mean the further extensions of the above mentioned quartiles by 1.5 times of IQR (IQR = $\rho_{75\%\text{ percentile}} - \rho_{25\%\text{ percentile}}$)

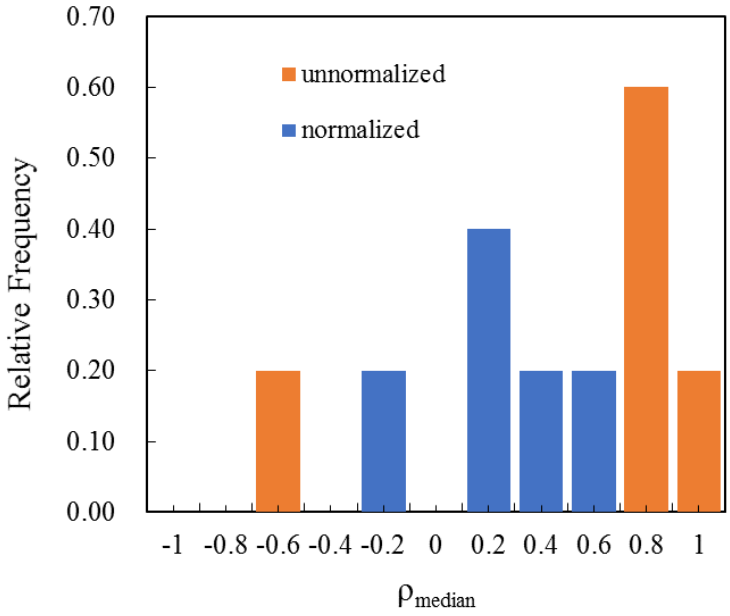

Figure 2.2. The histograms of site-specific ρ_{median} for normalized vs. non-normalized parameter pairs in ROCK/9/4069

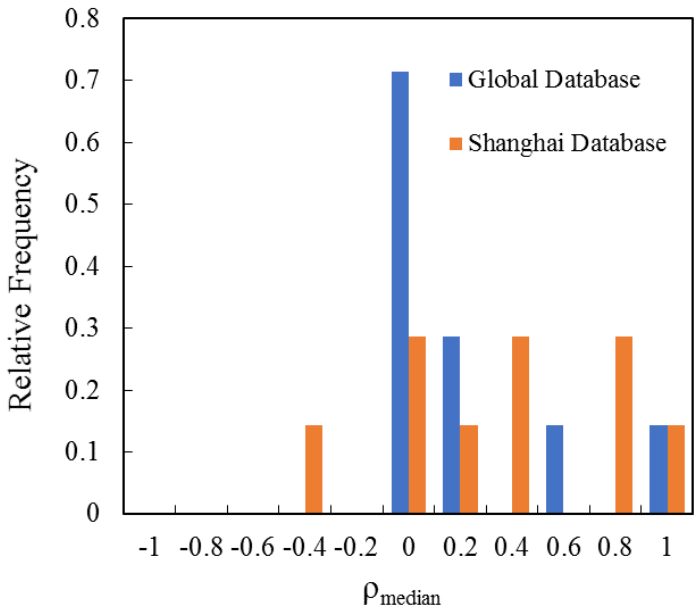

Figure 2.3. The histograms of site-specific ρ_{median} for global vs. Shanghai municipal clay sites

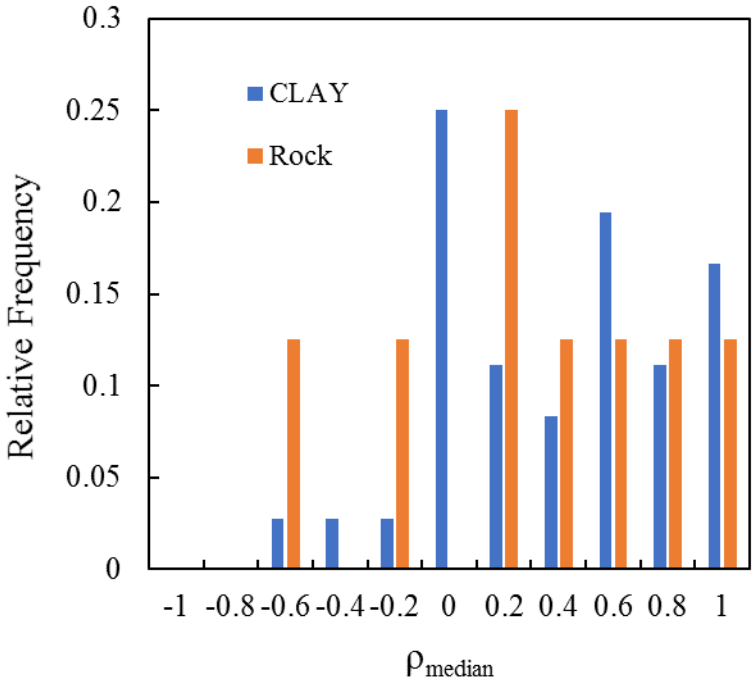

Figure 2.4. The histograms of site-specific ρ_{median} of normalized parameters for clay vs. rock

2.4 References

Ching, J. and Phoon, K.K. (2014). Transformations and correlations among some clay parameters—the global database. Canadian Geotechnical Journal, 51(6), 663-685.

Ching, J., Lin, G. H., Chen, J. R., and Phoon, K. K. (2017). Transformation models for effective friction angle and relative density calibrated based on generic database of coarse-grained soils. Canadian Geotechnical Journal, cgj-2016-0318.

Ching, J., Li, K. H., Phoon, K. K., and Weng, M. C. (2018). Generic transformation models for some intact rock properties. Canadian Geotechnical Journal, cgj-2017-0537.

Ching, J., Phoon, K.K., Ho, Y., and Weng, M. C. (2020). Quasi-site-specific prediction for deformation modulus of rock mass. Canadian Geotechnical Journal, in press.

Ching, J. (2020). Unpublished databases.

Evans, J.D. Straightforward statistics for the behavioral sciences. Brooks/ Cole Publishing, Pacific Grove, Calif, 1996.

Zhang, D., Zhou, Y., Phoon, K. K., and Huang, H. (2020). Multivariate probability distribution of shanghai clay properties. Engineering Geology, 105675.

Table 2.2. Summary of site-specific correlations for CLAY/10/7490, CLAY/8/12225, and CLAY/12/3997

Property pairs	No. of sites	No. of tests/site		Type of correlation	Value				
		Range	Mean		2.5% percentile	25% percentile	Median	75% percentile	97.5% percentile
w-C_c	70	10-639	30	Kendall	-0.06	0.29	0.52	0.66	0.91
	70	10-639	30	Pearson	-0.37	0.43	0.72	0.86	0.98
	70	10-639	30	Spearman	-0.07	0.38	0.70	0.83	0.98
w-C_s	18	10-35	16	Kendall	-0.40	0.02	0.34	0.48	0.73
	18	10-35	16	Pearson	-0.58	0.16	0.33	0.68	0.90
	18	10-35	16	Spearman	-0.58	0.08	0.37	0.66	0.89
w-s_u/σ'_v	99	10-57	16	Kendall	-0.70	-0.24	-0.05	0.24	0.72
	101	10-57	16	Pearson	-0.92	-0.38	-0.06	0.35	0.85
	99	10-57	16	Spearman	-0.83	-0.35	-0.05	0.32	0.84
w-K_0	21	10-41	18	Kendall	-0.59	-0.08	0.20	0.48	1.00
	23	10-41	17	Pearson	-0.91	-0.13	0.01	0.54	1.00
	21	10-41	18	Spearman	-0.72	-0.14	0.29	0.64	1.00
w-E_u/σ'_v	41	10-50	15	Kendall	-0.58	-0.29	-0.02	0.34	0.72
	41	10-50	15	Pearson	-0.94	-0.41	-0.07	0.58	0.82
	41	10-50	15	Spearman	-0.75	-0.33	-0.03	0.46	0.85
LL-PI	263	10-623	20	Kendall	0.31	0.69	0.82	0.89	0.96
	279	10-623	20	Pearson	0.41	0.89	0.96	0.99	1.00
	263	10-623	20	Spearman	0.37	0.84	0.94	0.97	0.99
LL-C_c	67	10-605	32	Kendall	-0.01	0.31	0.53	0.68	0.86
	67	10-605	32	Pearson	-0.07	0.47	0.67	0.87	0.97
	67	10-605	32	Spearman	-0.04	0.42	0.71	0.86	0.96
LL-C_s	14	10-33	14	Kendall	-0.44	0.04	0.27	0.42	0.87
	14	10-33	14	Pearson	-0.51	0.01	0.46	0.58	0.95
	14	10-33	14	Spearman	-0.55	0.02	0.36	0.59	0.95
LL-s_u/σ'_v	86	10-57	16	Kendall	-0.70	-0.27	-0.02	0.25	0.84
	86	10-57	16	Pearson	-0.77	-0.40	0.00	0.31	0.85
	86	10-57	16	Spearman	-0.83	-0.35	-0.04	0.36	0.93
LL-K_0	20	10-41	19	Kendall	-0.32	-0.02	0.18	0.33	0.73
	23	10-40	19	Pearson	-0.57	-0.02	0.12	0.39	0.88
	20	10-41	19	Spearman	-0.44	-0.04	0.21	0.49	0.83
LL-E_u/σ'_v	35	10-29	15	Kendall	-0.52	-0.19	0.02	0.44	0.72
	35	10-29	15	Pearson	-0.60	-0.40	0.06	0.50	0.84
	35	10-29	15	Spearman	-0.69	-0.27	0.09	0.58	0.84
PI-C_c	65	10-605	27	Kendall	-0.02	0.26	0.42	0.63	0.87
	65	10-605	27	Pearson	0.08	0.29	0.56	0.81	0.97
	65	10-605	27	Spearman	-0.01	0.35	0.55	0.77	0.96
PI-C_s	15	10-33	14	Kendall	-0.43	0.05	0.29	0.52	0.67
	15	10-33	14	Pearson	-0.46	0.12	0.45	0.60	0.90
	15	10-33	14	Spearman	-0.52	0.03	0.41	0.68	0.86
LI-S_t	45	10-113	19	Kendall	-0.40	0.06	0.29	0.54	0.80
	45	10-113	19	Pearson	-0.57	0.12	0.53	0.68	0.87
	45	10-113	19	Spearman	-0.52	0.06	0.42	0.69	0.94
LI-OCR	74	10-57	16	Kendall	-0.73	-0.25	-0.11	0.34	0.54
	77	10-57	16	Pearson	-0.79	-0.38	-0.03	0.29	0.83
	74	10-57	16	Spearman	-0.85	-0.39	-0.16	0.41	0.70
LI-s_u/σ'_v	64	10-57	16	Kendall	-0.69	-0.16	0.06	0.29	0.59
	64	10-57	16	Pearson	-0.88	-0.22	-0.04	0.33	0.78
	64	10-57	16	Spearman	-0.82	-0.26	0.10	0.39	0.78
LI-K_0	9	11-41	19	Kendall	-0.74	-0.33	-0.10	0.16	0.79

Property pairs	No. of sites	No. of tests/site		Type of correlation	Value				
		Range	Mean		2.5% percentile	25% percentile	Median	75% percentile	97.5% percentile
	9	11-41	19	Pearson	-0.85	-0.41	-0.14	0.14	0.69
	9	11-41	19	Spearman	-0.90	-0.43	-0.17	0.17	0.87
	34	10-27	15	Kendall	-0.74	-0.39	-0.14	0.10	0.72
LI-E_u/σ'_v	39	10-27	16	Pearson	-0.88	-0.49	-0.01	0.10	0.88
	34	10-27	15	Spearman	-0.87	-0.6	-0.15	0.16	0.89
	38	10-41	15	Kendall	-0.88	-0.72	-0.52	-0.24	0.44
B_q-OCR	38	10-41	15	Pearson	-0.98	-0.90	-0.68	-0.38	0.50
	38	10-41	15	Spearman	-0.95	-0.85	-0.70	-0.25	0.56
	30	10-40	15	Kendall	-0.86	-0.50	-0.16	0.06	0.39
B_q-s_u/σ'_v	30	10-40	15	Pearson	-0.93	-0.73	-0.03	0.10	0.67
	30	10-40	15	Spearman	-0.96	-0.63	-0.12	0.06	0.58
	25	10-24	16	Kendall	-0.76	-0.58	-0.28	-0.09	0.64
B_q-E_u/σ'_v	25	10-24	16	Pearson	-0.88	-0.75	-0.55	-0.26	0.65
	25	10-24	16	Spearman	-0.90	-0.76	-0.38	-0.13	0.78
	44	10-60	16	Kendall	-0.40	0.24	0.48	0.74	0.92
q_{t1}-OCR	44	10-60	16	Pearson	-0.47	0.44	0.82	0.93	0.99
	44	10-60	16	Spearman	-0.56	0.30	0.62	0.89	0.98
	90	10-59	15	Kendall	-0.76	-0.30	0.17	0.63	0.96
OCR-s_u/σ'_v	92	10-59	15	Pearson	-0.89	-0.35	0.30	0.96	0.99
	90	10-59	15	Spearman	-0.89	-0.38	0.25	0.81	0.99
	37	10-40	17	Kendall	-0.44	0.41	0.79	0.86	0.97
OCR-K_0	39	10-40	17	Pearson	-0.49	0.42	0.81	0.93	0.98
	37	10-40	17	Spearman	-0.53	0.48	0.87	0.96	0.99
	25	10-50	15	Kendall	0.07	0.27	0.42	0.59	0.93
OCR-E_u/σ'_v	25	10-50	15	Pearson	0.27	0.46	0.77	0.91	0.99
	25	10-50	15	Spearman	0.10	0.38	0.59	0.74	0.98
	37	10-59	16	Kendall	-0.59	-0.01	0.29	0.62	0.82
q_{t1}-s_u/σ'_v	37	10-59	16	Pearson	-0.79	-0.13	0.59	0.91	0.99
	37	10-59	16	Spearman	-0.71	-0.05	0.40	0.79	0.94
	7	13-43	19	Kendall	0.18	0.38	0.51	0.66	0.87
q_{t1}-K_0	8	12-43	18	Pearson	0.00	0.29	0.599	0.81	0.86
	7	13-43	19	Spearman	0.22	0.47	0.67	0.82	0.97
	42	10-33	16	Kendall	-0.33	0.19	0.43	0.61	0.83
q_{t1}-E_u/σ'_v	42	10-33	16	Pearson	-0.37	0.54	0.71	0.91	0.99
	42	10-33	16	Spearman	-0.41	0.27	0.56	0.77	0.95
	27	10-38	16	Kendall	-0.11	0.15	0.53	0.71	0.95
s_u/σ'_v-E_u/σ'_v	27	10-38	16	Pearson	-0.22	0.52	0.82	0.95	0.99
	27	10-38	16	Spearman	-0.20	0.17	0.74	0.71	0.99
	18	10-39	17	Kendall	-0.79	-0.46	-0.01	0.38	0.84
s_u/σ'_v-K_0	21	10-39	16	Pearson	-0.83	-0.44	0.00	0.53	0.98
	18	10-39	17	Spearman	-0.87	-0.64	0.00	0.51	0.94
	1	18-18	18	Kendall	0.05	0.05	0.05	0.05	0.05
s_u/σ'_v-C_c	1	18-18	18	Pearson	0.07	0.07	0.07	0.07	0.07
	1	18-18	18	Spearman	0.06	0.06	0.06	0.06	0.06
	4	10-17	14	Kendall	-0.07	0.06	0.33	0.57	0.69
E_u/σ'_v-K_0	5	10-17	13	Pearson	-0.19	0.05	0.35	0.43	0.60
	4	10-17	14	Spearman	-0.09	0.10	0.46	0.71	0.85
	1	10	10	Kendall	-0.21	-0.21	-0.21	-0.21	-0.21
K_0-C_c	1	10	10	Pearson	-0.28	-0.28	-0.28	-0.28	-0.28
	1	10	10	Spearman	-0.28	-0.28	-0.28	-0.28	-0.28
C_c-C_s	33	10-115	22	Kendall	-0.15	0.15	0.33	0.58	0.86
	33	10-115	22	Pearson	-0.48	0.20	0.46	0.73	0.96

Property pairs	No. of sites	No. of tests/site		Type of correlation	Value				
		Range	Mean		2.5% percentile	25% percentile	Median	75% percentile	97.5% percentile
	33	10-115	22	Spearman	-0.25	0.19	0.47	0.74	0.95

Note: red means very strong, orange means strong, yellow means moderate, green means weak and blue means very weak.

Table 2.3. Summary of site-specific correlations for SH-CLAY/11/4051

Property pairs	No. of sites	No. of tests/site		Type of correlation	Value				
		Range	Mean		2.5% percentile	25% percentile	Median	75% percentile	97.5% percentile
LL-PI	18	40-496	124	Kendall	0.78	0.82	0.84	0.86	0.96
	18	40-496	124	Pearson	0.94	0.95	0.97	0.98	1.00
	18	40-496	124	Spearman	0.92	0.95	0.96	0.97	1.00
LL-K_0	11	10-59	19	Kendall	0.29	0.48	0.56	0.71	0.86
	11	10-59	19	Pearson	0.40	0.61	0.80	0.88	0.97
	11	10-59	19	Spearman	0.35	0.64	0.76	0.87	0.94
LL-s_u/σ'_v	14	10-38	24	Kendall	-0.67	-0.45	-0.22	-0.07	0.08
	14	10-38	24	Pearson	-0.75	-0.63	-0.47	-0.34	-0.05
	14	10-38	24	Spearman	-0.83	-0.64	-0.34	-0.18	0.07
PI-K_0	11	10-59	19	Kendall	0.23	0.45	0.56	0.75	0.82
	11	10-59	19	Pearson	0.50	0.64	0.79	0.87	0.95
	11	10-59	19	Spearman	0.32	0.63	0.75	0.88	0.93
LI-St	12	10-38	26	Kendall	-0.17	-0.03	0.16	0.32	0.57
	12	10-38	26	Pearson	-0.21	0.07	0.20	0.38	0.79
	12	10-38	26	Spearman	-0.24	0.00	0.22	0.40	0.76
LI-K_0	11	10-59	19	Kendall	-0.24	-0.05	0.15	0.34	0.48
	11	10-59	19	Pearson	-0.18	-0.14	0.29	0.57	0.60
	11	10-59	19	Spearman	-0.35	-0.10	0.21	0.47	0.62
LI-s_u/σ'_v	14	10-38	24	Kendall	-0.29	0.15	0.28	0.35	0.49
	14	10-38	24	Pearson	-0.30	0.18	0.31	0.42	0.67
	14	10-38	24	Spearman	-0.48	0.20	0.39	0.49	0.66
w-K_0	11	10-59	19	Kendall	0.33	0.49	0.60	0.73	0.90
	11	10-59	19	Pearson	0.42	0.64	0.75	0.90	0.95
	11	10-59	19	Spearman	0.41	0.64	0.78	0.88	0.97
w-s_u/σ'_v	18	10-41	23	Kendall	-0.45	-0.35	-0.10	0.05	0.33
	18	10-41	23	Pearson	-0.73	-0.38	-0.19	-0.03	0.37
	18	10-41	23	Spearman	-0.66	-0.50	-0.15	0.06	0.41
K_0-s_u/σ'_v	1	12	12	Kendall	0.03	0.03	0.03	0.03	0.03
	1	12	12	Pearson	-0.05	-0.05	-0.05	-0.05	-0.05
	1	12	12	Spearman	0.05	0.05	0.05	0.05	0.05
p_s/σ'_v-K_0	3	10-21	14	Kendall	-0.51	-0.42	-0.16	0.16	0.27
	3	10-21	14	Pearson	-0.80	-0.74	-0.56	0.04	0.25
	3	10-21	14	Spearman	-0.70	-0.61	-0.35	0.19	0.37
p_s/σ'_v-s_u/σ'_v	13	11-41	24	Kendall	-0.18	0.25	0.42	0.46	0.58
	13	11-41	24	Pearson	0.06	0.61	0.68	0.85	0.94

Property pairs	No. of sites	No. of tests/site		Type of correlation	Value				
		Range	Mean		2.5% percentile	25% percentile	Median	75% percentile	97.5% percentile
	13	11-41	24	Spearman	-0.20	0.33	0.57	0.63	0.76

Note: red means very strong, orange means strong, yellow means moderate, green means weak and blue means very weak.

Table 2.4. Summary of site-specific correlations for SAND/7/2794 and SAND/10/4113

Property pairs	No. of sites	No. of tests/site		Type of correlation	Value				
		Range	Mean		2.5% percentile	25% percentile	Median	75% percentile	97.5% percentile
D_r-Q_{tn}	21	10-228	36	Kendall	0.53	0.62	0.73	0.83	0.91
	21	10-228	36	Pearson	0.72	0.83	0.91	0.94	0.96
	21	10-228	36	Spearman	0.69	0.81	0.88	0.94	0.98
D_r-M_n	4	12-72	40	Kendall	0.13	0.18	0.28	0.37	0.42
	4	12-72	40	Pearson	-0.04	0.09	0.26	0.36	0.43
	4	12-72	40	Spearman	0.16	0.26	0.40	0.50	0.56
K_0-M_n	5	12-72	38	Kendall	0.33	0.35	0.47	0.65	0.92
	5	12-72	38	Pearson	0.71	0.76	0.85	0.92	0.98
	5	12-72	38	Spearman	0.62	0.63	0.71	0.78	0.98
$(N_1)_{60}$-Q_{tn}	15	10-21	14	Kendall	-0.54	0.00	0.38	0.69	0.75
	15	10-21	14	Pearson	-0.70	0.23	0.48	0.85	0.91
	15	10-21	14	Spearman	-0.73	0.05	0.55	0.86	0.91
$(N_1)_{60}$-K_{DMT}	21	10-21	15	Kendall	-0.60	-0.03	0.20	0.46	0.82
	21	10-21	15	Pearson	-0.70	-0.08	0.34	0.64	0.90
	21	10-21	15	Spearman	-0.76	-0.04	0.23	0.61	0.94
Q_{tn}-K_{DMT}	45	10-31	17	Kendall	-0.41	0.14	0.37	0.53	0.77
	45	10-31	17	Pearson	-0.57	0.16	0.55	0.75	0.89
	45	10-31	17	Spearman	-0.52	0.21	0.52	0.69	0.91
E_{DMTn}-M_n	2	12-30	21	Kendall	0.43	0.43	0.52	0.61	0.61
	2	12-30	21	Pearson	0.55	0.55	0.59	0.63	0.63
	2	12-30	21	Spearman	0.59	0.59	0.68	0.78	0.78
K_{DMT}-M_n	2	12-30	21	Kendall	0.54	0.54	0.59	0.64	0.64
	2	12-30	21	Pearson	0.65	0.65	0.69	0.72	0.72
	2	12-30	21	Spearman	0.71	0.71	0.76	0.81	0.81

Note: red means very strong, orange means strong, yellow means moderate, green means weak and blue means very weak.

Table 2.5. Summary of site-specific correlations for ROCK/9/4069

Property pairs	No. of sites	No. of tests/site		Type of correlation	Value				
		Range	Mean		2.5% percentile	25% percentile	Median	75% percentile	97.5% percentile
γ_d-σ_{ci}	31	10-66	19	Kendall	-0.11	0.36	0.66	0.79	1.00
	31	10-66	19	Pearson	-0.26	0.51	0.83	0.93	0.99
	31	10-66	19	Spearman	-0.14	0.45	0.83	0.93	1.00
γ_d-E_i	11	10-66	24	Kendall	-0.04	0.17	0.29	0.61	0.75
	11	10-66	24	Pearson	-0.04	0.11	0.42	0.84	0.90
	11	10-66	24	Spearman	-0.09	0.27	0.41	0.78	0.90
γ_d-V_P	29	10-66	20	Kendall	-0.46	0.10	0.67	0.92	1.00

Property pairs	No. of sites	No. of tests/site		Type of correlation	Value				
		Range	Mean		2.5% percentile	25% percentile	Median	75% percentile	97.5% percentile
	29	10-66	20	Pearson	-0.55	0.14	0.83	0.93	0.99
	29	10-66	20	Spearman	-0.58	0.15	0.84	0.97	1.00
	11	10-45	20	Kendall	-0.65	-0.62	-0.52	-0.35	0.33
n-σ_{bt}	11	10-45	20	Pearson	-0.90	-0.79	-0.70	-0.44	0.38
	11	10-45	20	Spearman	-0.84	-0.78	-0.68	-0.45	0.53
	26	10-55	25	Kendall	-0.84	-0.67	-0.54	-0.31	0.13
n-σ_{ci}	26	10-55	25	Pearson	-0.92	-0.88	-0.73	-0.45	0.05
	26	10-55	25	Spearman	-0.96	-0.85	-0.73	-0.45	0.19
	17	10-45	24	Kendall	-0.71	-0.63	-0.55	-0.36	0.02
n-E_i	17	10-45	24	Pearson	-0.91	-0.81	-0.72	-0.47	-0.11
	17	10-45	24	Spearman	-0.90	-0.80	-0.72	-0.46	-0.01
	20	10-55	24	Kendall	-0.87	-0.76	-0.55	-0.34	0.16
n-V_P	20	10-55	24	Pearson	-0.95	-0.88	-0.72	-0.46	0.14
	20	10-55	24	Spearman	-0.96	-0.89	-0.71	-0.43	0.27
	9	13-145	41	Kendall	0.05	0.28	0.54	0.67	0.76
R_L-I_{s50}	9	13-145	41	Pearson	0.05	0.38	0.70	0.88	0.89
	9	13-145	41	Spearman	0.06	0.40	0.74	0.83	0.90
	19	10-145	30	Kendall	-0.13	0.42	0.59	0.75	0.82
R_L-σ_{ci}	19	10-145	30	Pearson	-0.21	0.60	0.82	0.90	0.97
	19	10-145	30	Spearman	-0.22	0.60	0.75	0.90	0.93
	9	10-44	25	Kendall	-0.21	0.39	0.57	0.74	0.74
R_L-E_i	9	10-44	25	Pearson	-0.27	0.65	0.78	0.89	0.93
	9	10-44	25	Spearman	-0.30	0.54	0.70	0.89	0.90
	8	13-145	40	Kendall	-0.33	0.35	0.57	0.71	0.80
R_L-V_P	8	13-145	40	Pearson	-0.44	0.55	0.76	0.89	0.97
	8	13-145	40	Spearman	-0.53	0.50	0.73	0.86	0.93
	20	10-45	22	Kendall	0.16	0.51	0.65	0.75	0.91
σ_{bt}-σ_{ci}	20	10-45	22	Pearson	0.19	0.70	0.82	0.92	0.96
	20	10-45	22	Spearman	0.21	0.67	0.76	0.87	0.96
	13	10-43	21	Kendall	-0.50	0.08	0.58	0.74	0.87
σ_{bt}-I_{s50}	13	10-43	21	Pearson	-0.51	0.05	0.81	0.90	0.94
	13	10-43	21	Spearman	-0.64	0.07	0.74	0.89	0.96
	8	10-36	20	Kendall	-0.28	0.32	0.51	0.72	0.81
σ_{bt}-V_P	8	10-36	20	Pearson	-0.44	0.50	0.66	0.82	0.92
	8	10-36	20	Spearman	-0.40	0.48	0.68	0.87	0.94
	36	10-145	28	Kendall	-0.25	0.50	0.64	0.78	1.00
I_{s50}-σ_{ci}	36	10-145	28	Pearson	-0.46	0.68	0.83	0.92	0.99
	36	10-145	28	Spearman	-0.34	0.68	0.80	0.82	1.00
	12	10-62	30	Kendall	-0.05	0.25	0.43	0.63	0.79
I_{s50}-E_i	12	10-62	30	Pearson	-0.12	0.38	0.63	0.81	0.98
	12	10-62	30	Spearman	-0.04	0.34	0.59	0.79	0.93
	18	10-145	28	Kendall	-0.15	0.50	0.61	0.82	1.00
I_{s50}-V_P	18	10-145	28	Pearson	-0.20	0.63	0.78	0.95	0.99
	18	10-145	28	Spearman	-0.23	0.68	0.77	0.95	1.00
	35	10-66	26	Kendall	0.15	0.46	0.62	0.73	0.88
σ_{ci}-E_i	35	10-66	26	Pearson	-0.13	0.57	0.83	0.92	0.98
	35	10-66	26	Spearman	0.16	0.63	0.79	0.88	0.96
	35	10-145	28	Kendall	0.03	0.58	0.68	0.84	1.00
σ_{ci}-V_P	35	10-145	28	Pearson	0.05	0.73	0.89	0.94	0.99
	35	10-145	28	Spearman	0.03	0.76	0.86	0.94	1.00
n-E_i/σ_{ci}	17	10-45	24	Kendall	-0.48	-0.13	-0.05	0.18	0.54

Property pairs	No. of sites	No. of tests/site		Type of correlation	Value				
		Range	Mean		2.5% percentile	25% percentile	Median	75% percentile	97.5% percentile
	17	10-45	24	Pearson	-0.77	-0.19	0.01	0.36	0.77
	17	10-45	24	Spearman	-0.63	-0.14	-0.06	0.26	0.71
R_L-E_i/σ_{ci}	9	10-44	25	Kendall	-0.35	-0.26	-0.14	0.09	0.34
	9	10-44	25	Pearson	-0.63	-0.43	-0.20	0.09	0.53
	9	10-44	25	Spearman	-0.45	-0.37	-0.23	0.05	0.41
R_L-I_{s50}/σ_{ci}	9	13-145	41	Kendall	-0.15	-0.05	0.06	0.10	0.17
	9	13-145	41	Pearson	-0.24	-0.07	0.13	0.28	0.31
	9	13-145	41	Spearman	-0.23	-0.08	0.10	0.11	0.24
I_{s50}/σ_{ci}-E_i/σ_{ci}	12	10-62	30	Kendall	-0.57	-0.02	0.10	0.28	0.45
	12	10-62	30	Pearson	-0.80	0.04	0.21	0.42	0.60
	12	10-62	30	Spearman	-0.79	0.04	0.13	0.40	0.63
σ_{bt}/σ_{ci}-I_{s50}/σ_{ci}	13	10-43	22	Kendall	-0.21	0.05	0.24	0.32	0.85
	13	10-43	22	Pearson	-0.15	0.22	0.46	0.83	0.94
	13	10-43	22	Spearman	-0.36	0.07	0.36	0.45	0.93

Note: red means very strong, orange means strong, yellow means moderate, green means weak and blue means very weak.

Table 2.6. Summary of site-specific correlations for ROCKMASS/9/5876

Property pairs	No. of sites	No. of tests/site		Type of correlation	Value				
		Range	Mean		2.5% percentile	25% percentile	Median	75% percentile	97.5% percentile
RQD-RMR	13	10-146	37	Kendall	0.18	0.39	0.60	0.65	0.70
	13	10-146	37	Pearson	0.01	0.56	0.80	0.84	0.87
	13	10-146	37	Spearman	0.23	0.52	0.75	0.79	0.85
RQD-Q	15	10-70	22	Kendall	0.23	0.48	0.61	0.73	0.98
	16	10-70	22	Pearson	-0.80	0.41	0.65	0.75	0.85
	15	10-70	22	Spearman	0.25	0.62	0.73	0.86	0.99
RQD-E_m/E_i	9	10-146	34	Kendall	-0.83	0.26	0.39	0.55	0.57
	9	10-146	34	Pearson	-0.92	0.37	0.50	0.68	0.69
	9	10-146	34	Spearman	-0.94	0.36	0.55	0.70	0.72
RMR-Q	20	10-330	43	Kendall	-0.01	0.43	0.53	0.72	0.89
	21	10-330	41	Pearson	-0.06	0.29	0.56	0.76	0.99
	20	10-330	43	Spearman	-0.05	0.56	0.70	0.88	0.96
RMR-GSI	9	11-60	26	Kendall	0.05	0.58	0.69	0.82	0.87
	9	11-60	26	Pearson	0.12	0.63	0.91	0.95	0.95
	9	11-60	26	Spearman	0.05	0.63	0.81	0.93	0.96
RMR-E_m	16	10-715	103	Kendall	0.09	0.46	0.60	0.72	0.76
	16	10-715	103	Pearson	0.00	0.58	0.68	0.86	0.86
	16	10-715	103	Spearman	0.11	0.62	0.75	0.89	0.91
RMR-E_{em}	9	11-418	63	Kendall	0.09	0.23	0.50	0.62	0.76
	9	11-418	63	Pearson	0.00	0.41	0.50	0.68	0.86
	9	11-418	63	Spearman	0.11	0.36	0.66	0.78	0.91
E_m-E_{em}	15	10-418	43.8	Kendall	0.63	0.78	0.85	0.89	0.93
	16	10-418	42.75	Pearson	0.55	0.92	0.94	0.98	0.99
	15	10-418	43.8	Spearman	0.79	0.90	0.96	0.97	0.99

Note: red means very strong, orange means strong, yellow means moderate, green means weak and blue means very weak.

3. Summary of random field model parameters of geotechnical properties

Armin W. Stuedlein, Brigid Cami, Diego Di Curzio, Sina Javankhoshdel, Shin-ichi Nishumura, Wojciech Pula, Giovanna Vessia, Yu Wang, and Jianye Ching

3.1 Introduction

Random field theory (RFT) represents a robust framework for the evaluation of spatial variability. Whereas regression analyses invoke classical statistics with the necessary and fundamental assumption that all data (e.g., in-situ measurements) exhibit identical likelihoods of representation and lack of correlation, RFT acknowledges and leverages the location-specific dependence of soil properties. Specifically, soil properties within any one depositional unit are autocorrelated. A given soil measurement of interest, g(z), may be separated into two components including a trend function, t(z), and a randomly fluctuating component, w(z), as:

$$g(z) = t(z) + w(z) \tag{3.1}$$

where z = depth and w(z) represents inherent soil variability. It should be noted that the assessment of random fields commonly requires conditioning to obtain weak stationarity (i.e., statistical homogeneity), which may be achieved through progressive detrending, differencing, or variance transformation of the measured soil parameter. Acceptable stationarity may be characterized by a conditioned dataset with constant mean and an autocovariance that is a singular function of separation distance (Fenton 1999; Cafaro and Cherubini 2002).

The inherent spatial variability of a measured soil property can be sufficiently characterized by its mean, the variance or coefficient of inherent variability (COV), and the scale of fluctuation (i.e., measure of autocorrelation length; VanMarcke 1977, 1983). The coefficient of inherent variability is defined as:

$$\mathrm{COV}_w(z) = \frac{\sigma_w(z)}{t(z)} \tag{3.2}$$

where σ_w = standard deviation of the fluctuating component of a measured, stationary soil parameter. The scale of fluctuation, δ, or the lag distance within which soils exhibit relatively strong correlation is the third parameter required to completely describe a finite random field within the RFT framework. Smaller magnitudes of δ describe short autocorrelation lengths and more variable soil conditions, whereas larger δ indicate long-lived autocorrelation and more homogeneous soil conditions. The determination of COV_w and δ should proceed carefully in order to prevent over-fitting during conditioning of the data to achieve weak stationarity.

3.2 Summary Tables and Figures

Table 3.1 and Figures 3.1 and 3.2 summarize the typical ranges in the vertical and horizontal scale

of fluctuation, δ, reported in the literature. Table 3.2 provides a comprehensive summary of previously reported δ. Table 3.3 provides a comprehensive summary of previously-reported vertical and horizontal COV_w. Table 3.1 and Figure 3.1 are extracted from Cami et al. (2020), whereas many cases in Table 3.2 are also extracted from Cami et al. (2020).

3.3 Key Observations

1. In general, far more data is available in the vertical direction owing to the difficulty in obtaining sufficient data in the horizontal direction to compute random field model parameters (Table 3.1, Figure 3.1).
2. Data for the vertical direction is generally considered more reliable than that in the horizontal direction, owing to the use of more sophisticated methods available for determining the autocorrelation length when data is plentiful.
3. The available data suggest that the soil autocorrelation length anisotropy (i.e., δ_h / δ_v) ranges from 3 to 500 (Figure 3.2), whereas Table 3.3 indicates no significant difference between the horizontal and vertical COV_w. The most typical value for δ_h / δ_v is around 10-20 (Figure 3.2).
4. Random field model parameters reported in the literature span a wide range in geotechnical properties; however, those associated with the cone penetration test (CPT) are most frequent owing to the ease with which data may be obtained with the CPT and frequency of data samples associated with any given sounding.

Table 3.1. Ranges of δ_h and δ_v for various soil types (Cami et al. 2020)

Soil type	δ_h (m)				δ_v (m)			
	# studies	Min	Max	Average	# studies	Min	Max	Average
Alluvial	9	1.1	49	14.8	11	0.07	2.53	0.66
Ankara clay	-	-	-	-	1	1	6.2	3.63
Chicago clay	-	-	-	-	2	0.4	1.25	0.72
Clay	17	0.14	92.4	24.43	24	0.06	12.7	2.47
Clay, sand, silt mix	13	1	1546	152.38	28	0.07	21	1.65
Hangzhou clay	-	-	-	-	1	0.5	0.77	0.65
Marine clay	6	2	60	31.3	7	0.11	6	1.85
Marine sand	1	55	55	55	4	0.08	7.2	1.77
Offshore soil	5	14	67	34.71	9	0.05	9.1	2.37
Over consolidated clay	-	-	-	-	2	0.6	2.55	1.38
Sand	8	1.7	75	11.29	12	0.1	4	1.14
Sensitive clay	2	30	46	38	3	2	4	3
Silt	3	12.7	45.5	33.22	5	0.14	7.19	2.08
Silty clay	6	5	45.4	30.26	13	0.095	6.47	1.58
Soft clay	4	22.1	80	41.1	11	0.14	6	1.76
Undrained engineered soil	-	-	-	-	23	0.3	2.7	1.43
Water content	9	2	60	18.5	5	0.2	3	1.22

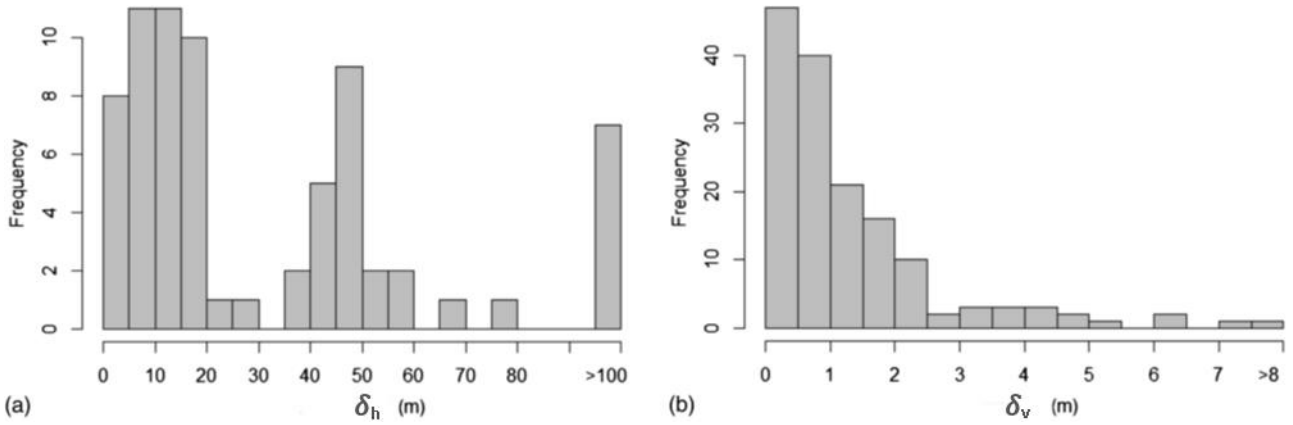

Figure 3.1. Histograms for δ_h and δ_v (extracted from Cami et al. 2020)

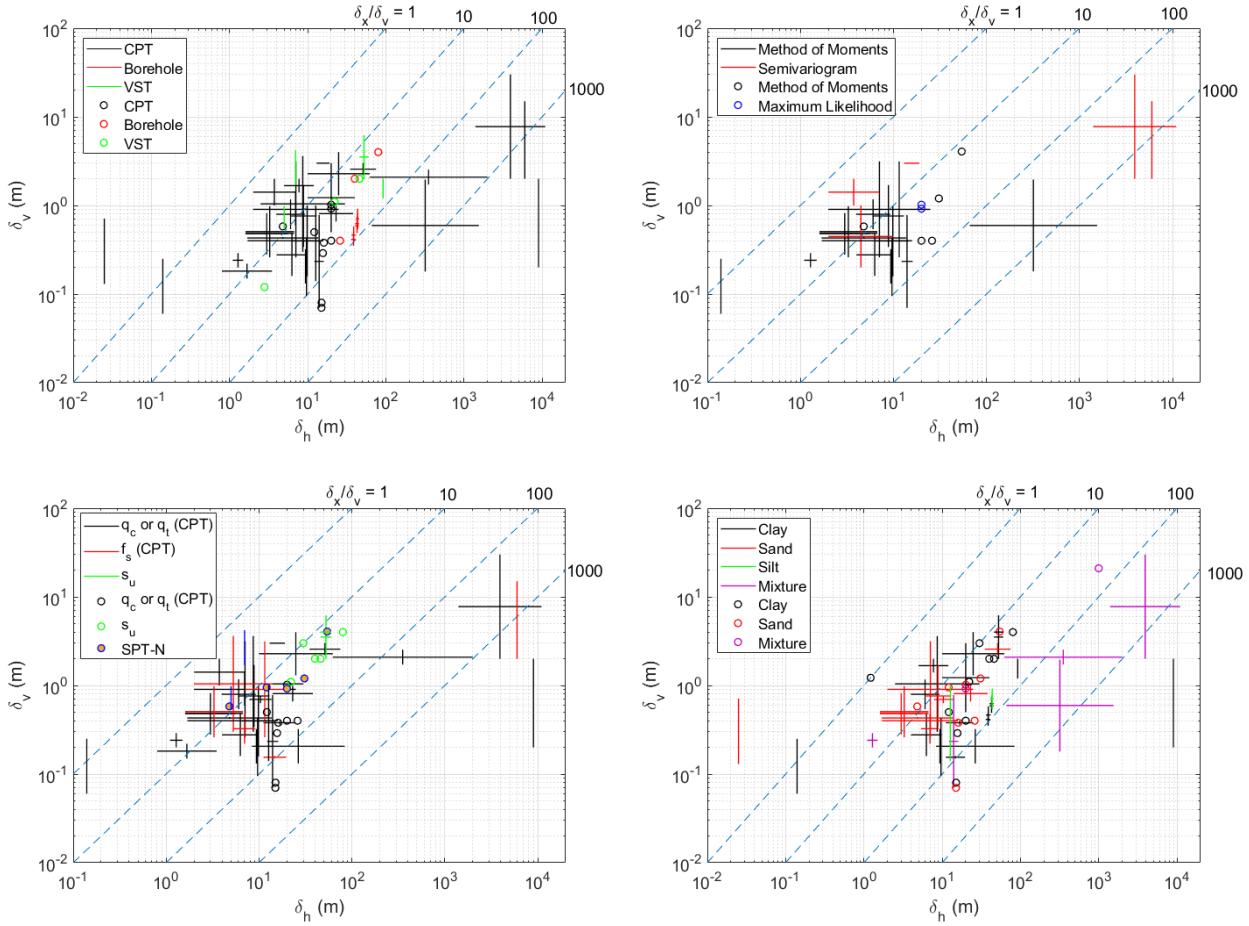

Figure 3.2. Variation of vertical scale of fluctuation, δ_v, with horizontal scale of fluctuation, δ_h, for various in-situ tests and soil conditions

3.4 References

Akkaya, A. D., & Vanmarcke, E. H. (2003). Estimation of spatial correlation of soil parameters based on data from the Texas A&M University NGES. Probabilistic site characterization at the National Geotechnical Experimentation Sites (eds GA Fenton and EH Vanmarcke), 29-40.

Akbas, S. O., & Kulhawy, F. H. (2010). Characterization and Estimation of Geotechnical Variability in

Ankara Clay: A Case History. Geotechnical and Geological Engineering, 28(5), 619-631.

Akkaya, A. D., & Vanmarcke, E. H. (2003). Estimation of Spatial Correlation of Soil Parameters Based on Data from the Texas A&M University NGES. In E. H. Vanmarcke & G. A. Fenton (Eds.), Probabilistic Site Characterization at the National Geotechnical Experimentation Sites (pp. 29-40): ASCE.

Al-Homoud, A. S., & Tanash, N. (2001). Monitoring and analysis of settlement and stability of an embankment dam constructed in stages on soft ground. Bulletin of Engineering Geology and the Environment, 59(4), 0259-0284.

Alonso, E. E., & Krizek, R. J. (1975, 15th-18th September). Stochastic Formulation of Soil Properties. Paper presented at the 2nd International Conference on Applications of Statistics and Probability in Soil and Structural Engineering, Aachen, Germany.

Asaoka, A., & Grivas, D. A. (1981). Spatial Variability of the Undrained Strength of Clays. ASCE Journal of the Geotechnical Engineering Division, 108(5), 743-756.

Bagińska, I., Kawa, M., & Janecki, W. (2016). Estimation of spatial variability of lignite mine dumping ground soil properties using CPTu results. Studia Geotechnica et Mechanica, 38(1), 3-13.

Baginska, I., Kawa, M., & Janecki, W. (2018). Estimation of Spatial Variability Properties of Mine Waste Dump Using CPTu Results-Case Study. Paper presented at the 4th International Symposium on Cone Penetration Testing (CPT'18), 21-22 June, 2018, Delft, The Netherlands.

Bergado, D. T., Patron, B. C., Youyongwatana, W., Chai, J.-C., & Yudhbir. (1994). Reliability-based analysis of embankment on soft Bangkok clay. Structural Safety, 13(4), 247-266.

Bombasaro, E., & Kasper, T. (2016). Evaluation of spatial soil variability in the Pearl River Estuary using CPTU data. Soils and Foundations, 56(3), 496-505.

Bong, T., & Stuedlein, A. W. (2017). Spatial variability of CPT parameters and silty fines in liquefiable beach sands. Journal of Geotechnical and Geoenvironmental Engineering, 143(12), 04017093.

Bong, T., & Stuedlein, A. W. (2018). Effect of cone penetration conditioning on random field model parameters and impact of spatial variability on liquefaction-induced differential settlements. Journal of Geotechnical and Geoenvironmental Engineering, 144(5), 04018018.

Bouayad, D. (2017). Assessment of Sandy Soil Variability Based on CPT Data. Procedia Engineering, 175, 310-315.

Cafaro, F., & Cherubini, C. (2002). Large sample spacing in evaluation of vertical strength variability of clayey soil. Journal of geotechnical and geoenvironmental engineering, 128(7), 558-568.

Cafaro, F., & Cherubini, C. (2002). Large Sample Spacing in Evaluation of Vertical Strength Variability of Clayey Soil. Journal of Geotechnical and Geoenvironmental Engineering, 128(7), 558-568.

Cai, G., Lin, J., Liu, S., & Puppala, A. J. (2016). Characterization of spatial variability of CPTU data in a liquefaction site improved by vibro-compaction method. KSCE Journal of Civil Engineering, 21(1), 209-219.

Cami, B., Javankhoshdel, S., Phoon, K.K., and Ching, J. (2020). Scale of fluctuation for spatially varying soils: estimation methods and values. ASCE-ASME Journal of Risk and Uncertainty in Engineering Systems, Part A: Civil Engineering, 6(4), 03120002.

Campanella, R. G., Wickremesinghe, D. S., & Robertson, P. K. (1987). Statistical Treatment of Cone

Penetrometer Test Data. Paper presented at the Fifth international conference on applications of statistics and probability in soil and structural engineering (ICASP-5), May 25-29, 1987, University of British Columbia, Vancouver, Canada.

Chai, J.-C., Miura, N., & Shen, S.-L. (2002). Performance of embankments with and without reinforcement on soft subsoil. Canadian Geotechnical Journal, 39(4), 838-848.

Cheon, J. Y., & Gilbert, R. B. (2014). Modeling spatial variability in offshore geotechnical properties for reliability-based foundation design. Structural Safety, 49, 18-26.

Cherubini C., Vessia G. (2005). The bearing capacity of piles evaluated by means of load tests according to reliability calculations. In Proceedings of ICOSSAR 2005 (Eds. G. Augusti, G.I. Schuëller, M. Ciampoli), Mill Press, Rotterdam. ISBN: 90-5966-040-4.

Cherubini C., Vessia G. (2006). Silt mixture CPT characterization for a reliability evaluation of pile total stress bearing capacity. In Proceedings of XIII Danube-European Conference on Geotechnical Engineering (Eds. J. Logar, A. Gaberc, B. Majes), Active Design in Infrastructure development, Vol. 2, pp. 19-24, Publisher: Slovensko geotechnisko drusko, Ljubljana, Slovenia. ISBN: 961-90043-9-6.

Cherubini C., Vessia G., Pula W. (2007). Statistical soil characterization of Italian sites for reliability análisis. In Proceedings of II International Workshop on Characterization & Engineering Properties of Natural Soils (Invited Paper), Singapore, 29 November,1 December, Vol. 4, pp. 2681-2706. ISBN: 041542691X

Chiasson, P., Lafleur, J., Soulié, M., & Law, K. T. (1995). Characterizing spatial variability of a clay by geostatistics. Canadian Geotechnical Journal, 32(1), 1-10.

Ching, J., Hu, Y.-G., Yang, Z.-Y., Shiau, J.-Q., Chen, J.-C., & Li, Y.-S. (2011). Reliability-based design for allowable bearing capacity of footings on rock masses by considering angle of distortion. International Journal of Rock Mechanics and Mining Sciences, 48(5), 728-740.

Dascal, O., & Tournier, J. P. (1975). Embankments on soft and sensitive clay foundation. Journal of Geotechnical and Geoenvironmental Engineering, 101(3), 297-314.

DeGroot, D. J., & Baecher, G. B. (1993). Estimating Autocovariance of In-Situ Soil Properties. Journal of Geotechnical Engineering, 119(1), 147-166.

Eslami Kenarsari, A., Jamshidi Chenari, R., & Eslami, A. (2013). Characterization of the correlation structure of residual CPT profiles in sand deposits. International Journal of Civil Engineering, 11(1), 29-37.

Ferkh, Z., & Fell, R. (1994). Design of Embankments on Soft Clay. Paper presented at the 13th International Conference on Soil Mechanics and Foundation Engineering, New Delhi, India.

Firouzianbandpey, S., Griffiths, D. V., Ibsen, L. B., & Andersen, L. V. (2014). Spatial correlation length of normalized cone data in sand: case study in the north of Denmark. Canadian Geotechnical Journal, 51(8), 844-857.

Flaate, K., & Preber, T. (1974). Stability of road embankments in soft clay. Canadian Geotechnical Journal, 11(1), 72-88.

Guo, L., Xu, W., Yang, A., and Liu, X. (2017). Application of spatial average method to estimation of scale of fluctuation of soil indexes. Journal of Engineering Geology, 25(6), 1424-1429. In Chinese.

Haldar, S., & Sivakumar Babu, G. L. (2009). Design of laterally loaded piles in clays based on cone

penetration test data: a reliability-based approach. Géotechnique, 59(7), 593-607.

Haldar, S., & Sivakumar Babu, G. L. (2009). Design of laterally loaded piles in clays based on cone penetration test data: a reliability-based approach. Géotechnique, 59(7), 593-607.

Hanzawa, H. (1983). Three Case Studies for Short Term Stability of Soft Clay Deposits. Soils and Foundations, 23(2), 140-154.

Hanzawa, H., Kishida, T., Fukasawa, T., & Asada, H. (1994). A Case Study of the Application of Direct Shear and Cone Penetration Tests to Soil Investigation, Design and Quality Control for Peaty Soils. Soils and Foundations, 34(4), 13-22.

Hanzawa, H., Matsuda, E., Suzuki, K., & Kishida, T. (1980). Stability Analysis and Field Behaviour of Earth Fills on an Alluvial Marine Clay. Soils and Foundations, 20(4), 37-51.

Hess, K. M., Wolf, S. H., & Celia, M. A. (1992). Large-scale natural gradient tracer test in sand and gravel, Cape Cod, Massachusetts: 3. Hydraulic conductivity variability and calculated macrodispersivities. Water Resources Research, 28(8), 2011-2027.

Hicks, M. A., & Samy, K. (2002). Influence of heterogeneity on undrained clay slope stability. Quarterly Journal of Engineering Geology and Hydrogeology, 35(1), 41-49.

Honjo, Y., & Kuroda, K. (1991). A New Look at Fluctuating Geotechnical Data for Reliability Design. Soils and Foundations, 31(1), 110-120.

Honjyo, Y. and Otake, Yu (2012). Verification of statistical estimation error evaluation theory of local average of geotechnical parameters, Journal of JSCE, Div.C, 68(3), 491-507.

Hsu, S.-C., & Nelson, P. P. (2006). Material Spatial Variability and Slope Stability for Weak Rock Masses. Journal of Geotechnical and Geoenvironmental Engineering, 132(2), 183-193.

Hufschmied, P. (1986). Estimation of Three-Dimensional Anisotropic Hydraulic Conductivity Field by Means of Single Well Pumping Tests Combined with Flowmeter Measurements. Hydrogeologie, 2, 163-174.

Imaide, K, Nishimura, S., Shuku, T., Shibata, T., Murakami, A. and Fujisawa, K. (2015). Estimation of distribution of cone penetration resistance inside earth-fills with use of geostatistical method, Proc. of JCOSSAR2015, 622-629.

Imaide, K., Nishimura, S., Shibata, T., Shuku, T., Murakami, A. and Fujisawa, K. (2019). Evaluation of liquefaction probability of earth-fill dam over next 50 years using geostatistical method based on CPT, Soils and Foundations, 59(6), DOI: https://doi.org/10.1016/j.sandf.2019.08.002, 1758-1771.

Ireland, H. O. (1954). Stability Analysis of the Congress Street Open Cut in Chicago. Géotechnique, 4(4), 163-168.

Jaksa, M. B. (1995). The Influence of Spatial Variability on the Geotechnical Design Properties of A Stiff, Overconsolidated Clay. (Ph.D.). University of Adelaide, Adelaide, Australia.

Jaksa, M. B., Kaggwa, W. S., & Brooker, P. I. (1999). Experimental Evaluation of the Scale of Fluctuation of A Stiff Clay. Paper presented at the 8th International Conference on Application of Statistics and Probability (ICASP8), December 1999, Sydney, Australia.

Jamshidi Chenari, R., & Kamyab Farahbakhsh, H. (2015). Generating non-stationary random fields of auto-correlated, normally distributed CPT profile by matrix decomposition method. Georisk: Assessment

and Management of Risk for Engineered Systems and Geohazards, 9(2), 96-108.

Jamshidi Chenari, R., & Kamyab Farahbakhsh, H. (2015). Generating non-stationary random fields of auto-correlated, normally distributed CPT profile by matrix decomposition method. Georisk: Assessment and Management of Risk for Engineered Systems and Geohazards, 9(2), 96-108.

Jamshidi Chenari, R., Kamyab Farahbakhsh, H., Heidarie Golafzani, S., & Eslami, A. (2018). Non-stationary realisation of CPT data: considering lithological and inherent heterogeneity. Georisk: Assessment and Management of Risk for Engineered Systems and Geohazards, 12(4), 265-278.

Japanese Geotechnical Society (1985). Reliability-based design of foundations, JGS.

Ji, J., Liao, H. J., & Low, B. K. (2012). Modeling 2-D spatial variation in slope reliability analysis using interpolated autocorrelations. Computers and Geotechnics, 40, 135-146.

Kawa, M., & Puła, W. (2020). 3D bearing capacity probabilistic analyses of footings on spatially variable c–φ soil. Acta Geotechnica 15, 1453–1466.

Khadija, N., Dias, D., Chapron, G., and Lebissonnais, H. (2020). Variability of the Ypresian plastic clay of Paris. Georisk: Assessment and Management of Risk for Engineered Systems and Geohazards, doi: 10.1080/17499518.2020.1753780.

Kulatilake, P. H., & Um, J. G. (2003). Spatial variation of cone tip resistance for the clay site at Texas A&M University. Geotechnical & Geological Engineering, 21(2), 149-165.

Lacasse, S., & de Lambellerie, J.-Y. N. (1995). Statistical Treatment of CPT Data. Paper presented at the 1st International Symposium on Cone Penetration Testing (CPT'95), October 4-5, 1995, Linkoping, Sweden.

Ladd, C. C. (1972). Test Embankment on Sensitive Clay. Paper presented at the Specialty Conference on Performance of Earth and Earth-Supported Structures, June 11-14, 1972, Lafayette, Indiana, USA

Li, X. and Xie, K. (2000). Numerical studies and statistic analyses on correlation distances of soil character parameters. Rock and Soil Mechanics, 21(4), 350-353. In Chinese.

Liu, C. N., and Chen, C. H. (2010). Estimating spatial correlation structures based on CPT data, Georisk: Assessment and Management of Risk for Engineered Systems and Geohazards, 4(2), 99-108.

Liu, C.-N., & Chen, C.-H. (2006). Mapping Liquefaction Potential Considering Spatial Correlations of CPT Measurements. Journal of Geotechnical and Geoenvironmental Engineering, 132(9), 1178-1187.

Liu, C.-N., & Chen, C.-H. (2010). Estimating spatial correlation structures based on CPT data. Georisk: Assessment and Management of Risk for Engineered Systems and Geohazards, 4(2), 99-108.

Lloret-Cabot, M. F. G. A., Fenton, G. A., and Hicks, M. A. (2014). On the estimation of scale of fluctuation in geostatistics. Georisk: Assessment and Management of Risk for Engineered Systems and Geohazards, 8(2), 129-140.

Lloret-Cabot, M., Fenton, G. A., & Hicks, M. A. (2014). On the estimation of scale of fluctuation in geostatistics. Georisk: Assessment and Management of Risk for Engineered Systems and Geohazards, 8(2), 129-140.

Lumb, P. (1975, 15th-18th September). Spatial Variability of Soil Properties. Paper presented at the 2nd International Conference on Application of Statistics and Probability in Soil and Structural Engineering, Aachen, Germany.

Luo, Q., Li, Y., and Tian, M. (2008). Study on space variability of soil parameter. Journal of Water Resources

and Architectural Engineering, 2. In Chinese.

Matsuo, M. (1984). Geotechnical engineering, -Theory and practice of reliability-based design-, Gihodo Publisher.

Matsuo, M. and Asaoka, A. (1977). Probability model of undrained strength of marine clay layer, Soils and Foundations, 17(3), 53-68.

Müller, R., Larsson, S., & Spross, J. (2014). Extended multivariate approach for uncertainty reduction in the assessment of undrained shear strength in clays. Canadian Geotechnical Journal, 51(3), 231-245.

Nadim, F. (2015). Accounting for Uncertainty and Variability in Geotechnical Characterization of Offshore Sites. Paper presented at the 5th International Symposium on Geotechnical Safety and Risk (ISGSR), October 13-16, 2015, Rotterdam, Netherlands.

Ng, I. T., & Zhou, C. Y. (2010). Uncertainty-Based Optimization of Site Characterization Using CPT. Paper presented at the 2nd International Symposium on Cone Penetration Testing (CPT'10), May 9-11, 2010, Huntington Beach, California, USA.

Nishimura, S., Fujisawa, K. and Murakami, A. (2010). Reliability-based design of earth-fill dams based on the spatial distribution of strength parameters, Georisk, 4(3), 140-147.

Nishimura, S., Shibata, T. Shuku, T. and Imaide, K. (2017). Geostatistical Analysis for Identifying Weak Soil Layers in Dikes, GEOTECHNICAL RISK ASSESSMENT AND MANAGEMENT, GSP285, ASCE, Proc. of the Geo-risk 2017, 529-538.

O'Neill, M. W., & Yoon, G. L. (2003). Spatial Variability of CPT Parameters at University of Houston NGES. Probabilistic Site Characterization at the National Geotechnical Experimentation Sites, 1-12.

Onyejekwe, S., & Ge, L. (2013). Scale of fluctuation of geotechnical parameters estimated from CPTu and laboratory test data. In Foundation engineering in the face of uncertainty: honoring Fred H. Kulhawy (pp. 434-443).

Overgård, I. E. V. (2015). Reliability-based Design of a Monopile Foundation for Offshore Wind Turbines based on CPT Data. (M.S. Master Thesis). Norwegian University of Science and Technology, Trondheim, Norway.

Phoon, K. K., Kulhawy, F. H., & Grigoriu, M. D. (1995). Reliability-based Design of Foundations for Transmission Line Structures (TR-105000).

Phoon, K.-K., & Kulhawy, F. H. (1999a). Characterization of geotechnical variability. Canadian Geotechnical Journal, 36(4), 612-624.

Phoon, K.-K., & Kulhawy, F. H. (1999b). Evaluation of geotechnical property variability. Canadian Geotechnical Journal, 36(4), 625-639.

Phoon, K.-K., Quek, S.-T., & An, P. (2003). Identification of Statistically Homogeneous Soil Layers Using Modified Bartlett Statistics. Journal of Geotechnical and Geoenvironmental Engineering, 129(7), 649-659.

Pieczyńska-Kozłowska J. M., Puła W. and Vessia G. (2017). A Collection of Fluctuation Scale Values and Autocorrelation Functions of Fine Deposits in Emilia Romagna Plain, Italy. Geo-Risk 2017 GSP 284, 290-299.

Pishgah, P., & Chenari, R. J. (2013). Reliability Measures for Consolidation Settlement by Means of CPT

Data. International Journal of Civil Engineering, 12(2B), 213-218.

Rackwitz, R. (2000). Reviewing probabilistic soils modelling. Computers and Geotechnics, 26(3-4), 199-223.

Rehfeldt, K. R., Boggs, J. M., & Gelhar, L. W. (1992). Field study of dispersion in a heterogeneous aquifer: 3. Geostatistical analysis of hydraulic conductivity. Water Resources Research, 28(12), 3309-3324.

Rehfeldt, K. R., Gelhar, L. W., Southard, J. B., & Dasinger, A. M. (1989). Estimates of Macrodispersivity base on Analyses of Hydraulic Conductivity Variability at the MADE Site (EN-6405).

Rehfeldt, K. R., Hufschmied, P., Gelhar, L. W., & Schaefer, M. E. (1989). Measuring Hydraulic Conductivity with the Borehole Flowmeter (EN-6511).

Ronold, K. O. (1990). Random Field Modeling of Foundation Failure Modes. Journal of Geotechnical Engineering, 116(4), 554-570.

Salgado, R., & Kim, D. (2014). Reliability Analysis of Load and Resistance Factor Design of Slopes. Journal of Geotechnical and Geoenvironmental Engineering, 140(1), 57-73.

Sasanian, S., Soroush, A., & Jamshidi Chenari, R. (2018). Effect of Sampling Interval on the Scale of Fluctuation of CPT Profiles Representing Random Fields. International Journal of Civil Engineering, 17(6), 871-880.

Sevaldson, R. A. (1956). The Slide in Lodalen, October 6th, 1954. Géotechnique, 6(4), 167-182.

Stuedlein, A. W. (2011). Random field model parameters for Columbia river silt. In Geo-Risk 2011: Risk Assessment and Management (pp. 169-177).

Stuedlein, A. W., Kramer, S. L., Arduino, P., & Holtz, R. D. (2012). Geotechnical characterization and random field modeling of desiccated clay. Journal of Geotechnical and Geoenvironmental Engineering, 138(11), 1301-1313.

Sudicky, E. A. (1986). A natural gradient experiment on solute transport in a sand aquifer: Spatial variability of hydraulic conductivity and its role in the dispersion process. Water Resources Research, 22(13), 2069-2082.

Uzielli, M., Vannucchi, G., & Phoon, K. K. (2005). Random field characterisation of stress-nomalised cone penetration testing parameters. Geotechnique, 55(1), 3-20.

Uzielli, M., Vannucchi, G., & Phoon, K. K. (2005). Random field characterisation of stress-nomalised cone penetration testing parameters. Géotechnique, 55(1), 3-20.

Vanmarcke, E. H. (1977). Probabilistic Modeling of Soil Profiles. Journal of the Geotechnical Engineering Division, 103(11), 1227-1246.

Vessia, G., Di Curzio, D., & Castrignanò, A. (2020). Modeling 3D soil lithotypes variability through geostatistical data fusion of CPT parameters. Science of The Total Environment, 698, 134340.

Vrouwenvelder, T., & Calle, E. O. F. (2003). Measuring Spatial Correlation of Soil Properties. Heron, 48(4), 297-311.

Wang, J., and Chen, J. (2019). A study on correlation distance of soil parameters of Ningbo mucky clay. Journal of Hubei University of Technology, 34(2), 92-97.

Wu, C., Zhu, X., and Liu, X. (2005). Studies on variability of shear strength indexes for several typical stratums in Hangzhou area. Chinese Jounal of Geotechnical Engineering, 1, 98-103. In Chinese.

Wu, T. H., Lee, I. M., Potter, J. C., & Kjekstad, O. (1987). Uncertainties in Evaluation of Strength of Marine Sand. Journal of Geotechnical Engineering, 113(7), 719-738.

Xiao, T., Li, D. Q., Cao, Z. J., & Zhang, L. M. (2018). CPT-based probabilistic characterization of three-dimensional spatial variability using MLE. Journal of Geotechnical and Geoenvironmental Engineering, 144(5), 04018023.

Xue, B. (2011). Study on the self-correlation of soil in Nanjing Hexi Area. Anhui Architecture, 018(006), 114-116. In Chinese.

Yan, S., Zhu, H., and Liu, R. (2009). Numerical studies and statistic analyses of correlation distances of soil properties in Tianjin Port. Rock and Soil Mechanics, 7, 2179-2185. In Chinese.

Zhang, J., Miao, L., Wang, H. (2009). Methods for characterizing variability of soil parameters. Chinese Journal of Geotechnical Engineering, 031(012), 1936-1940. In Chinese.

Zhang, J., Miu, L., and Chen, J. (2010). Statistical characterization of variability of lacustrine soft soil in central region of Jiangsu province. Rock and Soil Mechanics, 31(2), 471-477. In Chinese.

Zhang, L., & Chen, J.-J. (2012). Effect of spatial correlation of standard penetration test (SPT) data on bearing capacity of driven piles in sand. Canadian Geotechnical Journal, 49(4), 394-402.

Zhang, L., and Liu, C. (2011). Study on correlation distance of soil. Value engineering, 16, 6-7. In Chinese.

Table 3.2. Summary of scales of fluctuation reported in the literature

Site Location	Geomorphology	Soil type	Type of Measurement	Parameter	# soundings	Data interval (m)	SOF_h (m)	SOF_z (m)	Method	Model	Reference
Taiwan	Alluvial plane	Loose sandy soils, cohesive soils, medium dense to dense sands and clay layer	CPT	q_c	71	0.05		0.1-3.9	MM	SExp	Liu and Chen (2010)
			CPT	f_s	71	0.05		0.2-1.9			
Beaufort Region, Canada	artificial island	Filled sand in artificial island	CPT	q_c	18	0.02	1.69-13.69	0.42-0.44	MM	SExp	Lloret-Cabot et al. (2014)
Taiyuan, China		Silty clay	SPT	N value	6		39.4		MM		Li and Xie (2000)
Taiyuan, China		Clay	SPT	N value	6		45.1				
Hangzhou, China		Silty clay	SPT	N value	7		34.45				
Tianjin, China		Muck clay	CPT	q_c	25			0.18-0.54	MM		Guo et al. (2017)
Xian, China		Loess	CPT	q_c				0.22-1.13	MM		Zhang and Liu (2011)
			CPT	f_s				0.26-1.12			
Tianjin, China		Muck clay	CPT	q_c	65		6.53-14.83	0.158-1.0	MM		Yan et al. (2009)
		Clay	CPT	q_c	65		8.37	0.132-0.322			
		Silty clay	CPT	q_c	65		9.65	0.095-0.426	MM		
Ningbo, China		Mucky clay	CPT	q_c	9			0.32-0.49	MM		Wang and Chen (2019)
Nanjing, China		Silty clay	CPT	q_c	57			0.25-0.39	MM		Xue (2011)
		Silty sand	CPT	q_c	57			0.25-0.58			
Hangzhou, China		Silty clay	CPT	f_s	12			0.25-0.83	MM		Wu et al. (2005)
		Clay	CPT	f_s	12			0.16-1.26			
Xinjiang, China		Silty Clay	SPT	N value	109			0.41-0.82	MM		Luo et al. (2008)
		Silt	SPT	N value	109			0.46-0.75			
		Sand	SPT	N value	109			0.56-0.94			
College Station, TX,		Clay	CPT	q_c	6	0.02		0.1 – 0.55	MM	SExp	Kulatilake & Um (2003)

USA											
College Station, TX, USA		Sand site: Silty Sand	CPT	q_c	22	0.02		0.72 – 3.08	MM	SExp	Akkaya & Vanmarcke (2003)
		Sand site: Clean Sand	CPT	q_c	22	0.02		0.96 – 2.82	MM	SExp	
		Sand site: Clayey Sand	CPT	q_c	22	0.02		1.56 – 3.72	MM	SExp	
		Sand site: Hard Clay	CPT	q_c	22	0.02		0.61 – 1.95	MM	SExp	
		Clay site: very stiff clay	CPT	q_c	24	0.02		0.97 – 3.14	MM	SExp	
		Clay site: sand	CPT	q_c	24	0.02		0.38 – 0.77	MM	SExp	
		Clay site: very stiff clay	CPT	q_c	24	0.02		0.59 – 2.98	MM	SExp	
		Clay site: hard clay	CPT	q_c	24	0.02		0.26 – 1.33	MM	SExp	
		Sand site: Silty Sand	CPT	f_s	22	0.02		1.21 - 3.04	MM	SExp	
		Sand site: Clean Sand	CPT	f_s	22	0.02		0.83 – 2.34	MM	SExp	
		Sand site: Clayey Sand	CPT	f_s	22	0.02		1.25 – 3.53	MM	SExp	
		Sand site: Hard Clay	CPT	f_s	22	0.02		0.36 – 1.93	MM	SExp	
		Clay site: very stiff clay	CPT	f_s	24	0.02		3.34 – 12.00	MM	SExp	
		Clay site: sand	CPT	f_s	24	0.02		0.91 – 2.93	MM	SExp	
		Clay site: very stiff clay	CPT	f_s	24	0.02		0.34 – 0.78	MM	SExp	
		Clay site: hard clay	CPT	f_s	24	0.02		0.30 – 1.55	MM	SExp	
Missouri, USA		Clay	CPT	q_c	11	0.049		0.85 – 6.13	SVR	Sph	Onyejekwe & Ge (2013)
		Clay	CPT	q_t	11	0.049		0.91 – 4.94	SVR	Sph	
		Clay	Sample	C_c		0.305		0.88 – 3.05	SVR	Sph	
		Clay	Sample	e_0		0.305		0.55 – 4.66	SVR	Sph	
		Clay	Sample	γ		0.305		0.58 – 6.92	SVR	Sph	
		Clay	Sample	w_L		0.305		0.55 – 5.06	SVR	Sph	

		Clay	Sample	Preconsolidation stress, σ'_p		0.305		0.64 – 1.90	SVR	Sph	
		Clay	Sample	Friction angle, ϕ (°)		0.305		0.33 – 2.01	SVR	Sph	
		Clay	Sample	PL		0.305		0.55 – 4.42	SVR	Sph	
		Clay	Sample	S_u		0.305		0.82 – 1.43	SVR	Sph	
		Clay	Sample	w_n		0.305		0.91 – 7.10	SVR	Sph	
Longview, WA, USA		Silt	CPT	q_t	10	0.05		0.11 – 0.46	MM	Varies	Stuedlein (2011)
Baytown, TX, USA		Medium Stiff to Stiff Clay	CPT	q_t	9	0.02	4.0 to 9.90	0.16 – 0.48	MM	Varies	Stuedlein et al. (2012)
		Stiff to Very Stiff Clay	CPT	q_t	3	0.02	2.97 – 9.20	0.54 – 1.17	MM	Varies	
Hollywood, SC, USA	Beach Deposits	Clean and silty sand	CPT	q_t	25	0.02	1.6 – 6.7	0.33 – 0.78	MM	Varies	Bong and Stuedlein (2017)
				f_s	25	0.02	1.6 – 6.7	0.26 – 0.98			
Hollywood, SC, USA	Beach Deposits	Clean and silty sand	CPT	q_{c1N}	25	0.02	1.6 – 6.7	0.35 – 0.67	MM	Varies	Bong and Stuedlein (2018)
				q_{c1Ncs}	25	0.02	1.6 – 5.6	0.28 – 0.82			
Taranto, Italy		Clayey silt to silty clay: upper clay	CPT	q_t	5			0.20 – 0.44	MM	CExp	Cafaro & Cherubini (2002)
		Clayey silt to silty clay: lower		q_t	5			0.19 – 0.72			
Wufeng, Taiwan		Sand		q_t	7	0.05	7.86 – 13.65	0.63 – 0.77	ML, MM		Xiao et al. (2018)
				F_R	7	0.05	5.36 – 9.13	0.22 – 0.47	ML, MM		
		Clay		q_t	7	0.05	11.19 – 24.99	0.36 – 0.40	ML, MM		
				F_R	7	0.05	11.16 – 19.55	0.15 – 0.16	ML, MM		
Oakland, California, USA	-	Silt mixtures	CPT	q_{c1N}	2	0.05	-	0.82-0.96	MM	Mainly SMK; also SExp, and	Uzielli et al. (2005)[1]

[1] The soil types refer to the classification by Robertson (1990). The different number of soundings among the two parameters, at each location and for each soil type class, depends on cases where Autocorrelation models were not applicable or the CPT profiles were non-stationary.

										QExp	
Oakland, California, USA	-	Silt mixtures	CPT	F_R	1	0.05	-	0.49	MM	Mainly CExp; also SExp	
Oakland, California, USA	-	Sand mixtures	CPT	F_R	1	0.05	-	0.60	MM	CExp	
Oakland, California, USA	-	Clean sand	CPT	q_{c1N}	3	0.05	-	0.68-1.11	MM	Mainly QExp; also SMK, CExp, and SExp	
Oakland, California, USA	-	Clean sand	CPT	F_R	1	0.05	-	0.60	MM	Mainly SMK; also CExp, and SExp	
Mid-America earthquake regions, USA	-	Silt mixtures	CPT	q_{c1N}	2	0.05	-	0.33-0.73	MM	Mainly SMK; also SExp and QExp	
Mid-America earthquake regions, USA	-	Silt mixtures	CPT	F_R	1	0.05	-	0.40	MM	Mainly CExp; also SExp	
Mid-America earthquake regions, USA	-	Clean sand	CPT	q_{c1N}	19	0.05	-	0.39-0.97	MM	Mainly QExp; also SMK, CExp, and SExp	
Mid-America earthquake regions, USA	-	Clean sand	CPT	F_R	11	0.05	-	0.28-0.59	MM	Mainly SMK; also	

										CExp, and SExp	
Texas, USA	-	Silt mixtures	CPT	q_{c1N}	1	0.05	-	0.99	MM	Mainly SMK; also SExp, and QExp	
Texas, USA	-	Silt mixtures	CPT	F_R	2	0.05	-	0.12-0.13	MM	Mainly CExp; also SExp	
Texas, USA	-	Sand mixtures	CPT	q_{c1N}	1	0.05	-	0.35	MM	SMK	
Adapazari, Turkey	-	Clay, silty clay	CPT	q_{c1N}	5	0.05	-	0.28-0.64	MM	Mainly CExp; also SMK, SExp, and QExp	
Adapazari, Turkey	-	Clay, silty clay	CPT	F_R	3	0.05	-	0.26-0.45	MM	Mainly SExp; also SMK, and CExp	
Adapazari, Turkey	-	Clean sand	CPT	q_{c1N}	3	0.05	-	0.39-0.79	MM	Mainly QExp also SMK, CExp and SExp	
Adapazari, Turkey	-	Clean sand	CPT	F_R	2	0.05	-	0.19-0.26	MM	Mainly SMK; also CExp, and SExp	

Treasure Island, San Francisco Bay, California, USA-	-	Clay, silty clay	CPT	q_{c1N}	4	0.05	-	0.13-0.23	MM	Mainly CExp; also SMK, SExp and QExp	
Treasure Island, San Francisco Bay, California, USA	-	Clay, silty clay	CPT	F_R	3	0.05	-	0.13-0.28	MM	Mainly SExp; also SMK, and CExp	
Konaseema, India	-	Stiff clay	CPT	q_c	1	0.05	-	0.85	MM	SExp	Haldar and Sivakumar Babu (2009)
Yuanlin, Taiwan	-	Sandy and clayey layers	CPT	q_c	71	0.05	-	0.1-3.9	MM	SExp	Liu and Chen (2010)
Yuanlin, Taiwan	-	Sandy and clayey layers	CPT	f_s	71	0.05	-	0.2-1.9	MM	SExp	
Tarsuit P-45 island, Canadian Beaufort Sea, Canada	-	Sand	CPT	q_c	18	0.05	1.69-13.69	0.42-0.44	MM	SExp	Lloret-Cabot et al. (2014)
Urmia, Iran	-	Clay and organic clay, with silty and sandy inclusions	CPT	q_c	8	0.02-0.1	-	0.21-2.33	MM	-	Jamshidi Chenari and Kamyab Farahbakhsh (2015)
Central Europe	-	Lignite	CPT	q_c	42	0.05	-	0.44-0.56	MM	SExp	Baginska et al. (2016)
Central Europe	-	Lignite	CPT	f_s	42	0.05	-	0.36-0.45	MM	SExp	
Taranto, Italy	-	Yellow clay	CPT	q_c	15	0.05	-	0.195-0.436	MM	SExp	Kawa and Pula (2020)
Taranto, Italy	-	Blue-gray clay	CPT	q_c	15	0.05	-	0.185-0.720	MM	SExp	
Bologna district, Italy	-	Silt and sand mixtures	CPT	q_c	182	0.05	1400-11000	2-30	SVR	Sph	Vessia et al. (2020)
Bologna district, Italy	-	Silt and sand mixtures	CPT	f_s	182	0.05	6000	2-15	SVR	SExp (x); Sph(y)	
Bologna		Clay silt	CPT	q_c	7	0.05	-	0.13-1.03	MM	QExp,	Pieczyńska-Kozłowska

district, Italy										SExp	et al. (2017)
Brindisi, Italy		Silt mixture (silty clay and clayey silt)	CPT	s_u	6	0.02		1.6	MM	SExp	Cherubini and Vessia (2005)
Taranto, Italy		Stiff overconsolidated Taranto clay	CPT	q_c	15			0.2-0.4 (upper brownish-yellow layer) 0.2-0.7 (lower grey layer)	MM		Cherubini et al. (2007)
Fivizzano, Italy		Alluvial Deposits	Down Hole	S_u	2			1.4-2.6			Cherubini et al. (2007)
				S_u	2			1.8 -2.0			
Ankara, Turkey		Ankara Clay		w_L				4-6.2			Akbas and Kulhawy (2010)
		Ankara Clay		w_n				2.5-5.5			
		Ankara Clay		s_u				3-Jan			
		Ankara Clay	SPT	N value				3-3.8			
NGES at Texas A&M, USA		Sand	CPT	q_c, fs			2-25, 7-19	0.26-3.14	MM		Akkaya and Vanmarcke (2003)
		Clay	CPT	q_c, fs			2.5–30, 2–14	0.3-3.62	MM		
Karameh Dam, Jordan		-		s_u			2-10				Al-Homoud and Tanash (2001)
		Clean sand and sand fill	SPT	N value				0.3-4			Alonso and Krizek (1975), Lumb (1975), reported by Huber (2013)
		Organic soft clay	VST	S_u			-	1.2			Asaoka and Grivas (1981)
		Organic soft clay	VST	S_u			-	3.1			
New York		Soft clay, New York	VST	S_u				2.5-6		SExp	Asoaka et al (1981)
		Sensitive clay	VST	S_u			46	2			Baecher (1982)
Bełchatów (Central Poland)		Lignite mine waste dump	CPT	q_c	4		0.8-3.5	0.15-0.22		SExp	Baginska et al. (2018)
			CPT	q_c			Isotropic	0.36-0.56		SExp	Baginska et al. (2016)

										QExp CExp	
Bangkok, Thailand		Very soft clay	VST	S_u	41	1	22.1	1.1			Bergado et al. (1994)
Pearl River Estuary, China		Sand and clay	CPT	q_t	333	0.01/0.02	12.2-16.1	0.07-0.78	MM	SExp SMK QExp	Bombasaro and Kasper (2016)
		Marine Clay	CPT	q_c				0.78		SExp	
		Marine Sand	CPT	q_c				0.08		SMK	
		Continental Clay	CPT	q_c				0.21		SMK	
		Marine Alluvial Clay	CPT	q_c			12.15	0.5		SExp	
		Marine Alluvial clay with sand laminae	CPT	q_c			15.67	0.29		SExp	
		Marine Alluvial sand	CPT	q_c			15	0.07		SExp	
		Fluvial alluvial clay	CPT	q_c			15.06	0.08		SExp	
		Fluvial alluvial sand	CPT	q_c			16.11	0.38		SExp	
Jijel port, Algeria		Onshore sandy soils (loose to medium dense sands, dense fine sands and silty sands)	UC and DPL	q_c	10	0.02		0.32-1.32 (0.78)			Bouayad (2017)
Taranto, Italy		Taranto clay	CPT	q_c	15	0.2		0.195-0.72		CExp	Cafaro and Cherubini (2002)
Suqian City, China		Alluvial deposit	CPT	q_{c1N}	16	0.05	1.1-1.5	0.2-0.29	MM		Cai et al. (2016)
Deltaic Soils, Canada		Sand	CPT	q_c			0.025	0.13-0.71			Campanella et al. (1987)
Lian-Yun-Gang City, China		Undrained engineered slope	UC or VST	S_u				1.04	APM		Chai et al. (2002)
Saint-Hilaire, Canada			CPT, VST		16 CPT 27 VST	CPT: 0.02 VST: 0.5		1.5	SVR	Sph	Chiasson et al. (1995)
		Sandy soil	CPT	q_c				0.1-1.0		QExp	Cheng et al. (2000)

		Clay	CPT	q_c				0.1-1.8		CExp Bin	
		Soft clay	CPT	q_c				0.2-2.0			
Gulf of Mexico		Offshore soils	Sample	S_u	16		9000	7.1 - 9.1			Cheon and Gilbert (2014)
		Clay	CPT					042-0.96			Cherubini et al. (2016)
Montreal, Canada		Sensitiv clay	VST	S_u	27	X: 10m Y: 0.5m		4			Chiasson et al. (1995)
		Clay	VST	S_u			46–60	2.0–6.2		SExp	Ching et al. (2011)
		Undrained engineered slope	UC or VST	S_u				2.3	APM		Dascal and Tournier (1975)
James Bay, Quebec, Canada		Sensitive clay	VST	S_u	35						DeGroot and Baecher (1993)
		Undrained engineered slope	UC or VST	s_u				1.2	APM		Eide and Holmberg (1977)
Jutland, Denmark		Clayey silty sand	CPT	q_{c1N}	21	0.02		0.2-0.5	MM		Firouzianbandpey et al. (2014)
		Undrained engineered slope	UC or VST	S_u				0.62	APM		Flaate and Preber (1974)
		Undrained engineered slope	UC or VST	S_u				1	APM		
		Undrained engineered slope	UC or VST	S_u				0.6	APM		
		Undrained engineered slope	UC or VST	S_u				1.1	APM		
		Undrained engineered slope	UC or VST	S_u				1	APM		
		Undrained engineered slope	UC or VST	S_u				1.8	APM		
		Undrained engineered slope	UC or VST	S_u				1.25	APM		
		Undrained engineered slope	UC or VST	S_u				0.72	APM		Flaate and Preber(1974), La Rochelle et al.(1974)
		Shanghai silty clay						0.31-0.42		SExp CExp	Haldar and Sivakumar Babu (2009)
Konaseema site, India		Silty clay	CPT	q_c	1	0.2		0.8–6.1		SExp	
		Undrained	UC or	S_u				2.5	APM		Hanzawa (1983),

		engineered slope	VST								Kishida et al. (1983), Hanzawa et al. (1980), Hanzawa (1983), Hanzawa et al. (1994)
		Undrained engineered slope	UC or VST	S_u				2.5	APM		
		Undrained engineered slope	UC or VST	S_u				0.57	APM		
Cape Cod, Massachus, USA				k	16		2-10	0.2-1	SVR	SExp	Hess et al. (1992)
		Clay						0.25–2.5		SExp	Hicks and Samy (2002)
		Offshore soils	CPT	q_c			30				Hoeg (1977); Tang (1979)
		Marine clay (different levels)	CPT	q_c			35-60				
Tokyo, Japan		Soft clay	UCC	S_u	5	1 or 2	40	2			Honjo and Kuroda (1991)
Tokyo, Japan					5		80	4		SExp	
		Clay		σ_t			1.22	1.22		SExp	Hsu and Nelson (2006)
Emme Valley, Berne, Switzerland				k	16		15-20	0.63			Hufschmied (1986)
Chicago, USA		Undrained engineered slope	UC or VST	S_u	8			1.6	APM		Ireland (1954)
Adelaide, Australia		Clay	CPT	q_c	200	0.005	0.14	0.06-0.25 (mean 0.148)	MM	SExp	Jaksa (1995)
South Parlands, Adelaide, Australia		Relatively homogenous, stiff, overconsolidated clay known as Keswich Clay	CPT	q_c	30	0.005		0.63-2.55			Jaksa et al. (1999)
Urmia, Iran		clean sand, clay	CPT	q_c, fs	8	0.1 or 0.02		0.21-2.33		SExp	Jamshidi Chenari and Kamyab Farahbakhsh (2015)
		In situ soils					30–60	1.0–6.0		SExp	Ji et al. (2012)
		Offshore sand	CPT	q_c			14-38	0.66-0.99			Keaveny et al. (1989)
		Offshore soils	CPT				24.6-66.5				
		Offshore soils	Sample	S_u				0.48-7.14			
		Offshore soils	CPT	q_c			14-38				
		Offshore	Sample	S_u				0.66-.99			

		cohesive soil									
		Offshore soil	UU	S_u			-	3.6			
		Offshore soil	DST	S_u			-	1.4			
		Clean sand	CPT	q_c			-	1.6			Kulatilake and Ghosh (1988)
		Silty Clay	CPT		28		5-12	1.4-2			Lacasse and de Lambellerie (1995)
		Offshore sand	CPT	q_c			25-67c		MM	SExp	Lacasse and Nadim (1996)
		Laminated clay	CPT	q_c			9.6	-			
		Dense sand	CPT	q_c			37.5	-			
Portsmouth, N.H., USA		Undrained engineered slope	UC or VST	S_u	3			0.94	APM		Ladd (1972)
		Undrained engineered slope	UC or VST	S_u	3			2.5	APM		Lafleur et al. (1988)
		Taiyuan silty clay	DST				36.2–41.7	0.37–0.58		Bin	Li et al. (2003)
		Taiyuan silty clay	DST				36–41.4	0.35–0.49		Bin	
		Taiyuan silt	DST				41.5–45.1	0.6–0.84		Bin	
		Taiyuan silt	DST				41.8–45.5	0.54–0.92		Bin	
		Hangzhou silty clay	DST				40.5–45.4	0.52–0.75		Bin	
		Hangzhou silty clay	DST				40.4–45.2	0.49–0.71		Bin	
		Hangzhou clay	DST					0.5–0.77		Bin	
		Hangzhou clay	DST					0.59–0.73		Bin	
		Clay-bound sand	CPT	q_c			6-13	0.34-1.7	MM	SExp Sph	Lingwanda et al. (2017)
Yuanlin, Taiwan		Sand, silt, and clay	CPT	q_c, fs	71	0.05	126.9-163.9		MM	SExp	Liu and Chen (2006)
		Sand, silt, and clay	CPT	q_c, fs			66-1546	0.18-1.96	MM	SExp	
Yuanlin, Taiwan		onshore alluvial deposits (loose sandy soils, cohesive soils, medium dense to	CPT	q_c	71	0.05	62-2000	1.72-2.53		SExp	Liu and Chen (2010)

		dense sands and clay layers)									
		Offshore clays	CPT	q_c				0.05-1			Liu et al. (2015)
Tarsuit P-45, Canada		Filled sand in artificial Island	CPT	q_c	18		1.7–15.9	0.4	MM		Lloret-Cabot et al. (2014)
		Marine clay, Japan						1.3-2.7		SExp	Matsuo (1976)
							50-70		SVR	Sph	Mulla (1988)
							40-60		SVR	Sph	
							40-70		SVR	Sph	
							60-80		SVR	Sph	
							40-60		SVR	Sph	
Veda, Sweden		Clay	CPT	q_t	16		20	0.4	MM		Müller et al. (2014)
CDP1 Platform, North Sea		Different soil units	CPT	q_c	39			0.18-0.39			Nadim (2015)
		Clay and silt clay	CPT	q_c			283, 225		MM		Ng and Zhou (2010)
		Yan'an silty clay						1.47			Ni et al. (2002)
		Yan'an silty clay						1.44			
		Jiangzhang silty clay						6.47			
		Jiangzhang silty clay						2.96			
		Tongguan silt						7.19			
		Tongguan silt						1.2			
NGES-UH, USA		Alluvial deposit	CPT	q_c	A:12 B: 44	0.15	2-7	1-2	SVR		O'Neill and Yoon (2003)
		onshore alluvial deposits (loose sandy soils, cohesive soils, medium dense to dense sands and clay layers)	CPT	f_s				0.18-1.96			Oguz et al. (2019)
		Clayey silty sand	CPT	f_s				0.2			
North Sea		Offshore sand	CPT		18			0.4-2.9	ML		Overgård (2015)

		and clay sublayers									
		Onshore two clay sites						0.11-0.29			Pantelids and Christodoulou (2017)
		Clay		S_u	5			0.8-6.1 (2.5)			Phoon and Kulhawy (1999a),Phoon and Kulhawy (1999b)
		Sand, Clay	CPT	q_c	7			0.1-2.2 (0.9)			
		Clay	CPT	q_t	10			0.2-0.5 (0.3)			
		Clay	VST	S_u	6		46-60	2-6.2			
		Clay, loam		w_n	3			1.6-12.7 (5.7)			
		Clay	CPT	S_u	5			0.8-6.1(mean 2,5)			Phoon et al. (1995)
		Clay	CPT	q_t	x: 2 z: 7		23-66 (mean 44.5)	0.1-2.2 (mean 0.9)			
		Sand and clay	CPT	q_c	x:11 z: 10		3-80 (mean 47.9)	0.2-0.5 (mean 0.3)			
		Clay	VST	S_u	x: 3 z: 6		46-60(mean 50.7)	2-6.2 (mean 3.8)			
Treasure Island Naval Station, California, USA		Offshore sediments	CPT, Lab tests	S_u		0.02		0.38-0.8			Phoon et al. (2003)
		Undrained engineered slope	UC or VST	S_u				0.96-2.7	APM		Pilot (1972), Pilot et al. (1982), Talesnick and Baker (1984)
		Sand	SPT	N value			12.1	0.95			Popescu et al. (1995)
		-		S_u			Isotropic 0.5. rarely more than 10				Rackwitz (2000)
		Undrained engineered slope	UC or VST	S_u				2.5	APM		Ramalho-Ortigão et al. (1983), Ferkh and Fell (1994)
		Undrained engineered slope	UC or VST	S_u				1.8	APM		
Columbs, Mississippi, USA				k			12.7	1.6			Rehfeldt, Gelhar, et al. (1989),Rehfeldt, Hufschmied, et al. (1989), Young and Boggs (1990)

					58	0.15	7.5-22.6	1-2.3		SExp	Rehfeldt et al. (1992)
					58	0.15	25-50	1.5-3		SExp	
		Clay	DST				92.4	1.2-2		QExp	Ronold (1990)
							750		SVR	Sph	Rosenbaum (1987)
		Clay	CPT	q_c			10–62	1.3–4.0		SExp	Salgado and Kim (2014)
		Sand	CPT	q_c			35–75	2.2–3.0		SExp	
Lodalen, Oslo, Norway		Undrained engineered slope		S_u	14			1.8	APM		Sevaldson (1956)
		Very soft clay (sand inclusion)	UC or VST					0.16-0.32 (0.23)			Huwang and Linping (2015)
		Mud and very soft clay	CPT					0.14-1 (0.37)		SExp QExp CExp	
		very soft clay and clay	CPT					0.16-0.57 (0.37)			
		Clay	CPT					0.13-0.32 (0.24)			
		Silty Clay	CPT	q_c				0.1-0.43 (0.23)			
			CPT				13-19	3	SVR	SExp	Soulie' et al. (1990)
		Marine Clay		S_u				6			
		Sensitive clay		S_u			30	3			
Canadian Forces Base Borden, Ontario, Canada			VST	k		0.2-0.3	2.8	0.12			Sudicky (1986), Freyberg (1986)
							55			QExp	Tang (1979)
			CPT				35-60			QExp	
			CPT				5.68-9.27		SVR		Unlu et al. (1990)
							8.89-20		SVR		
							4.02-7.5		SVR		
Turkey and North America		Sand, Clay, Silt (Mixture)		q_c	40	0.05		0.13-1.11 (0.7)			Uzielli et al. (2005)
		Sand, Clay, Silt (Mixture)	CPT	F_R	25	0.05		0.12-0.6 (0.36)			
		Superficial soft	CPT	Soil layer			22.2				Valdez-Llamas et al.

		clay		thickness							(2003)
		Superficial soft clay		w_n				0.8-2.0			
		Deep deposits with alternating clayey and sandy soils		w_n			1000	21			
		New Liskeard varved clay		S_u, N value	25		46	5			Vanmarcke (1977)
Leidschendam, Netherlands		Sand		q_z	18	2-5	22-34			SExp	Vrouwenvelder and Calle (2003)
Deltaic Soils, Canada		Sand	CPT	q_c		0.025		0.24-0.32			Wickremesinghe and Campanella (1993)
		Undrained engineered slope	CPT	S_u				0.3	APM		Wilkes (1972)
		Chicago clay	UC or VST	S_u			-	0.4			Wu (1974)
North Sea		Fine sand	UC	q_c	24		26	0.4	MM	SExp	Wu et al. (1987)
		Clay	CPT				10–40	0.5–3.0		SExp	Wu et al. (2011)
		Alluvial soil					30–49	0.2–0.9		SExp	
		Ocean and lake sedimentary soils					40–80	1.3–8.0			
		Moraine soil						2			
		Aeolian soil						1.2–7.2			
		Undrained engineered slope		S_u				1.5	APM		Wu et al. (1977)
		Chicago clay	UC or VST					0.79–1.25		SExp	Xie (2009)
		Saturated clay, Japan						1.25–2.86			
		Tianjin port clay		q_c			8.37	0.132–0.322			Yan et al. (2009)
		Tianjin port silty clay	CPT	q_c			9.65	0.095–0.426			
		Tianjin port silt	CPT	q_c			12.7	0.140–1.0			
		Sandy	CPT	N value	3			1.36-3.01		SExp QExp	Zhang and Chen (2012)
		Sand, Clay, Silt	SPT	q_c			-	0.36–4.92	MM	-	Sasanian et al. (2018)

		(Mixture)									
Adapazari area, Turkey		Sand, Clay, Silt (Mixture)	CPT	q_c	1	0.02	-	0.16	VRF	-	Pishgah and Chenari (2013)
		Sand, Clay, Silt (Mixture)	CPT	q_c			-	0.44-1.52	MM, VRF	SExp	Eslami Kenarsari et al. (2013)
B.C., Canada		Sand, Clay, Silt (Mixture)	CPT	q_c	1		-	0.5		SExp	Jamshidi Chenari et al. (2018)
Canadian Beaufort sea shelf		(0-3 m below sea bottom)	CPT	q_c	6	9	55				Zhang et al. (2016)
		Fine to medium grained kaolinic sandstones overlain by consolidated clay-bound sands	CPT	q_c				0.6-1.4			Prastings (2019)
			CPT	q_c			7	0.59-1.44	APM		
			CPT	q_c				0.4-1.7			
			CPT	q_c				0.35-1.5	MM	Sph	
			CPT	q_c				0.34-1.4	MM	SExp	
			CPT	q_c			10		MM	Tri	
			CPT	N_{10}				0.3-1.8			
			DPL	N_{10}			5	0.54-0.98	APM		
			DPL	N_{10}				0.38-1.5	MM	Sph	
			DPL	N_{10}				0.37-1.59	MM	SExp	
			DPL	N_{60}			7	1.7-4.2	APM		
			SPT	M			7	2.5-2.9	APM		
Japan	Marine bay	Clay, Silty Clay	UC	S_u	1	0.25-0.5		1.2-2.5	MM	SExp	Matsuo and Asaoka (1977)
Tokyo Japan	Marine bay	Clay	UC	S_u	1	231	660		MM	SExp	Matsuo (1984)
Hokkaido Japan	Alluvial Layer	Organic clay	UC	S_u	1	36	105		MM	SExp	
Japan	Alluvial Layer	Sand	CPT	q_t	3	0.05		0.3-0.5	MM	SExp	Honjo and Otake (2012)
Okayama Japan	Embankment	Silty sand	CPT	q_t	10	X: 5 Y: 0.05	20	1.02	ML	SExp	Imaide, et al. (2015)
Kyoto Japan	Embankment	Silty sand	CPT	q_t	11	X: 5 Y: 0.05	20	0.92	ML	SExp	
Hiroshima Japan	Embankment	Silty sand	CPT	log (N value)	8	X: 2.0 Y: 0.05	4.8	0.58	MM	SExp	Imaide, et al. (2019)

Okayama Japan	Embankment, Alluvial layer	Silty sand, Clay, Sand	CPT	log (N value)	24	X: 5 Y: 0.05	20	0.92	ML	SExp	Nishimura et al. (2017)
Okayama Japan	Embankment	Silty sand	SWS	N value	15	X: 2 - 5 Y: 0.25	54.2	4.06	MM	SExp	Nishimura et al. (2016)
Okayama Japan	Embankment	Silty sand	SWS	N value	9	X: 5 Y: 0.25	30.8	1.20	MM	SExp	Nishimura et al. (2010)

Table 3.3. Summary of the coefficient of inherent variability reported in the literature

Site Location	Geomorphology	Soil type	Type of Measurement	Parameter	# soundings	Data interval (m)	COV_h (%)	COV_z (%)	Method	Model	Reference
Jiangsu, China		Clay		Cohesion, C (kPa)				9-16			Zhang et al. (2009)
		Clay		Friction angel, ϕ (°)				16-73			
		Clay		Young's modulus, E (MPa)				14-21			
Jiangsu, China		Silty clay		Natural moisture content, w (%)	49 sets (including 2695 samples)			2-18			Zhang et al. (2010)
		Clay		Natural moisture content, w (%)	15 sets (including 1185 samples)			3-15			
		Silty sand		Natural moisture content, w (%)	22 sets (including 550 samples)			3-17			
		Silty clay		Liquid limit, w_L (%)	42 sets (including 2100 samples)			4-18			
		Clay		Liquid limit, w_L (%)	12 sets (including 996 samples)			1-15			
		Silty clay		Unit weight, γ	50 sets (including 2900 samples)			1-5			
		Clay		Unit weight, γ	15 sets (including 1200 samples)			1-4			
		Silty sand		Unit weight, γ	21 sets (including 504 samples)			1-4			
		Silty clay		Plasticity index, PI	14 sets (including 364 samples)			9-38			
		Silty clay		Liquidity index, LI	14 sets (including 364 samples)			11-47			
		Silty clay		Void ratio, e	16 sets (including 512 samples)			5-15			
		Silty sand		Void ratio, e	14 sets (including 252 samples)			6-19			

		Silty clay		Young's modulus, E (MPa)	30 sets (including 960 samples)			5-48			
		Clay		Young's modulus, E (MPa)	7 sets (including 427 samples)			12-34			
		Silty sand		Young's modulus, E (MPa)	12 sets (including 252 samples)			15-51			
		Silty clay		Cohesion, C (kPa)	43 sets (including 1419 samples)			7-51			
		Clay		Cohesion, C (kPa)	12 sets (including 540 samples)			13-44			
		Silty sand		Cohesion, C (kPa)	12 sets (including 192 samples)			23-106			
		Silty clay		Friction angle, ϕ (°)	43 sets (including 1419 samples)			7-54			
		Clay		Friction angle, ϕ (°)	12 sets (including 540 samples)			7-28			
		Silty sand		Friction angle, ϕ (°)	12 sets (including 192 samples)			7-31			
Paris, France		Ypresian plastic clay		Natural moisture content, w (%)	656 samples			4.2-37			Khadija et al. (2020)
				Plasticity index, PI	153 samples			15-36			
				Clay content (<2µm)	143 samples			7.8-33			
			CD and CU triaxial tests	Friction angel, ϕ (°)	91 samples			23.8-24.1			
			CD and CU triaxial tests	Cohesion, C (kPa)	65 samples			13-38			
				Young's modulus, E (MPa)	123 samples			59-68			
			Oedometer test	Coefficient of earth pressure at rest, K_0	70 samples			6.8-33			
College Station, TX, USA		Clay	CPT	q_c	6	0.02		5 - 36	MM	SExp	Kulatilake & Um (2003)
College Station, TX, USA		Sand site: Silty Sand	CPT	q_c	22	0.02		32 – 69	MM	SExp	Akkaya & Vanmarcke (2003)
		Sand site: Clean Sand	CPT	q_c	22	0.02		15 – 75			
		Sand site: Clayey	CPT	q_c	22	0.02		33 - 70			

		Sand									
		Sand site: Hard Clay	CPT	q_c	22	0.02		4 - 53			
		Clay site: very stiff clay	CPT	q_c	24	0.02		30 – 66			
		Clay site: sand	CPT	q_c	24	0.02		7 – 31			
		Clay site: very stiff clay	CPT	q_c	24	0.02		48 – 100			
		Clay site: hard clay	CPT	q_c	24	0.02		15 – 72			
		Sand site: Silty Sand	CPT	f_s	22	0.02		44 – 82			
		Sand site: Clean Sand	CPT	f_s	22	0.02		18 – 67			
		Sand site: Clayey Sand	CPT	f_s	22	0.02		34 – 71			
		Sand site: Hard Clay	CPT	f_s	22	0.02		8 – 56			
		Clay site: very stiff clay	CPT	f_s	24	0.02		30 – 58			
		Clay site: sand	CPT	f_s	24	0.02		15 – 44			
		Clay site: very stiff clay	CPT	f_s	24	0.02		39 – 82			
		Clay site: hard clay	CPT	f_s	24	0.02		15 - 60			
Longview, WA, USA	Alluvial deposits	NC Silt	CPT	q_t	10	0.05		8.2 – 24.1	MM	Varies	Stuedlein (2011)
Baytown, TX, USA	Marine deposits	Medium Stiff to Stiff Clay	CPT	q_t	9	0.02	13 – 55	16.1 – 76.8	MM	Varies	Stuedlein et al. (2012)
	Marine Deposits	Stiff to Very Stiff	CPT	q_t	3	0.02	9 - 14	7.8 – 10.8			

		Clay									
Hollywood, SC, USA	Beach Deposits	Clean and silty sand	CPT	q_t	25	0.02	9 – 80	37.8 – 55.8	MM	Varies	Bong and Stuedlein (2017)
				f_s	25	0.02	17 – 66	17.2 – 70.2			
Hollywood, SC, USA	Beach Deposits	Clean and silty sand	CPT	q_{c1N}	25	0.02	9 - 81	34.8 – 52.1	MM	Varies	Bong and Stuedlein (2018)
				q_{c1Ncs}	25	0.02	4.2 - 35	11.1 – 38.0			
Oakland, California, USA	-	Silt mixtures	CPT	q_{c1N}	2	0.05	-	18-20	MM	Mainly SMK; also SExp, and QExp	Uzielli et al. (2005)[2]
Oakland, California, USA	-	Silt mixtures	CPT	F_R	1	0.05	-	17	MM	Mainly CExp; also SExp	
Oakland, California, USA	-	Sand mixtures	CPT	F_R	1	0.05	-	38	MM	CExp	
Oakland, California, USA	-	Clean sand	CPT	q_{c1N}	3	0.05	-	18-25	MM	Mainly QExp; also SMK, CExp, and SExp	
Oakland, California, USA	-	Clean sand	CPT	F_R	1	0.05	-	22	MM	Mainly SMK; also CExp, and SExp	
Mid-America	-	Silt mixtures	CPT	q_{c1N}	2	0.05	-	19-28	MM	Mainly SMK;	

[2] COV_z values refer to the Inherent Coefficient of Variation, calculated after the vertical trend removal.

earthquake regions, USA										also SExp, and QExp	
Mid-America earthquake regions, USA	-	Silt mixtures	CPT	F_R	1	0.05	-	18	MM	Mainly CExp; also SExp	
Mid-America earthquake regions, USA	-	Clean sand	CPT	q_{c1N}	19	0.05	-	17-38	MM	Mainly QExp; also SMK, CExp, and SExp	
Mid-America earthquake regions, USA	-	Clean sand	CPT	F_R	11	0.05	-	10-31	MM	Mainly Second-order Markov; also CExp, and SExp	
Texas, USA	-	Silt mixtures	CPT	q_{c1N}	1	0.05	-	33	MM	Mainly SMK; also SExp, and QExp	
Texas, USA	-	Silt mixtures	CPT	F_R	2	0.05	-	13-15	MM	Mainly CExp; also SExp	
Texas, USA	-	Sand mixtures	CPT	q_{c1N}	1	0.05	-	24	MM	SMK	
Adapazari, Turkey	-	Clay, silty clay	CPT	q_{c1N}	5	0.05	-	11-21	MM	Mainly CExp; also	

										SMK, SExp, and QExp	
Adapazari, Turkey	-	Clay, silty clay	CPT	F_R	3	0.05	-	14-21	MM	Mainly SExp; also SMK, and CExp	
Adapazari, Turkey	-	Clean sand	CPT	q_{c1N}	3	0.05	-	20-24	MM	Mainly QExp; also SMK, CExp, and SExp	
Adapazari, Turkey	-	Clean sand	CPT	F_R	2	0.05	-	48-59	MM	Mainly SMK; also CExp, and SExp	
Treasure Island, San Francisco Bay, California, USA-	-	Clay, silty clay	CPT	q_{c1N}	4	0.05	-	2-5	MM	Mainly CExp; also SMK, SExp, and QExp	
Treasure Island, San Francisco Bay, California, USA	-	Clay, silty clay	CPT	F_R	3	0.05	-	10-18	MM	Mainly SExp; also SMK, and CExp	
Konaseema, India	-	Stiff clay	CPT	q_c	1	0.05	-	37	MM	SExp	Haldar and Sivakumar Babu (2009)

Central Europe	-	Lignite	CPTu	q_c	42	0.05	-	23.55-88.16	MM	SExp	Baginska et al. (2016)
Central Europe	-	Lignite	CPTu	f_s	42	0.05	-	31.99-111.53	MM	SExp	
Bologna district, Italy		Clay silt	CPT	s_u	7	0.05		17-51	Detrend +Residuals Analyses		Pieczyńska-Kozłowska et al. (2017)
Matera, Italy		Matera blue clay	Undrained shear test	su	89			32.7			Cherubini and Vessia (2005)
			Atterberg Limits	LL	181			14.1			
			Atterberg Limits	PL	181			16.2			
			Unit weight	γ	579			4.6			
			Natural water content	w_n	579			12.9			
Brindisi, Italy		Silt mixture (silty clay and clayey silt)	Atterberg limits	LL				21.8			Cherubini and Vessia (2005)
			Atterberg limits	PL				20.7			
			Unit weight	γ				4.9			
			Natural water content	w_n				26.4			
Fivizzano, Italy		Alluvial Deposits	Down Hole	V_{SH}	2			7-9.2			Cherubini et al. (2007)
				V_P	2			6.8-7.9			
Japan	Marine bay	Clay, or Silty Clay	UC	S_u	1	0.25-0.5			MM	SExp	Matsuo and Asaoka (1977)
Tokyo Japan	Marine bay	Clay	UC	S_u	1	231			MM	SExp	Matsuo (1984)
Hokkaido Japan	Alluvial Layer	Organic clay	UC	S_u	1	36			MM	SExp	
Japan	Alluvial Layer	Sand	CPT	q_t	3	0.05			MM	SExp	Honjo and Otake (2012)
Okayama	Embankment	Silty sand	CPT	q_t	10	X: 5.0 Y: 0.05			ML	SExp	Imaide, et al. (2015)

Japan											
Kyoto Japan	Embankment	Silty sand	CPT	q_t	11	X: 5.0 Y: 0.05			ML	SExp	
Hiroshima Japan	Embankment	Silty sand	CPT	log (N value)	8	X: 2.0 Y: 0.05			MM	SExp	Imaide, et al. (2019)
Okayama Japan	Embankment + Alluvial layer	Silty sand, Clay, Sand	CPT	log (N value)	24	X: 5.0 Y: 0.05			ML	SExp	Nishimura et al. (2017)
Okayama Japan	Embankment	Silty sand	SWS	N value	15	X: 2-5 Y: 0.25			MM	SExp	Nishimura et al. (2016)

Notations

Type of measurement:

CPT Cone/piezoncone penetration test
VST Vane shear test
UC Unconfined compression
SPT Standard penetration test
DST Direct shear test
DPL Dynamic probing light
SWS Surface wave seismology

Properties:

q_c Cone tip resistance
q_{c1N} Normalized cone tip resistance
q_t Corrected cone tip resistance
f_s Sleeve friction
F_R Friction ratio
S_u Undrained shear strength
k Hydraulic conductivity
N value SPT-N value
N_{10} Number of blows per 100 mm of penetration for DPL
N_{60} Energy normalized SPT-N value
w_n Natural water content
w_L Liquid limit

w_P	Plastic limit
Cc	Compression index
Cs	Swell index
LI	Liquid index
γ	Unit weight
e_0	Void ratio

Method:

APM	Approximate method proposed by Vanmarcke (1977)
MM	Autocorrelation function fitting (method of moments)
ML	Maximum likelihood
VRF	Variance reduction function fitting
SVR	Semivariogram

Autocorrelation model:

SExp:	Single exponential
SMK:	Second-order Markov
QExp:	Squared exponential
Bin:	Binary
CExp:	Cosine exponential
Sph:	Spherical
Tri:	Triangular

4. Statistics for geotechnical design model factors

Chong Tang and Richard Bathurst

4.1 Introduction

During the historical development of the mechanics of deformable solids, the problems in geotechnical engineering are often categorized into two distinct groups, namely elasticity and stability (e.g., Terzaghi 1943; Terzaghi and Peck. 1948; Chen 1975). The elasticity problems deal with stress or deformation of soil without failure, such as point stress beneath a footing or behind an earth retaining wall, deformation around a tunnel or an excavation, and settlement analysis. The stability problems are associated with the determination of a load that will cause the failure of soil, such as bearing capacity, passive and active earth pressure, and slope stability. In many design codes/manuals (e.g., CEN 2004; AASHTO 2017; JRA 2017; CSA 2019), elasticity is usually considered as a serviceability limit state (SLS), while stability is frequently considered as an ultimate limit state (ULS). For practical design convenience, many useable and oftentimes analytically tractable models (link between theory and practice) have been developed for elasticity and stability analyses of geotechnical structures. Because of the natural (or inherent) variability of geomaterial properties, assumptions and simplifications made by calculation models and the difficulty to model construction disturbance, the predicted response will deviate from the measured one (typically on the safe side). This deviation can be directly captured by a ratio of the measured value (X_m) (e.g., load test) to the calculated value (X_c) that is called a model factor M ($=X_m/X_c$) (ISO 2015). This method is practical, familiar to engineers, and grounded realistically on a load test database. The quantity X could be a load, a resistance, or a displacement, etc.

The simplest way to characterize the model factor M is to calculate the mean (bias) and coefficient of variation (COV) (dispersion). The mean of M would provide an engineer with a sense of the hidden factor of safety (FS) that either adds or subtracts from the nominal global FS, depending on whether the calculation method is conservative (mean>1) or unconservative (mean<1) in the average sense. It should not be inferred that a calculation method is conservative or otherwise for a specific case because M takes a range of values in actuality (hence it is random) that may depend on the scenarios covered in the database used in calibration. This random nature is practically significant, because it implies that a calculation method can be unconservative when applied to a specific case even though the method is conservative on the average. Therefore, it is also necessary to consider the degree of scatter (dispersion) in M and to ensure probability of a measured value being lower than the calculated value is capped at a known value say p%. This idea is conceptually

similar to EN 1997-1:2004 (CEN 2004), 2.4.5.2 (11) which recommends a cautious estimation (or characteristic value) for a geotechnical design parameter can be "derived such that the calculated probability of a worse value governing the occurrence of the limit state under consideration is not greater than 5%." The model factor statistics (mean and COV) have been widely used to develop load and resistance factor design (LRFD) of foundations (e.g., Paikowsky et al. 2004, 2010; Salgado et al. 2011; Ng and Fazia 2012; Abu-Farsakh et al. 2013; AbdelSalam et al. 2015; Seo et al. 2015; Stark et al. 2017; Asem et al. 2018; Machairas et al. 2018; Asem and Gardoni 2019; Heidarie Golafzani et al. 2020; Petek et al. 2020; Tang and Phoon 2021). The Federal Highway Administration mandated the use of LRFD for all federally funded new bridges after September 2007 (e.g., Brown et al. 2010, 2018; Hannigan et al. 2016; AASHTO 2017).

4.2 Summary Table

Table 4.1 summarizes previous studies on the characterization of model factors – mean (bias) and COV (dispersion). The dataset used in calibration include laboratory (scaled model or prototype in a centrifuge facility) (representing controlled soil condition) or in situ (representing natural soil condition) load tests. The results cover various geotechnical structures (e.g., shallow foundations, offshore spudcans, pipes, anchors, drilled shafts, driven piles, rock sockets, helical piles, mechanically stabilized earth walls, soil nail walls, slopes and braced excavations) and a wide range of geomaterials from soft clay to soft rock. Two typical limit states (i.e., ULS and SLS) are calibrated. The mean and COV values and number of tests (N) averaged over n-data groups that belong to the same geotechnical structure, limit state, and geomaterial are presented in Figure 4.1.

4.3 Key Observations

1. Characterization of ULS model factor received most of the attention in the literature (foundation capacity is the most prevalent), while characterization of SLS model factor is relatively limited. This is because only strength parameters (e.g., cohesion, friction angle, or uniaxial compressive strength) are required in stability analysis that are familiar to engineers and are most often measured in field or laboratory tests.
2. Based on the mean of model factor, the bias of calculation model is classified as (1) unconservative (mean<1), (2) moderately conservative (1≤mean≤3), and (3) highly conservative (mean>3). Based on the COV of model factor, the dispersion of calculation model is classified as: (1) low (COV<0.3), (2) medium (0.3≤COV≤0.6), and (3) high (COV>0.6). Note that "low dispersion" means "high precision" and vice-versa. This three-tier classification scheme is deemed reasonable based on the extensive statistical analyses covering numerous geotechnical structures and soil types. It is consistent with the three-tier classification for soil properties

(Phoon et al. 2003), the degree of site and model understanding in the Canadian Highway Bridge Design Code (CSA 2019) and the geotechnical complexity class being considered in the new draft for Eurocode 7 Part 1 – EN 1997-1:202x.

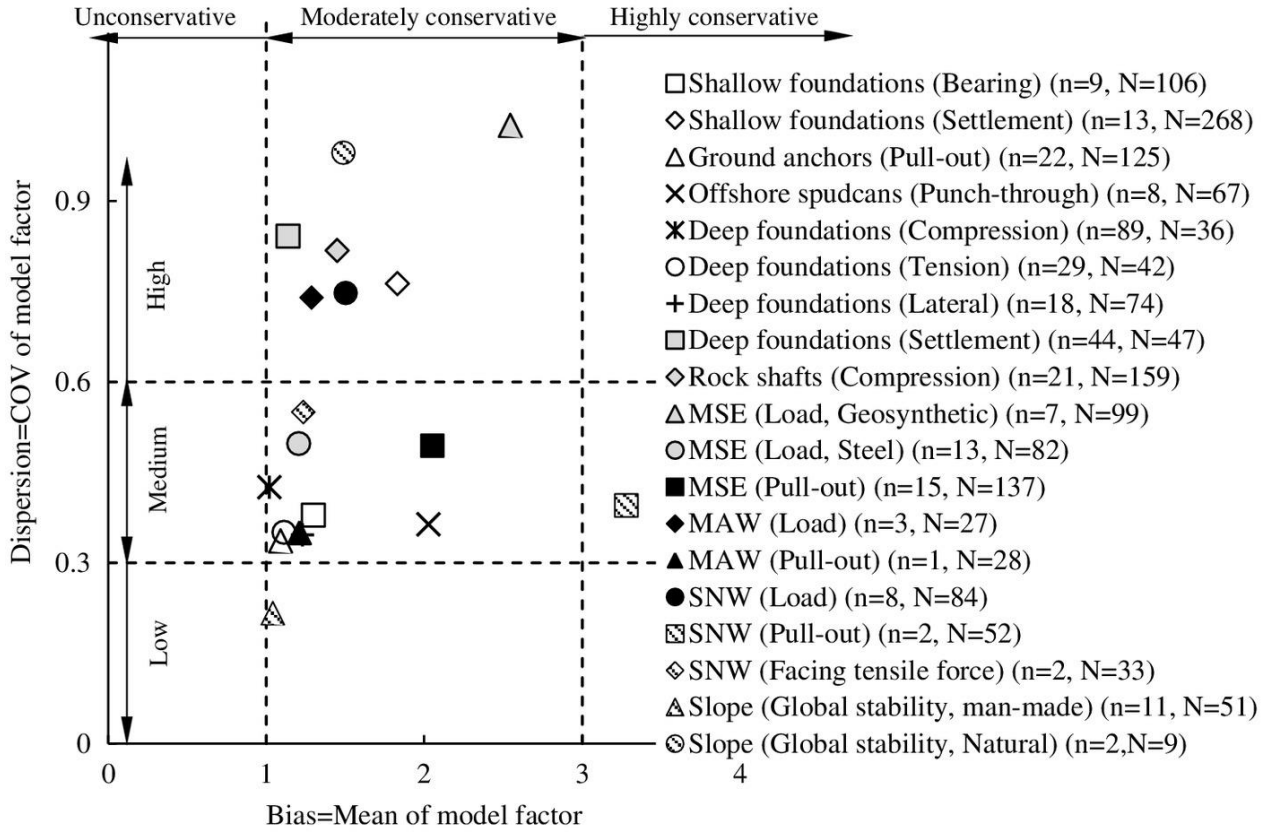

Figure 4.1. Classification of model uncertainty based on the mean (bias) and COV (dispersion) of model factor, where n = number of data groups, N = number of tests averaged over n-data groups, MSE = mechanically stabilized earth wall, MAW = multi-anchor wall, and SNW = soil nail wall. (Image taken from Tang et al. 2020a)

3. Few calculation methods are of low dispersion (or high precision). The model factor COV values for (1) the factor of safety of man-made slopes, (2) the pullout capacity of pipes (laboratory tests on scaled models in 1g condition) and (3) the punch-through capacity of offshore spudcans in stiff-over-soft clays or clay with sand (centrifuge tests that are laboratory tests on scaled models in ng condition) are around 0.3. For these three cases, soil samples are well-prepared, corresponding to lower geotechnical variability. In addition, slope stability is an important and classical problem in geotechnical engineering that has been extensively studied since the 1930s, leading to the better understanding of slope failure mechanism and improved analysis methods (Duncan et al. 2014). For pullout capacity of pipes and punch-through capacity of offshore spudcans, due to the increasing demand of offshore oil and gas, many laboratory tests were performed to study the underlying mechanism and improve the performance of the calculation models as reviewed by Tang and Phoon (2021). Therefore, they

correspond to a high to typical degree of site and model understanding (i.e. low to medium dispersion).

4. Calculation methods for the capacity of shallow and deep foundations in soil, steel reinforced earth walls and soil nail walls are of medium dispersion. This is explained by the fact that field load tests or observations are mainly used, corresponding to higher geotechnical variability than laboratory tests. Foundation analysis and design in soil is another important and classical problem in geotechnical engineering that has been studied over one century (e.g., load-displacement response and load-transfer mechanism). They correspond to a typical degree of site and model understanding.
5. Calculation methods for foundation settlement, foundation capacity in rock, and geosynthetic reinforced earth walls are of high dispersion (low precision). The reasons may include: (1) soil stiffness is more difficult to predict than strength parameters; (2) only rock compressive strength is incorporated into calculations that is insufficient, as rock mass is usually composed of joints, seams, faults, and bedding planes; and (3) the interaction between geosynthetic and soil is more complicated than that between steel reinforcements and soil. They correspond to a lower degree of site and model understanding.
6. Assessment of design methods for large-diameter open-ended piles (LDOEPs) (Petek et al. 2020) and laterally loaded piles (e.g., Phoon and Kulhawy 2005; Briaud and Wang 2018) is relatively limited. This is because significant challenges are involved addressing both problems, such as complicated behaviour (e.g., plug and development of internal friction) and difficulty in LDOEPs installation and obvious deficiencies in current limit state design methods for laterally loaded piles that only cover a specific behavior and lack the ability to properly accommodate both ULS and SLS.

4.4 References

AASHTO. 2007. LRFD bridge design specifications. 4th ed. Washington, DC: AASHTO.

AASHTO. 2014. LRFD bridge design specifications. 7th ed. Washington, DC: AASHTO.

AASHTO. 2017. LRFD bridge design specifications. 8th ed. Washington, DC: AASHTO.

Abchir, Z., S. Burlon, R. Frank, J. Habert, and S. Legrand. 2016. t-z Curves for Piles from pressuremeter test results. Géotechnique, 66(2): 137-148.

AbdelSalam, S., F. Baligh, and H. M. El-Naggar. 2015. A database to ensure reliability of bored pile design in Egypt. Proceedings of the Institution of Civil Engineers–Geotechnical Engineering, 168(2): 131-143.

Abu-Farsakh, M. Y., Q. M. Chen, and M. N. Haque. 2013. Calibration of resistance factors for drilled shafts for the new FHWA design method. Report No. FHWA/LA.12/495. Baton Rouge, LA: Louisiana Transportation Research Centre.

Abu-Farsakh, M. Y. and H. H. Titi. 2007. Probabilistic CPT method for estimating the ultimate capacity of

friction piles. Geotechnical Testing Journal, 30(5): 387-398.

Abu-Hejleh, N. and W. J. Attwooll. 2005. Colorado's axial load tests on drilled shafts socketed in weak rocks: synthesis and future needs. Report No. CDOT-DTD-R-2005-4, Colorado Department of Transportation.

Akbas, S. O. 2007. Deterministic and probabilistic assessment of settlements of shallow foundations in cohesionless soils. Ph.D. thesis, Cornell University, Ithaca, New York.

Allen, T. M. and R. J. Bathurst. 2015. Improved Simplified Method for Prediction of Loads in Reinforced Soil Walls. Journal of Geotechnical and Geoenvironmental Engineering, 141 (11): 04015069.

Allen, T. M. and R. J. Bathurst. 2018. Application of the Simplified Stiffness Method to Design of Reinforced Soil Walls. Journal of Geotechnical and Geoenvironmental Engineering, 144 (5): 04018024.

Alpan, I. 1964. Estimating the settlements of foundations on sands. Civil Engineering and Public Works Review, 59(700): 1415-1418.

Amirmojahedi, M. and M. Abu-Farsakh. 2019. Evaluation of 18 direct CPT methods for estimating the ultimate pile capacity of driven piles. Transportation Research Record, 2673(9): 127-141.

Anagnostopoulos, A. G., B. P. Papadopoulos, and M. J. Lavvadas. 1991. Direct estimation of settlements on sand based on SPT results. Proceedings of the tenth European Conference on Soil Mechanics and Foundation Engineering, Vol. 2, pp. 293-296. Rotterdam: A. A. Balkema.

Aoki, N. and D. A. Velloso. 1975. An approximate method to estimate the bearing capacity of piles. Proceedings of the Fifth Pan-American Conf. of Soil Mechanics and Foundation Engineering, International Society of Soil Mechanics and Geotechnical Engineering, Buenos Aires, Vol. 1, pp. 367-376.

API (American Petroleum Institute). 1974. Recommendations for timber piles design manufacture and installation of concrete piles. Report No. 543R-74. Washington, DC: API.

API (American Petroleum Institute). 1984. Recommended practice for planning, designing and constructing fixed offshore platforms. API RP2A, 15th Ed. Washington, DC: API.

API (American Petroleum Institute). 1989. Recommended practice for planning, designing and constructing fixed offshore platforms–Load and Resistance Factor Design. API RP2ALRFD. Washington, DC: API.

API (American Petroleum Institute). 2000. Recommended practice for planning, designing, and constructing fixed offshore platforms–working stress design. 22nd ed. Washington, DC: API.

API (American Petroleum Institute). 2007. Recommended practice for planning, designing and constructing fixed offshore platforms–working stress design. 22nd ed. Washington, DC: API.

ARGEMA (Association de Recherché en Géotechnique Marine). 1992. Design guides for offshore structures: offshore pile design. Paris, France: ARGEMA.

Asem, P. 2019. Base resistance of drilled shafts in soft rock using in situ load tests: a limit state approach. Soils and Foundations, 59(6): 1639-1658.

Asem, P. and P. Gardoni. 2019. Evaluation of peak side resistance for rock socketed shafts in weak sedimentary rock from an extensive database of published field load tests: a limit state approach. Canadian Geotechnical Journal, 56(12): 1816-1831.

Asem, P., J. H. Long, and P. Gardoni. 2018. Probabilistic model and LRFD resistance factors for the tip

resistance of drilled shafts in soft sedimentary rock based axial load tests. Proceedings of Innovations in Geotechnical Engineering: Honoring Jean-Louis Briaud (GSP 299), pp. 1-49. Reston, VA: ASCE.

Bahsan, E., H. J. Liao, J. Y. Ching, and S. W. Lee. 2014. Statistics for the calculated safety factors of undrained failure slopes. Engineering Geology, 172: 85-94.

Bathurst, R. J., T. M. Allen, Y. Miyata, and B. Huang. 2013. Lessons learned from LRFD calibration of reinforced soil wall structures. In Modern design codes of practice: Development, calibration, and experiences, edited by P. Arnold, M. Hicks, T. Schweckendiek, B. Simpson, and G. Fenton, 261–276. Amsterdam, Netherlands: IOS Press.

Bathurst, R. J., N. Bozorgzadeh, Y. Miyata, and T. M. Allen. 2020. Reliability-based design and analysis for internal limit states of steel grid-reinforced mechanically stabilized earth walls. Canadian Geotechnical Journal, in press.

Bathurst, R. J., and Y. Yu. 2018. Probabilistic prediction of reinforcement loads for steel MSE walls using a response surface method. International Journal of Geomechanics, 18(5): 04018027.

Bazaraa, A. R. and M. M. Kurkur. 1986. N-values used to predict settlements of piles in Egypt. Proceedings of Use of In Situ Tests in Geotechnical Engineering, pp. 462-474. New York, NY: ASCE.

Berardi, R. and R. Lancellotta. 1994. Prediction of settlements of footings on sands: accuracy and reliability. Proceedings of vertical and horizontal deformations of foundations and embankments – Settlement'94 (GSP 40), pp. 640-651. New York, NY: ASCE.

Berg, R. R., B. R. Christopher, and N. C. Samtani. 2009a. Design of mechanically stabilized earth walls and reinforce soil slopes – Volume I. Report No. FHWA-NHI-10-024. Washington, DC: National Highway Institute, Federal Highway Administration, and U.S. Department of Transportation.

Berg, R. R., B. R. Christopher, and N. C. Samtani. 2009b. Design of mechanically stabilized earth walls and reinforce soil slopes – Volume II. Report No. FHWA-NHI-10-025. Washington, DC: National Highway Institute, Federal Highway Administration, and U.S. Department of Transportation.

Bishop, A. W. 1955. The use of the slip circle in the stability analysis of earth slopes. Géotechnique, 5(1): 7-17.

Bjerrum, L. and O. Eide. 1956. Stability of strutted excavations in clay. Géotechnique, 6(1): 32-47.

Bloomquist, D., M. McVay, and Z. Hu. 2007. Updating Florida Department of Transportation's (FDOT) pile/shaft design procedures based on CPT & DTP data. UF Project 00005780. Gainesville, FL: University of Florida.

Bozorgzadeh, N., R. J. Bathurst, T. M. Allen, and Y. Miyata. 2020. Reliability-based analysis of internal limit states for MSE walls using steel-strip reinforcement. Journal of Geotechnical and Geoenvironmental Engineering, 146(1): 04019119.

Bransby, M. F., T. A. Newson, and P. Brunning. 2002. The upheaval capacity of pipelines in jetted clay backfill. Offshore and Polar, 12(4): 280-287.

Briaud, J. L. and L. M. Tucker. 1984. Piles in sand: a method including residual stresses. Journal of Geotechnical Engineering, 110(11): 1666-1680.

Briaud, J. L. and L. M. Tucker. 1988. Measured and predicted axial response of 98 piles. Journal of

Geotechnical Engineering, 114(9): 984-1001.

Briaud, J. L. and Y. C. Wang. 2018. Synthesis of load-deflection characteristics of laterally loaded large diameter drilled shafts. Report No. FHWA/TX-18/0-6956-R1. Austin, TX: Texas Department of Transportation.

Briaud, J. L., L. M. Tucker, J. S. Anderson, D. Perdomo, and H. M. Coyle. 1986. Development of an improved pile design procedure for single piles in clays and sands. Research Report 4981-1 to the Mississippi State Highway Department, Civil Engineering, Texas A&M University, College Station, Texas.

Broms, B. B. 1964a. Lateral resistance of piles in cohesive soils. Journal of the Soil Mechanics and Foundations Division, 90(2): 27-63.

Broms, B. B. 1964b. Lateral resistance of piles in cohesionless soils. Journal of the Soil Mechanics and Foundations Division, 90(3), 123-156.

Brown, D. A., J. P. Turner, and R. J. Castelli. 2010. Drilled shafts: construction procedures and LRFD design methods. Publication FHWA-NHI-10-016. Washington, DC: Federal Highway Administration.

Brown, D.A., Turner, J.P., Castelli, R.J., and Loehr, E.J. 2018. Drilled shafts: construction procedures and design methods. Report No. FHWA NHI-18-024. Washing, DC: U.S. Department of Transportation and Federal Highway Administration.

BSI (British Standards Institution). 2010. Code of practice for strengthened/reinforced soil and other fills. BS8006-1:2010+A1:2016. Milton Keynes: British Standards Institution.

BSI (British Standards Institution). 2020a. Petroleum and natural gas industries–site specific assessment of mobile offshore units–Part 1: Jack-ups. BS EN ISO 19905-1:2016–Tracked Changes. London, UK: BSI.

BSI (British Standards Institution). 2020b. Petroleum and natural gas industries-specific requirements for offshore structures. Part 4: Geotechnical and foundation design considerations. BS EN ISO 19901-4:2016–Tracked Changes. London, UK: BSI.

Burland, J. B. 1973. Shaft friction of piles in clay–a simple fundamental approach. Ground Engineering, 6(3), 30-42.

Burland, J. B. and M. C. Burbidge. 1985. Settlement of foundations on sand and gravel. Proceedings of the Institution of Civil Engineers, 78(6): 1325-1381.

Bustamante, M. and L. Gianeselli. 1982. Pile bearing capacity prediction by means of static penetrometer CPT. Proceedings of the Second European Symposium on Penetration Testing, pp. 493-500. Amsterdam: A. A. Balkema.

Bustamante, M. and L. Gianeselli. 1983. Prevision de la capacite portante des pieux par la méthode penetrometrique. Compte Rendu de Recherché F.A.E.R. 1.05.02.2, Laboratoires Central des Ponts et Chaussées.

Byrne, B. W., J. Schupp, C. M. Martin, A. Maconochie, and D. Cathie. 2013. Uplift of shallowly buried pipe sections in saturated very loose sand. Géotechnique, 63(5): 382-390.

CABR (China Architecture & Building Press). 2012. Technical Specification for Retaining and Protection of Building Foundation Excavations.

Carter, J. P. and F. H. Kulhawy. 1988. Analysis and design of drilled shaft foundations socketed into rock. Report No. EL-5918. Palo Alto, CA: EPRI.

CECS (China Association for Engineering Construction Standardization). 1997. Specifications for Soil Nailing in Foundation Excavations.

CEN. 2004. Eurocode 7: Geotechnical Design – Part 1: General Rules. EN 1997-1:2004. Brussels, Belgium: European Committee for Standardization (CEN).

CGS (Canadian Geotechnical Society). 2006. Canadian foundation engineering manual. 4th ed. BiTech Publisher Ltd., Vancouver, Canada.

Chen, W. F. 1975. Limit analysis and soil plasticity. Amsterdam: Elsevier.

Cherry, J. A. and M. Souissi. 2010. Helical pile capacity to torque ratios, current practice, and reliability. Proceedings of GeoTrends: The Progress of Geological and Geotechnical Engineering in Colorado at the Cusp of a New Decade (GPP 6), Eds. C. M. Goss, J. B. Kerringan, J. C. Malama, W. O. McCarron, and R. L. Wiltshire, pp. 43-52. Reston, VA: ASCE.

Chin, F. K. 1970. Estimation of the ultimate load of piles not carried to failure. Proceedings of the second Southeast Asian Conference on Soil Mechanics, pp. 81-90. Singapore: Southeast Asian Society of Soil Engineering.

Clausen, C. J. F., P. M. Aas, and K. Karlsrud. 2005. Bearing capacity of driven piles in sand, the NGI approach. Proceedings of the 1st International Symposium on Frontiers in Offshore Geotechnics, Perth, Australia, pp. 677-682.

Clisby, M. B., R. M. Scholtes, M. W. Corey, H. A. Cole, P. Teng, and J. D. Webb. 1978. An evaluation of pile bearing capacities. Volume I, Final Report. Jackson, MS: Mississippi State Highway Department.

Coates, D. F. 1967. Rock mechanics principle. Department of Energy, Mines, and Resources, Canada.

Coyle, H. M. and R. R. Castello. 1981. New design correlations for piles in sand. Journal of the Geotechnical Engineering Division, 107(7): 965-986.

CSA (Canadian Standards Association). 2019. Canadian highway bridge design code. CAN/CSA-S6-14. Mississauga, ON, Canada: CSA.

Davisson, M. T. 1972. High capacity piles. Proceedings of Lecture Series on Innovations in Foundation Construction. Reston, VA: ASCE.

Décourt, L. 1995. Prediction of load-settlement relationships for foundations on the basis of the SPT-T. Ciclo de Conferencias Inter. “Leonardo Zeevaert”, UNAM, Mexico, pp. 85-104.

De Ruiter, J. and F. L. Beringen. 1979. Pile foundations for large North Sea structures. Marine Geotechnology, 3(3): 267-314.

DNV (Det Norske Veritas). 2007. Global Buckling of Submarine Pipelines-Structural Design Due to High Temperature High Pressure. DNV-RP-F110. Oslo, Norway.

D'Appolonia, D. J., E. D. D'Appolonia, and R. F. Brisssette. 1970. Closure to “Settlement of spread footings on sand”. Journal of the Soil Mechanics and Foundations Division, 96(SM2): 754-761.

Duncan, J.M., Wright, S.G. and Brandon, T.L. 2014. Soil strength and slope stability. 2nd Ed. Hoboken, NJ: John Wiley & Sons, Inc.

Eslami, A. and Fellenius, B. H. 1997. Pile capacity by direct CPT and CPTu methods applied to 102 case histories. Canadian Geotechnical Journal, 34(6): 886-904.

Esrig, M. I., and R. C. Kirby. 1979. Soil capacity for supporting deep foundation members in clay. Behavior of Deep Foundations, ASTM STP. No. 670, Ed. R. Lundgren, pp. 27-63.

Fateh, A. M. A., A. Eslami, and A. Fahimifar. 2017. Direct CPT and CPTu methods for determining bearing capacity of helical piles. Marine Georesources & Geotechnology, 35(2): 193-207.

Frank, R. & Zhao, S. R. (1982). Estimation par les paramètres pressiométriques de l'enfocement sous charge axiale de pieux forés dans des sols fins. Bulletin de Liaison des Laboratoires des Ponts et Chaussées, 119: 17-24.

GEO (Geotechnical Engineering Office). 2007 Good practice in design of steel soil nails for soil cut slopes. GEO technical guidance note No. 23. Hong Kong.

Gibbs, H. J. and W. H. Holtz. 1957. Research on determining the density of sands by spoon penetration testing. Proceedings of 4th International Conference on Soil Mechanics and Foundation Engineering, vol. 1, London, pp. 35-39.

Goodman, R. E. 1989. Introduction to Rock Mechanics. Second edition. New York: Wiley.

Gupton, C. and T. Logan. 1984. Design guidelines for drilled shafts in weak rocks of south Florida. Proceedings of the South Florida Annual ASCE Meeting. Miami, FL, ASCE.

Gurbuz, A. 2007. The uncertainty in the displacement evaluation of deep foundations. Ph.D. thesis, University of Massachusetts Lowell.

Hannigan, P.J., Rausche, F., Likins, G.E., Robinson, B.R. and Becker, M.L. 2016. Design and construction of driven pile foundations, volume I. Washington, DC: Federal Highway Administration (FHWA).

Hansen, J. B. 1961. The ultimate resistance of rigid piles against transversal forces. Bulletin No. 12, pp. 5-9. Copenhagen: Danish Geotechnical Institute.

Hansen, J. B. 1963. Discussion of “Hyperbolic stress-strain response: cohesive soils.” Journal of the Soil Mechanics and Foundations Division, 89(4): 241-242.

Hansen, J.B. 1970. A revised and extended formula for bearing capacity. Bulletin No. 28, 5-11. Copenhagen: Danish Geotechnical Institute.

Heidarie Golafzani, S., R. Jamshidi Chenari, and A. Eslami. 2020. Reliability based assessment of axial pile bearing capacity: static analysis, SPT and CPT-based methods. Georisk: Assessment and Management of Risk for Engineered Systems and Geohazards, 14 (3): 216-230.

Hirany, A. and F. H. Kulhawy. 1988. Conduct and interpretation of load tests on drilled shaft foundations: detailed guidelines. Report No. EL-5915. Palo Alto, CA: EPRI.

Horvath, R. and T. Kenney, 1979. Shaft resistance of rock-socketed drilled piers. Proceedings of Symposium on Deep Foundations, Atlanta, Edited by F. Fuller, pp. 182-214. New York: ASCE.

Hough, B. K. 1959. Compressibility as the basis for soil bearing value. Journal of the Soil Mechanics and Foundations Division, 85(4): 11-40.

Housel, W. S. 1966. Pile load capacity: estimates and test results. Journal of the Soil Mechanics and Foundations Division, 92(4), 1-30.

Hoyt, R. M. and S. P. Clemence. 1989. Uplift capacity of helical anchors in soil. Proceedings of the 12th International Conference on Soil Mechanics and Foundation Engineering, Vol. 2, pp. 1019-1022. Rotterdam, Netherlands: A. A. Balkema.

Hu, Z., M. McVay, D. Bloomquist, D. Horhota, and P. Lai. 2012. New ultimate pile capacity prediction method based on cone penetration test (CPT). Canadian Geotechnical Journal, 49(8): 961-967.

Huang, B. Q. and R. J. Bathurst. 2009. Evaluation of Soil-Geogrid Pullout Models Using a Statistical Approach. Geotechnical Testing Journal, 32(6): 489-504.

Huang, B. Q., R. J. Bathurst, and T. M. Allen. 2012. LRFD calibration for steel strip reinforced soil walls. Journal of Geotechnical and Geoenvironmental Engineering, 138(8): 922-933.

IEEE. 2001. IEEE guide for transmission structure foundation design and testing. IEEE Std 691-2001. New York: IEEE.

InSafeJIP. 2011. Improved guidelines for the prediction of geotechnical performance of spudcan foundations during installation and removal of jack-up units. Singapore: RPS Energy and Képpel Offshore Technology Development.

Ismail, S., S. S. Najjar, and S. Sadek. 2018. Reliability Analysis of Buried Offshore Pipelines in Sand Subjected to Upheaval Buckling. Proceedings of the Offshore Technology Conference (OTC). Houston, TX: American Petroleum Institute. OTC-28882-MS.

ISO. 2015. General Principles on Reliability of Structures. ISO 2394. Geneva, Switzerland: International Organization for Standardization (ISO).

Jewell, R. A., G. W. E. Milligan, R. W. Sarsby, and D. Dubois. 1984. Interaction between soil and geogrids. Proceedings of Symposium on Polymer Grid Reinforcement in Civil Engineering, 18–30. London, UK: Thomas Telford.

JRA (Japan Road Association). 2017. Specifications for highway bridges. Part 4, Substructures. Tokyo: JRA.

JSA (Japanese Society of Architecture). 1988. Guidelines of Design and Construction of Deep Excavation. Tokyo, Japan: JSA.

Jardine, F. M., F. C., Chow, R. F. Overy, and J. R. Standing, 2005. ICP design methods for driven piles in sands and clays. London, UK: Thomas Telford.

Karlsrud, K., C. J. F. Clausen, and P. M. Aas. 2005. Bearing capacity of driven piles in clay, the NGI approach. Proceedings of the 1st International Symposium on Frontiers in Offshore Geotechnics, Taylor & Francis, University of Western Australia, Perth, pp. 775-782.

Kempfert, H. G. and Becker, P. 2010. Axial pile resistance of different pile types based on empirical values. Proceedings of Deep Foundations and Geotechnical In Situ Testing (Geo-Shanghai 2010) (GSP 205), Eds. R. Y. Liang, F. Zhang, and K. Yang, pp. 149-154, Reston, VA: ASCE.

Kolk, H. J., A. E. Baaijens, and M. Senders. 2005. Design criteria for pipe piles in silica sands. Proceedings of the 1st International Symposium on Frontiers in Offshore Geotechnics, Perth, Western Australia, pp. 711-716.

Kulhawy, F. H. 1978. Geomechanical model for rock foundation settlement. Journal of the Geotechnical Engineering Division, ASCE, 104(2), 211-227.

Kulhawy, F. H. and J. P. Carter. 1992. Socketed foundation in rock masses. Engineering in Rock Masses (Ed. F. H. Bell), pp. 509-529. Oxford: Butterworth-Heinemann.

Kulhawy, F. H. and K. K. Phoon. 1993. Drilled shaft side resistance in clay soil to rock. Proceedings of Design and Performance of Deep Foundations: Piles and Piers in Soil and Soft Rock (GSP 38), 172-183. Reston, VA: ASCE.

Lazarte, C. A., H. Robinson, J. E. Gómez, A. Baxter, A. Cadden, and R. Berg. 2015. Soil nail walls – reference manual. Report No. FHWA-NHI-14-007. Washington, DC: National Highway Institute and U.S. Department of Transportation.

Lehane, B. M., F. C. Chow, B. A. McCabe, and R. J. Jardine. 2000. Relationships between shaft capacity of driven piles and CPT end resistance. Proceedings of the Institution of Civil Engineers–Geotechnical Engineering, 143(2): 93-101.

Lehane, B. M., Y. Li, and R. Williams. 2013. Shaft capacity of displacement piles in clay using the cone penetration test. Journal of Geotechnical and Geoenvironmental Engineering, 139(2): 253-266.

Lehane, B. M., J. A. Schneider, and X. T. Xu, 2005. The UWA-05 method for prediction of axial capacity of driven piles in sand. Proceedings of the 1st International Symposium on Frontiers in Offshore Geotechnics, Perth, Western Australia, pp. 683-690.

Lin, P. Y., R. J. Bathurst, and J. Y. Liu. 2017a. Statistical evaluation of the FHWA simplified method and modifications for predicting soil nail loads. Journal of Geotechnical and Geoenvironmental Engineering, 143 (3): 04016107.

Lin, P. Y., R. J. Bathurst, S. Javankhoshdel, and J. Y. Liu. 2017b. Statistical analysis of the effective stress method and modifications for prediction of ultimate bond strength of soil nails. Acta Geotechnica, 12: 171-182.

Lin, P. Y. and R. J. Bathurst. 2018. Reliability-based internal limit state analysis and design of soil nails using different load and resistance models. Journal of Geotechnical and Geoenvironmental Engineering, 144 (5): 04018022.

Liu, H. F., L. S. Tang, P. Y. Lin, and G. X. Mei. 2018. Accuracy assessment of default and modified Federal Highway Administration (FHWA) simplified models for estimation of facing tensile forces of soil nail walls. Canadian Geotechnical Journal, 55 (8): 1104-1115.

Lutenegger, A. J. 2015. Quick design guide for screw-piles and helical anchors in soils. International Society for Helical Foundations (ISHF).

Machairas, N., G. A. Highley, and M. G. Iskander. 2018. Evaluation of FHWA pile design method against the FHWA Deep Foundation Load Test Database version 2.0. Transportation Research Record, 2672(52): 268-277.

Mayne, P. W. and D. E. Harris. 1993. Axial load-displacement behavior of drilled shaft foundation in piedmont residuum. Publication No. 41-30-3175. Atlanta: Georgia Institute of Technology.

Mazurkiewicz, B. K. 1972. Test loading of piles according to Polish regulations. Report No. 35. Stockholm: Royal Swedish Academy of Engineering Sciences Commission on Pile Research.

Meigh, A. C. and W. Wolski. 1979. Design parameters for weak rock. Proceedings of the Seventh European

Conference on Soil Mechanics and Foundation Engineering, Brighton, Vol. 5, pp. 59-79. London: British Geotechnical Society.

Meyerhof, G. G. 1965. Shallow foundations. Journal of the Soil Mechanics and Foundations Division, 91(SM2): 21-31.

Meyerhof, G. G. 1976. Bearing capacity and settlement of pile foundations. Journal of Geotechnical Engineering Division, 102(3): 197-228.

Meyerhof, G. G. 1983. Scale effects of ultimate pile capacity. Journal of Geotechnical Engineering, 109(6): 797-806.

Meyerhof, G. G. and J. I. Adams. 1968. The ultimate uplift capacity of foundations. Canadian Geotechnical Journal, 5(4): 225-244.

Miller, A. D. 2003. Prediction of ultimate side shear for drilled shafts in Missouri shale. M.Sc. thesis, University of Missouri-Columbia.

Miyata, Y. and R. J. Bathurst. 2012a. Measured and Predicted Loads in Steel Strip Reinforced c-ϕ Soil Walls in Japan. Soils and Foundations, 52 (1): 1-17.

Miyata, Y. and R. J. Bathurst. 2012b. Analysis and Calibration of Default Steel Strip Pullout Models Used in Japan. Soils and Foundations, 52 (3): 481-497.

Miyata, Y. and R. J. Bathurst. 2012c. Reliability Analysis of Soil-Geogrid Pullout Models in Japan. Soils and Foundations, 52 (4): 620-633.

Miyata, Y. and R. J. Bathurst. 2019. Statistical Assessment of Load Model Accuracy for Steel Grid-Reinforced Soil Walls. Acta Geotechnica, 14 (1): 57-70.

Miyata, Y., R. J. Bathurst, and T. Konami. 2009. Measured and predicted loads in multi-anchor reinforced soil walls in Japan. Soils and Foundations, 49 (1): 1-10.

Miyata, Y., R. J. Bathurst, and T. Konami, 2011. Evaluation of Two Anchor Plate Capacity Models for MAW Systems. Soils and Foundations, 51 (5): 885-895.

Miyata, Y., Y. Yu, and R. J. Bathurst. 2018. Calibration of Soil-Steel Grid Pullout Models Using a Statistical Approach. Journal of Geotechnical and Geoenvironmental Engineering, 144 (2): 04017106.

Moshfeghi, S. and A. Eslami. 2018. Study on pile ultimate capacity criteria and CPT-based direct methods. International Journal of Geotechnical Engineering, 12(1): 28-39.

MSHD (Mississippi State Highway Department). 1972. Soil design manual. Mississippi State Highway Department.

Muganga, R. 2008. Uncertainty evaluation of displacement and capacity of shallow foundations on rock. Master of Science, University of Massachusetts Lowell.

Nabeshima, Y., T. Matsui, S. G. Zhou, and S. Tsuruta. 1999. Elucidation of reinforcing mechanism and evaluation of bearing resistance in steel grid reinforced earth. J. JSCE, 638/III-49, 251–258 (in Japanese).

Ng, T. and Fazia, S. 2012. Development and validation of a unified equation for drilled shaft foundation design in New Mexico. Report No. NM10MSC-01. Albuquerque, NM: New Mexico Department of Transportation.

Nordlund, R. L. 1963. Bearing capacity of piles in cohesionless soils. Journal of the Soil Mechanics and Foundations Division, 89(3): 1-35.

Nottingham, L. C. and J. H. Schmertmann. 1975. An investigation of pile capacity design procedures. Report No. D629. Gainesville: University of Florida.

Okamura, M., J. Takemura, and T. Kimura. 1998. Bearing capacity predictions of sand overlying clay based on limit equilibrium methods. Soils and Foundations, 38(1): 181-194.

Paikowsky, S. G., B. Birgisson, M. McVay, T. Nguyen, C. Kuo, G. Baecher, B. Ayyub, K. Stenersen, K. O'Malley, L. Chernauskas, and M. O'Neill. 2004. Load and resistance factor design (LRFD) for deep foundations. NCHRP Report 507. Washington, DC: National Academy of Sciences.

Paikowsky, S. G., M. C. Canniff, K. Lesny, A. Kisse, S. Amatya, and R. Muganga. 2010. LRFD design and construction of shallow foundations for highway bridge structures. NCHRP Report 651. Washington, DC: National Academy of Sciences.

Parry, R. H. G. 1971. A direct method of estimating settlements in sands from SPT values. Proceedings of Symposium on Interaction of Structure and Foundation, pp. 29-37.

Peck, R. B. and A. R. S. S. Bazaraa. 1969. Discussion on settlement of spread footings on sand. Journal of the Soil Mechanics and Foundations Division, 95(SM3): 905-909.

Peck, R. B., W. E. Hanson, and T. H. Thornburn. 1974. Foundation engineering. 2nd Ed. New York: Wiley.

Pedersen, P. T. and J. J. Jensen, 1988. Upheaval creep of buried heated pipelines with initial imperfections. Marine Structures, 1(1): 11-22.

Perko, H. A. 2009. Helical piles: a practical guide to design and installation. Hoboken, NJ: John Wiley & Sons, Inc.

Petek, K., M. McVay, and R. Mitchell. 2020. Development of guidelines for bearing resistance of large diameter open-end steel piles. Report No. FHWA-HRT-20-011. McLean, VA: Federal Highway Administration.

Peterson, L. M., and L. R. Anderson. 1980. Pullout resistance of welded wire mats embedded in soil. Report to the Hilfiker Company. Logan, UT: Utah State University.

Philipponnat, G. 1980. Méthode pratique de calcul d'un pieu isolé à l'aide du pénétromètre statique. Revue Française de Géotechnique, 10: 55-64.

Phoon, K. K. and F. H. Kulhawy. 2005. Characterisation of model uncertainties for laterally loaded rigid drilled shafts. Géotechnique, 55(1): 45-54.

Phoon, K. K., F. H. Kulhawy, and M. D. Grigoriu. 2003. Multiple resistance factor design for shallow transmission line structure foundations. Journal of Geotechnical and Geoenvironmental Engineering, 129 (9): 807-818.

Phoon, K. K. and C. Tang. 2017. Model uncertainty for the capacity of strip footings under positive combined loading. Proceedings of Geotechnical Safety and Reliability: Honoring Wilson H. Tang (GSP 286), Eds. C. H. Juang, R. B. Gilbert, L. M. Zhang, J. Zhang, and L. L. Zhang, pp. 40-60. Reston, VA: ASCE.

Phoon, K. K. and C. Tang. 2019a. Characterisation of geotechnical model uncertainty. Georisk: Assessment

and Management of Risk for Engineered Systems and Geohazards, 13(2): 101-130.

Phoon, K. K. and C. Tang. 2019b. Effect pf extrapolation on interpreted capacity and model statistics of steel H-piles. Georisk: Assessment and Management of Risk for Engineered Systems and Geohazards, 13(4): 291-302.

Poulos, H. G. 1994. Settlement prediction for driven piles and pile groups. Proceedings of Vertical and Horizontal Deformations of Foundations and Embankments (GSP 40), pp. 1629-1649. Reston, VA: ASCE.

Price, G. and I. F. Wardle. 1982. A comparison between cone penetration test results and the performance of small diameter instrumented piles in stiff clay. Proceedings of the Second European Symposium on Penetration Testing, Vol. 2, pp. 775-780.

PWRC (Public Works Research Centre). 1988. Design method, construction manual and specifications for steel strip reinforced retaining walls. 2nd ed. Tsukuba, Ibaraki: Public Works Research Centre (in Japanese).

PWRC (Public Works Research Centre). 2002. Design method, construction manual and specifications for multi-anchored reinforced retaining wall. Tsukuba, Ibaraki: Public Works Research Centre (in Japanese).

PWRC (Public Works Research Centre). 2003. Design method, construction manual and specifications for steel strip reinforced retaining walls. 3rd ed. Tsukuba, Ibaraki: Public Works Research Centre (in Japanese).

PWRC (Public Works Research Centre). 2014. Design method, construction manual and specifications for steel strip reinforced retaining walls. 4th ed. Tsukuba, Ibaraki: Public Works Research Centre (in Japanese).

Randolph, M. F. and G. T. Houlsby. 1984. The limiting pressure on a circular pile loaded laterally in cohesive soil. Géotechnique, 34(4): 613-623.

Reese, L. C. 1958. Discussion of 'Soil modulus for laterally loaded piles. Transactions of the American Society of Civil Engineers, 123, 1071-1074.

Reese, L. C., W. R. Cox, and F. D. Coop. 1974. Analysis of laterally loaded piles in sand. Proceedings of the Sixth Offshore Technology Conference, Paper No. OTC2080, pp. 473-483.

Reese, L. C. and M. W. O'Neill. 1988. Drilled Shaft: construction procedures and design methods. Report No. FHWA-HI-88-042. McLean, VA: Federal Highway Administration.

Reese, L. C. and M. W. O'Neill. 1989. New design method for drilled shaft from common soil and rock tests. Foundation Engineering: current principles and practices (Ed. F. H. Fellenius), Vol. 2, pp. 1026-1039. New York, NY: ASCE.

Reese, L. C. and S. J. Wright. 1977. Construction Procedures and Design for Axial Loading. Report No. FHWA-IP-77-21. Washington, DC: Federal Highway Administration.

Reynolds, R. T. and T. J. Kaderabek. 1981. Miami limestone foundation design and construction. Journal of the Geotechnical Engineering Division, 107(7): 859-872.

Rosenberg, P. and N. L. Journeaux. 1976. Friction and end bearing tests on bedrock for high capacity socket design. Canadian Geotechnical Journal, 13(3): 324-333.

Rowe, R. K. and H. H. Armitage. 1987. A design method for drilled piers in soft rock. Canadian Geotechnical Journal, 24(1): 126-142.

Salgado, R., S. I. Woo, and D. Kim. 2011. Development of load and resistance factor design for ultimate and serviceability limit states of transportation structure foundations. Report No. FHWA/IN/JTRP-2011/03. Indianapolis, IN: Indiana Department of Transportation.

Samtani, N. C. and T. M. Allen. 2018. Expanded database for service limit state calibration of immediate settlement of bridge foundations on soil. Report No. FHWA-HIF-18-008. Washington, DC: Federal Highway Administration.

Saye, S. R., D. A. Brown, and A. J. Lutenegger. 2013. Assessing adhesion of driven pipe piles in clay using adaption of stress history and normalized soil engineering parameter concept. Journal of Geotechnical and Geoenvironmental Engineering, 139(7): 1062-1074.

Schaminee, P. E. L., N. F. Zorn, and G. J. M. Schotman. 1990. Soil response for pipeline upheaval buckling analyses: full-scale laboratory tests and modelling. Proceedings of the 22nd Annual Offshore Technology Conference, OTC 6486, 563-572. Houston, TX: OTC.

Schmertmann, J. H. 1978. Guidelines for cone penetrometer test (performance and design). Report No. FHWA TS-78-209. Washington, DC: Federal Highway Administration.

Schmertmann, J. H., P. R. Brown, and J. P. Hartman. 1978. Improved strain influence factor diagrams. Journal of the Geotechnical Engineering Division, 104(8): 1131-1135.

Schultze, F. and G. Sherif. 1973. Prediction of settlements from evaluated settlement observations for sand. Proceedings of 8th International Conference on Soil Mechanics and Foundation Engineering, Vol. 3, Moscow, pp. 225-230.

Shioi, Y. and J. Fukui. 1982. Application of N-value to design of foundations in Japan. Proceeding of the Second European Symposium on Penetration Testing, Vol. 1, pp. 40-93.

Spencer, E. 1967. A method of analysis of the stability of embankments assuming parallel inter-slice forces. Géotechnique, 17(1): 11-26.

Stark, T. D., J. H. Long, A. Osouli, and A. K. Baghdady, 2017. Modified standard penetration test-based drilled shaft design method for weak rocks (Phase 2 study). Report No. FHWA-ICT-17-018. Springfield, IL: Illinois Department of Transportation.

Stevens, J. B. and J. M. E. Audibert. 1979. Re-examination of p-y curve formulations. Proceedings of the 11th Offshore Technology Conference, Paper No. OTC 3402, pp. 397-403.

Strahler, A. W. and A. W. Stuedlein. 2014. Accuracy, uncertainty, and reliability of the bearing-capacity equation for shallow foundations on saturated clay. Proceeding of Geo-Congress 2014: Geo-characterization and modeling for sustainability (GSP 234), Eds. M. Abu-Farsakh, X. Yu, and L. R. Hoyos, pp. 3262-3273. Reston, VA: ASCE.

Stuyts, B., D. Cathie, and T. Powell. 2016. Model uncertainty in uplift resistance calculations for sandy backfills. Canadian Geotechnical Journal, 53(11): 1831-1840.

Tang, C. and K. K. Phoon. 2016. Model uncertainty of cylindrical shear method for calculating the uplift capacity of helical anchors in clay. Engineering Geology, 207: 14-23.

Tang, C. and K. K. Phoon. 2017. Model uncertainty of Eurocode 7 approach for bearing capacity of circular footings on dense sand. International Journal of Geomechanics, 17(3): 04016069.

Tang, C., K. K. Phoon, L. Zhang, and D. Q. Li. 2017. Model uncertainty for predicting the bearing capacity of sand overlying clay. International Journal of Geomechanics, 17(7): 04017015.

Tang, C. and K. K. Phoon. 2018a. Evaluation of model uncertainties in reliability-based design of steel H-piles in axial compression. Canadian Geotechnical Journal, 55(11): 1513-1532.

Tang, C. and K. K. Phoon. 2018b. Statistics of model factors in reliability-based design of axially loaded driven piles in sand. Canadian Geotechnical Journal, 55(11): 1592-1610.

Tang, C. and K. K. Phoon. 2018c. Statistics of model factors and consideration in reliability-based design of axially loaded helical piles. Journal of Geotechnical and Geoenvironmental Engineering, 144(8): 04018050.

Tang, C. and K. K. Phoon. 2019a. Evaluation of stress-dependent methods for the punch-through capacity of foundations in clay with sand. ASCE-ASME Journal of Risk and Uncertainty in Engineering Systems, Part A: Civil Engineering, 5(3): 04019008.

Tang, C. and K. K. Phoon. 2019b. Characterization of model uncertainty in predicting axial resistance of piles driven into clay. Canadian Geotechnical Journal, 56(8): 1098-1118.

Tang, C. and K. K. Phoon. 2019c. Reply to the discussion by Flynn and McCabe on “Statistics of model factors in reliability-based design of axially loaded driven piles in sand”. Canadian Geotechnical Journal, 56(1): 148-152.

Tang, C., K. K. Phoon, and Y.-J. Chen. 2019. Statistical analyses of model factors in reliability-based limit-state design of drilled shafts under axial loading. Journal of Geotechnical and Geoenvironmental Engineering, 145(9): 04019042.

Tang, C. and K. K. Phoon. 2020. Statistical evaluation of model factors in reliability calibration of high-displacement helical piles under axial loading. Canadian Geotechnical Journal, 57(2): 246-262.

Tang, C., K. K. Phoon, D. Q. Li, and S. O. Akbas. 2020a. Expanded database assessment of design methods for spread foundations under axial compression and uplift loading. Journal of Geotechnical and Geoenvironmental Engineering, 146 (11): 04020119.

Tang, C., K. K. Phoon, D. Q. Li, and F. Xu. 2020b. Expanded database assessment and consideration of model factors in reliability-based design of rock sockets for axial loading. Engineering Geology, under revision.

Tang, C., and K. K. Phoon. 2021 (Forthcoming). Model uncertainties in foundation design. London: CRC Press.

Tappenden, K.M. 2007. Predicting the axial capacity of screw piles installed in Western Canadian soils. M.Sc. thesis, University of Alberta.

Teng, W. C. 1962. Foundation Design. New Jersey: Prentice Hall.

Terzaghi, K. 1943. Theoretical soil mechanics. New York: John Wiley and Sons, Inc.

Terzaghi, K. and R. B. Peck. 1948. Soil mechanics in engineering practice. New York: Wiley.

Togliani, G. 2008. Pile capacity prediction for in situ tests. Proceedings of the Third International Conference

on Site Characterization, pp. 1187-1192. London, UK: Taylor and Francis Group.

Tomlinson, M. J. 1986. Foundation Design and Construction. 5th ed. London: English Language Book Society.

Travis, Q., M. Schmeeckle, and D. Sebert. 2011a. Meta-analysis of 301 slope failure calculations. I: database description. Journal of Geotechnical and Geoenvironmental Engineering, 137(5): 453-470.

Travis, Q., M. Schmeeckle, and D. Sebert. 2011b. Meta-analysis of 301 slope failure calculations. II: database analysis. Journal of Geotechnical and Geoenvironmental Engineering, 137(5): 471-482.

Tumay, M. T. and M. Fakhroo. 1982. Friction pile capacity prediction in cohesive soils using electric quasi-static penetration tests. Interim Research Report 1. Baton Rouge, LA: Louisiana Department of Transportation and Development.

Ullah, S. N., S. Stanier, Y. Hu, and D. White. 2017. Foundation punch through in clay with sand: analytical modelling. Géotechnique, 67(8): 672-690.

Van Dijk, B. F. J., and H. J. Kolk. 2010. CPT-based design method for axial capacity of offshore piles in clays. Proceedings of the Second International Symposium on Frontiers in Offshore Geotechnics, Ed. S. Gourvenec, and D. White, pp. 555-560. Boca Raton, FL: CRC Press.

Verbrugge, J. C. 1981. Évaluation du tassement des pieux à partir de l'essai de pénétration statique. Revue Française de Géotechnique, 15: 75-82.

Vesić, A. S. 1963. Bearing capacity of deep foundations in sand. Highway Research Record 39, 112-153. Washington, DC: National Academy of Sciences.

Vesić, A. S. 1973. Analysis of ultimate loads of shallow foundations. Journal of the Soil Mechanics and Foundations Divisions, 99(1): 45-73.

Vesić, A. S. 1977. Design of pile foundation. NCHRP No. 42. Washington, DC: Transportation Research Board.

Vijayvergiya, V. N. and J. A. Focht. 1972. A new way to predict the capacity of piles in clay. Proceedings of the 4th Annual Offshore Technology Conference, Houston, pp. 269-284.

White, D., A. Barefoot, and M. Bolton. 2001. Centrifuge modelling of upheaval buckling in sand. International Journal of Physical Modelling in Geotechnics, 1(2): 19-28.

White, D., C. Cheuk, and M. Bolton. 2008. The uplift resistance of pipes and plate anchors buried in sand. Géotechnique, 58(10): 771-779.

Williams, A. F., I. W. Johnston, and I. B. Donald, 1980. The design of sockets in weak rock. Proceedings of International Conference on Structural Foundations on Rock, Sydney, edited by P. J. N. Pells, Vol. 1, pp. 327-347.

Wu, S. H., C. Y. Ou, and J. Y. Ching. 2014. Calibration of model uncertainties in base heave stability for wide excavations in clay. Soils and Foundations, 54(6): 1159-1174.

Xu, J., W. Gong, R. P. Gamage, Q. Zhang, and G. Dai. 2020. A new method for predicting the ultimate shaft resistance of rock-socketed drilled shafts. Proceedings of the Institution of Civil Engineers – Geotechnical Engineering, 173(2): 169-186.

Yu, Y., and R. J. Bathurst. 2015. Analysis of soil-steel bar mat pullout models using a statistical approach.

Journal of Geotechnical and Geoenvironmental Engineering, 141(5): 04015006.

Yuan, J., P. Y. Lin, R. Huang, and Y. Que. 2019. Statistical Evaluation and Calibration of Two Methods for Predicting Nail Loads of Soil Nail Walls in China. Computers and Geotechnics, 108: 269-279.

Zhang, L.M. and L.F. Chu. 2009a. Calibration of methods for designing large-diameter bored piles: ultimate limit state. Soils and Foundations, 49(6): 883-895.

Zhang, L.M. and L.F. Chu. 2009b. Calibration of methods for designing large-diameter bored piles: serviceability limit state. Soils and Foundations, 49(6): 897-908.

Zhang, L. and H. H. Einstein. 1998. End bearing capacity of drilled shafts in rock. Journal of Geotechnical and Geoenvironmental Engineering, 124(7): 574-584.

Zhou, J., Y. Xie, Z. Zuo, M. Luo, and X. Tang. 1982. Prediction of limit load of driven pile by CPT. Proceedings of the Second European Symposium on Penetration Testing, Vol. 2, pp. 957-961. Amsterdam: A. A. Balkema.

Table 4.1. Summary of mean and coefficient of variation (COV) for geotechnical design model factor $M = X_m/X_c$

Geo-structure	Limit state	Calibration database				Method to determine X_m	Calculation method for X_c/reference	M		Source
		Ground condition		Data range	N			λ	COV	
Shallow foundation	Bearing	Clay (natural)		B=0.3–3.1 m s_u=20–139 kPa	30	Chin (1970)	Hansen (1970)	1.25	0.37	Strahler and Stuedlein (2014)
				B=0.3–5.0 m D/B=0.0–5.7 s_u=9–200 kPa	42	Hirany and Kulhawy (1988)	Vesić (1973)	1.05	0.29	Tang et al. (2020a)
		Sand	Controlled	B≤0.1 m	138	Vesić (1963)	AASHTO (2007)	1.67	0.25	Paikowsky et al. (2010)
				0.1<B≤1.0 m	21			1.48	0.39	
			Natural	B>1.0 m	6			1.01	0.23	
				0.1<B≤1.0 m	8			0.99	0.41	
			Field (θ=0°)	B=0.25–4.0 m D/B=0.0–6.1	113	Housel (1966)	Vesić (1973)	1.33	0.62	Tang et al. (2020a)
					106	Hirany and Kulhawy (1988)		1.64	0.47	
					76	10%B		1.77	0.43	
			Chamber (θ=0°)	B=0.30–1.22 m D/B=0.0–2.0 ϕ=27–46°	17	Housel (1966)		2.34	0.56	
					72	10%B		2.45	0.62	
			Chamber (θ>0°)	B=0.30 m D/B=0.0–3.0 ϕ=35–40°	27	Hirany and Kulhawy (1988)		1.21	0.33	
			Centrifuge (θ=0°)	B=0.30–7.0 m D/B=0.0–3.0 ϕ=41–48°	48	Peak		1.20	0.35	
			Centrifuge	B=0.90–2.54 m	93			1.09	0.22	

			(θ>0°)	D/B=0.0 ϕ=41–44°					
		Rock (natural)		RMR≥85	7	Hirany and Kulhawy (1988)	Carter and Kulhawy (1988)	1.81	0.84	Paikowsky et al. (2010)
				65≤RMR<85	22			3.54	0.49	
				44≤RMR<65	8			11.1	0.40	
				3≤RMR<44	21			24.3	0.55	
				RMR≥85	7		Goodman (1989)	1.46	0.14	
				65≤RMR<85	22			1.22	0.74	
				44≤RMR<65	8			1.06	0.44	
				3≤RMR<44	21			1.24	0.44	
	Eccentric	Sand		B=0.05–1.0 m	43	Vesić (1963)	Effective width	1.83	0.35	
					41	Two-slope		1.61	0.40	
					43	Vesić (1963)	Full width	1.05	0.42	
					41	Two-slope		0.92	0.46	
	Inclined	Sand		B=0.05–1.0 m	39	Vesić (1963)	AASHTO (2007)	1.43	0.30	
Shallow foundation	Inclined	Sand		B=0.05–1.0 m	37	Two-slope	AASHTO (2007)	1.29	0.35	
	Tension	Clay (natural)		B=0.38–3.05 m	118	Housel (1966)	IEEE (2001)	1.15	0.36	Tang et al. (2020a)
				s_u=15–300 kPa	74		Meyerhof and Adams (1968)	1.37	0.38	
		Sand (natural)		B=0.61–2.5 m ϕ=30–49°	106		IEEE (2001)	1.10	0.33	
							Meyerhof and Adams (1968)	1.19	0.42	
	Punch-through	Sand-over-clay (centrifuge)		B=0.8–3.0 m H_s/B=0.5–3.0 D_r=88%, ϕ_{cv}=32° s_{u0}=8.7–45 kPa	27	Peak	Load spread (1H:3V) (BSI 2020a)	1.49	0.31	Tang and Phoon (2019a)
							Load spread (1H:5V) (BSI 2020a)	2.37	0.38	
							Punching shear (BSI 2020a)	1.61	0.46	
							Punching shear (InSafeJIP 2011)	1.69	0.39	
							Okamura et al. (1998)	0.90	0.12	
							Ullah et al. (2017)	0.82	0.19	

	Settlement	Sand (natural)	B=1.0–10.0 m	268	s_m at elastic limit L_1 (Hirany and Kulhawy 1988)	Terzaghi and Peck (1948)	3.71	0.65	Akbas (2007)
						Gibbs and Holtz (1957)	1.37	0.64	
						Alpan (1964)	1.70	1.04	
						Meyerhof (1965)	2.40	0.90	
						Peck and Bazaraa (1969)	1.62	0.70	
						Peck et al. (1974)	2.76	0.92	
						D'Appolonia et al. (1970)	1.45	0.60	
						Schultze and Sherif (1973)	1.07	0.65	
						Anagnostopoulos et al. (1991)	1.44	0.84	
						Burland and Burbidge (1985)	1.45	0.63	
						Parry (1971)	1.24	0.87	
						Schmertmann et al. (1978)	2.03	0.69	
						Berardi and Lancelotta (1991)	1.55	0.79	
			Bridge	57	All	Schmertmann et al. (1978)	1.21	1.13	Samtani and Allen (2018)
				40	All (s_c>12.7 mm)		0.87	0.86	
				61	All	Hough (1959)	0.90	1.01	
				49	All (s_c>12.7 mm)		0.66	0.45	
Anchor	Pullout	Sand (natural)	B=0.30–2.39 m	45	Housel (1966)	IEEE (2001)	1.48	0.39	Tang et al. (2020a)
						Meyerhof and Adams (1968)	1.45	0.37	
		Sand (controlled)	B=0.10–0.44 m	162		IEEE (2001)	0.94	0.47	
						Meyerhof and Adams (1968)	0.99	0.45	
Pipeline	Upheaval buckling	Sand (1g-model 53%, centrifuge 29%, full-scale 18%)	D_r=5–85% D/B=0–20	>300	Peak	Pedersen and Jensen (1988)	0.93	0.21	Stuyts et al. (2016)
						White et al. (2008)	1.05	0.21	
						Byrne et al. (2013)	0.88	0.20	
		Sand (controlled)	B=0.015–0.45 m L=0.075–3 m	143	Peak	Schaminee et al. (1990)	1.21	0.39	Ismail et al. (2018)
						Bransby et al. (2002)	1.41	0.37	

			D/B=0.1–8			White et al. (2001)	1.02	0.30	
						DNV (2007)	1.09	0.32	
Offshore spudcan	Punch-through	Sand-over-clay (centrifuge)	B=3.0–20.0 m α=0-21° H_s/B=0.16–1.17 D_r=44–99% ϕ_{cv}=31–34° s_{u0}=7.2–44.8 kPa	103	Peak	Load spread (1H:3V) (BSI 2020a)	1.89	0.27	Tang and Phoon (2019a)
						Load spread (1H:5V) (BSI 2020a)	2.48	0.32	
						Punching shear (BSI 2020a)	2.86	0.30	
						Punching shear (InSafeJIP 2011)	2.44	0.24	
						Okamura et al. (1998)	0.87	0.22	
						Ullah et al. (2017)	1.02	0.17	
		Clay-sand-clay (centrifuge)	B=6.0–16.0 m α=0-13° H_s/B=0.25–1.04 D_r=44–89%, ϕ_{cv}=31° s_{u0}=4.4–34 kPa	28	Peak	Load spread (1H:3V) (BSI 2020a)	1.59	0.18	
						Load spread (1H:5V) (BSI 2020a)	2.02	0.22	
						Punching shear (BSI 2020)	1.94	0.23	
						Punching shear (InSafeJIP 2011)	1.71	0.17	
						Okamura et al. (1998)	1.00	0.21	
						Ullah et al. (2017)	1.06	0.13	
Rock socket	Bearing	Rock (natural)	RMR≥85	16	Hirany and Kulhawy (1988)	Carter and Kulhawy (1988)	3.42	0.55	Paikowsky et al. (2010)
			65≤RMR<85	35			3.93	0.45	
			44≤RMR<65	9			6.82	0.92	
			RMR≥85	16		Goodman (1989)	1.59	0.51	
			65≤RMR<85	35			1.40	0.52	
			44≤RMR<65	9			1.47	0.62	
			B=0.10–2.5 m D/B=1.0–31.3 σ_c=0.5–99 MPa E_m=7.82–75113 MPa GSI=7.5–95 RQD=20–100%	128	Hirany and Kulhawy (1988)	Teng (1962)	24.4	1.07	Tang et al. (2020a)
						Coates (1967)	1.63	1.07	
						Rowe and Armitage (1987)	1.95	1.07	
						Zhang and Einstein (1998)	1.11	0.86	
						Asem (2019)	1.78	1.01	
						ARGEMA (1992)	1.23	0.93	

				118		Abu-Hejleh and Attwooll (2005)	1.74	0.87	
				127		Stark et al. (2017)	1.38	0.81	
				125		Asem et al. (2018)	1.07	0.50	
				265	Maximum load	Teng (1962)	18.4	1.43	
						Coates (1967)	1.23	1.43	
						Rowe and Armitage (1987)	1.47	1.43	
						Zhang and Einstein (1998)	1.02	1.00	
						Asem (2019)	1.38	1.34	
						ARGEMA (1992)	1.40	0.88	
	Shearing		B=0.10–2.44 m D/B=0.54–17.3 σ_c=0.48–20 MPa E_m=47.6–6061 MPa	169	Peak	Reynolds and Kaderabek (1980)	1.13	0.70	Tang et al. (2020b)
						Gupton and Logan (1984)	1.70	0.70	
						Rosenberg and Journeaux (1976)	1.23	0.79	
						Horvath and Kenney (1979)	2.20	0.80	
						Williams et al. (1980)	1.18	0.89	
						Rowe and Armitage (1987)	1.01	0.80	
						Kulhawy and Phoon (1993)	1.01	0.80	
						Miller (2003)	1.14	0.80	
						AASHTO (2017)	1.43	0.80	
						Asem and Gardoni (2019b)	1.19	0.60	
						Xu et al. (2020)	1.39	0.88	
						Meigh and Wolski (1979)	1.97	0.73	
						Abu-Hejleh and Attwooll (2005)	1.31	0.70	
	Settlement	Rock (natural)		37	s_m at Q=50%Q_{L2}	Kulhawy (1978)	1.64	1.73	Muganga (2008)
Steel H pile	Bearing	Clay (natural)	B=0.28–0.41 m D/B=16–95	26	Davisson (1972)	API (1974)	1.26	0.56	Tang and Phoon (2018a)
						Burland (1973)	0.96	0.61	
				16		Vijayvergiya and Focht (1972)	0.74	0.39	Paikowsky et al.

				17		Tomlinson (1986)	0.82	0.40	(2004)
				16		API (1989)	0.90	0.41	
		Sand (natural)	B=0.28–0.42 m D/B=22–110	36	Davisson (1972)	SPT-Meyerhof (1976)	1.52	0.66	Tang and Phoon (2018a)
						Burland (1973)	0.78	0.47	
						Nordlund (1963)	0.82	0.52	
				19		Nordlund (1963)	0.94	0.40	Paikowsky et al. (2004)
				18		SPT-Meyerhof (1976)	0.81	0.38	
				19		Esrig and Kirby (1979)	0.78	0.51	
				18		SPT-97	1.35	0.43	
		Mixed (natural)	B=0.28–0.42 m D/B=17–85	29		Burland (1973)	0.81	0.40	Tang and Phoon (2018a)
				20		Tomlinson (1986)/Nordlund (1963)	0.59	0.39	Paikowsky et al. (2004)
				34		API (1989) /Nordlund (1963)	0.79	0.44	
				32		Esrig and Kirby (1979)	0.48	0.48	
				40		SPT-97	1.23	0.45	
Steel pipe pile	Bearing	Clay (natural)	B=0.1–0.81 m D/B=7.9–200 PI=11–160% OCR=1–43.2 S_t=1–17	110	10%B	BSI (2020b)	1.02	0.32	Tang and Phoon (2019b)
						NGI-05 (Karlsrud et al. 2005)	1.10	0.29	
						SHANSEP (Saye et al. 2013)	1.14	0.27	
						ICP-05 (Jardine et al. 2005)	1.06	0.28	
				18	Davisson (1972)	Tomlinson (1986)	0.64	0.50	Paikowsky et al. (2004)
				19		API (1989)	0.79	0.54	
				12		Esrig and Kirby (1979)	0.45	0.60	
				19		Vijayvergiya and Focht (1972)	0.67	0.55	
				12		SPT-97	0.39	0.62	

		Sand (natural)	B=0.14–0.76 m D/B=13–251 ϕ=30–42° D_r=15–93%	68	10%B	BSI (2020b)	1.11	0.54	Tang and Phoon (2018b, 2019b)
						NGI-05 (Clausen et al. 2005)	1.05	0.41	
				29		ICP-05 (Jardine et al. 2005)	1.13	0.30	
						Fugro-05 (Kolk et al. 2005)	0.95	0.36	
						UWA-05 (Lehane et al. 2005)	1.08	0.37	
				19	Davisson (1972)	Nordlund (1963)	1.48	0.52	Paikowsky et al. (2004)
				20		Esrig and Kirby (1979)	1.18	0.62	
				20		SPT-Meyerhof (1976)	0.94	0.59	
				19		SPT-97	1.58	0.52	
		Mixed (natural)		13		Tomlinson (1986)/Nordlund (1963)	0.74	0.59	
				32		API (1989)/Nordlund (1963)	0.80	0.45	
				29		Esrig and Kirby (1979)	0.54	0.48	
				33		SPT-97	0.76	0.38	
Concrete pile	Bearing	Clay (natural)	B=0.1–0.81 m D/B=7.9–200 PI=11–160% OCR=1–43.2 S_t=1–17	65	10%B	BSI (2020b)	1.09	0.34	Tang and Phoon (2019b)
						NGI-05 (Karlsrud et al. 2005)	0.95	0.26	
						SHANSEP (Saye et al. 2013)	1.01	0.34	
						ICP-05 (Jardine et al. 2005)	1.04	0.35	
				18	Davisson (1972)	Vijayvergiya and Focht (1972)	0.76	0.29	Paikowsky et al. (2004)
				17		API (1989)	0.81	0.26	
				8		Esrig and Kirby (1979)	0.81	0.51	
				18		Tomlinson (1986)	0.87	0.48	
		Sand (natural)	B=0.14–0.76 m D/B=13–251 ϕ=30–42°	50	10%B	BSI (2020b)	0.95	0.37	Tang and Phoon (2018b, 2019b)
						NGI-05 (Clausen et al. 2005)	0.83	0.33	
				40		ICP-05 (Jardine et al. 2005)	1.13	0.29	

			D_t=15–93%			Fugro-05 (Kolk et al. 2005)	0.87	0.41	
						UWA-05 (Lehane et al. 2005)	1.00	0.33	
				36	Davisson (1972)	Nordlund (1963)	1.02	0.48	Paikowsky et al. (2004)
				35		Esrig and Kirby (1979)	1.10	0.44	
				36		SPT-Meyerhof (1976)	0.61	0.61	
				36		SPT-97	1.21	0.47	
		Mixed (natural)		33		Tomlinson (1986)/Nordlund (1963)	0.96	0.49	
				80		API (1989)/Nordlund (1963)	0.87	0.48	
				80		Esrig and Kirby (1979)	0.81	0.38	
				71		SPT-97	1.81	0.50	
				30		Nottingham and Schmertmann (1975)	0.84	0.31	
			B=0.356–0.914 m D=11–61 m	80	Modified Davisson (AASHTO 2017)	Bustamante and Gianeselli (1982)	1.07	0.39	Amirmojahedi and Abu-Farsakh (2019)
						Nottingham and Schmertmann (1975)	1.21	0.35	
						De Ruiter and Beringen (1979)	0.95	0.36	
						Price and Wardle (1982)	0.83	0.34	
						Fugro-05 (Kolk et al. 2005; Van Dijk and Kolk 2010)	1.34	0.45	
						ICP-05 (Jardine et al. 2005)	1.33	0.45	
						NGI-05 (Clausen et al. 2005; Karlsrud et al. 2005)	1.24	0.45	
						Tumay and Fakhroo (1982)	1.36	0.35	
						Aoki and Velloso (1975)	0.77	0.51	
						Salgado et al. (2011)	1.29	0.56	

						UWA-05 (Lehane et al. 2005, 2013)	1.17	0.31	
Concrete/steel pile	Bearing	Sand (natural)	B=0.235–1.372 m D/B=17.1–85.2	43	Hansen (1963)-80%	CPT-Meyerhof (1983)	0.91	0.45	Moshfeghi and Eslami (2018)
						Nottingham and Schmertmann (1975)	0.86	0.31	
						De Ruiter and Beringen (1979)	0.69	0.41	
						Kempfert and Becker (2010)	0.98	0.41	
						Bustamante and Gianeselli (1982)	0.93	0.43	
						Eslami and Fellenius (1997)	1.12	0.19	
						Fugro-05 (Kolk et al. 2005)	1.00	0.43	
						ICP-05 (Jardine et al. 2005)	1.00	0.43	
						NGI-05 (Clausen et al. 2005)	1.12	0.42	
						UWA-05 (Lehane et al. 2005)	0.88	0.40	
	Bearing/ Tension	Mixed (natural)	B=0.114–1.50 m D/B=10.3–111	60	Hansen (1963)-80%	Schmertmann (1978)	1.12	0.35	Heidarie Golafzani et al. (2020)
						De Ruiter and Beringen (1979)	1.14	0.41	
						Bustamante and Gianeselli (1982)	1.29	0.47	
						CPT-Meyerhof (1983)	0.99	0.44	
						Eslami and Fellenius (1998)	0.99	0.33	
						SPT-Meyerhof (1976)	1.13	0.52	
						Shioi and Fukui (1982)	0.98	0.43	
						Bazaraa and Kurkur (1986)	1.57	0.50	
						Briaud and Tucker (1988)	0.85	0.40	
						Décourt (1995)	1.12	0.54	
						API (2000)	1.14	0.44	
						CGS (2006)	0.87	0.86	
Driven pile	Bearing	Clay (natural)	B=0.254–1.524 m	41	Davisson (1972)	Tomlinson (1986)	1.20	0.47	Machairas et al.

		Sand (natural)	D=3.05–55 m	114		Nordlund (1963)	1.60	0.88	(2018)
		Mixed (natural)		58		Tomlinson (1986)/Nordlund (1963)	1.43	0.94	
RC		Soil (natural)		29		Tomlinson (1986)/Nordlund (1963)	2.30	0.70	
SC				135		Tomlinson (1986)/Nordlund (1963)	1.28	0.65	
Steel H pile				9		Tomlinson (1986)/Nordlund (1963)	0.90	0.56	
SPC				27		Tomlinson (1986)/Nordlund (1963)	1.45	0.96	
SPO				11		Tomlinson (1986)/Nordlund (1963)	2.37	1.24	
Helical pile	Bearing	Clay (natural)	d=38–114 mm	176	10%B+QL/AE	Capacity-to-torque correlation	1.10	0.23	Tang and Phoon (2018c)
		Sand (natural)	D/B=3–70	115			1.39	0.33	
		Clay (natural)	d=38–57 mm	53		Individual plate bearing	1.25	0.41	
		Sand (natural)	D/B=8.4–110	49			1.46	0.42	
		Clay/sand (natural)	d=38–89 mm	27		Least value of individual plate bearing, cylindrical shear and capacity-to-torque correlation	1.79	0.50	Cherry and Souissi (2010)
				27			1.79	0.60	
				21			1.78	0.54	
				18			1.99	0.52	
		Clay/sand (natural)	d=0.168–0.508 m	83	5%B	Capacity-to-torque correlation	1.25	0.36	Tang and Phoon (2018c, 2020)
			B=0.356–1.016 m	47		CGS (2006)	1.17	0.36	
			D/B=4.1–20	47		ISHF (Lutenegger 2015)	1.06	0.45	
			s_u=12-305 kPa	47		BSI (2016)	1.04	0.35	
			ϕ=30–45°, n=2–6						

			S/B=1.5–4.5						
		Soil/rock (natural)		46	NA	Bearing (SPT) and cylindrical shear	1.06	0.55	Perko (2009)
Drilled shaft	Bearing	Clay (natural)	B=0.35–1.52 m D/B= 1.6–56 s_u=41–246 kPa	64	Modified Davisson (AASHTO 2017)	Brown et al. (2010)	1.41	0.63	Tang et al. (2019)
			B≥0.6 m	22	Davisson (1972)		1.02	0.41	AbdelSalam et al. (2015)
				53		Reese and O'Neill (1988)	0.90	0.47	Paikowsky et al. (2004)
				13			0.84	0.50	
				40			0.88	0.48	
		Sand (natural)	B=0.35–2.00 m D/B=5.1–59 ϕ=30–41°	44	Modified Davisson (AASHTO 2017)	Brown et al. (2010)	1.19	0.39	Tang et al. (2019)
			B≥0.6 m	45	Davisson (1972)		0.91	0.40	AbdelSalam et al. (2015)
			B=0.458–2.135 m D/B=4.05–45.3	24	5%B	O'Neill and Reese (1999)	1.14	0.58	Ng and Fazia (2012)
						Brown et al. (2010)	1.21	0.60	
			B=1.0–1.8 m D/B=11.2–64.2	11	Davisson (1972)	O'Neill and Reese (1999)	0.60	0.58	Zhang and Chu (2009a)
				17			1.06	0.28	
				32		Reese and Wright (1977)	1.22	0.67	Paikowsky et al. (2004)
				12			1.45	0.50	
				9			1.32	0.62	
				32		Reese and O'Neill (1988)	1.71	0.60	
				12			2.27	0.46	
				9			1.62	0.74	

		Mixed (natural)	B≥0.6 m	90	Davisson (1972)	Brown et al. (2010)	0.81	0.37	AbdelSalam et al. (2015)
			B=0.61–1.83 m D/B=7.2–34.5	34	5%B	O'Neill and Reese (1999)	1.27	0.30	Abu-Farsakh et al. (2013)
						Brown et al. (2010)	0.99	0.30	
				44	Davisson (1972)	Reese and O'Neill (1988)	1.19	0.30	Paikowsky et al. (2004)
				21			1.04	0.29	
				12			1.32	0.28	
				10			1.29	0.27	
				44		Reese and Wright (1977)	1.09	0.35	
				21			1.01	0.42	
				12			1.20	0.32	
				10			1.16	0.25	
		Gravel (natural)	B=0.59–1.50 m D/B=6.2–30 ϕ=37–47°	41	Modified Davisson (AASHTO 2017)	Brown et al. (2010)	1.69	0.47	Tang et al. (2019)
Pile foundation	Bearing	Soil (natural)	B=0.36–0.46 m (square concrete) B=0.30–0.41 m (drilled shaft) D=3.0–25.0 m	68	10%B+QL/AE	Bustamante and Gianeselli (1983)	1.15	0.43	Briaud and Tucker (1988)
				15		Bustamante and Gianeselli (1982)	1.32	0.44	
				77		Coyle and Castello (1981)	1.19	0.66	
				63		MSHD (1972)	1.15	0.70	
				53		Briaud and Tucker (1984)	1.40	0.51	
				68		De Ruiter and Beringen (1979)	1.49	0.42	
				68		Clisby et al. (1978)	0.72	0.38	
				77		API (1984)	0.92	0.58	
				68		Schmertmann (1978)	1.48	0.74	
				23		Tumay and Fakhroo (1982)	1.99	0.43	
				53		SPT-Meyerhof (1976)	1.73	0.72	

				68		Briaud et al. (1986)	2.78	0.59	
Steel pipe pile	Tension	Clay (natural)	B=0.1–0.81 m D/B=12–110 PI=12–110% OCR=1–43.2 S_t=1–8.3	64	10%B	BSI (2020b)	0.88	0.28	Tang and Phoon (2019b)
						NGI-05 (Karlsrud et al. 2005)	0.99	0.26	
						SHANSEP (Saye et al. 2013)	1.04	0.30	
						ICP-05 (Jardine et al. 2005)	1.02	0.34	
		Sand (natural)	B=0.25–0.76 m D/B=19–84 ϕ=30–42° D_r=31–97%	63		BSI (2020b)	1.15	0.61	
						NGI-05 (Clausen et al. 2005)	1.16	0.49	
				40		ICP-05 (Jardine et al. 2005)	1.26	0.36	Tang and Phoon (2018b)
						Fugro-05 (Kolk et al. 2005)	1.49	0.77	
						UWA-05 (Lehane et al. 2005)	1.20	0.36	
Drilled shaft	Tension	Clay (natural)	B=0.36–1.80 m D/B=3.4–55 s_u=21–250 kPa	32	Modified Davisson (AASHTO 2017)	Brown et al. (2010)	1.11	0.28	Tang et al. (2019)
				13	Davisson (1972)	Reese and O'Neill (1988)	0.87	0.37	Paikowsky et al. (2004)
		Sand (natural)	B=0.30–1.31 m D/B=2.5–43 ϕ=30–45°	30	Modified Davisson (AASHTO 2017)	Brown et al. (2010)	1.28	0.33	Tang et al. (2019)
				11	Davisson (1972)	Reese and O'Neill (1988)	1.09	0.51	Paikowsky et al. (2004)
						Reese and Wright (1977)	0.83	0.54	
		Gravel	B=0.43–2.26 m D/B=1.77–17.3 ϕ=42–48°	109	Modified Davisson (AASHTO 2017)	Brown et al. (2010)	1.14	0.43	Tang et al. (2019)
				14	Davisson (1972)	Reese and O'Neill (1988)	1.25	0.29	Paikowsky et al. (2004)
						Reese and Wright (1977)	1.24	0.41	

				16		Carter and Kulhawy (1988)	1.18	0.46	
						O'Neill and Reese (1999)	1.25	0.37	
				39		Reese and O'Neill (1988)	1.08	0.41	
				25		Reese and Wright (1977)	1.07	0.48	
Helical pile	Tension	Clay (natural)	d=38–114 mm D/B=10–62	147	10%B+QL/AE	Capacity-to-torque correlation	0.95	0.27	Tang and Phoon (2018c)
		Sand (natural)		105			1.09	0.31	
		Clay/sand (natural)	d=38–89 mm B=0.152–0.508 m n=2–14	91	NA	Cylindrical shear	1.50	0.79	Hoyt and Clemence (1989)
						Individual plate bearing	1.56	0.82	
						Capacity-to-torque correlation	1.49	0.59	
			d=38–89 mm	25	10%B+QL/AE	Least value of individual plate bearing, cylindrical shear and capacity-to-torque correlation	1.43	0.43	Cherry and Souissi (2010)
				39			1.31	0.54	
				20			1.56	0.43	
				25			2.08	0.53	
		Clay/sand (natural)	d=0.168–0.406 m B=0.304–1.016 m D/B=4.2–24 s_u=24-300 kPa ϕ=30–45°, n=2–6 S/B=1.5–3	28	5%B	Capacity-to-torque correlation	0.92	0.38	Tang and Phoon (2018c, 2020)
				31		CGS (2006)	1.26	0.32	
				31		ISHF (Lutenegger 2015)	1.22	0.39	
				31		BSI (2020b)	1.18	0.33	
		Soil/rock (natural)		66	NA	Bearing (SPT) and cylindrical shear	0.87	0.46	Perko (2009)
		Clay/sand (natural)	d=0.089–0.406 m B=0.355–0.762 m D/B=6.43–23.9 n=1–5 S/B=1.5–4.5	36	Average of failure loads interpreted by Modified Davisson (AASHTO 2017), Hansen (1963)-80%, and Mazurkiewicz (1972)	Meyerhof (1983)	1.79	0.71	Fateh et al. (2017)
						Schmertmann (1978)	1.42	0.49	
						De Ruiter and Beringen (1979)	1.4	0.54	
						Bustamante and Gianeselli (1982)	1.06	0.51	
						Eslami and Fellenius (1997)	1.98	0.55	

					methods	Fugro-05 (Kolk et al. 2005; Van Dijk and Kolk 2010)	1.58	0.52	
						ICP-05 (Jardine et al. 2005)	0.84	0.68	
						UWA-05 (Lehane et al. 2005, 2013)	0.9	0.46	
						NGI-05 (Clausen et al. 2005; Karlsrud et al. 2005)	1.07	0.39	
						Kempfert and Becker (2010)	1.71	0.56	
		Clay/sand (natural)	d=0.114–0.406 m B=0.356–0.914 m D/B=6.43–18.8 n=1–3, S/B=1.5–3	23	Mazurkiewicz (1972)	Bustamante and Gianeselli (1982)	0.76	0.46	Tappenden (2007)
		Clay (natural)	d=73–114 mm B=0.203–0.457 m D/B=2.57–66 n=1–4	47	NA	Individual plate bearing	1.03	0.46	Perko (2009)
		Sand (natural)		54			1.16	0.72	
				54		Individual plate bearing (SPT)	1.34	0.61	
		Clay (natural)		32		Cylindrical shear	0.82	0.32	
		Sand (natural)		42		Cylindrical shear	1.07	0.54	
		Clay (natural)		47		Lest value of individual plate	1.03	0.46	
		Sand (natural)		54		Bearing (SPT) and cylindrical shear	1.34	0.6	
		Soil/rock (natural)		112		Bearing (SPT) and cylindrical shear	0.97	0.53	
Drilled shaft	Lateral	Clay (controlled)	B=0.089–0.175 m D/B=3.00–7.98 h/D=0.03–4.01	45	Lateral or moment limit (Hirany and Kulhawy 1988)	Reese (1958)	0.90	0.24	Phoon and Kulhawy (2005)
						Hansen (1961)	1.22	0.25	
						Broms (1964a)	1.46	0.36	
						Stevens and Audibert (1979)	0.70	0.24	

						Randolph and Houlsby (1984)	0.84	0.24	
		Clay (natural)	B=0.08–1.98 m D/B=2.25–10.49 h/D=0.03–6.83	27		Reese (1958)	0.94	0.35	
						Hansen (1961)	1.24	0.32	
						Broms (1964a)	1.55	0.42	
						Stevens and Audibert (1979)	0.73	0.33	
						Randolph and Houlsby (1984)	0.87	0.34	
		Clay (controlled)	B=0.089–0.175 m D/B=3.00–7.98 h/D=0.03–4.01	47	Chin (1970)	Reese (1958)	1.43	0.26	
						Hansen (1961)	1.95	0.28	
						Broms (1964a)	2.28	0.35	
						Stevens and Audibert (1979)	1.12	0.28	
						Randolph and Houlsby (1984)	1.33	0.27	
		Clay (natural)	B=0.08–1.98 m D/B=2.25–10.49 h/D=0.03–6.83	27		Reese (1958)	1.40	0.33	
						Hansen (1961)	1.85	0.31	
						Broms (1964a)	2.29	0.41	
						Stevens and Audibert (1979)	1.09	0.32	
						Randolph and Houlsby (1984)	1.30	0.32	
		Sand (controlled)	B=0.076–0.152 m D/B=2.61–9.03 h/D=0.06–4.99	53	Lateral or moment limit (Hirany and Kulhawy 1988)	Hansen (1961)	0.71	0.36	
						Broms (1964b)	1.20	0.42	
						Reese et al. (1974)	0.82	0.51	
		Sand (natural)	B=0.05–1.62 m D/B=2.49–7.03 h/D=0.00–5.37	22		Hansen (1961)	0.56	0.39	
						Broms (1964b)	1.26	0.35	
						Reese et al. (1974)	0.81	0.39	
		Sand (controlled)	B=0.076–0.152 m D/B=2.61–9.03 h/D=0.06–4.99	55	Chin (1970)	Hansen (1961)	1.05	0.32	
						Broms (1964b)	1.77	0.44	
						Reese et al. (1974)	1.19	0.48	
		Sand (natural)	B=0.05–1.62 m	22		Hansen (1961)	0.83	0.30	

			D/B=2.49–7.03 h/D=0.00–5.37			Broms (1964b)	1.89	0.33	
						Reese et al. (1974)	1.19	0.30	
Driven pile	Settlement	Clay (natural)	s_u=9.6–500 kPa	21	s_m at Q=50%Q_{uc}	Coyle (Briaud et al. 1986)	1.26	0.45	Briaud and Tucker (1988)
				12		Penpile (Clisby et al. 1978)	1.51	0.35	
				30		Verbrugge (1981)	1.82	0.44	
Pile foundation				22		'FZ' model (Frank and Zhao 1982)	1.41	0.44	Abchir et al. (2016)
						'AB1' model (Abchir et al. 2016)	0.78	0.40	
						'AB2' model (Abchir et al. 2016)	0.66	0.67	
Driven pile		Mixed (natural)		23	s_m at Q=50%Q_{uc}	Coyle (Briaud et al. 1986)	0.44	1.30	Briaud and Tucker (1988)
				10		Penpile (Clisby et al. 1978)	0.99	0.72	
				22		Briaud and Tucker (1988)	0.57	1.07	
				19		Verbrugge (1981)	0.71	0.77	
				33		Coyle (Briaud et al. 1986)	1.49	0.76	
				20		Penpile (Clisby et al. 1978)	1.56	0.60	
				32		Briaud and Tucker (1988)	1.18	1.01	
				27		Verbrugge (1981)	1.02	0.63	
CEP				29	s_m at Q=50%Q_{DA}	Load transfer analysis	1.18	0.78	Gurbuz (2007)
						Elastic solution (Poulos 1994)	1.11	0.65	
CFA				31		Load transfer analysis	0.94	0.50	
Pile foundation				62		'FZ' model (Frank and Zhao 1982)	1.23	0.64	Abchir et al. (2016)
						'AB1' model (Abchir et al. 2016)	1.02	0.71	
						'AB2' model (Abchir et al. 2016)	0.88	0.99	
Drilled shaft		Soil (natural)	B=1.0–1.8 m D/B=11.2–64.2	24	s_m at Q=50%Q_{DA}	Vesić (1977)	0.24	0.38	Zhang and Chu (2009b)
				12		Mayne and Harris (1993)	0.64	0.22	
				19		Reese and O'Neill (1989)	1.80	0.31	
				19		Load transfer curves using Hong	0.90	0.39	

						Kong beta method			
				12		Load transfer curves using correlations with SPT blow count	1.05	0.41	
		Rock (natural)	B=1.0–1.5 m D/B=17.5–58.3 σ_c=15–202 MPa RQD=29–100% RMR=17–79%	14		Vesić (1977)	0.87	0.30	
				14		Kulhawy and Carter (1992) (100%)	0.81	0.24	
				14		Kulhawy and Carter (1992) (85%)	1.01	0.24	
				14		Kulhawy and Carter (1992) (70%)	1.22	0.34	
				14		Load transfer method using the ASTM correlation	1.21	0.30	
				5		Load transfer method using correlation with RMR	0.57	0.61	
				14		Load transfer method using correlation with RQD	1.11	0.30	
Displacement pile		Soil (natural)	B=0.156–1.02 m D=4.0–54.0 m	51	s_m at Q=40%Q_{uc}	'FZ' model (Frank and Zhao 1982)	1.26	0.56	Abchir et al. (2016)
						'AB1' model (Abchir et al. 2016)	0.93	0.60	
						'AB2' model (Abchir et al. 2016)	0.81	0.77	
Replacement pile			B=0.196–1.92 m D=3.5–43.4 m	39	s_m at Q=40%Q_{uc}	'FZ' model (Frank and Zhao 1982)	1.26	0.66	Abchir et al. (2016)
						'AB1' model (Abchir et al. 2016)	1.02	0.75	
						'AB2' model (Abchir et al. 2016)	0.89	1.09	
Pile foundation			B=0.156–1.92 m D=3.5–54.0 m	90		'FZ' model (Frank and Zhao 1982)	1.26	0.60	
						'AB1' model (Abchir et al. 2016)	0.97	0.66	
						'AB2' model (Abchir et al. 2016)	0.84	0.90	
Slope	Global stability	Real case histories	θ=2–90° LL=19–197% PL=5–107%	83	FS_A=1	Direct	1.07	0.21	Travis et al. (2011)
				134		Bishop (1955)	1.00	0.20	
				43		Force	0.95	0.20	

			PI=6–105%	41		Complete	0.97	0.15	
		Embankment (fill)	θ=18–47° H=2–18.7 m	27	FS_A=1	Bishop (1955)	1.11	0.28	Bahsan et al. (2014)
						Spencer (1967)	1.19	0.27	
		Excavation (cut)	θ=27–45° H=5–18.8 m	7		Bishop (1955)	0.89	0.28	
						Spencer (1967)	0.90	0.26	
		Natural slope	θ=26–57° H=7.6–34 m	9		Bishop (1955)	1.41	1.00	
						Spencer (1967)	1.57	0.96	
Excavation	Base heave stability	Real case histories	H_e=3.0–19.7 m H_d=0.3–23.7 m B_e=4.0–70.0 m	24	FS_A=0.8 (total failure) FS_A=1.2 (near failure) FS_A=1.2 (non-failure)	Modified Terzaghi (1943)	1.02	0.16	Wu et al. (2014)
						Bjerrum and Eide (1956)	1.09	0.15	
						Slip circle (JSA 1988)	1.27	0.22	
MSE	Load	Geosynthetic	Cohesionless backfill	114		AASHTO (2014)	0.45	0.92	Allen and Bathurst (2018)
			Cohesive backfill	79			0.16	1.46	
			All soil	193			0.33	1.14	
			Stiff wall face (sand)	73			0.33	0.96	
			Flexible wall face (sand)	41			0.66	0.73	
			Battered wall (all soil)	50			0.58	0.92	Allen and Bathurst (2015)
			Vertical wall (all soil)	143			0.24	1.05	
		Steel strip	Strip (ϕ>45°)	21		PWRC (2003)	2.57	0.44	Miyata and Bathurst (2012a)
			Strip (35<ϕ≤45°)	93			1.12	0.33	
			Strip (ϕ≤35°)	40			0.53	0.48	

			Strip	104		AASHTO (2014)	1.29	0.58	Allen and Bathurst (2018)
			Bar mat	29			0.85	0.41	
			Welded wire	52			1.07	0.4	
			All	185			1.16	0.55	
			Cohesionless soil	104		Allen and Bathurst (2015, 2018)	0.95	0.31	Bozorgzadeh et al. (2020)
						Bathurst et al. (2013)	1.00	0.47	
						Bathurst and Yu (2018)	1.00	0.39	
		Steel grid	c=0, ϕ>0	97		BSI (2010)	1.36	0.50	Miyata and Bathurst (2019)
						Simplified method (AASHTO 2017)	1.01	0.45	
						PWRC (2014)	1.41	0.47	
			c≥0, ϕ>0	113		BSI (2010)	1.19	0.64	
						AASHTO (2017)	0.89	0.59	
						PWRC (2014)	1.23	0.63	
			c=0, ϕ>0	97		Coherent gravity method (AASHTO 2017)	1.36	0.50	Bathurst et al. (2020)
						Bathurst and Yu (2018)	1.00	0.32	
						Allen and Bathurst (2015, 2018)	0.99	0.35	
	Pull-out	Geosynthetic	Uniaxial HDPE	159		AASHTO (2007)	2.02	0.47	Huang and Bathurst (2009)
			Biaxial PP	25			2.68	0.5	
			Woven PET	134			2.41	0.59	
			All	318			2.23	0.55	
						Huang and Bathurst (2009)	1.07	0.36	
		Geogrid	Gravel to fine sand	194		PWRC (2000)	1.11	0.23	Miyata and Bathurst (2012c)
			Sand	160			1.28	0.27	
			Silty sand	149			1.75	0.37	

			All	503			1.35	0.38	
		Smooth steel strip		47		Berg et al. (2009a, b)	2.73	0.48	Huang et al. (2012)
		Ribbed steel strip		38			2.5	0.54	
			Soil type A(laboratory)	36		PWRC (1988)	1.45	0.39	Miyata and Bathurst (2012b)
			Soil type A(in situ)	128			1.42	0.5	
			Soil type B (in situ)	43			3.27	0.4	
		Strip	Cohesionless soil	180		AASHTO (2017)	2.53	0.46	Bozorgzadeh et al. (2020)
						PWRC (2014)	2.34	0.47	
						Miyata and Bathurst (2012b)	1.00	0.40	
		Steel grid	Laboratory, c=0, ϕ>0	129		Peterson and Anderson (1980)	0.64	0.87	Miyata et al. (2018)
			Laboratory, c>0, ϕ>0	56			2.39	0.76	
			Laboratory, c≥0, ϕ>0	185			1.17	1.17	
			In situ, c≥0, ϕ>0	17			4.06	1.12	
			Laboratory, c=0, ϕ>0	129		Jewell et al. (1984)	2.49	0.77	
			Laboratory, c>0, ϕ>0	56			12.56	0.78	
			Laboratory, c≥0, ϕ>0	185			5.54	1.31	
			In situ, c≥0, ϕ>0	17			24.74	1.51	
			Laboratory, c=0, ϕ>0	129		Nebeshima et al. (1999)	1.16	0.79	
			Laboratory, c>0, ϕ>0	56			3.46	0.62	
			Laboratory, c≥0, ϕ>0	185			1.86	0.95	
			In situ, c≥0, ϕ>0	17			5.39	1.03	
			Laboratory, c=0, ϕ>0	129		Berg et al. (2009a, b)	1.33	0.44	
			Laboratory, c>0, ϕ>0	56			2.44	0.52	
			Laboratory, c≥0, ϕ>0	185			1.67	0.59	
			In situ, c≥0, ϕ>0	17			1.53	0.69	

			Laboratory, c=0, ϕ>0	129		Revised Berg et al. (2009a, b)	1.15	0.43	
			Laboratory, c>0, ϕ>0	56			2.16	0.53	
			Laboratory, c≥0, ϕ>0	185			1.45	0.61	
			In situ, c≥0, ϕ>0	17			1.35	0.71	
			Laboratory, c=0, ϕ>0	129		Yu and Bathurst (2015)	1.07	0.34	
			Laboratory, c>0, ϕ>0	56			2.26	0.32	
			Laboratory, c≥0, ϕ>0	185			1.43	0.52	
			In situ, c≥0, ϕ>0	17			2.65	0.56	
			Laboratory, c=0, ϕ>0	129		Revised Yu and Bathurst (2015)	1.00	0.34	
			Laboratory, c>0, ϕ>0	56			1.01	0.33	
			Laboratory, c≥0, ϕ>0	185			1.00	0.34	
			In situ, c≥0, ϕ>0	17			1.14	0.35	
MAW	Load		c=0, ϕ>0	18		PWRC (2002)	0.98	0.67	Miyata et al. (2009)
			c>0, ϕ>0	18			0.57	0.79	
			c≥0, ϕ>0	36			0.78	0.76	
	Pull-out		c≥0, ϕ>0	28		PWRC (2002)	1.21	0.35	Miyata et al. (2011)
SNW	Load	Long-term	All soil	54		AASHTO (2014)	0.95	0.38	Lin et al. (2017a)
		Short-term	All soil	45			0.66	0.52	
			Cohesive	92		CABR (2012)	0.6	1.01	Yuan et al. (2019)
			Cohesionless	52			0.64	0.92	
			All soil	144			0.62	0.97	
			Cohesive	92		CECS (1997)	0.65	0.74	
			Cohesionless	52			0.58	0.71	
			All soil	144			0.62	0.73	
	Pull-out	Hong Kong data	CDG soil	74		GEO (2007)	2.98	0.36	Lin et al. (2017b)
			CDV soil	30			3.58	0.43	

	Face tensile	Long term	All facing	42		Lazarte et al. (2015)	0.85	0.43	Liu et al. (2018)
		Short term		23			0.77	0.67	

Note:

1. X_m=measured response; X_c=calculated response; M=model factor (=X_m/X_c); N=number of tests or data points; λ=mean (bias) of model factor; B=foundation width; s_u or s_{u0}=undrained shear strength at the surface of the clay layer; D/B=embedment ratio; θ=slope angle; ϕ=friction angle; RMR=rock mass rating; H_s/B=ratio of thickness of sand layer to foundation width; D_r=relative density; ϕ_{cv}=constant volume friction angle of sand; s_m=measured settlement; s_c=calculated settlement; L=length of pipeline; α=foundation base cone angle; σ_c=uniaxial compressive strength of rock; E_m=elasticity modulus of rock mass; GSI=geological strength index; RQD=rock quality designation; Q_{L2}=failure load interpreted by the L_1-L_2 method in Hirany and Kulhawy (1988); PI=plasticity index; OCR=overconsolidation ratio; S_t=soil sensitivity; d=shaft diameter of helical pile; n=number of bearing helices; S/B=ratio of helix spacing to diameter; Q=applied load; L=pile length; A=cross-sectional area of pile; E=elasticity modulus of pile material; h/D=ratio of lateral load eccentricity to shaft depth; Q_{uc}=calculated capacity; Q_{DA}=failure load interpreted by the Davisson (1972) offset limit method; SPT=standard penetration test; ASTM=American Society for Testing and Materials; LL=liquid limit; PL=plasticity limit; FS_A=actual factor of safety; H=slope height or wall height; H_e=excavation depth; H_d=wall embedment depth; B_e=excavation width; CEP=closed-ended pile; CFA=continuous flight auger pile; RC=round concrete; SC=square concrete; SPC=steel pipe closed; SPO = steel pipe open; SNW=soil nail wall; and MSE=mechanically stabilized earth wall.
2. The mean (bias) λ and COV values in Akbas (2007) for shallow foundation settlement, Stuyts et al. (2016) for upheaval buckling of offshore pipeline, and Machairas et al. (2018) for driven pile capacity were calculated for the ratio of calculated over measured response.

5. Statistics for transformation uncertainties

Jianye Ching and Ali Noorzad

5.1 Introduction

Transformation models (Phoon and Kulhway 1999) quantify correlation behaviors among various soil/rock parameters. Transformation models are used to infer geotechnical properties from indirect measurements. A site-specific transformation model can be calibrated with direct and indirect measurements from a site. When such a model is used, spatial variability, measurement errors, and statistical uncertainty propagate into the uncertainty of the spatial average, which is the variable of interest in most geotechnical analyses (van der Kroget et al. 2019). Useful compilations of these models are available in the literature (e.g., Kulhawy and Mayne 1990; Mayne et al. 2001; Zhang 2016).

A transformation model is usually developed by regression based on a soil/rock dataset, so it is suitable for the range of conditions found in the dataset. The resulting regression equation does not provide an exact fit to the dataset, and the variability is called the transformation uncertainty. When implemented to a future case that is not within the regression dataset, a transformation model may exhibit both bias and variability. Ching and Phoon (2014) defined the bias (b) and coefficient of variation (COV) (δ) as the sample mean and sample COV of the following ratio:

$$\varepsilon = \frac{\text{measured target value}}{\text{prediction made by a transformation model}} \tag{5.1}$$

The bias (b) and COV (δ) of a transformation model can be calibrated by a generic soil/rock database. Table 5.1 gives the details of some generic soil/rock databases, labelled as (material type)/(number of parameters of interest)/(number of data points). For instance, consider the first transformation model in Table 5.2. The target value is s_u^{re}/P_a (s_u^{re} is the remolded undrained shear strength; P_a is one atmosphere pressure), and the prediction is $0.0144\times LI^{-2.44}$ (LI is liquidity index). For all cases in the CLAY/10/7490 database (see Table 5.1) with simultaneous knowledge of s_u^{re} and LI, their ε ratios can be computed, and b and δ are simply the sample mean and sample COV of these ε ratios. In principle, b = 1 is desirable because this means that the prediction is unbiased, whereas $\delta = 0$ is desirable because this means that b×prediction is 100% accurate. In this report, b and δ of some existing transformation models found in the literature are calibrated by the generic soil/rock databases in Table 5.1.

5.2 Summary Tables

Tables 5.2 to 5.5 summarize the calibrated b and δ values of some existing transformation models for clay, sand, rock, and rock mass, respectively. The n value in the third column is the number of calibration cases with simultaneous knowledge of measured value and prediction.

Table 5.2. Soil/rock databases

Database	Reference	Parameters of interest	# data points	# sites/ studies
CLAY/10/7490	Ching and Phoon (2014)	LL, PI, LI, σ'_v/P_a, σ'_p/P_a, s_u/σ'_v, S_t, q_{t1}, q_{tu}, B_q	7490	251 studies
SAND/7/2794	Ching et al. (2017)	D_{50}, C_u, D_r, σ'_v/P_a, ϕ', Q_{tn}, $(N_1)_{60}$	2794	176 studies
ROCK/9/4069	Ching et al. (2018)	γ, n, R_L, S_h, σ_{bt}, I_{s50}, V_p, σ_{ci}, E_i	4069	184 studies
ROCKMass/9/5876	Ching et al. (2020)	RQD, RMR, Q, GSI, E_m, E_{em}, E_{dm}, E_i, σ_{ci}	5784	225 studies
CLAY/8/12225	Ching (2020)	LL, PI, w, e, σ'_v, C_c, C_s, c_v	12225	427 studies
CLAY/12/3997	Ching (2020)	LL, PI, LI, σ'_v/P_a, σ'_p/P_a, s_u/σ'_v, K_0, E_u/σ'_v, B_q, q_{t1}, $N_{60}/(\sigma'_v/P_a)$	3997	237 studies
SAND/10/4113	Ching (2020)	e, D_r, σ'_v/P_a, σ'_p/P_a, K_0, E_{d1}, Q_{tn}, B_q, $(N_1)_{60}$, K_{DMT}	4113	172 studies

Note: γ = unit weight; ϕ' = effective friction angle; σ'_p = preconsolidation stress; σ'_v = vertical effective stress; σ_{bt} = Brazilian tensile strength; σ_{ci} = uniaxial compressive strength of intact rock; $(N_1)_{60} = N_{60}/(\sigma'_v/P_a)^{0.5}$; B_q = CPT pore pressure ratio = $(u_2-u_0)/(q_t-\sigma_v)$; C_c = compression index; C_s = swelling index; C_u = coefficient of uniformity; c_v = coefficient of consolidation; D_{50} = median grain size; D_r = relative density; e = void ratio; E_d = drained modulus of sand; $E_{d1} = (E_d/P_a)/(\sigma'_v/P_a)^{0.5}$; E_{dm} = dynamic modulus of rock mass; E_{em} = elasticity modulus of rock mass; E_i = Young's modulus of intact rock; E_m = deformation modulus of rock mass; E_u = undrained modulus of clay; GSI = geological strength index; I_{s50} = point load strength index for diameter 50 mm; K_0 = at-rest lateral earth pressure coefficient; K_{DMT} = dilatometer horizontal stress index; LI = liquidity index; LL = liquid limit; n = porosity; N_{60} = corrected SPT-N; P_a = atmospheric pressure = 101.3 kPa; PI = plasticity index; Q = Q-system; q_c = cone tip resistance; q_t = corrected cone tip resistance; $Q_{tn} = (q_t/P_a)/(\sigma'_v/P_a)^{0.5}$; $q_{t1} = (q_t-\sigma_v)/\sigma'_v$ = normalized cone tip resistance; $q_{tu} = (q_t-u_2)/\sigma'_v$ = effective cone tip resistance; R_L = L-type Schmidt hammer hardness; RMR = rock mass rating; RQD = rock quality designation; S_h = Shore scleroscope hardness; SPT-N = standard penetration test blow count; S_t = sensitivity; s_u = undrained shear strength for clay; s_u^{re} = remoulded s_u; u_0 = hydrostatic pore pressure; u_2 = CPTU pore pressure; V_p = P-wave velocity; w = water content.

Figure 5.1 shows the calibrated (b, δ) values. According to the classification for model bias proposed by Phoon and Tang (2019), a similar classification is adopted for the transformation bias:

1. Highly overestimation ($b < 0.5$);
2. Moderately overestimation ($0.5 \leq b < 1$);
3. Moderately underestimation ($1 \leq b < 2$);
4. Highly underestimation ($2 \leq b < 3$);
5. Very highly underestimation ($b \geq 3$).

According to the classification for model COV proposed by Phoon and Tang (2019), a similar classification is adopted for the transformation COV:

1. Low variability ($\delta < 0.3$);
2. Medium variability ($0.3 \leq \delta < 0.6$);
3. High variability ($0.6 \leq \delta < 0.9$);
4. Very high variability ($\delta \geq 0.9$).

5.3 Key observations

1. Most transformation models have $0.5 < b < 2$ (namely, moderate underestimate or moderate underestimate).
2. Most soil models (clay and sand) and intact rock models have $0.3 < \delta < 0.9$ (median to high variability). However, rock mass models have the largest variability. Most of them are with $\delta > 0.9$ (very high variability).
3. Most clay models for s_u and OCR (or σ'_p) have $0.3 < \delta < 0.6$ (median variability).
4. Most clay models for C_c and C_s have $0.6 < \delta < 0.9$ (high variability).
5. Most sand models for ϕ' and D_r have $\delta < 0.3$ (low variability). In particular, all sand models for ϕ' have very low variability ($\delta \approx 0.1$).

6. All soil models for modulus (e.g., E_{PMT}, E_{DMT}, and M′) have $\delta > 0.6$ (high to very high variability). Moreover, they are fairly biased with $1.5 < b < 2.3$ (moderate to high underestimation).
7. All soil models for K_0 have $0.3 < \delta < 0.9$ (median to high variability).
8. In general, the COVs for transformation uncertainties are significantly larger than those for spatial variability. The latters (COVs for spatial variability) usually range from 0.1 to 0.5.

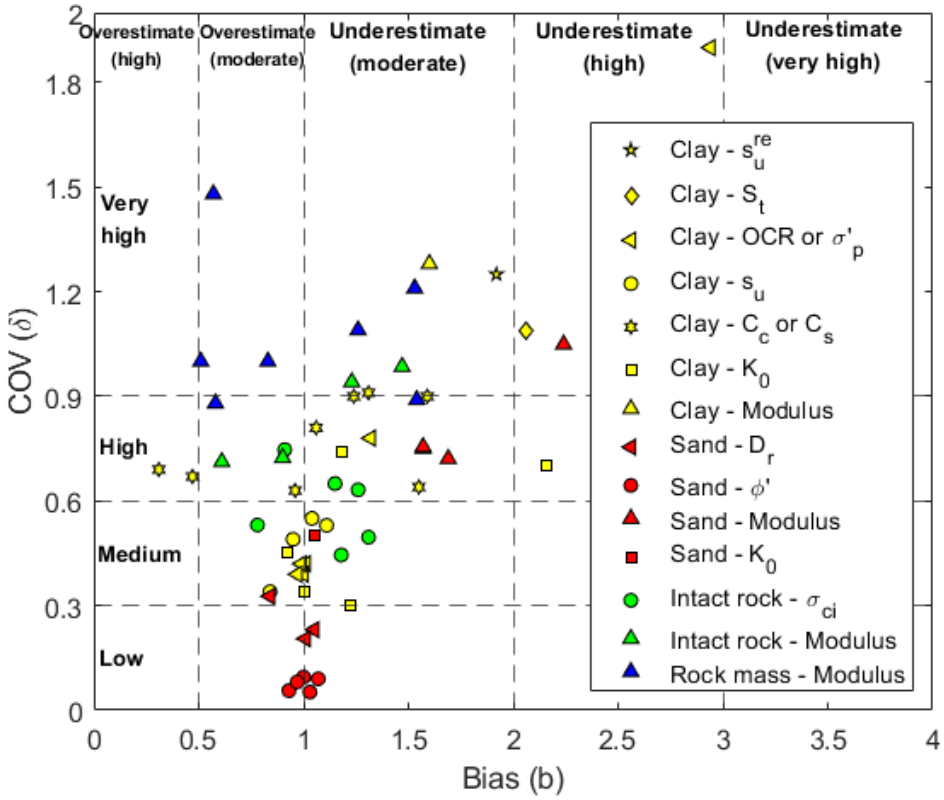

Figure 5.1. Calibrated (b, δ) values

5.4 References

Altindag, R. and Guney, A. (2010). Predicting the relationships between brittleness and mechanical properties (UCS, TS and SH) of rocks. Scientific Research and Essays, 5(16), 2107-2118.

Bieniawski, Z.T. (1975). The point load test in geotechnical practice. Engineering Geology, 9, 1-11.

Bieniawski, Z.T. (1978). Determining rock mass deformability: Experience from case histories. International Journal of Rock Mechanics and Mining Sciences, 15, 237-247.

Bjerrum, L. (1954). Geotechnical properties of Norwegian marine clays. Geotechnique, 4(2), 49-69.

Bolton, M.D. 1986. The strength and dilatancy of sands. Geotechnique, 36(1), 65-78.

Chen, B.S.Y. and Mayne, P.W. (1996). Statistical relationships between piezocone measurements and stress history of clays. Canadian Geotechnical Journal, 33 (3), 488-498.

Chen, J.-R. 2004. Axial behavior of drilled shafts in gravelly soils. PhD Thesis, Cornell Univ., Ithaca, N.Y.

Ching, J. and Phoon, K.K. (2012a), Establishment of generic transformations for geotechnical design parameters. Structural Safety, 35, 52-62.

Ching, J. and Phoon, K.K. (2012b), Modeling parameters of structured clays as a multivariate normal distribution. Canadian Geotechnical Journal, 49(5), 522-545.

Ching, J. and Phoon, K.K. (2014). Transformations and correlations among some parameters of clays – the global database. Canadian Geotechnical Journal, 51(6), 663-685.

Ching, J., Lin, G.H., Chen, J.R., and Phoon, K.K. (2017). Transformation models for effective friction angle and relative density calibrated based on a multivariate database of coarse-grained soils. Canadian Geotechnical Journal, 54(4), 481-501.

Ching, J., Li, K.H., Phoon, K.K., and Weng, M.C. (2018). Generic transformation models for some intact rock properties. Canadian Geotechnical Journal, 55(12), 1702-1741.

Ching, J., Phoon, K.K., Ho, Y.H., and Weng, M.C. (2020). Quasi-site-specific prediction for deformation modulus of rock mass. Canadian Geotechnical Journal, in press.

Ching, J. (2020). Unpublished soil databases.

Coon, R.F. and Merritt, A.H. (1970). Predicting in situ modulus of deformation using rock quality indexes. In Determination of the In Situ Modulus of Deformation of Rock, ASTM International, 154-173.

Deere, D.U. and Miller, R.P. (1966). Engineering Classification and Index Properties for Intact Rock. Technical Report No. AFWL-TR-65-116, Air Force Weapons Lab, Kirtland Air Force Base, Albuquerque, NM.

Gokceoglu, C., Sonmez, H., and Kayabasi, A. (2003). Predicting the deformation moduli of rock masses. International Journal of Rock Mechanics and Mining Sciences, 40(5), 701-710.

Grimstad E. and Barton N. (1993). Updating the Q-System for NMT. In: Proceedings of the international symposium on sprayed concrete-modern use of wet mix sprayed concrete for underground support, Oslo, Norwegian Concrete Association.

Hatanaka, M., Suzuki, Y., Kawasaki, T., and Endo, M. 1988. Cyclic undrained shear properties of high quality undisturbed Tokyo gravel. Soils and Foundations, 28(4), 57-68.

Hoek, E. and Diederichs, M.S. (2006). Empirical estimation of rock mass modulus. International Journal of Rock Mechanics and Mining Sciences, 43(2), 203-215.

Isik, N. S. (2009). Estimation of Swell Index of Fine Grained Soils Using Regression Equations and Artificial Neural Networks. Scientific Research and Essay, 4(10), 1047-1056.

Jamiolkowski, M., Ladd, C.C., Germain, J.T., and Lancellotta, R. (1985). New developments in field and laboratory testing of soils. Proceeding of the 11th International Conference on Soil Mechanics and Foundation Engineering, San Francisco, 1, 57-153.

Kahraman, S. (2001). Evaluation of simple methods for assessing the uniaxial compressive strength of rock. International Journal of Rock Mechanics and Mining Sciences, 38(7), 981-994.

Kahraman, S. and Gunaydin, O. (2009). The effect of rock classes on the relation between uniaxial compressive strength and point load index. Bulletin of Engineering Geology and the Environment, 68(3), 345-353.

Katz, O., Reches, Z., and Roegiers, J.C. (2000). Evaluation of mechanical rock properties using a Schmidt hammer. International Journal of Rock Mechanics and Mining Sciences, 37(4), 723-728.

Kılıç, A. and Teymen, A. (2008). Determination of mechanical properties of rocks using simple methods. Bulletin of Engineering Geology and the Environment, 67(2), 237-244.

Kulhawy, F. H., Jackson, C. S., and Mayne, P. W. (1989). First Order Estimation of K_0 in Sands and Clays, Foundation Engineering: Current Principles and Practices, Ed. F. H. Kulhawy, ASCE, New York.

Kulhawy, F.H. and Mayne, P.W. (1990). Manual on Estimating Soil Properties for Foundation Design, Report EL-6800, Electric Power Research Institute, Cornell University, Palo Alto.

Locat. J. and Demers. D. (1988). Viscosity, yield stress, remoulded strength, and liquidity index relationships

for sensitive clays. Canadian Geotechnical Journal, 25, 799-806.

Mayne, P. W. (2007). Invited Overview Paper: In-situ test calibrations for evaluating soil parameters, Characterization and Engineering Properties of Natural Soils, vol. 3 (Proc. IS-Singapore), Taylor & Francis Group, London: 1602 – 1652.

Mayne, P. W. and Frost, D. D. (1989). "Dilatometer Experience in Washington D.C. and Vicinity." Research Record 1169, Transportation Research Board, Washington D.C., 16 – 23.

Mayne, P. W., and Kulhawy, F. H. (1990). Direct and Indirect Determinations of In-Situ K_0 in Clays. Transportation Research Record 1278.

Mayne, P.W., Christopher, B.R., and DeJong, J. (2001). Manual on Subsurface Investigations. National Highway Institute Publication No. FHWA NHI-01-031, Federal Highway Administration, Washington, D.C.

Mesri, G. (1975). Discussion on "New design procedure for stability of soft clays". Journal of the Geotechnical Engineering Division, ASCE, 101(4), 409-412.

Mesri, G. (1989). A re-evaluation of $s_{u(mob)} = 0.22\ \sigma'_p$ using laboratory shear tests. Canadian Geotechnical Journal, 26(1), 162-164.

Mesri, G. and Huvaj, N. (2007). Shear strength mobilized in undrained failure of soft clay and silt deposits. Advances in Measurement and Modeling of Soil Behaviour (GSP 173), Ed. D.J. DeGroot et al., ASCE, 1-22.

Mishra, D.A. and Basu, A. (2013). Estimation of uniaxial compressive strength of rock materials by index tests using regression analysis and fuzzy inference system. Engineering Geology, 160, 54-68.

Morales, T., Uribe-Etxebarria, G., Uriarte, J.A., and de Valderrama, I.F. (2004). Probabilistic slope analysis – state-of-play. Engineering Geology, 71, 343-362.

Nagaraj, T. S., and Srinivasa Murthy, B. R. (1986). A critical reappraisal of compression index equations. Géotechnique, 36(1), 27–32.

Ohya, S. Imai, T., Matsubara, M. (1982). Relation between N value by SPT and LLT pressuremeter results. Proc., 2nd European Symposium on Penetration Testing, Amsterdam, vol. 1, pp. 125 – 130.

Peck, R. B., and Reed, W. C. (1954). Engineering Properties of Chicago Subsoils. University of Illinois at Urbana Champaign, College of Engineering. Engineering Experiment Station.

Phoon, K.K. and Kulhawy, F.H. (1999). Evaluation of geotechnical property variability. Canadian Geotechnical Journal, 36(4), 625-639.

Phoon, K.K. and Tang, C. (2019). Characterisation of geotechnical model uncertainty, Georisk: Assessment and Management of Risk for Engineered Systems and Geohazards, 13(2), 101-130.

Powell, J. J. M., and Uglow, I. M. (1986). Dilatometer testing in stiff overconsolidated clays. Proc. 39th Canadian Geotech. Conf., In Situ Testing and Field Behaviour, Canadian Geotechnical Society, 317 – 326.

Prakoso, W.A., and Kulhawy, F.H. (2011). Effects of testing conditions on intact rock strength and variability. Geotechnical and Geological Engineering, 29(1), 101-111.

Serafim, J.L. and Pereira, J.P. (1983). Considerations on the geomechanical classification of Bieniawski. In: Proceedings of the symposium on engineering geology and underground openings, Lisboa, Portugal, 1133-1144.

Skempton, A. W. and Jones, O. T. (1944). Notes on the Compressibility of Clays. Quarterly Journal of the Geological Society, 100(1-4), 119–135.

Sousa, L.M.O., del Rio, L.M.S., Calleja, L., de Argandona, V.G.R., and Rey, A.R. (2005). Influence of microfractures and porosity on the physico-mechanical properties and weathering of ornamental granites. Engineering Geology, 77, 153-168.

Stas, C. V. and Kulhawy, F. H. (1984). Critical evaluation of design methods for foundations under axial uplift and compressive loading. Electric Power Research Institute, Palo Alto, Calif. Report EL-3771.

Terzaghi, K., and Peck, R. B. (1967). Soil Mechanics in Engineering Practice. 2nd Ed., John Willey and Sons, New York, 729p.

Van der Krogt, M.G., Schweckendiek, T., and Kok, M. (2019) Uncertainty in spatial average undrained shear strength with a site-specific transformation model, Georisk: Assessment and Management of Risk for Engineered Systems and Geohazards, 13(3), 226-236.

Wroth, C. P., and Wood, D. M., (1978). The Correlation of Index Properties with Some Basic Engineering Properties of Soils. Canadian Geotechnical Journal, 15(3), 137-145.

Yaşar, E. and Erdogan, Y. (2004). Correlating sound velocity with the density, compressive strength and Young's modulus of carbonate rocks. International Journal of Rock Mechanics and Mining Sciences, 41(5), 871-875.

Zhang, L. and Einstein, H. H. (2004). Using RQD to estimate the deformation modulus of rock masses. International Journal of Rock Mechanics and Mining Sciences, 41(2), 337-341.

Zhang, L. (2016). Engineering Properties of Rocks, 2nd Edition. Elsevier Ltd., Cambridge, MA, USA.

Table 5.2. Transformation models for clay

Model	Literature	n	Transformation model	b	δ	Data restriction / Application range	Calibration database
$s_u{}^{re} - LI$	Locat and Demers (1988)	899	$s_u^{re}/P_a \approx 0.0144 \times LI^{-2.44}$	1.92	1.25		CLAY/10/7490
$S_t - LI$	Bjerrum (1954)	1279	$S_t \approx 10^{0.8LI}$	2.06	1.09		CLAY/10/7490
$\sigma'_p - LI - S_t$	Stas and Kulhawy (1984)	249	$\sigma'_p/P_a \approx 10^{1.11-1.62\times LI}$	2.94	1.90	$S_t < 10$	CLAY/10/7490
	Ching and Phoon (2012b)	489	$\sigma'_p/P_a \approx 0.235 \times LI^{-1.319} \times S_t{}^{0.536}$	1.32	0.78		CLAY/10/7490
$s_u - \sigma'_p$	Mesri (1975, 1989)	1155	$s_u(mob)/\sigma'_p \approx 0.22$	1.04	0.55		CLAY/10/7490
$\left(\frac{s_u}{\sigma'_v}\right) - OCR$	Jamiolkowski et al. (1985)	1402	$s_u(mob)/\sigma'_v \approx 0.23 \times OCR^{0.8}$	1.11	0.53		CLAY/10/7490
$\left(\frac{s_u}{\sigma'_v}\right) - OCR - S_t$	Ching and Phoon (2012b)	395	$s_u(mob)/\sigma'_v \approx 0.223 \times OCR^{0.823} \times S_t{}^{0.121}$	0.84	0.34		CLAY/10/7490
$\left(\frac{s_u}{\sigma'_v}\right) - CPT$	Ching and Phoon (2012a)	423	$s_u(mob)/\sigma'_v \approx \frac{(q_t - \sigma_v)/\sigma'_v}{29.1 \times \exp(-0.513B_q)}$	0.95	0.49		CLAY/10/7490
$OCR - CPT$	Chen and Mayne (1996)	690	$OCR \approx 0.259 \times [(q_t - \sigma_v)/\sigma'_v]^{1.107}$	1.01	0.42		CLAY/10/7490
	Kulhway and Mayne (1990)	690	$OCR \approx 0.32 \times (q_t - \sigma_v)/\sigma'_v$	1.00	0.39		CLAY/10/7490
$\sigma'_p - CPT$	Chen and Mayne (1996)	690	$\sigma'_p/P_a \approx 0.227 \times [(q_t - \sigma_v)/P_a]^{1.200}$	0.99	0.42		CLAY/10/7490
	Kulhway and Mayne (1990)	690	$\sigma'_p \approx 0.33 \times (q_t - \sigma_v)$	0.97	0.39		CLAY/10/7490
$C_c - LL$	Skempton (1944)	3398	$C_c \approx 0.007 \times (LL - 10)$	1.59	0.90	Remolded clay	CLAY/8/12225
	Terzaghi and Peck (1967)	3398	$C_c \approx 0.009 \times (LL - 10)$	1.24	0.90		CLAY/8/12225
$C_c - PI$	Kulhawy and Mayne (1990)	2964	$C_c \approx PI/73$	1.31	0.91		CLAY/8/12225
$C_c - LL - G_s$	Nagaraj and Murty (1985)	1523	$C_c \approx 0.2343 \times (LL/100) \times G_s$	1.06	0.81		CLAY/8/12225
$C_s - e_0$	Peck and Reed (1954)	668	$C_s \approx 0.208 \times e_0 + 0.0083$	0.31	0.69		CLAY/8/12225
$C_s - \omega$	Azzouz et al. (1976)	771	$C_s \approx 0.003 \times (\omega + 7)$	0.47	0.67		CLAY/8/12225

$C_s - PI$	Kulhawy and Mayne (1990)	847	$C_s \approx PI/385$	0.96	0.63		CLAY/8/12225
$C_s - LL$	Isik (2009)	846	$C_s \approx 0.0007 \times \mathrm{LL} + 0.0062$	1.55	0.64		CLAY/8/12225
$K_0 - OCR$	Mayne and Kulhawy (1990)	1009	$K_0 \approx [1 - \sin(\phi')] \times OCR^{\sin(\phi')}$	1.00 (ϕ' = 25°)	0.34 (ϕ' = 25°)		CLAY/12/3997
$K_0 - K_{DMT}$		124	$K_0 \approx 0.27 \times K_{DMT}$	0.92	0.45		CLAY/12/3997
	Powell and Uglow (1988)	124	$K_0 \approx 0.34 \times {K_{DMT}}^{0.55}$	1.22	0.30		CLAY/12/3997
$K_0 - N_{60} - \sigma'_v$	Kulhawy et al. (1989)	74	$K_0 \approx 0.073 \times N_{60}/(\sigma'_v/P_a)$	2.16	0.70		CLAY/12/3997
$K_0 - CPT$		74	$K_0 \approx 0.1 \times (q_t - \sigma_v)/\sigma'_v$	1.18	0.74		CLAY/12/3997
$E_{PMT} - N_{60}$	Kulhway and Mayne (1990), Ohya et al. (1982)	812	$E_{PMT}/P_a \approx 19.3 \times {N_{60}}^{0.63}$	1.60	1.28		CLAY/12/3997
$M' - CPT$	Mayne (2007)	111	$M' \approx 5 \times (q_t - \sigma_v)$	1.57	0.75		CLAY/12/3997

Note: s_u(mob) = undrained shear strength mobilized in embankment and slope failures (Mesri and Huvaj 2007) ; E_{PMT} = pressuremeter modulus; M′ = effective constrained modulus.

Table 5.3. Transformation models for sand

Model	Literature	n	Transformation model	b	δ	Data restriction / Application range	Calibration database
$D_r - SPT$	Terzaghi and Peck (1967)	198	$D_r(\%) \approx 100 \times \sqrt{(N_1)_{60}/60}$	1.05	0.23	$(N_1)_{60} < 60$	SAND/7/2794
	Kulhawy and Mayne (1990)	199	$D_r(\%) \approx 100 \times \sqrt{\frac{(N_1)_{60}}{[60 + 25\log_{10}(D_{50})] \times OCR^{0.18}}}$	1.01	0.21		SAND/7/2794
$D_r - CPT$	Jamiolkowski et al. (1985)	681	$D_r(\%) \approx 68 \times [\log_{10}(Q_{tn}) - 1]$	0.84	0.33	$Q_{tn} < 300$	SAND/7/2794
$\phi' - D_r$	Bolton (1986)	391	$\phi' \approx {\phi'}_{CV} + 3 \times \left(D_r \left[10 - \ln\left({p'}_f\right)\right] - 1\right)$	1.03	0.052		SAND/7/2794
$\phi' - SPT$	Hatanaka et al. (1998)	58	$\phi' \approx \begin{cases} \sqrt{15.4 \times (N_1)_{60}} + 20 & (N_1)_{60} \le 26 \\ 40 & (N_1)_{60} > 26 \end{cases}$	1.07	0.090	$(N_1)_{60} < 150$	SAND/7/2794

	Chen (2004)	59	$\phi' \approx 27.5 + 9.2 \times \log_{10}[(N_1)_{60}]$	1.00	0.095		SAND/7/2794
$\phi' - CPT$	Robertson and Campanella (1983)	99	$\phi' \approx \tan^{-1}[0.1 + 0.38 \times \log_{10}(q_t/\sigma'_v)]$	0.93	0.056		SAND/7/2794
	Kulhawy and Mayne (1990)	376	$\phi' \approx 17.6 + 11 \times \log_{10}(Q_{tn})$	0.97	0.081		SAND/7/2794
$E_{PMT} - N_{60}$	Kulhway and Mayne (1990), Ohya et al. (1982)	1081	$E_{PMT}/P_a \approx 9.08 \times {N_{60}}^{0.66}$	2.24	1.05		SAND/10/4113
$E_{DMT} - N_{60}$	Mayne and Frost (1989)	591	$E_{PMT}/P_a \approx 22 \times {N_{60}}^{0.82}$	1.69	0.72		SAND/10/4113
$M' - CPT$	Mayne (2007)	113	$M' \approx 5 \times (q_t - \sigma_v)$	1.57	0.76		SAND/10/4113
$K_0 - OCR$	Mayne and Kulhawy (1990)	1207	$K_0 \approx [1 - sin(\phi')] \times OCR^{sin(\phi')}$	1.05 (ϕ' = 30°)	0.50 (ϕ' = 30°)		SAND/10/4113

Note: E_{DMT} = pressuremeter modulus; E_{PMT} = pressuremeter modulus; M′ = effective constrained modulus.

Table 5.4. Transformation models for intact rock

Model	Literature	n	Transformation model	b	δ	Data restriction / Application range	Calibration database
$\sigma_{ci} - n$	Kilic and Teymen (2008)	911	$\sigma_{ci} \approx 147.16 \times e^{-0.0835n}$	0.91	0.75	0.16 < n < 37.81	ROCK/9/4069
$\sigma_{ci} - R_L$	Karaman and Kesimal (2015)	664	$\sigma_{ci} \approx 0.1383 \times {R_L}^{1.743}$	0.78	0.53	11.82 < R_L < 59.59	ROCK/9/4069
$\sigma_{ci} - S_h$	Altindag and Guney (2010)	297	$\sigma_{ci} \approx 0.1821 \times {S_h}^{1.5833}$	1.15	0.65	9 < S_h < 100	ROCK/9/4069
$\sigma_{ci} - \sigma_{bt}$	Prakoso and Kulhawy (2011)	525	$\sigma_{ci} \approx 7.8 \times \sigma_{bt}$	1.31	0.50	5 < σ_{bt} < 25.64	ROCK/9/4069
$\sigma_{ci} - I_{s\,50}$	Mishra and Basu (2013)	1074	$\sigma_{ci} \approx 14.63 \times I_{s\,50}$	1.18	0.45	1.15 < $I_{s\,50}$ < 14.13	ROCK/9/4069
$\sigma_{ci} - V_P$	Kahraman (2001)	1247	$\sigma_{ci} \approx 9.95 \times {V_P}^{1.21}$	1.26	0.63	1.02 < V_P < 6.3	ROCK/9/4069
$E_i - R_L$	Katz et al. (2000)	289	$E_i \approx 0.00013 \times {R_L}^{3.09074}$	1.47	0.99	24.01 < R_L < 73.3	ROCK/9/4069
$E_i - S_h$	Deere and Miller (1966)	197	$E_i \approx 0.739 \times S_h + 11.51$	0.61	0.71	11 < S_h < 105	ROCK/9/4069
$E_i - \sigma_c$	Deere and Miller (1966)	1152	$E_i \approx 0.303 \times \sigma_{ci} - 0.8745$	1.23	0.94	21 < σ_{ci} < 1330	ROCK/9/4069
$E_i - V_P$	Yasar and Erdogan (2004)	192	$E_i \approx 10.67 \times V_P - 18.71$	0.90	0.72	3.11 < V_P < 5.6	ROCK/9/4069

Note: σ_{ci} in MPa; E_i in GPa; I_{s50} in MPa; σ_{bt} in MPa; V_P in km/s; n in %.

Table 5.5. Transformation models for rock mass

Model	Literature	n	Transformation model	b	δ	Data restriction / Application range	Calibration database
$E_m - E_i - RQD$	Coon and Merritt (1970)	147	$E_m/E_i = 0.0231 \times RQD - 1.32$	1.26	1.09	57 < RQD < 100	ROCKMass/9/5876
	Zhang and Einstein (2004)	161	$E_m/E_i = 10^{0.0186 \times RQD - 1.91}$	1.54	0.89	0 < RQD < 100	ROCKMass/9/5876
$E_m - RMR$	Bieniawski (1978)	1091	$E_m = 2 \times RMR - 100$	0.57	1.48	50 < RMR < 85	ROCKMass/9/5876
	Gokceoglu et al. (2003)	1749	$E_m = 0.0736 \times e^{0.0755 \times RMR}$	1.53	1.21	20 < RMR < 85	ROCKMass/9/5876
	Serafim and Pereira (1983)	1749	$E_m = 10^{\frac{(RMR-10)}{40}}$	0.51	1.00	20 < RMR < 85	ROCKMass/9/5876
$E_m - Q$	Grimstad and Barton (1993)	288	$E_m = 25 \times log_{10}(Q)$	0.58	0.88	1.1 < Q < 1000	ROCKMass/9/5876
$E_m - GSI$	Hoek and Diederichs (2006)	349	$E_m = 100 \times \frac{(1 - D/2)}{1 + e^{\frac{75+25D-GSI}{11}}}$	0.83 (D = 0)	1.00 (D = 0)	10 < GSI < 100	ROCKMass/9/5876

Note: σ_{ci} in MPa; E_m in GPa; D is disturbance factor (Hoek and Diederichs 2006).

6. Determining characteristic values of geotechnical parameters and resistance: an overview

Zi-Jun Cao, Jianye Ching, Guo-Hui Gao, Mikhail Kholmyansky, Ali Noorzad, Timo Schweckendiek, Johan Spross, Mohammad Tabarroki, Xiaohui Tan, Yu Wang, Tengyuan Zhao, Yan-Guo Zhou (Alphabetical Order)

6.1 Introduction

Determining design values of geotechnical parameters or resistance is indispensable in geotechnical design practice. Depending on design approaches adopted, the design values of geotechnical parameters and resistance are often derived from their respective characteristic values. For example, when partial material factor design methods (e.g., Design Approach 3 in Eurocode 7) are applied, characteristic values of geotechnical parameters are needed while characteristic values of geotechnical resistance (e.g., pile compressive resistance) are used in resistance factor design methods (e.g., Design Approach 2 in Eurocode 7) (CEN 2004; Orr 2017). Selection of characteristic values of geotechnical parameters and resistance is an intriguing issue and has attracted much attention (e.g., Schneider 1997; Hicks and Samy 2002; Honjo 2009; Schneider and Schneider 2013; Hicks 2013; Orr 2000, 2017; Wang et al. 2017; Zhao et al. 2018; Shen et al. 2019; Hicks et al. 2019; Prästings et al. 2019; van der Krogt et al. 2019; Ching et al. 2020; Tabarroki et al. 2020; Länsivaara et al. 2020). Despite these efforts, the ways of determining the characteristic values of geotechnical parameters and resistance remain debatable. A diversity of definitions and selection methods of characteristic values of geotechnical parameters and resistance can be found in the geotechnical literature and national (or regional) design codes with consideration of various factors. For example, in Eurocode 7, Clause 2.4.5.2(4)P lists the following six factors that shall be taken into account for selection of characteristic values of geotechnical parameters:

- *geological and other background information, such as data from previous projects;(F1)*
- *the variability of the measured property values and other relevant information, e.g. from existing knowledge; (F2)*
- *the extent of the field and laboratory investigation; (F3)*
- *the type and number of samples; (F4)*
- *the extent of the zone of ground governing the behaviour of the geotechnical structure at the limit state being considered; (F5)*
- *the ability of the geotechnical structure to transfer loads from weak to strong zones in the ground. (F6)*

Note that the "*F1*"-"*F6*" in parentheses following each item are added by authors of this report for the convenience of discussions. The above six factors include aspects on prior knowledge (*F1* and *F2*), spatial variability and statistical uncertainties (*F2* and *F3*), data quantity and quality (*F4*), and limit state & response of the geotechnical structure (*F*5 and *F6*). Although some of these aspects may have been considered in other national (or regional) geotechnical codes as well, definitions of

characteristic values are often worded to avoid being too prescriptive, allowing geotechnical engineers to exercise their engineering judgment and experience to select characteristic values at a site in a subjective way. Nevertheless, it has been observed that such a subjective reasoning might result in a wide spread of selected characteristic values for a given set of site investigation data (Bond and Harries 2008; Orr 2017). Differences between engineers' subjective estimates of characteristic values can be attributed to differences in their level of expertise obtained from their educational background, differences in deliberate practices, as well as various cognitive biases and limitations (Vick 2002; Cao et al. 2016).

Alternatively, statistical methods can be employed in selection of characteristic values of geotechnical parameters and resistance. Several statistical methods have been developed in the literature. To facilitate the understanding and selection of these methods, this report presents an overview on existing statistical methods of determining characteristic values of geotechnical parameters and resistance. The overview covers both frequentist and Bayesian formulas to calculate characteristic values of geotechnical parameters. Frequentist and Bayesian schools assert different interpretations of probability, i.e., relative frequency versus degrees-of-belief (e.g., Vrouwevelder 2002; Baecher and Christian 2003). This leads to the use of different probabilistic terminologies in practice, such as "confidence interval" in frequentist approaches versus Bayesian "credibility interval". Nevertheless, this report will not strictly pursue the implication of the difference in frequentistic and Bayesian interpretations of probability since frequentist probability axioms are identical to Bayesian probability axioms. This allows interchangeably implementing frequentist and Bayesian approaches in practice, e.g., statistics estimated from Bayesian approaches can be used in frequentist formulas to calculate the characteristic values.

6.2 Definition of characteristic values of geotechnical parameters and resistance

Tables 6.1 and 6.2 summarize, respectively, definitions of characteristic values of geotechnical parameters and resistance in geotechnical design codes (including Eurocodes, CHBDC in Canada, ASSHTO LRFD BDS in USA, Australia Standard, and CIGE in China) and the literature. A glance reveals that these definitions are far from a clear cut. Canadian Foundation Engineering Manual (CFEM) (CGS 2006), AASHTO LRFD BDS (i.e., AASHTO 2017), Australian Standard AS5100.3 (SA 2004), and CIGE (MOHURDPRC 2009) incorporate the conservatism into selection of characteristic values, X_k, of geotechnical parameters. Eurocode 7 (CEN 2004) and CHBDC 2019 (CSA 2019) share a similar definition of X_k that considers both the conservatism (i.e., "*a cautious estimate*") and physical mechanism (i.e., "*affecting the occurrence of the limit state*" and "*within the zones of influence of applied loads*"). Moreover, Eurocode 7 distinguishes two scenarios involving global and local failures, for which the zones of ground affect the behavior of geotechnical structures at the limit state are of different sizes with respect to the scale of fluctuation (SOF) of geotechnical parameters (e.g., Frank 2004; Orr 2017; Prästings et al. 2019). For the global failure scenario with a size of the influence zone much greater than the SOF, the X_k should be a cautious

estimate of the mean value within the influence zone affecting the occurrence of limit state. The influence zone can be a surface or volume of ground, depending on the design problems concerned. For the local failure scenario with a size of the influence zone smaller than the SOF, the X_k should be taken as a cautious estimate of the lowest or highest value within the influence zone. These considerations highlight the significant role of geotechnical spatial variability and its interaction with ground mechanical responses in selection of characteristic geotechnical parameters.

Table 6.1. Definition of characteristic values of geotechnical parameters

Sources	Clause	Definition
EN 1997-1 (CEN 2004)	2.4.5.2(4)P	The characteristic value of a geotechnical parameter shall be selected as a cautious estimate of the value affecting the occurrence of the limit state.
	2.4.5.2(11)	If statistical methods are used, the characteristic value should be derived such that the calculated probability of a worse value governing the occurrence of the limit state under consideration is not greater than 5%. NOTE In this respect, a cautious estimate of the mean value is a selection of the mean value of the limited set of geotechnical parameter values, with a confidence level of 95%; where local failure is concerned, a cautious estimate of the low value is a 5% fractile.
CHBDC 2019 (CSA 2019)	6.2	**Characteristic geotechnical parameter** — a cautious estimate of the mean value of a geotechnical parameter for individual strata within the zones of influence of applied loads.
CFEM (CGS 2006)		Frequently, the mean value, or a value slightly less than the mean is selected by geotechnical engineers as the characteristic value.
AS5100.3 (SA 2004)		the characteristic value of a geotechnical parameter should be a conservatively assessed value of the parameter
AASHTO LRFD BDS (AASHTO 2017)	C10.4.6.1	For strength limit states, average measured values of relevant laboratory test data, in situ test data, or both were used to calibrate the resistance factors…it may not be possible to reliably estimate the average value of the properties needed for design. In such cases, the Engineer may have no choice but to use a more conservative selection of design parameters to mitigate the additional risks created by potential variability or the paucity of relevant data.
CIGE (MOHURDPRC 2009)	2.1.13	Representative value of geotechnical parameters and it usually taken as the 5% quantile value.

Table 6.2. Definition of characteristic values of geotechnical resistance

Sources	Clause	Definition
EN 1997-1 (CEN 2004)	7.6.2.2(7)P	When deriving the ultimate characteristic compressive resistance $R_{c;k}$ from values $R_{c;m}$ measured in one or several pile load tests, an allowance shall be made for the variability of the ground and the variability of the effect of pile installation.
	8.4(10)P	For grouted anchorages and screw anchorages, the characteristic value of the pull-out resistance, $R_{a;k}$, shall be determined on the basis of suitability tests according to 8.7 or comparable experience. The design resistance shall be checked by acceptance tests after execution.
	8.5.2(3)	The characteristic value should be related to the suitability test results by applying a correlation factor ξ_a. NOTE 8.5.2(3) refers to those types of anchorage that are not individually checked by acceptance tests. If a correlation factor ξ_a is used, it must be based on experience or provided for in the National annex.
CHBDC 2019 (CSA 2019)	6.2	**Serviceability geotechnical resistance** — the load that the ground can support at serviceability limit states, usually at a predefined deformation in the ground or structure, estimated using characteristic geotechnical parameters; **Ultimate geotechnical resistance** — the maximum load that the ground can support at ultimate limit states, estimated using characteristic geotechnical parameters.
NBCC User's Guide (NRC 2011)	Commentary K	the [characteristic] resistance is the engineer's best estimate of the ultimate resistance
NCHRP Report 507(Paikowsky et al. 2004)		The nominal values (e.g., the nominal strength, R_n) are those calculated by the specific calibrated design method and are not necessarily the means (i.e., the mean loads or mean resistance (Figure 1).
AASHTO LRFD BDS (AASHTO 2017)	10.6.3.1.2a	The nominal bearing resistance shall be estimated using accepted soil mechanics theories and should be based on measured soil parameters. The soil parameters used in the analyses shall be representative of the soil shear strength under the considered loading and subsurface conditions..
	10.6.3.2.2	The nominal bearing resistance of rock should be determined using empirical correlation with the Geomechanics RMR system. Local experience shall be considered in the use of these semi-empirical procedures.
	10.6.3.2.3	The nominal bearing resistance of foundations on rock shall be determined using established rock mechanics principles based on the rock mass strength parameters. The influence of discontinuities on the failure mode shall also be considered.

Characteristic values of geotechnical resistance are needed in resistance factor design approaches (e.g., Design Approach 2 in Eurocode 7 and LRFD in North America). It shall be pointed out that, in some design codes (e.g., ASSHTO LRFD BDS), the terminology "nominal resistance" is used in lieu of "characteristic resistance" while it is also included in this report because it plays the same role of "characteristic resistance" in design calculations. Fenton et al. (2016) summarized definitions of characteristic geotechnical resistance in geotechnical design codes, including Eurocodes, CHBDC, NBCC, ASSHTO LRFD BDS, and Australian Standard. In general, with design calculation models, the characteristic geotechnical resistance can be calculated based on characteristic values of geotechnical parameters. Fenton et al. (2016) observed different degrees of conservatism in characteristic geotechnical resistance adopted in Eurocodes and North American design codes. Eurocode 7 also allows deriving characteristic values of pile resistances from load test results and soil test profiles and pull-out resistance of anchors from the suitability test results by applying correlation factors (e.g., Bauduin 2002; Orr 2017).

6.3 Methods of determining characteristic values of geotechnical parameters

An overview of existing statistical methods of determining characteristic values of geotechnical parameters give two observations:

- Different methods may be developed based on probability distributions of different random variables, such as the basic variable X (e.g., soil shear strength parameters), statistical mean (X_m), spatial average (X_A), and effective (or mobilized) property (X_E) of X within influence zones;
- Sophistication of different methods varies in a wide spread to account for different uncertainty sources, as discussed below.

6.3.1 Characteristic value based on the probability distribution of the basic random variable

Assume that the basic random variable X that represents an uncertain geotechnical parameter follows a Gaussian distribution. If Gaussian distribution parameters can be determined based on unlimited test results, the X_k can be calculated as:

$$\text{MP1:}\quad X_k = \mu_X - N_{95}\sigma_X = \mu_X(1 - N_{95}V_X) \tag{6.1}$$

where μ_X, σ_X, and V_X ($=\sigma_X/\mu_X$) are the mean value, standard deviation, and coefficient of variation of X, respectively; and N_{95} = 1.645. Eq. (6.1) gives the point estimate of 5% quantile of the Gaussian random variable X as the characteristic value. It accounts for the uncertainty in estimated value of X in a gross manner. Neither statistical uncertainty nor spatial averaging are considered by Eq. (6.1). In this report, methods for determining characteristic values of geotechnical parameters and resistance are denoted by "MP#" and "MR#", respectively, which will not be defined again in the remaining part of this report. Moreover, most of the methods summarized in this report provide formulas to calculate the characteristic values based on the Gaussian assumption. When the

coefficient of variation is large, it is more appropriate to assume the lognormal distribution to avoid negative values. It is straightforward to extend Gaussian-based formulas to obtain formulas for the lognormal distribution. This report will give lognormal counterparts of some methods for illustration, but not provide all of them for the sake of conciseness.

6.3.2 Characteristic value considering the statistical uncertainty

With a limited number of test data, it is impossible to determine the statistics (i.e., mean value and standard deviation) of X with complete certainty. Statistical uncertainty is unavoidable. Hence, the statistics (e.g., mean value X_m) of X are random variables themselves. Depending on whether the standard deviation (i.e., σ_X) of X is known or not, a different type of distribution should be adopted (JGS 2004; DNV 2010; ISO2394 2015). When the σ_X is known or assumed based on the prior knowledge, the normal distribution is adopted. For the global failure scenario, the X_k can be taken as the 5% factile of X_m:

$$\text{MP2:}\quad X_k = X_m - N_{95}\frac{\sigma_X}{\sqrt{n}} = X_m\left(1 - N_{95}\frac{V_X}{\sqrt{n}}\right) \tag{6.2a}$$

where n is the number of test data. For the local failure scenario, the X_k can be taken as the 5% factile of X with the consideration of the statistical uncertainty in X_m, i.e.,

$$\text{MP3:}\quad X_k = X_m - N_{95}\sqrt{1+\frac{1}{n}}\sigma_X = X_m\left(1 - N_{95}\sqrt{1+\frac{1}{n}}V_X\right) \tag{6.2b}$$

When the σ_X is unknown, the Student's t-distribution is adopted. Similarly, for the global failure scenario, the X_k can be taken as the 5% factile of X_m:

$$\text{MP4:}\quad X_k = X_m - t_{95,n-1}\frac{S_X}{\sqrt{n}} = X_m\left(1 - t_{95,n-1}\frac{V_X}{\sqrt{n}}\right) \tag{6.3a}$$

where S_X is the sample estimate of standard deviation; $t_{95,n-1}$ is a Student's-t factor evaluated for a 95% confidence level and n-1 degrees of freedom. For the local failure scenario, the X_k can be taken as the 5% factile of X with the consideration of the statistical uncertainty in X_m, i.e.,

$$\text{MP5:}\quad X_k = X_m - t_{95,n-1}\sqrt{1+\frac{1}{n}}S_X = X_m\left(1 - t_{95,n-1}\sqrt{1+\frac{1}{n}}V_X\right) \tag{6.3b}$$

Although the X_k given by MP2 and MP4 are defined based on the distribution of X_m with a 95% confidence level, different confidence levels can be applied to represent different degrees of conservatism. For example, in Russian Code of Practice (e.g., SP 22.13330.2016; SP 23.13330.2018), 95% confidence level is used to selecting characteristic values for design verification of ultimate limit states using MP4 while 85% confidence level is adopted for serviceability limit states.

For considerations of practical implementations, Schneider (1997) proposed the following simple formula based on MP2 and MP4:

$$\text{MP6:}\quad X_k = X_m(1-\frac{V_X}{2}) \tag{6.4}$$

The MP6 generally provides a good, but slightly conservative, approximation to MP2 for $n > 10$ and MP4 for $n > 13$. Similarly, CIGE of China (MOHURDPRC 2009) provides another approximate formula of MP4 to avoid the misuse of Student's-t factor when n is relatively small:

$$\text{MP7:}\quad X_k = X_m[1-(\frac{1.704}{\sqrt{n}}+\frac{4.678}{n^2})V_X] \tag{6.5}$$

MP7 gives the same X_k value as MP6 for $n = 13$. MP2-MP7 account for the statistical uncertainty in X_m, which is indicated by the number, n, of test results in the formulas. For illustration, Figure 6.1 compares characteristic values calculated from MP1-MP7 based on prescribed values of $\mu = 30$, $\sigma_X = 6$, $X_m = 27.68$, $S_X = 7.37$, $V_X = 0.27$, and $n = 16$, among which X_m, S_X, and V_X are estimated from 16 random samples of a Gaussian random variable with $\mu = 30$ and $\sigma_X = 6$. It is shown that the MP2, MP4, MP6, and MP7 for the global failure scenario give higher characteristic values than MP3 and MP5 for the local failure scenario and MP1 with unlimited test results.

While spatial variability and averaging will be the focus of the methods discussed in the next section, it is important to notice that spatial averaging is already involved in the methods eluded on hitherto. The implicit assumption for the global failure scenario addressed by MP2 and MP4 (and to some degree MP6 and MP7) is that all spatial variability averages. Hence, for the global failure scenario, only the statistical uncertainty in the spatial average is considered. For the local failure scenario addressed by MP3 and MP5, on the other hand, the implicit assumption is that no averaging at all occurs, and that the lowest ground property value in the considered volume governs the failure behavior of the geotechnical structure. These two extremes are in fact the upper and lower bound cases for the more sophisticated treatment of spatial averaging discussed in the next section.

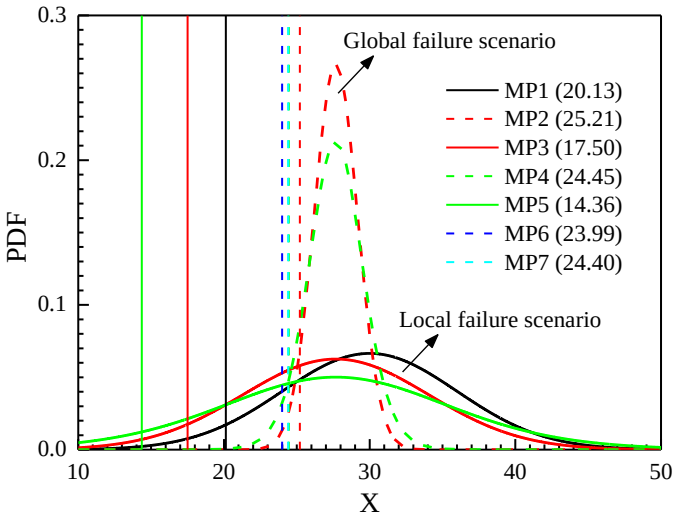

Figure 6.1. Comparison of characteristic values calculated from MP1-MP7

6.3.3 Characteristic value based on the probability distribution of the spatial average

The size of influence zones affecting geotechnical structure responses can be much larger than that involved in-situ and/or laboratory tests. It is more appropriate to consider the spatial average of geotechnical parameters over the influence zone of geotechnical structure responses than their values at a point (or testing) level (Vanmarcke 1977). The estimate of the spatial average, X_A, of X may also be affected by other uncertainty sources arising during site investigation, such as measurement errors, statistical uncertainty, and transformation uncertainty. Its total coefficient of variation, V_{TOT}, can be written as (Phoon and Kulhawy 1999):

$$V_{TOT} = \sqrt{\Gamma_I^2 V_I^2 + V_M^2 + V_T^2 + V_S^2} \tag{6.6}$$

where Γ_I^2 is the variance reduction function quantifying the extent of reduction in variance due to spatial averaging (Vanmarcke 1977); V_I, V_M, V_T, and V_S are coefficients of variation representing inherent spatial variability, measurement errors, transformation uncertainty, and statistical uncertainty, respectively. Note that Eq. (6.6) is based on an additive uncertainty model, by which the total uncertainty is attributed to inherent spatial variability ε_I, measurement errors ε_M, transformation uncertainty ε_T, and statistical uncertainty ε_S, and these uncertainties are assumed to be independent. Herein, the definition of V_I, V_M, V_T, and V_S is non-traditional in the sense that they are defined as the ratio of their respective standard deviations over the mean value of X, rather than their respective mean values that are usually equal to zero. Moreover, when calibrating a design code, the code writer shall define which uncertainty sources are included in characteristic values and which are considered by partial factors. For example, if V_T has been considered in calibration of partial factors, it can be set to zero in Eq. (6.6), to avoid accounting for it more than once during the design process.

For a separable correlation function, the Γ_I^2 can be written as (e.g., Vanmarcke 2010; Schneider and Schneider 2013; Orr 2017):

$$\Gamma_I^2 = \Gamma_X^2 \Gamma_Y^2 \Gamma_Z^2 \tag{6.7}$$

where Γ_i^2, $i = X, Y, Z$ are the respective variance reduction functions in the two horizontal directions (X and Y) and the vertical direction (Z), and the Γ_i^2 can be approximately calculated as (Schneider and Schneider 2013; Orr 2017):

$$\Gamma_i^2 = \left(\delta_i / L_i\right)\left[1 - \left(\delta_i / 3L_i\right)\right] \quad \text{for} \quad L_i > \delta_i \tag{6.8}$$

$$\Gamma_i^2 = 1 - \left(\delta_i / 3L_i\right) \quad \text{for} \quad L_i \le \delta_i \tag{6.9}$$

where δ_i, $i = X, Y, Z$ is the scale of fluctuation (SOF) in the i direction; L_i is the length of the influence zone along the i direction.

Depending on the value of V_{TOT}, Schneider and Schneider (2013) suggested the normal and lognormal distributions of X_A, based on which the X_k can be calculated as the 5% quantile of X_A:

MP8: $X_k = X_m\left(1 - N_{95} V_{TOT}\right)$ for $V_{TOT} < 0.3$, Normal distribution (6.10a)

MP9: $X_k = X_m \cdot \dfrac{0.2^{\sqrt{\ln(1+V_{TOT}^2)}}}{\sqrt{1+V_{TOT}^2}}$ for $V_{TOT} \ge 0.3$, Lognormal distribution (6.10b)

As indicated by Eqs. (6.8)-(6.10), MP8 and MP9 account for not only various uncertainties in estimated X_A (i.e., *F2* and *F3*) but also "*the extent of the zone of ground governing the behavior of the geotechnical structure at limit state*" (i.e., *F5*). Van der Krogt et al. (2019) observed that Eq. (6.6) assumes that the measurement errors, statistical uncertainty, and transformation uncertainty are systematic errors that are not subject to spatial averaging. This assumption is conservative since it leads to overestimation of V_{TOT}. They also demonstrated that considering the spatial averaging of measurement errors and transformation uncertainty may lead to further reduction in uncertainty, resulting in a higher characteristic value. It is noteworthy that Ching et al. (2016) presented some real cases showing that transformation uncertainty is indeed not subjected to spatial averaging.

By ignoring measurement errors, statistical uncertainty, and transformation uncertainty, MP8 and MP9 can be simplified as:

MP10: $X_k = X_m\left(1 - N_{95} V_I \Gamma_I\right)$ for $V_I < 0.3$, Normal distribution (6.11a)

MP11: $X_k = X_m \dfrac{0.2^{\sqrt{\ln(1+V_I^2 \Gamma_I^2)}}}{\sqrt{1+V_I^2 \Gamma_I^2}}$ for $V_I \geq 0.3$, Lognormal distribution (6.11b)

Similarly, an evolution committee of CEN proposed another simplified formula (Orr 2017):

MP12: $X_{\mathrm{k}} = X_m - a(X_m - X_{extr})\sqrt{\delta_Z / L_Z}$ (6.12)

where X_{extr} is the expected extreme value of X given a large number of tests; a can be taken as 0.5, 0.75, and 1.0, reflecting the extent and quality of field and laboratory investigations or estimation method, type of tests for selecting derived values, and sampling methods and levels of experience (Orr 2017). Assume the X_{extr} is smaller than X_m by 3 times of standard deviation, and δ_Z is taken as a typical value of 1m. Then, MP12 is re-written as:

MP13: $X_{\mathrm{k}} = X_m - 3aS_X\sqrt{1/L_Z} = X_m(1-3aV_X\sqrt{1/L_Z})$ (6.13)

Shen et al. (2019) performed a comparative study on MP1, MP4, MP6, MP11, and MP13 from a perspective of design robustness. Based on the comparative study, the following formula for calculating X_k was proposed:

MP14: $X_{\mathrm{k}} = X_m(1-AV_X)$ (6.14)

Shen et al. (2019) commented that the optimal value of A in Eq. (6.14) depends on many factors, such as the preference in a trade-off consideration (e.g., cost versus robustness), the cost function in local practice, the level of variation of the noise factors (including the effect of spatial variability), and the "calculated risk", and they suggested a value of a =0.7, with which Eq. (6.14) has the same format as MP6 suggested by Schneider (1997), but more conservative.

6.3.4 Characteristic value based on the Bayesian theory

All the above formulas for the characteristic value are frequentist ones. Ching et al. (2021) derive the Bayesian formulas for the characteristic value. The derivations assume that both μ_X and σ_X^2 are unknown and follow a prior probability density function (PDF) that is normal-inverse-gamma. If the prior PDF is non-informative, Ching et al. (2021) show that:

MP15: $X_k = X_m\left(1-t_{95,n-1}\sqrt{\Gamma_I^2V_I^2+V_S^2+V_T^2+V_M^2/n}\right)$ for normal distribution (6.15a)

MP16: $X_k = \left(\prod_{i=1}^{n} X_i\right)^{1/n} \times e^{-t_{95,n-1}\sqrt{\Gamma_I^2V_I^2+V_S^2+V_T^2+V_M^2/n}}$ for lognormal distribution (6.15b)

Herein, it is necessary to distinguish V_X and V_I in this report. The V_I denotes the coefficient of

variation of the inherent spatial variability, but the V_X in MP1-MP7, MP13, and MP14 represents the coefficient of variation of X estimated from data without distinguishing different uncertainty sources. Moreover, the V_{TOT} is the coefficient of variation of the total uncertainty with explicit quantification of different uncertainty sources (i.e., ε_I, ε_M, ε_T, and ε_S).

6.3.5 Characteristic value based on responses of geotechnical structures in spatial variability

In terms of the ultimate limit state (ULS), effects of spatial variability on the response of the geotechnical structure are two-fold: the spatial averaging effect that results in the uncertainty reduction, and the weak-path effect that seeks out the failure mechanism with the least resistance and causes the reduction in the mean value of the effective or mobilized shear strength (Hicks and Samy 2002; Hicks 2013; Ching and Phoon 2013; Hu and Ching 2015; Ching et al. 2016, 2017). The effective or mobilized property, X_E, is defined as the homogeneous property that gives the same response (e.g., factor of safety, FS) as the response with explicit modelling of the spatial variability. The former factor (spatial averaging) has been considered by MP8-MP13, MP15 and MP16, but the latter factor (weak path) has not been considered. Hicks and Samy (2002) and Hicks (2013) proposed to select geotechnical characteristic parameters based on the random finite element method (RFEM) (Fenton and Griffiths 2008), which is referred to as the "MP17" in this report. The MP17 provides reliability-based characteristic values either based on the probability distribution of X_E or, equivalently, by back-calculating the quantile of X from 5% fractile of FS determined from the RFEM. Detailed implementation procedures of MP17 are not repeated here, which can be referred to Hicks and Samy (2002), Hicks (2013), and Hicks et al. (2019).

The MP17 successfully considers both the spatial averaging effect and the weak-path effect. Nevertheless, it requires RFEM, which is not trivial for geotechnical practitioners. To address this issue, Ching and Phoon (2013), Hu and Ching (2015), and Ching et al. (2016, 2017) proposed a weakest-path model (WPM) to model X_E. Based on the WPM, the X_E is modeled as the minimum of the X_A values along a number, n_s, of independent representative potential slip curves (RPSCs), i.e., $X_E = min(X_{A,1}, X_{A,2}, \ldots, X_{A,ns})$, where $X_{A,i}$, i = 1, 2., n_s denotes the spatial average of X along the i-th RPSC. However, Ching and Phoon (2013), Hu and Ching (2015), and Ching et al. (2016, 2017) called X_E as the mobilized strength rather than the effective strength, although the two terms are equivalent. Tabarroki et al. (2020) further calibrated the WPM by X_E values simulated by RFEM and developed the simplified formula for the 5% fractile of X_E, defined as the mobilization-based characteristic value, X_k^{mob}, and referred to as "MP18" and "M19" in this report:

MP18: $$X_k^{mob} = X_m \times \left(1 + \alpha_{5\%} \Gamma_I V_{TOT}\right) \quad \text{for Normal distribution} \qquad (6.16a)$$

MP19: $$X_k^{mob} = X_m \times \exp\left(\alpha_{5\%} \times \sqrt{\ln\left[1 + \Gamma_I^2 V_{TOT}^2\right]}\right) \Big/ \sqrt{1 + \Gamma_I^2 V_{TOT}^2} \quad \text{for Lognormal distribution} \qquad (6.16b)$$

where $\alpha_{5\%}$ is the 5% fractile of the minimum of n_s standard normal random variables, and it can be

calculated as (Tabarroki et al. 2020):

$$\alpha_{5\%} = \Phi^{-1}\left[1-0.95^{1/n_s}\right] \tag{6.17}$$

As indicated by Eq. (6.17), the $\alpha_{5\%}$ is reduced to -1.645 when n_s = 1. The $\alpha_{5\%}$ has been calibrated from RFEM for several geotechnical problems for a scenario of V_X = 0.3 and $\delta_X = 10\times\delta_Z$, as shown in Table 3. The Γ_I in Eq. (6.16) is the variance reduction factor along a classical slip surface. It can be determined by Eqs. (6.8) and (6.9) with L = the length of the classical slip surface and δ_L = SOF along the classical slip surface, which can be approximately estimated as (Vanmarcke 1977):

$$\delta_L \approx \left[\left(\frac{\Delta x}{\Delta x+\Delta z_1+\Delta z_2}\right)\times\frac{1}{\delta_X}+\left(\frac{\Delta z_1+\Delta z_2}{\Delta x+\Delta z_1+\Delta z_2}\right)\times\frac{1}{\delta_Z}\right]^{-1} \tag{6.18}$$

where Δz_1, Δz_2, and Δx are the length of segments approximating the classical slip surface, e.g., see Figure 6.2 for the footing foundation. Note that characteristic values derived from MP17-MP19 correspond to the 5% quantile of the geotechnical structure response while the characteristic values derived from MP1-MP16 refer to the 5% quantile of a single soil parameter. This makes a huge difference for multi-layered and multi-variate problems, as discussed later.

Table 6.3. Equations for $\alpha_{5\%}$ for different problems (source: Tabarroki et al. 2020)

Problem	**Type of slip curve**	**$\alpha_{5\%}$ (for V_X = 0.3 and $\delta_X = 10\times\delta_Z$)**
Soil column subjected to axial loading	Slip curve is lowly constrained	$\alpha_{5\%} = -0.48\times(\delta_L/L)^{-0.36}-1.645$
Shallow foundation Basal heave stability	Slip curve is intermediately constrained	$\alpha_{5\%} = -0.21\times(\delta_L/L)^{-0.55}-1.645$
Retaining wall	Slip curve is highly constrained	$\alpha_{5\%} = -0.04\times(\delta_L/L)^{-0.87}-1.645$
Friction pile (compressive loading)	Slip curve is fully constrained	$\alpha_{5\%} = -1.645$

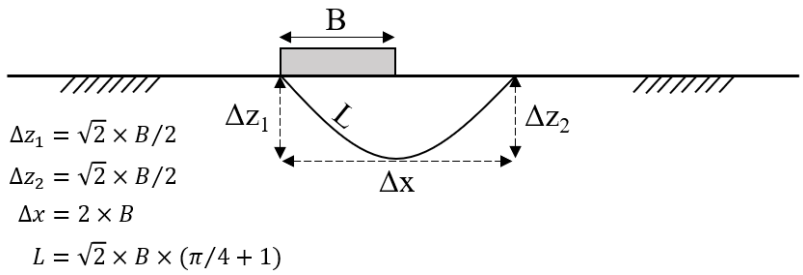

Figure 6.2. Approximation of the classical slip curve for a footing foundation (ϕ=0) (source: Tabarroki et al. 2020)

6.3.6 Characteristic value of the profile of geotechnical parameters over depth

Some geotechnical parameters may exhibit an obvious spatial trend over depth. Such a spatial trend was not considered by MP1-MP19 described previously. For example, if a linear spatial trend is observed, the profile of X over depth can be represented as (e.g., Frank 2004):

$$X = X_m + b\left(z - \overline{z}\right) \tag{6.19}$$

where $\overline{z}$ is the depth of the gravity center of a number, n, of X measurements (i.e., $[x_1, x_2, \ldots, x_n]$) at different depths $z_1, z_2, \ldots, z_n$; X_m is the statistical mean of the n measurements; b is a regression coefficient and represents the slope of the linear trend line over depth. Then, for local and global failure scenarios, the characteristic values, $X_{k,z}$, of X at the depth z can be calculated using the following formulas (e.g., Frank 2004; Prästings et al. 2019):

MP20: $X_{k,z} = \left[X_m + b\left(z - \overline{z}\right)\right] - t_{95,n-2} \times s_{x|z}$ for local failure scenarios (6.20a)

MP21: $X_{k,z} = \left[X_m + b\left(z - \overline{z}\right)\right] - t_{95,n-2} \times s_{\overline{x}|z}$ for global failure scenarios (6.20b)

where $t_{95,n-2}$ is a Student's-t factor evaluated for a 95% confidence level and n-2 degrees of freedom; $s_{x|z}$ and $s_{\overline{x}|z}$ are respective standard deviations of X and its mean value at a depth of z, and they are given by:

$$s_{x|z} = \sqrt{\frac{1}{n-2}\left(1 + \frac{1}{n} + \frac{\left(z - \overline{z}\right)^2}{\sum_{i=1}^{n}\left(z_i - \overline{z}\right)^2}\right)\sum_{i=1}^{n}\left[\left(x_i - X_m\right) - b\left(z_i - \overline{z}\right)\right]^2} \tag{6.21a}$$

$$s_{\overline{x}|z} = \sqrt{\frac{1}{n-2}\left(\frac{1}{n} + \frac{\left(z - \overline{z}\right)^2}{\sum_{i=1}^{n}\left(z_i - \overline{z}\right)^2}\right)\sum_{i=1}^{n}\left[\left(x_i - X_m\right) - b\left(z_i - \overline{z}\right)\right]^2} \tag{6.21b}$$

Determining the characteristic value of the profile of geotechnical parameters over depth can be more challenging if a non-linear spatial trend is exhibited by test data though some methods have been suggested to assess such trends (e.g., Müller et al 2016; Spross and Larsson 2019). This challenge is more profound when only sparse data over depth are obtained from site investigation. Recently, Wang and Zhao (2017) and Zhao et al. (2018) proposed a Bayesian compressive sensing (BCS) approach for probabilistic interpolation of the profile of geotechnical parameters over depth from sparse data. Ching and Phoon (2020) proposed a Bayesian approach that can handle MUSIC-X site investigation data, where M stands for "multivariate", U for "uncertain and unique",

S for "sparse", I for "incomplete", C for "possibly corrupted", and X for "spatially varying". This approach considers both the spatial correlation (correlation among different locations) and cross correlation (cross correlation among different soil properties) when interpolating the profile of geotechnical parameters. These approaches not only provide the expected (or mean) profile of the geotechnical parameter concerned but also give the confidence interval of the estimated profile to quantify its associated uncertainty. The lower bound of the confidence interval can be taken as a quantile profile of the geotechnical parameter. For example, the lower bound of the 90% confidence interval of the estimated profile from BCS corresponds to the 5% quantile profile, which can be taken as the characteristic value over depth. These BCS-based and MUSIC-X methods for determining the profile of the characteristic value are referred to as "MP22" and "MP23" in this report. Detailed algorithms and implementation of BCS and MUSIC-X can be referred to Wang and Zhao (2017), Zhao et al. (2018), Zhao and Wang (2020), Zhao et al. (2020), and Ching and Phoon (2020).

6.3.7 Characteristic value of multiple correlated geotechnical parameters

Geotechnical designs may involve multiple geotechnical parameters as input. A straightforward way to determine multivariate characteristic values is to specify the same fractile (e.g., 5% fractile) for each geotechnical parameter to obtain a vector (i.e., $\underline{X}_k$) of characteristic values of multiple geotechnical parameters (e.g., Tang et al. 2018; Ching et al. 2020). This method, however, does not consider the correlation among geotechnical parameters. Alternatively, multivariate characteristic values can be back-calculated from the cumulative distribution function (CDF) of the performance function concerned in design, which gives reliability-based multivariate characteristic values (e.g., Hicks et al. 2019; Ching et al. 2020). Determining reliability-based multivariate characteristic values often requires probabilistic analyses that may not be familiar to geotechnical practitioners. To address this issue, Ching et al. (2020) proposed a practical approach to determine reliability-based multivariate characteristic values based on the "effective random dimension" (ERD). The ERD characterizes the degree of redundancy of the performance function, and it represents the effective number of independent standard normal random variables that affect the limit state (Ching et al. 2015). Detailed calculations of ERD for a given performance function are referred to Ching et al. (2015, 2020). Based on the ERD, the required η for selecting multivariate characteristic values for the 5% fractile performance is determined as follows:

$$\eta=\Phi\left[-1.645/\sqrt{ERD}\right] \tag{6.22}$$

Varkey et al. (2020) further extended Eq. (22) to account for the spatial averaging effect over the influence zone:

$$\eta=\Phi\left[-1.645\times \Gamma_1/\sqrt{ERD}\right] \tag{6.23}$$

where Γ_I^2 is the variance reduction function quantifying the variance reduction due to spatial averaging over the influence zone. Once η is computed, the characteristic value for each of the multivariate inputs should be taken as its η fractile, rather than the 5% fractile. This method of selecting multivariate characteristic values is referred to as "MP24" in this report.

6.3.8 Characteristic value as an average with qualitative adjustment to factors F1-F6

Rather than trying to address the effect of factors *F1-F6* by calculation, the Swedish Implementation Commission of European Standards in Geotechnics (IEG) introduced a practice where a best-estimate value is adjusted to the relevant features of *F1-F6* through a conversion factor η. This practice utilizes an opening in Eurocode EN 1990, principle 4.2(4)P, which states that "*a conversion factor shall be applied [to the characteristic value] where it is necessary to convert the test results into values which can be assumed to represent the behaviour of the material or product in the structure or the ground*".

For convenience, the Swedish practice redefines the characteristic value so that the conversion factor becomes an integrated part of it:

MP25: $X_k = \eta X_{chosen}$ (6.24)

where X_{chosen} is either a subjective, best-estimate (i.e. non-cautious) mean value, or a calculated mean value, X_m. The X_{chosen} may be a weighted mean value with respect to the accuracy of the used investigation method, e.g. through a multivariate approach (Ching et al. 2010; Prästings et al. 2017). All uncertainty in the characteristic value is consequently assigned to η. The Swedish implementation guidelines to Eurocode 7 (IEG, 2008) defines η as a product of eight sub-factors: $\eta = \eta_1\ \eta_2\ \eta_3\ \eta_4\ \eta_5\ \eta_6\ \eta_7\ \eta_8$. Table 6.4 shows their respective purposes. Each sub-factor η_i has been calibrated by IEG for a large number of combinations of geotechnical structure types and soil types, to address the features of *F2-F6* (while *F1* is addressed by X_{chosen}). The number of possible combinations are extensive and not presented here. Though, to give a brief example, sub-factor η_3 is either 0.9, 0.95, 1.0, 1.05, or 1.1, when evaluating undrained shear strength in a slope stability problem; the selected value depends both on how many different investigation methods that were used and on the judged variability of the results, as detailed in a description for each value.

Typically, the total η would end up between 0.8 and 1.2 for most combinations of geotechnical structures and soil types. Thus, the X_k can notably be larger than X_m, which may seem counterintuitive at first, considering the often expressed need for cautiousness in determining characteristic values. The reason is that the later applied fixed partial factor, γ_M, provides a substantial safety margin when determining the design value ($X_d = X_k / \gamma_M$) and such a large safety margin was not found to be needed for all situations, i.e. in case of very favorable conditions with high-quality geotechnical investigations. By adopting the conversion factor η, IEG managed to

create a flexible framework that allows detailed adjustments to account for *F1-F6*, while still following the Eurocode requirements. The method does however come with a degree of subjectivity, as the selection of some η_i requires engineering judgement. Further details on the Swedish method to determine characteristic values can be found in Prästings et al. (2017; 2019), and in the Swedish implementation guidelines to Eurocode 7 (IEG, 2008) [Swedish only].

Table 6.4. Definition of conversion sub-factors η_i that modifies X_k in the Swedish implementation guidelines to Eurocode 7, and their connection to factors *F1-F6*

η_i	**Definition**	***F1-F6***
η_1	The inherent variability of the material properties	*F2*
η_2	Number of independent measurement points	*F3*
η_3	Uncertainty related to the assessment of soil properties	*F2, F3, F4*
η_4	The location of measurement points in relation to the structure	*F3*
η_5	The extent of the ground zone governing the behaviour of the geotechnical structure at the limit state being considered	*F5*
η_6	The ability of the geotechnical structure to transfer loads from weak to strong zones in the ground	*F6*
η_7	Type of failure mechanism (i.e. ductile or brittle failure)	(-)
η_8	The sensitivity of the material design property on the limit state	(-)

6.4 Methods of determining characteristic values of geotechnical resistance

When resistance factor design methods are applied, the characteristic value, R_k, of geotechnical resistance is needed. It can be estimated from characteristic values of geotechnical parameters using a design calculation model *M*, which can be written as (Bond and Harries 2008):

MR1: $R_k = M(\underline{X}_k)$ (6.25)

Fenton et al. (2016) pointed out that the variability of geotechnical resistance is generally less than the variability of geotechnical parameters at a point level due to spatial averaging, and suggested that the R_k can be evaluated as:

MR2: $R_k = \mu_R / k_R = \mu_R(1-1.645V_R)$ (6.26)

where k_R is the resistance bias factor; μ_R and V_R are the mean value and coefficient of variation of geotechnical resistance, respectively. As indicated by Eq. (6.26), the resistance bias factor k_R (i.e., μ_R/R_k) is equal to $1/(1\text{-}1.645V_R)$. Assuming V_R = 0.15, the k_R is calculated as 1.33 for Design Approach 2 in Eurocode 7 (Fenton et al. 2016). The same k_R was also assumed for Australia by Fenton et al. (2016) while the k_R = 1.1 was assumed in North American design codes (e.g., CHBDC, NBCC, and AASHTO LRFD BDS).

For pile designs, Eurocode 7 also provides correlation factors to determine characteristic values of pile resistance based on static pile load tests, ground test results, and dynamic impact tests.

$$\text{MR3:}\quad R_k = \text{Min}\left\{\frac{R_{mean}}{\xi_i};\frac{R_{min}}{\xi_j}\right\}\quad i = 1, 3, 5 \text{ and } j = 2, 4, 6 \tag{6.27}$$

where R_{mean} and R_{min} are the mean and minimum values of the pile resistance measured from load tests or calculated from ground test results; ξ_1 and ξ_2 are correlation factors to derive characteristic values from static pile load tests; ξ_3 and ξ_4 are correlation factors to derive characteristic values from ground test results; ξ_5 and ξ_6 are correlation factors to derive characteristic values from dynamic impact tests. The values of ξ_1- ξ_6 are provided in Appendix A.3.3.3 of Eurocode 7 (CEN 2004), which are shown in Table 6.5-6.7. Detailed discussions on these correlation factors can be found in Bauduin (2002) and Orr (2017).

Table 6.5. Correlation factors ξ to derive characteristic values from static pile load tests (After CEN 2004)

ξ for n =	1	2	3	4	≥ 5
ξ_1	1.40	1.30	1.20	1.10	1.00
ξ_2	1.40	1.20	1.05	1.00	1.00

Table 6.6. Correlation factors ξ to derive characteristic values from ground test results (After CEN 2004)

ξ for n =	1	2	3	4	5	7	10
ξ_3	1.40	1.35	1.33	1.31	1.29	1.27	1.25
ξ_4	1.40	1.27	1.23	1.20	1.15	1.12	1.08

Table 6.7. Correlation factors ξ to derive characteristic values from dynamic impact tests (After CEN 2004)

ξ for n =	≥ 2	≥ 5	≥ 10	≥ 15	≥ 20
ξ_5	1.60	1.5	1.45	1.42	1.40
ξ_6	1.60	1.35	1.3	1.25	1.25

Table 6.8. Overview of factors (*F1-F6*) addressed by different methods (MP1-MP25) for determining geotechnical characteristic parameters

Methods	***F1***	***F2***	***F3***	***F4***	***F5***	***F6***
MP1	○	◑	○	○	○	○
MP2	○	◑	○	◑	○	○
MP3	○	◑	○	◑	○	○
MP4	○	◑	○	◑	○	○
MP5	○	◑	○	◑	○	○
MP6	○	◑	○	○	○	○
MP7	○	◑	○	◑	○	○
MP8	○	●	◑	◑	◑	○
MP9	○	●	◑	◑	◑	○
MP10	○	●	○	○	◑	○
MP11	○	●	○	○	◑	○
MP12	○	●	○	○	◑	○
MP13	○	●	○	○	◑	○
MP14	○	◑	○	○	○	○
MP15	◑	●	◑	◑	◑	○
MP16	◑	●	◑	◑	◑	○
MP17	◑	●	◑	◑	●	●
MP18	○	●	◑	◑	●	○
MP19	○	●	◑	◑	●	○
MP20	◑	●	●	◑	○	○
MP21	◑	●	●	◑	○	○
MP22	●	●	●	◑	○	○
MP23	●	●	●	●	○	○
MP24	◑	●	◑	◑	●	○
MP25	◑	◑	◑	◑	◑	◑

Note: ●: Addressed; ◑ Partially addressed; ○: Not addressed

6.5 Summary

This report provides an overview of statistical methods of determining characteristic values of geotechnical parameters and resistance. Definitions of characteristic values of geotechnical parameters and resistance in geotechnical design codes (including Eurocodes, CHBDC in Canada, ASSHTO LRFD BDS in USA, Australia Standard, and CIGE in China) and the literature were summarized in Tables 6.1 and 6.2. These definitions of geotechnical characteristic values are often worded to avoid being too prescriptive. This provides flexibility to geotechnical engineers to select characteristic values of geotechnical parameters and resistance for a specific project by exercising their engineering judgment and experience in a subjective way.

Statistical methods (including frequentist and Bayesian approaches) allow determining characteristic values of geotechnical parameters (e.g., MP1-MP25) and resistance (e.g., MR1-MR3) in a quantifiable way. The MP1-MP19 were developed based on distributions of different random variables (including basic random variable X, statistical mean X_m, spatial average X_A, and effective or mobilized property X_E). The MP20-MP23 can be used to determine the profile of characteristic geotechnical parameters over depth, and the MP24 gives the characteristic values of multiple parameters with consideration of cross-correlation among them. Characteristic values derived from MP1-MP16 and MP20-MP22 refer to the 5% quantile of a single soil parameter or its profile over depth, and MP23 (MUSIC-X method) is able to give the profiles of multivariate characteristic values as the same quantile of multiple soil parameters. In contrast, the characteristic values calculated by MP17-MP19 and MP24 correspond to the 5% quantile of the geotechnical structure response. The MP1-MP24 were developed based on different assumptions considering different uncertainties in estimated geotechnical parameters, and some factors among *F1-F6* mentioned in Eurocode 7, Clause 2.4.5.2(4)P were taken into account, as summarized in Table 6.8.

The MP17 and MP25 were found to be the only methods that are able to address all the six factors. For MP17 this is thanks to the prominent flexibility of uncertainty and deterministic modelling provide by RFEM. Nevertheless, it shall be pointed out that, in practice, whether characteristic values derived from MP17 account for all the six factors is a matter of detailed modelling in implementation. MP25 addresses the factors *F1-F6* in a more qualitative way through a combination of many pre-calibrated conversion factors, which are provided to the engineer in a large number of tables. While less mathematically rigorous than many of the other methods, MP25 provides a straightforward way for the practicing engineer to account explicitly for all aspects *F1-F6*.

As for characteristic geotechnical resistance, it can be calculated either from characteristic values of geotechnical parameters using a design calculation model (i.e., MR1) or by applying the resistance bias factor (i.e., MR2). Eurocode 7 also provides correlation factors to determine characteristic pile resistances based on static pile load tests, ground test results, and dynamic impact tests (i.e., MR3).

6.6 References

American Association of State Highway and Transportation Officials (AASHTO). (2017). LRFD Bridge Design Specifications. Washington, D.C.

Baecher, G. B. and Christian, J. T. (2003). Reliability and Statistics in Geotechnical Engineering, John Wiley & Sons, Hoboken, New Jersey, 605p.

Bauduin, C. (2002). “Design of Axially Loaded Piles According to Eurocode 7.” Paper presented at the proceedings 5th international conference on Piling and Deep Foundations, DFI, Nice, Presses de L’ENPC, Paris, June.

Bond, A., Harris, A., (2008). Decoding Eurocode 7. Taylor & Francis, London and New York.

Canadian Geotechnical Society (CGS). (2006). Canadian foundation engineering manual. 4th ed. Montreal, Quebec.

Cao, Z., Wang, Y., & Li, D. (2016). Quantification of prior knowledge in geotechnical site characterization. Engineering Geology, 203, 107-116.

Ching, J., Cao, Z. J., Spross, J., Schweckendiek, T. (2021). Bayesian formulas for the characteristic value in Eurocode 7, in preparation.

Ching, J., Wu, T.J., and Phoon, K.K. (2016). Spatial correlation for transformation uncertainty and its applications, Georisk: Assessment and Management of Risk for Engineered Systems and Geohazards, 10(4), 294-311.

Ching, J., Phoon, K. K., Chen, K. F., Orr, T. L., & Schneider, H. R. (2020). Statistical determination of multivariate characteristic values for Eurocode 7. Structural Safety, 82, 101893.

Ching, J., Phoon, K. K., & Sung, S. P. (2017). Worst case scale of fluctuation in basal heave analysis involving spatially variable clays. Structural Safety, 68, 28–42.

Ching, J., Phoon, K. K., & Chen, Y. C. (2010). Reducing shear strength uncertainties in clays by multivariate correlations. Canadian Geotechnical Journal, 47(1), 16-33.

Ching, J., Lee, S. W., & Phoon, K. K. (2016). Undrained strength for a 3D spatially variable clay column subjected to compression or shear. Probabilistic Engineering Mechanics, 45, 127–39.

Ching, J. Y., Phoon, K. K., & Yang, J. J. (2015). Role of redundancy in simplified geotechnical reliability-based design - A quantile value method perspective. Structural Safety, 55, 37-48.

Ching, J., & Phoon, K. K. (2013). Probability distribution for mobilized shear strengths of spatially variable soils under uniform stress states. Georisk: Assessment and Management of Risk for Engineered Systems and Geohazards, 7(3), 209–24.

Ching, J. and Phoon, K.K. (2020). Constructing a site-specific multivariate probability distribution using sparse, incomplete, and spatially variable (MUSIC-X) data. ASCE Journal of Engineering Mechanics, 146(7), 04020061.

Canadian Standards Association (CSA). (2019). Canadian Highway Bridge Design Code (CHBDC). CAN/CSA-S6:19, Mississauga, Ont.

DNV. (2010). Statistical Representation of Soil Data. http://www.dnv.com.

European Committee for Standardization (CEN). (2004). EN 1997-1 Eurocode 7: Geotechnical design – Part 1: General rules. Brussels.

Fenton, G.A. and Griffiths, D.V. (2008). Risk Assessment in Geotechnical Engineering. Hoboken, N.J., John Wiley & Sons.

Fenton, G. A., Naghibi, F., Dundas, D., Bathurst, R. J., & Griffiths, D. V. (2016). Reliability-based geotechnical design in 2014 Canadian Highway Bridge Design Code. Canadian Geotechnical Journal, 53(2), 236-251.

Frank R., Bauduin C., Driscoll R., Kavvadas M., Krebs Ovesen N., Orr T., & Schuppener B. (2004). Designer's Guide to EN 1997-1 Eurocode 7: Geotechnical design – general rules. Thomas Telford Publishing, Thomas Telford Ltd, 1 Heron Quay, London E14 4JD.

Hicks, M. A., Varkey, D., van den Eijnden, A. P., de Gast, T., & Vardon, P. J. (2019). On characteristic values and the reliability-based assessment of dykes. Georisk: Assessment and Management of Risk for Engineered Systems and Geohazards, 13(4), 313-319.

Hicks, M.A. (2013). An explanation of characteristic values of soil properties in Eurocode7. In Modern geotechnical design codes of practice: implementation, application, and development. Edited by P. Arnold, G.A. Fenton, M.A. Hicks, T. Schweckendiek, and B. Simpson. Advances in Soil Mechanics and Geotechnical Engineering, IOS Press, pp. 277–294.

Hicks, M. A., & Samy, K. (2002). Reliability-based characteristic values: a stochastic approach to Eurocode 7. Ground Engineering, 35(12).

Honjo, Y. (2009). General vs. Local RBD and Determination of Characteristic Values. In Contemporary Topics in In Situ Testing, Analysis, and Reliability of Foundations (pp. 395-402).

Hu, Y. G., & Ching, J. (2015). Impact of spatial variability in undrained shear strength on active lateral force in clay. Structural Safety, 52, 121–31.

IEG (Implementation Commission of European Standards in Geotechnics). (2008). Implementation guidelines: General rules of Eurocode 7. Report 2:2008, 3rd edition. Swedish Geotechnical Society, Linköping, Sweden.

ISO2394: 2015. General Principles on Reliability for Structures. Geneva, International Organization for Standardization.

JGS. (2004). Principles for Foundation Design Grounded on a Performance-based Design Concept (GeoGuide). Tokyo: Japanese Geotechnical Society.

Länsivaara, T., Phoon, K.K., and Ching, J. (2020). What is a characteristic value for soils? in preparation.

Müller, R., Larsson, S., & Spross, J. (2016). Multivariate stability assessment during staged construction. Canadian Geotechnical Journal, 53(4), 603-618.

Ministry of Housing and Urban-Rural Development of the People's Republic of China (MOHURDPRC). (2009). Code for investigation of geotechnical engineering (CIGE). GB 50021-2001, China Building Industry Press, Beijing (in Chinese).

National Research Council (NRC). 2011. User's Guide – NBC 2010 Structural Commentaries (Part 4 of Division B), 3rd ed. National Research Council of Canada, Ottawa, Ont.

Orr, T. L. (2017). Defining and selecting characteristic values of geotechnical parameters for designs to Eurocode 7. Georisk: Assessment and Management of Risk for Engineered Systems and Geohazards, 11(1), 103-115.

Orr, T. L. (2000). Selection of characteristic values and partial factors in geotechnical designs to Eurocode 7. Computers and Geotechnics, 26(3-4), 263-279.

Paikowsky, S. G., Birgisson, B., MvVay, M., Nguyen, T., Kuo, C., Baecher, G., Ayyub, B., Stenersen, K., O'Malley, K., Chernauskas, L., and O'Neill, M. (2004). Load and resistance factor design (LRFD) for deep foundations, National Cooperative Highway Research Program (NCHRP) Report 507, Transportation Research Board, National Research Council, Washington, D.C.

Phoon, K. K., & Kulhawy, F. H. (1999). Evaluation of geotechnical property variability. Canadian Geotechnical Journal. 36(4), 625-639.

Prästings, A., et al. (2017). Implementing the extended multivariate approach in design with partial factors for a retaining wall in clay. ASCE-ASME Journal of Risk and Uncertainty in Engineering Systems, Part A: Civil Engineering, 3(4), 04017015.

Prästings, A., Spross, J., & Larsson, S. (2019). Characteristic values of geotechnical parameters in Eurocode 7. Proceedings of the Institution of Civil Engineers-Geotechnical Engineering, 172(4), 301-311.

Schneider, H. R., & Schneider, M. A. (2013). Dealing with uncertainties in EC7 with emphasis on determination of characteristic soil properties. Edited by P. Arnold, G.A. Fenton, M.A. Hicks, T. Schweckendiek, and B. Simpson. Advances in Soil Mechanics and Geotechnical Engineering, IOS Press, pp. 87-101.

Schneider, H. R. (1997). Definition and determination of characteristic soil properties. Proceedings of the XII International Con-ference on Soil Mechanics and Geotechnical Engineering, Hamburg, 2271-2274, Balkema, Rotterdam.

Shen, M., Khoshnevisan, S., Tan, X., Zhang, Y., & Juang, C. H. (2019). Assessing characteristic value selection methods for design with load and resistance factor design (LRFD)—design robustness perspective. Canadian Geotechnical Journal, 56(10), 1475-1485.

Spross, J., & Larsson, S. (2021). Probabilistic observational method for design of surcharges on vertical drains. Géotechnique, In press.

SP 22.13330. (2016) (Russian Code of Practice) Soil bases of buildings and structures, in Russian.

SP 23.13330. (2018) (Russian Code of Practice) Foundation of hydraulic structures, in Russian.

Standards Australia (SA). (2004). Bridge design. Part 1: Scope and general principles. Australian Standard AS 5100.1–2004, Sydney, Australia.

Tabarroki, M., Ching, J., Phoon, K.K., and Chen, Y.Z. (2020). Mobilization-based characteristic value of shear strength for ultimate limit states, Georisk: Assessment and Management of Risk for Engineered Systems and Geohazards, in press.

Tang, X. S., Li, D. Q., Wang, X. G., & Phoon, K. K. (2018). Statistical characterization of shear strength parameters of rock mass for hydropower projects in China. Engineering Geology, 245, 258-265.

Van der Krogt, M. G., Schweckendiek, T., & Kok, M. (2019). Uncertainty in spatial average undrained shear strength with a site-specific transformation model. Georisk: Assessment and Management of Risk for Engineered Systems and Geohazards, 13(3), 226-236.

Vanmarcke, E. H., 1977. Probabilistic modeling of soil profiles. Journal of the Geotechnical Engineering Division, 103 (11), 1227-1246.

Varkey, D., Hicks, M.A., van den Eijnden, A.P., and Vardon, P.J. (2020). On characteristic values for calculating factors of safety for dyke stability. Géotechnique Letters, 10(2), 353-359.

Vick, S.G., 2002. Degrees of Belief: Subjective Probability and Engineering Judgment. ASCE Press, Reston, Virginia.

Vrouwenvelder, A. C. W. M. (2002). Developments towards full probabilistic design codes. Structural safety, 24(2-4), 417-432.

Wang, Y., Arroyo, M., Cao, Z. J., Ching, J. Y., Länsivaara, T., Orr, T., Phoon, K. K., Schneider, H., and Simpson B. (2017). Selection of characteristic values for rock and soil properties using Bayesian

statistics and prior knowledge, Chapter 5, Joint TC205/TC304 working group report on “Discussion of statistical/reliability methods for Eurocodes”, International Society for Soil Mechanics and Geotechnical Engineering (ISSMGE).

Wang, Y., & Zhao, T. (2017). Statistical interpretation of soil property profiles from sparse data using Bayesian compressive sampling. Géotechnique, 67(6), 523-536.

Zhao, T., & Wang, Y. (2020). Interpolation and stratification of multilayer soil property profile from sparse measurements using machine learning methods. Engineering Geology, 265, 105430.

Zhao, T., Xu, L., & Wang, Y. (2020). Fast non-parametric simulation of 2D multi-layer cone penetration test (CPT) data without pre-stratification using Markov Chain Monte Carlo simulation. Engineering Geology, 105670.

Zhao, T., Montoya-Noguera, S., Phoon, K. K., & Wang, Y. (2018). Interpolating spatially varying soil property values from sparse data for facilitating characteristic value selection. Canadian Geotechnical Journal, 55(2), 171-181.

7. Numerical evidences for worst-case scale of fluctuation

Giovanna Vessia, Yan-Guo Zhou, Andy Leung, Wojciech Pula, Diego Di Curzio, Mohammad Tabarroki, and Jianye Ching

7.1 Introduction

The worst-case scale of fluctuation (worst-case SOF) is a phenomenon observed in the literature (e.g., Fenton and Griffiths 2003; Jaksa et al. 2005; Fenton et al. 2005; Breysse et al. 2005; Griffiths et al. 2006; Soubra et al. 2008; Vessia et al. 2009; Ching and Phoon 2013; Ahmed and Soubra 2014; Hu and Ching 2015; Stuedlein and Bong 2017) where more complex non-classical mechanisms can occur when the SOF of the soil spatial variability (usually modeled by a random field) is comparable to some multiple of the characteristic length of the geotechnical structure (e.g., width of a footing, distance between shallow pads, height of a retaining wall). The complex behavior typically manifests itself most clearly when the mean response from random field realizations is compared with the nominal response produced by a soil mass taking mean properties everywhere. At the worst-case SOF, the discrepancy between the mean response and the nominal response is the largest. The existence of a worst-case SOF indicates that adopting the nominal response is unconservative. The concept of the worst-case SOF is valuable in reliability-based design (RBD), because in the absence of a site-specific SOF, the use of the worst-case SOF may ensure a conservative design.

7.2 Summary Table

Table 7.1 summarizes past studies that report worst-case SOFs. The characteristic length in the fifth column is mostly chosen by the current report rather than by the past studies. Right now, the characteristic length is mostly chosen to be related to the dimension of the geotechnical structure.

7.3 Key observations

1. In terms of problem types, only five problem types have been investigated by the past studies in Table 7.1, including footing (43% of the studies), retaining wall (14%), soil column (18%), basal heave (7%), slope (11%), and pile (7%). In terms of limit states, 75% of the studies are for the ultimate limit state (ULS) (strength and capacity), whereas 25% are for the serviceability limit state (SLS) (settlement and deformation).
2. All studies adopted numerical models to investigate worst-case SOFs. Among them, 72% of the studies adopted random finite element analyses (RFEA), 7% adopted random finite difference analyses (RFDA), 11% adopted random limit equilibrium methods (RLEM), and 11% adopted numerical models calibrated by RFEA/FFDA/RLEM. None of the studies in the table investigated worst-case SOFs based on real-world field tests or model tests.
3. In terms of problem dimensions, 7% of the studies investigated 1D problems, 75% investigated 2D problems, and 18% investigated 3D problems.

4. The definitions for worst-case SOFs are not uniform. Most of them are defined as the SOF that produces the minimal mean strength/capacity/FS, maximal under-design probability, or maximal mean demand (e.g., mean settlement, mean moment, mean lateral force, etc.).
5. For many cases in the table, the worst-case SOFs are found to be around the characteristic length (worst-case SOF ≈ characteristic length), but there are also cases where the worst-case SOF is far from the characteristic length.
6. For the cases focusing on ULS, the ratio (worst-case mean response)/(nominal response) varies from 0.5 to 1.0, where "nominal response" refers to the response produced by a homogenous analysis with soil parameter fixed at the mean value of the random field. This ratio seems to depend on the following three factors: (a) COV of random field; (b) problem type; (c) isotropy/anisotropy. Figure 7.1 shows how this ratio varies with COV. Figure 1a shows that the ratio is larger for anisotropic cases ($\delta_h > \delta_v$) and smaller for isotropic cases ($\delta_h = \delta_v$). Figure 7.1b shows that the ratio is the largest for retaining wall and smallest for soil column.
7. For compressive strength of a soil column, some studies investigated 3D problems. Figure 7.1c shows the ratios (worst-case mean response)/(nominal response) for both 2D and 3D cases. It seems that this ratio is not significantly affected by the problem dimension.

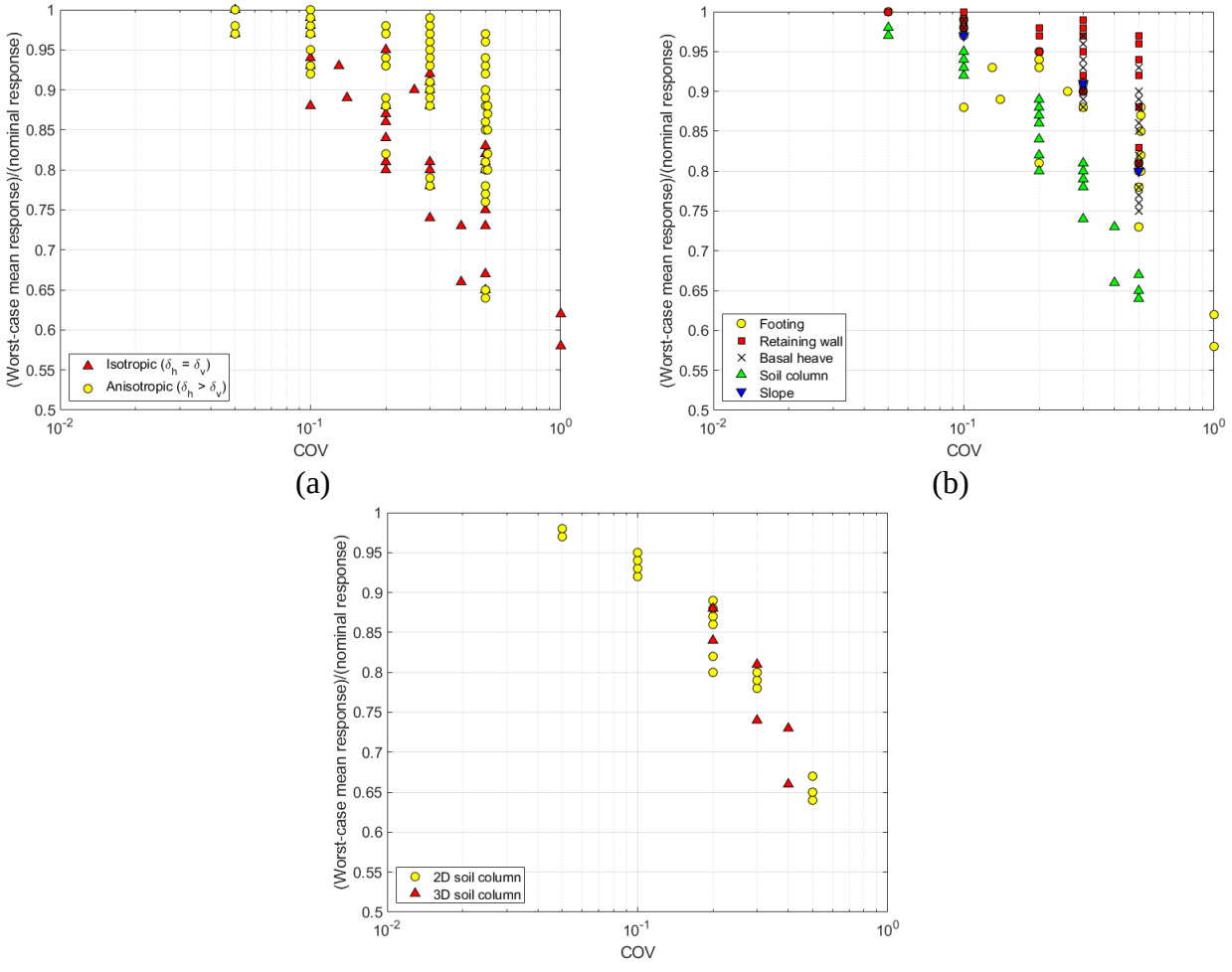

Figure 7.1. Variation of (worst-case mean response)/(nominal response) with respect to COV: (a) isotropic v.s. anisotropic cases; (b) different problem types; (c) 2D v.s. 3D soil column

7.4 References

Ali, A., Huang, J., Lyamin, A.V., Sloan, S.W., Griffiths, D.V., Cassidy, M.J., and Li, J.H. (2014). Simplified quantitative risk assessment of rainfall-induced landslides modelled by infinite slopes. Engineering Geology, 179, 102-116.

Ahmed, A. and Soubra, A.H. (2014). Probabilistic analysis at the serviceability limit state of two neighboring strip footings resting on a spatially random soil, Structural Safety, 49, 2-9.

Allahverdizadeh, P., Griffiths, D.V., and Fenton, G.A. (2016). Influence of soil shear strength spatial variability on the compressive strength of a block. Georisk: Assessment and Management of Risk for Engineered Systems and Geohazards, 10(1), 2-10.

Breysse, D., Niandou, H., Elachachi, S., and Houy, L. (2005). A generic approach to soil-structure interaction considering the effects of soil heterogeneity. Géotechnique, 55(2), 143-150.

Ching, J. and Phoon, K.K. (2013). Probability distribution for mobilised shear strengths of spatially variable soils under uniform stress states. Georisk: Assessment and Management of Risk for Engineered Systems and Geohazards, 7(3), 209-224.

Ching, J., Phoon, K.K., and Sung, S.P. (2017). Worst case scale of fluctuation in basal heave analysis involving spatially variable clays. Structural Safety, 68, 28-42.

Fenton, G.A. and Griffiths, D.V. (2003). Bearing capacity prediction of spatially random c-ϕ soil. Canadian Geotechnical Journal, 40(1), 54-65.

Fenton, G.A., Griffiths, D.V., and Williams, M.B. (2005). Reliability of traditional retaining wall design. Geotechnique, 55(1), 55-62.

Fenton, G.A. and Griffiths, D.V. (2005). Three-dimensional probabilistic foundation settlement. Journal of Geotechnical and Geoenvironmental Engineering, 131(2), 232-239.

Griffiths, D.V., Fenton, G.A., and Manoharan, N. (2006). Undrained bearing capacity of two-strip footings on spatially random soil. International Journal of Geomechanics, 6(6), 421-427.

Griffiths, D.V., Fenton, G.A., and Ziemann, H.R. (2008). Reliability of passive earth pressure. Georisk: Assessment and Management of Risk for Engineered Systems and Geohazards, 2(2), 113-121.

Hu, Y.G. and Ching, J. (2015). Impact of spatial variability in undrained shear strength on active lateral force in clay. Structural Safety, 52, 121-131.

Jaksa, M.B., Goldsworthy, J.S., Fenton, G.A., Kaggwa, W.S., Griffiths, D.V., Kuo, Y.L., and Poulos, H.G. (2005). Towards reliable and effective site investigations. Geotechnique, 55(2), 109-121.

Javankhoshdel, S., Luo, N., and Bathurst, R. J. (2017). Probabilistic analysis of simple slopes with cohesive soil strength using RLEM and RFEM. Georisk: Assessment and Management of Risk for Engineered Systems and Geohazards, 11(3), 231-246.

Leung, Y.F. and Lo, M.K. (2018). Probabilistic assessment of pile group response considering superstructure stiffness and three-dimensional soil spatial variability. Computers and Geotechnics, 103, 193-200.

Luo, N. and Bathurst, R.J. (2017). Reliability bearing capacity analysis of footings on cohesive soil slopes using RFEM. Computers and Geotechnics, 89, 203-212.

Naghibi, F., Fenton, G.A., and Griffiths, D.V. (2016). Probabilistic considerations for the design of deep foundations against excessive differential settlement. Canadian Geotechnical Journal, 53(7),1167-1175.

Namikawa, T. and Koseki, J. (2013). Effects of spatial correlation on the compression behavior of a

cement-treated column. Journal of Geotechnical and Geoenvironmental Engineering, 139(8), 1346-1359.

Pan, Y., Liu, Y., Fook, H.X., Lee, H., and Phoon, K.K. (2018). Effect of spatial variability on short-and long-term behaviour of axially-loaded cement-admixed marine clay column. Computers and Geotechnics, 94, 150-168.

Puła, W., Pieczyńska-Kozłowska, J.M., and Chwała, M. (2017). Search for the worst-case correlation length in the bearing capacity probability of failure analyses. Geo-Risk 2017 in ASCE Geotechnical Special Publication, GSP 283, 534-544.

Soubra, A.H., Massih, D.S.Y.A., and Kalfa, M. (2008). Bearing capacity of foundations resting on a spatially random soil. ASCE Geotechnical Special Publication, (178), 66-73.

Stuedlein, A.W. and Bong, T. (2017). Effect of spatial variability on static and liquefaction-induced differential settlements. ASCE Geotechnical Special Publication, (GSP 282), 31-51.

Tabarroki, M., Ahmad, F., Banaki, R., Jha, S.K., and Ching, J. (2013). Determining the factors of safety of spatially variable slopes modeled by random fields. Journal of Geotechnical and Geoenvironmental Engineering, 139(12), 2082-2095.

Tabarroki, M. (2020). PhD Dissertation (in preparation), Dept of Civil Engineering, National Taiwan University.

Vessia, G., Cherubini, C., Pieczyńska, J., and Puła W. (2009). Application of random finite element method to bearing capacity design of strip footing. Journal of Geoengineering, 4(3), 103-112.

Table 7.1. Summary of worst-case SOFs in the literature

Reference	Response & problem type	Worst-case definition	Simulation method	Characteristic length	Random field characteristics: 1D/2D/3D Isotropic/anisotropic COV	Worst-case SOF	(Worst-case mean response)/ (nominal response)
Jaksa et al. (2005)	Settlement of a nine-pad footing system	Under-design probability is maximal	RFEA	Footing spacing (S)	3D random field of E δ_h/δ_v = 1 and 2 COV = 0.1 and 0.5	1×S	
Fenton and Griffiths (2005)	Differential settlement between two footings	Standard deviation of different settlement is maximal	RFEA	Footing spacing (S)	3D random field of E δ_h/δ_v = 1 COV = 0.1 to 4	1×S	
Fenton and Griffiths (2003)	Bearing-capacity factor of a strip footing on a c-ϕ soil	Mean of log bearing-capacity factor is minimal	RFEA	Footing width (B)	2D random fields of c and ϕ δ_h/δ_v = 1 COV = 0.1 to 5	1 to 5×B	0.88 for COV = 0.1 0.81 for COV = 0.2 0.73 for COV = 0.5 0.62 for COV = 1 0.51 for COV = 2 0.45 for COV = 5
Soubra et al. (2008)	Bearing capacity under punching failure mode for a strip footing	Mean bearing capacity is minimal	RFDA	Footing width (B)	2D random fields of c and ϕ δ_h/δ_v = 0.25 to 25 COV_c = 0.2 to 0.4 COV_ϕ = 0.1 to 0.15	1×B for isotropic 5×B for anisotropic	0.93 for COV_c = 0.2 & COV_ϕ = 0.1 0.90 for COV_c = 0.4 & COV_ϕ = 0.1 0.89 for COV_c = 0.2 & COV_ϕ = 0.15
Fenton et al. (2005)	Active lateral force for a retaining wall	Under-design probability is maximal	RFEA	Wall height (H)	2D random fields of ϕ and γ δ_h/δ_v = 1 COV = 0.02 and 0.5	0.5 to 1×H	
Breysse et al. (2005)	Settlement of a footing system	Mean footing rotation is maximal	Numerical model + MCS	Footing spacing (S) & Pipe length (L)	1D random field of soil subgrade modulus k	0.5×S	
		Mean sewer pipe bending moment is maximal				1 to 2×L	
		Mean different settlement between footings is				Very complicated	

		maximal					
Griffiths et al. (2006)	Bearing capacity of a strip footing on ϕ=0 soil	Mean bearing capacity is minimal	RFEA	Footing width (B)	2D isotropic random field of s_u δ_h/δ_v = 1 COV = 0.25 to 8	0.5 to 1×B	0.58 for COV = 1
Vessia et al. (2009)	Bearing capacity of a strip footing on c-ϕ soil	Mean bearing capacity is minimal	RFEA	Footing width (B)	2D random fields of c and ϕ δ_h/δ_v = 0.5 to 25 COV_c = 0.56 & COV_ϕ = 0.24	1×B for isotropic 0.3 to 0.5×B for anisotropic	0.80 for δ_h/B = 1 0.82 for δ_h/B = 5 0.85 for δ_h/B = 10 0.87 for δ_h/B = 30 0.88 for δ_h/B = 50
Ching and Phoon (2013)	Compressive strength of a undrained soil column	Mean strength is minimal	RFEA	Column width (W)	2D random field of s_u δ_h/δ_v = 1 & ∞ COV = 0.2	1×W	0.8 for δ_h/δ_v = 1 0.82 for δ_h/δ_v = ∞
Ahmed and Soubra (2014)	Differential settlement between strip footings	Under-design probability is maximal	RFDA	Footing spacing (S)	2D random field of E δ_h/δ_v = 1 to 30 COV = 0.15	1×S	
Hu and Ching (2015)	Active lateral force for a retaining wall in clay	Mean active lateral force is maximal	RLEM	Wall height (H)	2D random field of s_u δ_h/δ_v = 1 COV = 0.1 to 0.3	0.1 to 0.2×H	1.24 for COV = 0.3
Stuedlein and Bong (2017)	Differential settlement of footings	Under-design probability is maximal	Numerical model + MCS	Footing spacing (S)	2D conditional random field based on CPT data	1×S	
Ali et al. (2014)	Risk of an infinite slope	Risk of rainfall induced slope failure is maximal	RLEM	Slope thickness (H)	1D random field of hydraulic conductivity k COV = 1	1×H	
Pan et al. (2018)	Compressive strength of a cement-treated clay column	Mean strength is minimal	RFEA	Column diameter (D)	3D random field of s_u δ_h/δ_v = 1 COV = 0.2 to 0.4	1×D	0.84 for COV = 0.2 0.74 for COV = 0.3 0.66 for COV = 0.4
Pula et al. (2017)	Bearing capacity of a strip footing on c-ϕ soil	Under-design probability is maximal	RFEA	Footing width (B)	Scenario 1: 2D random fields of c δ_h/δ_v = 1 COV_c = 0.1 to 4 Scenario 2: 2D random fields	Scenario 1: 8×B Scenario 2: local maximum effect not observed	

					of c and ϕ δ_h/δ_v = 1 Case A: COV_c = 0.1 to 4 and COV_ϕ = 0.2 Case B: COV_ϕ = variable and COV_c = const.		
Javankhoshdel et al. (2017)	FS of a cohesive slope	Probability of failure is maximal	RFEA/RLEM	Slope height (H)	2D random field of s_u δ_h/δ_v varies COV = 0.5		
Luo and Bathurst (2017)	Bearing-capacity factor of a strip footing on a cohesive slope	Mean bearing-capacity factor is minimal	RFEA	Footing width (B)	2D random field of s_u δ_h/δ_v = 1 to 20 COV = 0.5	0.25 to 1×B	Very complicated, depending on several factors
Allahverdizadeh et al. (2016)	Compressive strength of a square block	Mean compressive strength is minimal	RFEA	Block width (B)	2D random fields of c and ϕ δ_h/δ_v = 1 COV_c = COV_ϕ = 0.2 to 0.5	0.1 to 1×B	0.86 for COV = 0.2 0.80 for COV = 0.3 0.67 for COV = 0.5
Griffiths et al. (2008)	Passive lateral force for a retaining wall	Under-design probability is maximal	RFEA	Wall height (H)	2D random fields of c and ϕ δ_h/δ_v = 1 COV = 0.02 to 0.5	0.1 to 0.5×H	
Tabarroki et al. (2013)	FS of a cohesive slope	Mean FS is minimal	RFEA/RLEM	Slope height (H)	2D random field of s_u δ_h/δ_v = 1 COV = 0.1 to 0.5	0.1~1×H	0.97 for COV = 0.1 0.91 for COV = 0.3 0.80 for COV = 0.5
Namikawa and Koseki (2013)	Compressive strength of a cement-treated column	Mean strength is minimal	RFEA	Column diameter (D)	3D random field of q_u δ_h/δ_v = 1 COV = 0.2 to 0.4	0.5×D	0.88 for COV = 0.2 0.81 for COV = 0.3 0.73 for COV = 0.4
Ching et al. (2017)	FS for basal heave of an excavation in clay	Mean FS is minimal	RFEA	Wall penetration depth (H_p)	2D random field of s_u/σ'_v δ_h/δ_v = 1 to 100 COV = 0.1 to 0.5	0.1~0.4×H_p	0.98 for δ_h/δ_v = 1 & COV = 0.1 0.9 for δ_h/δ_v = 1 & COV = 0.3 0.81 for δ_h/δ_v = 1 & COV = 0.5 0.98 for δ_h/δ_v = 10 & COV = 0.1 0.93 for δ_h/δ_v = 10 & COV = 0.3 0.86 for δ_h/δ_v = 10 & COV = 0.5 0.98 for δ_h/δ_v = 30 & COV = 0.1 0.94 for δ_h/δ_v = 30 & COV = 0.3 0.89 for δ_h/δ_v = 30 & COV = 0.5 0.98 for δ_h/δ_v = 100 & COV = 0.1

							0.96 for δ_h/δ_v = 100 & COV = 0.3 0.9 for δ_h/δ_v = 100 & COV = 0.5
Naghibi et al. (2016)	Differential settlement of a two-pile system	Mean differential settlement is maximal	Semi-theoretical model validated by RFEA	Pile spacing (S)	2D random field of E δ_h/δ_v = 1 COV = 0.1 to 0.5	1×S	
Leung and Lo (2018)	Differential settlement of a pile group	Standard deviation of differential settlement is maximal	RFEA	Width of pile group (B) Length of pile group (L)	3D random field of E δ_h/B = 0.5, 1 and $\propto$ δ_v/L = 0.15 to 1 COV = 0.25 and 0.5	0.5 to 1×B	
Tabarroki (2020)	Mobilized shear strength of a soil column under compression	Mean mobilized shear strength is minimal	RFEA	Column width (W)	Scenario A: 2D random field of s_u Scenario B: 2D random field of s_u/σ'_v Scenario C: 2D random field of tan ϕ' δ_h/δ_v = 1 to 100 For A & B: COV = 0.1 to 0.5 For C: COV = 0.05 to 0.2	0.5×W	Scenario A: 0.93 for δ_h/δ_v = 1 & COV = 0.1 0.78 for δ_h/δ_v = 1 & COV = 0.3 0.65 for δ_h/δ_v = 1 & COV = 0.5 0.93 for δ_h/δ_v = 10 & COV = 0.1 0.78 for δ_h/δ_v = 10 & COV = 0.3 0.64 for δ_h/δ_v = 10 & COV = 0.5 0.92 for δ_h/δ_v = 30 & COV = 0.1 0.78 for δ_h/δ_v = 30 & COV = 0.3 0.65 for δ_h/δ_v = 30 & COV = 0.5 0.93 for δ_h/δ_v = 100 & COV = 0.1 0.79 for δ_h/δ_v = 100 & COV = 0.3 0.65 for δ_h/δ_v = 100 & COV = 0.5 Scenario C: 0.97 for δ_h/δ_v = 1 & COV = 0.05 0.94 for δ_h/δ_v = 1 & COV = 0.1 0.87 for δ_h/δ_v = 1 & COV = 0.2 0.97 for δ_h/δ_v = 10 & COV = 0.05 0.95 for δ_h/δ_v = 10 & COV = 0.1 0.88 for δ_h/δ_v = 10 & COV = 0.2 0.97 for δ_h/δ_v = 30 & COV = 0.05 0.95 for δ_h/δ_v = 30 & COV = 0.1 0.88 for δ_h/δ_v = 30 & COV = 0.2 0.98 for δ_h/δ_v = 100 & COV = 0.05 0.95 for δ_h/δ_v = 100 & COV = 0.1

							0.89 for δ_h/δ_v = 100 & COV = 0.2
	Mobilized shear strength of a retaining wall			Wall height (H)		0.05×H	Scenario A: 0.98 for δ_h/δ_v = 1 & COV = 0.1 0.9 for δ_h/δ_v = 1 & COV = 0.3 0.81 for δ_h/δ_v = 1 & COV = 0.5 0.99 for δ_h/δ_v = 10 & COV = 0.1 0.95 for δ_h/δ_v = 10 & COV = 0.3 0.88 for δ_h/δ_v = 10 & COV = 0.5 1 for δ_h/δ_v = 30 & COV = 0.1 0.98 for δ_h/δ_v = 30 & COV = 0.3 0.94 for δ_h/δ_v = 30 & COV = 0.5 1 for δ_h/δ_v = 100 & COV = 0.1 0.99 for δ_h/δ_v = 100 & COV = 0.3 0.97 for δ_h/δ_v = 100 & COV = 0.5 Scenario B: 0.99 for δ_h/δ_v = 1 & COV = 0.1 0.92 for δ_h/δ_v = 1 & COV = 0.3 0.83 for δ_h/δ_v = 1 & COV = 0.5 1 for δ_h/δ_v = 10 & COV = 0.1 0.97 for δ_h/δ_v = 10 & COV = 0.3 0.92 for δ_h/δ_v = 10 & COV = 0.5 1 for δ_h/δ_v = 30 & COV = 0.1 0.99 for δ_h/δ_v = 30 & COV = 0.3 0.96 for δ_h/δ_v = 30 & COV = 0.5 1 for δ_h/δ_v = 100 & COV = 0.1 0.99 for δ_h/δ_v = 100 & COV = 0.3 0.97 for δ_h/δ_v = 100 & COV = 0.5 Scenario C: 1 for δ_h/δ_v = 1 & COV = 0.05 0.98 for δ_h/δ_v = 1 & COV = 0.1 0.95 for δ_h/δ_v = 1 & COV = 0.2 1 for δ_h/δ_v = 10 & COV = 0.05 0.99 for δ_h/δ_v = 10 & COV = 0.1 0.97 for δ_h/δ_v = 10 & COV = 0.2

							1 for δ_h/δ_v = 30 & COV = 0.05 0.99 for δ_h/δ_v = 30 & COV = 0.1 0.98 for δ_h/δ_v = 30 & COV = 0.2 1 for δ_h/δ_v = 100 & COV = 0.05 0.99 for δ_h/δ_v = 100 & COV = 0.1 0.97 for δ_h/δ_v = 100 & COV = 0.2
	Mobilized shear strength of a strip footing			Footing width (B)		0.1 to 0.5×B	Scenario A: 0.98 for δ_h/δ_v = 1 & COV = 0.1 0.9 for δ_h/δ_v = 1 & COV = 0.3 0.8 for δ_h/δ_v = 1 & COV = 0.5 0.98 for δ_h/δ_v = 10 & COV = 0.1 0.9 for δ_h/δ_v = 10 & COV = 0.3 0.81 for δ_h/δ_v = 10 & COV = 0.5 0.98 for δ_h/δ_v = 30 & COV = 0.1 0.9 for δ_h/δ_v = 30 & COV = 0.3 0.8 for δ_h/δ_v = 30 & COV = 0.5 0.97 for δ_h/δ_v = 100 & COV = 0.1 0.88 for δ_h/δ_v = 100 & COV = 0.3 0.78 for δ_h/δ_v = 100 & COV = 0.5 Scenario B: 0.98 for δ_h/δ_v = 1 & COV = 0.1 0.9 for δ_h/δ_v = 1 & COV = 0.3 0.8 for δ_h/δ_v = 1 & COV = 0.5 0.98 for δ_h/δ_v = 10 & COV = 0.1 0.9 for δ_h/δ_v = 10 & COV = 0.3 0.8 for δ_h/δ_v = 10 & COV = 0.5 0.98 for δ_h/δ_v = 30 & COV = 0.1 0.9 for δ_h/δ_v = 30 & COV = 0.3 0.8 for δ_h/δ_v = 30 & COV = 0.5 0.99 for δ_h/δ_v = 100 & COV = 0.1 0.91 for δ_h/δ_v = 100 & COV = 0.3 0.81 for δ_h/δ_v = 100 & COV = 0.5 Scenario C: 1 for δ_h/δ_v = 1 & COV = 0.05

							0.98 for δ_h/δ_v = 1 & COV = 0.1 0.95 for δ_h/δ_v = 1 & COV = 0.2 1 for δ_h/δ_v = 10 & COV = 0.05 0.98 for δ_h/δ_v = 10 & COV = 0.1 0.94 for δ_h/δ_v = 10 & COV = 0.2 1 for δ_h/δ_v = 30 & COV = 0.05 0.98 for δ_h/δ_v = 30 & COV = 0.1 0.94 for δ_h/δ_v = 30 & COV = 0.2 1 for δ_h/δ_v = 100 & COV = 0.05 0.98 for δ_h/δ_v = 100 & COV = 0.1 0.93 for δ_h/δ_v = 100 & COV = 0.2
	Mobilized shear strength of a deep excavation in clay			Penetration depth (H_p)		$0.2\times H_p$	Scenario A: 0.99 for δ_h/δ_v = 1 & COV = 0.1 0.88 for δ_h/δ_v = 1 & COV = 0.3 0.75 for δ_h/δ_v = 1 & COV = 0.5 0.98 for δ_h/δ_v = 10 & COV = 0.1 0.88 for δ_h/δ_v = 10 & COV = 0.3 0.76 for δ_h/δ_v = 10 & COV = 0.5 0.98 for δ_h/δ_v = 30 & COV = 0.1 0.88 for δ_h/δ_v = 30 & COV = 0.3 0.77 for δ_h/δ_v = 30 & COV = 0.5 0.98 for δ_h/δ_v = 100 & COV = 0.1 0.89 for δ_h/δ_v = 100 & COV = 0.3 0.78 for δ_h/δ_v = 100 & COV = 0.5 Scenario B: 0.98 for δ_h/δ_v = 1 & COV = 0.1 0.91 for δ_h/δ_v = 1 & COV = 0.3 0.82 for δ_h/δ_v = 1 & COV = 0.5 0.98 for δ_h/δ_v = 10 & COV = 0.1 0.93 for δ_h/δ_v = 10 & COV = 0.3 0.85 for δ_h/δ_v = 10 & COV = 0.5 0.98 for δ_h/δ_v = 30 & COV = 0.1 0.94 for δ_h/δ_v = 30 & COV = 0.3 0.88 for δ_h/δ_v = 30 & COV = 0.5 0.98 for δ_h/δ_v = 100 & COV = 0.1

							0.97 for δ_h/δ_v = 100 & COV = 0.3 0.93 for δ_h/δ_v = 100 & COV = 0.5